8524

SANDIA REPORT

SAND87—2456 • UC—70
Unlimited Release
Printed December 1987

Interpretation of the WIPP-13 Multipad Pumping Test of the Culebra Dolomite at the Waste Isolation Pilot Plant (WIPP) Site

Richard L. Beauheim

Prepared by
Sandia National Laboratories
Albuquerque, New Mexico 87185 and Livermore, California 94550
for the United States Department of Energy
under Contract DE-AC04-76DP00789

Issued by Sandia National Laboratories, operated for the United States Department of Energy by Sandia Corporation.

Printed in the United States of America
Available from
National Technical Information Service
U.S. Department of Commerce
5285 Port Royal Road
Springfield, VA 22161

NTIS price codes
Printed copy: A08
Microfiche copy: A01

SAND87-2456
Unlimited Release
Printed December 1987

Distribution
Category UC-70

Interpretation of the WIPP-13 Multipad Pumping Test of the Culebra Dolomite at the Waste Isolation Pilot Plant (WIPP) Site

Richard L. Beauheim
Earth Sciences Division
Sandia National Laboratories
Albuquerque, NM 87185

Abstract

A large-scale pumping test of the Culebra Dolomite Member of the Rustler Formation was performed in early 1987 at the Waste Isolation Pilot Plant (WIPP) site in southeastern New Mexico. This test (the WIPP-13 or northern) multipad test, complemented the H-3 (or southern) multipad test (conducted in late 1985 and early 1986) by creating a hydraulic stress that could be measured over the northern portion of the WIPP site. The test consisted of pumping well WIPP-13 at a rate of 30 gpm for 36 days and monitoring drawdown and recovery responses in 17 observation wells and one WIPP shaft. Responses were observed in 14 of these wells, including one well 20 550 ft from WIPP-13 and in the WIPP exhaust shaft. Several of these wells had also responded during the H-3 multipad test.

Individual well tests at locations around the WIPP site have demonstrated that the Culebra is a heterogeneous, water-bearing unit. The responses measured at observation wells to pumping tests in heterogeneous systems cannot be rigorously interpreted using standard analytical (as opposed to numerical) techniques developed for tests in homogeneous, porous media. Application of analytical techniques to data from heterogeneous media results in evaluations of average hydraulic properties between pumping and observation wells that are nonunique in the sense that they are representative only of the responses observed when a hydraulic stress is imposed at a certain location. These "apparent" hydraulic properties do, however, provide a qualitative understanding of the nature and distribution of both hydraulic properties and heterogeneities or boundaries within the tested area.

The interpretations of the responses at the pumping and observation wells are consistent with the following conceptualization: The Culebra is a fractured, double-porosity system around WIPP-13, H-6, and DOE-2, with

(continued)

Abstract (continued)

relatively high transmissivity (~70 ft^2/day) and relatively low storativity (5×10^{-6} to 8×10^{-6}). This system appears to extend further to the north toward WIPP-30, although WIPP-30 itself lies in a lower transmissivity zone. The apparent transmissivity between WIPP-13 and observation wells toward the center of the WIPP site to the south and east, where fracturing in the Culebra decreases, decreases to 16 to 28 ft^2/day, and apparent storativity increases to 3.6×10^{-5} to 5.5×10^{-5}. To the west toward Nash Draw, the apparent transmissivity increases to 265 to 650 ft^2/day, reflecting increased fracturing in that direction, while the apparent storativity increases to 5.2×10^{-5} to 6.4×10^{-5}.

The analyses of the responses measured at observation wells to the WIPP-13 multipad pumping test provide a qualitative conceptualization of three distinct domains within a heterogeneous portion of the Culebra north of the center of the WIPP site. This conceptualization is being refined by using numerical-modeling techniques to simulate the WIPP-13 multipad test and other tests at the WIPP site in an attempt to define the distribution of hydraulic properties that will reproduce the responses observed.

Acknowledgments

The author thanks Wayne Stensrud, Michael Bame, Kent Lantz, Jeff Palmer, and George Saulnier for their efforts in performing the WIPP-13 multipad test. George Saulnier, Jerry Mercer, Ken Brinster, and Al Lappin provided helpful review comments on the original manuscript of this document. Mary Gonzales's help with the data preparation is especially appreciated.

Contents

Contents (continued)

Figures

Figures (continued)

Tables

Interpretation of the WIPP-13 Multipad Pumping Test of the Culebra Dolomite at the Waste Isolation Pilot Plant (WIPP) Site

1. Introduction

This report presents the results of a large-scale pumping test performed on the Culebra Dolomite Member of the Rustler Formation over the northern portion of the Waste Isolation Pilot Plant (WIPP) site in southeastern New Mexico (Figure 1-1). The WIPP is a US Department of Energy research and development facility designed to demonstrate safe disposal of transuranic radioactive wastes resulting from the nation's defense programs. The WIPP facility lies in bedded halite in the lower Salado Formation. The pumping test discussed in this report was conducted in the Rustler Formation, which overlies the Salado Formation. The test was performed by INTERA Technologies, Inc., under the technical direction of Sandia National Laboratories, Albuquerque, New Mexico.

The pumping well for the test was WIPP-13, which is located ~8600 ft northwest of the center of the WIPP site. WIPP-13 was pumped at a rate of ~30 gallons per minute (gpm) from January 12 to February 17, 1987 (Julian days 12 to 48), to provide data on the hydraulic properties of the Culebra at WIPP-13 and to create a hydraulic stress that could be measured over the northern part of the WIPP site. The test is termed a "multipad" test because responses were observed in wells completed on a number of drilling pads. The test was intended to complement the H-3 (or southern) multipad test conducted between October and December 1985 (Beauheim, 1987a). Together, the two multipad tests provided measurable, and spatially overlapping, hydraulic responses over most of the 16-mi^2 WIPP site (Figure 1-1).

During the WIPP-13 (or northern) multipad test, water levels were measured on a regular basis in 17 observation wells completed in the Culebra dolomite at locations ranging from 4210 to 20 550 ft from WIPP-13. Responses to the pumping were observed at 14 of these wells, including the observation well farthest from WIPP-13. Five of these wells had also shown responses to the H-3 multipad test. Fluid-pressure responses were also observed in the exhaust shaft at the WIPP site during the WIPP-13 multipad test. The interpretation of the fluid-pressure and water-level responses resulting from the WIPP-13 multipad test is the subject of this report.

2. Site Hydrogeology

The WIPP site is located in the northern part of the Delaware Basin in southeastern New Mexico. WIPP-site geologic investigations have concentrated on the upper seven formations typically found in that part of the Delaware Basin. These are, in ascending order, the Bell Canyon Formation, the Castile Formation, the Salado Formation, the Rustler Formation, the Dewey Lake Red Beds, the Dockum Group, and the Gatuna Formation (Figure 2-1). All of these formations are of Permian age, except for the Dockum Group, which is of Triassic age, and the Gatuna, which is a Quaternary deposit. Of these formations, only the Bell Canyon and the Rustler contain regionally continuous, saturated intervals with sufficient permeability to allow well testing by standard hydrogeological techniques.

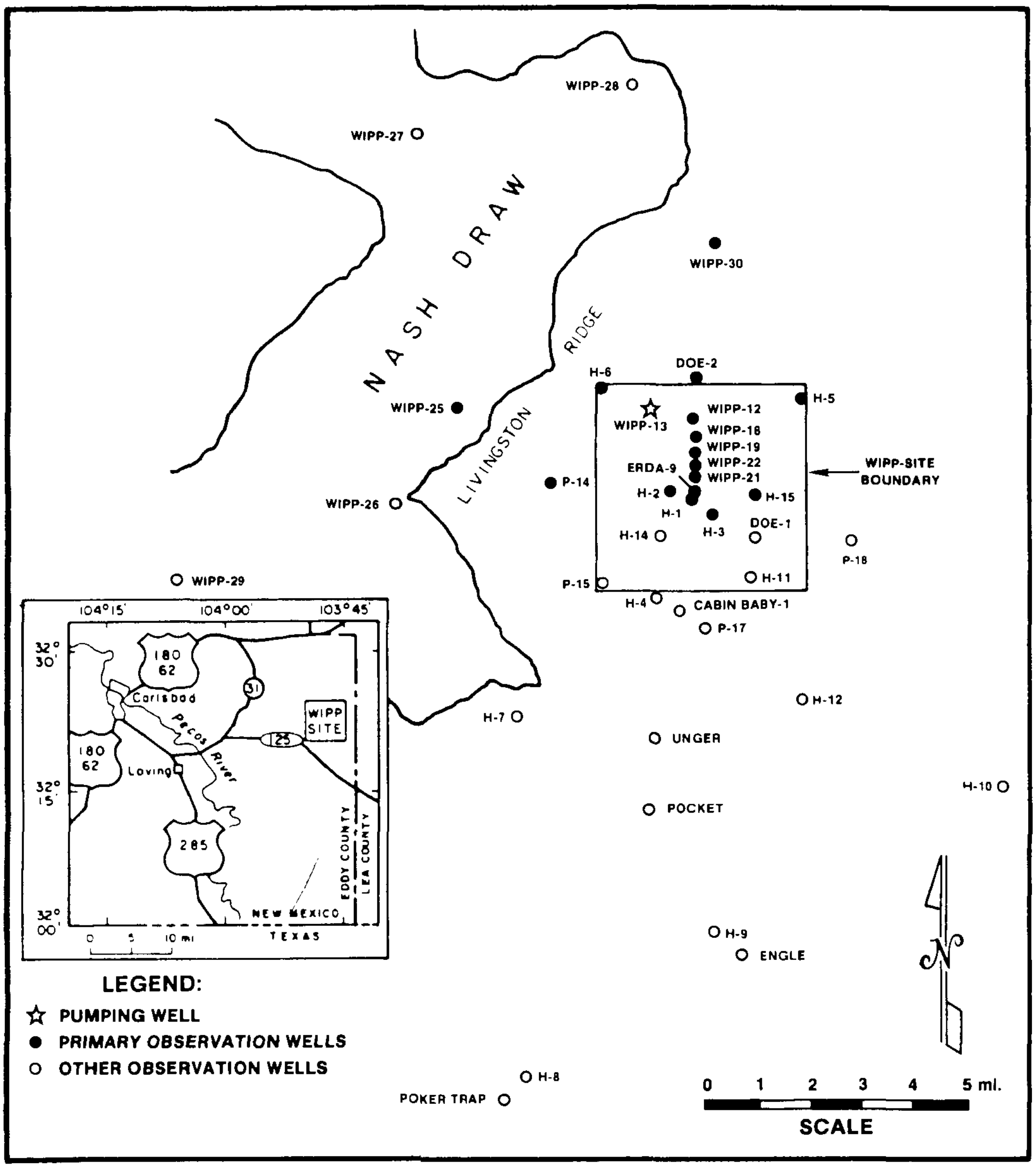

Figure 1-1. Locations of the WIPP Site and Observation Wells

The Rustler Formation lies from 517 to 846 ft below ground surface at the WIPP-13 pad (Sandia and USGS, 1979a). At this location, the Rustler consists of five members (in ascending order): the unnamed lower member, the Culebra Dolomite Member, the Tamarisk Member, the Magenta Dolomite Member, and the Forty-niner Member. The Culebra dolomite, which lies from 703 to 726 ft deep, is the principal water-bearing member of the Rustler. At WIPP-13, the Culebra is a fractured, light olive-gray, finely crystalline, vuggy, silty dolomite. The Culebra is considered to be the most important potential groundwater-transport pathway for radionuclides that may escape from the WIPP facility to reach the accessible environment. The vast majority of hydrologic tests performed at the WIPP site have examined the hydraulic properties of the Culebra.

The Culebra is confined by the underlying unnamed member, which is composed of a layered sequence of mudstone, siltstone, anhydrite, and halite, and by the overlying Tamarisk Member, which is composed of anhydrite and gypsum with a single mudstone/claystone interbed. The Culebra water level in December 1986 at WIPP-13 was ~351 ft below ground surface (Stensrud et al., 1987) or ~352 ft above the top of the Culebra.

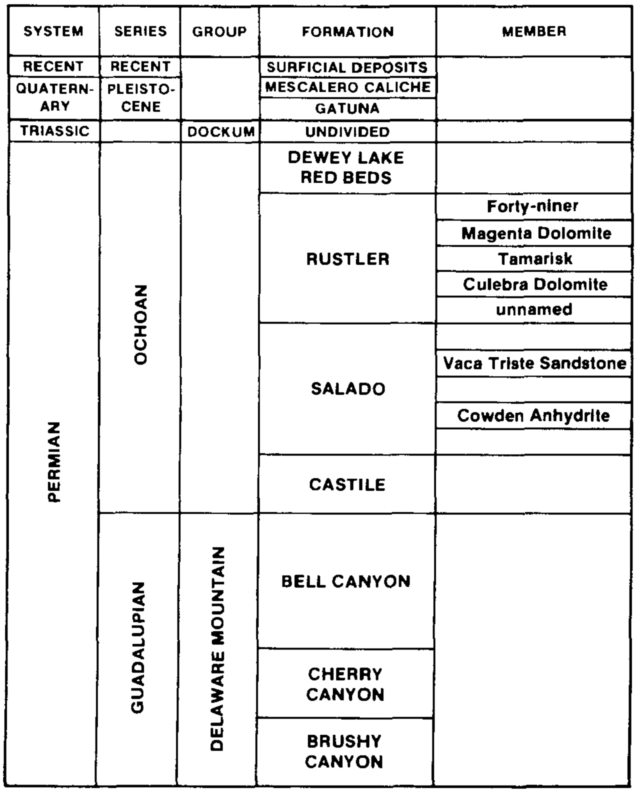

Figure 2-1. WIPP-Area Stratigraphic Column

The Culebra fluid at WIPP-13 has a total dissolved solids concentration of ~63 000 mg/L, primarily due to sodium and chloride (Randall et al., in preparation), and a specific gravity of ~1.046 at 25°C (Stensrud et al., 1987).

3. Observation Wells

The fluid pressure in WIPP-13 was monitored throughout the pumping test by a computerized data-acquisition system (DAS), described in Section 4. In addition, water levels were measured regularly in 17 key Culebra wells during the WIPP-13 multipad test. These include WIPP-12, WIPP-18, WIPP-19, WIPP-21, WIPP-22, WIPP-25, WIPP-30, H-1, H-2b2, H-3b2, H-5b, H-6a, H-6b, H-15, DOE-2, P-14, and ERDA-9 (Figure 1-1). Of these, all but H-3b2, H-5b, and H-15 showed distinct responses to the test. Pressure transducers installed in the Culebra dolomite in the exhaust shaft at the WIPP site were also monitored during the test and showed a response to the pumping. The transducers in the construction and salt-handling (C&SH) and waste-handling shafts were not operational during this time. The rest of the wells in the vicinity of the WIPP site were monitored biweekly to monthly during the WIPP-13 test as part of the ongoing regional water-level monitoring (Stensrud et al., 1987). Except for other wells on the H-2 hydropad, none of the other Culebra wells responded to the WIPP-13 pumping. Distances and directions from WIPP-13 to the key observation wells are listed in Table 3-1.

Table 3-1. Positions of Observation Wells Relative to Pumping Well WIPP-13

Observation Well	Distance From WIPP-13 (ft)	Direction From WIPP-13
WIPP-12	4 210	S 55° E
WIPP-18	4 990	S 45° E
WIPP-19	5 980	S 37° E
WIPP-21	7 270	S 29° E
WIPP-22	6 340	S 34° E
WIPP-25	20 550	S 88° W
WIPP-30	18 330	N 12° E
H-1	8 780	S 16° E
H-2b2	8 520	S 0° W
H-3b2	11 490	S 17° E
H-5b	13 980	N 83° E
H-6a	7 190	N 20° W
H-6b	7 180	N 20° W
H-15	11 740	S 48° E
DOE-2	4 840	N 45° E
P-14	13 870	S 58° W
ERDA-9	8 260	S 24° E
Exhaust Shaft	7 920	S 26° E

The key observation wells are completed in a variety of fashions. WIPP-13 (Figure 3-1), WIPP-12 (Figure 3-2), DOE-2 (Figure 3-3), and ERDA-9 (Figure 3-4) are completed with casing cemented from the surface to the upper Salado, perforations across the Culebra intervals, and bridge plugs lower in the casing isolating open intervals of the wells. WIPP-13, WIPP-12, and DOE-2 were all acidized following perforation in an effort to improve the hydraulic connections between the wellbores and the formation (Saulnier et al., 1987). Because of drilling-fluid residue on the water surface in ERDA-9, 2.375-in. tubing was installed from the ground surface to a depth of ~523 ft (~68 ft below the water surface) to provide a cleaner access for the water-level probe during the test (Figure 3-4).

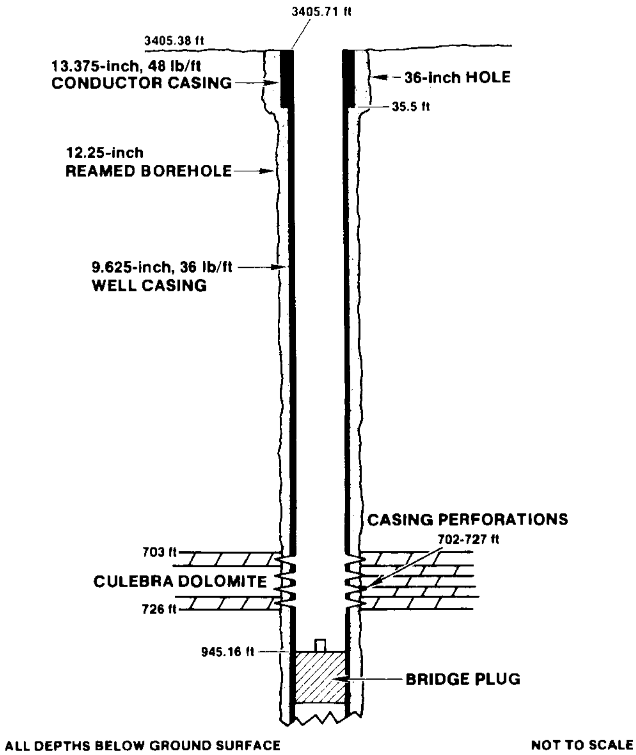

Figure 3-1. Well Configuration for WIPP-13

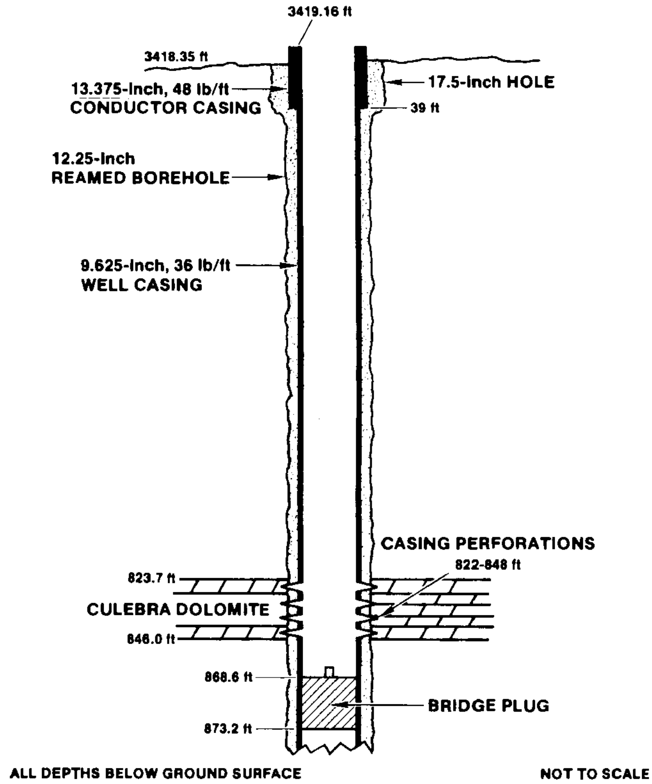

Figure 3-3. Well Configuration for DOE-2

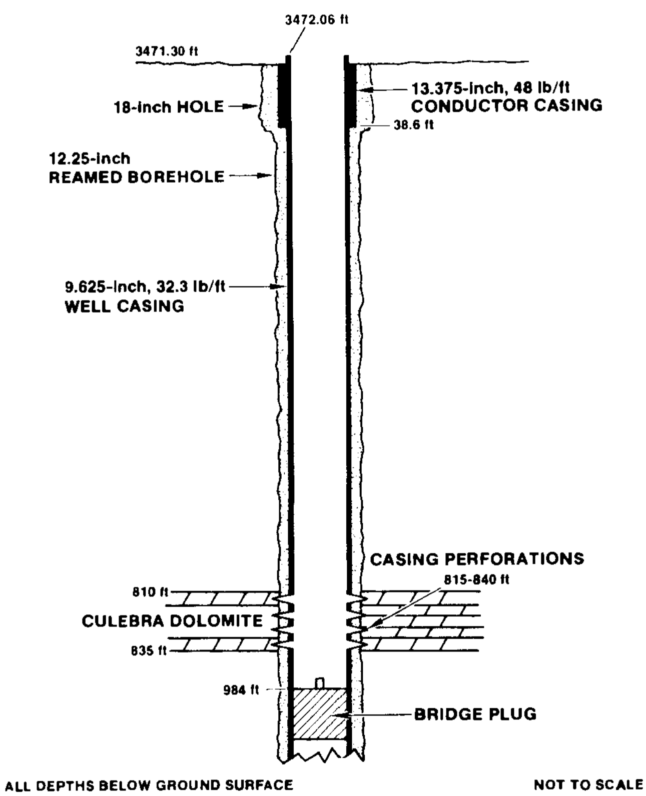

Figure 3-2. Well Configuration for WIPP-12

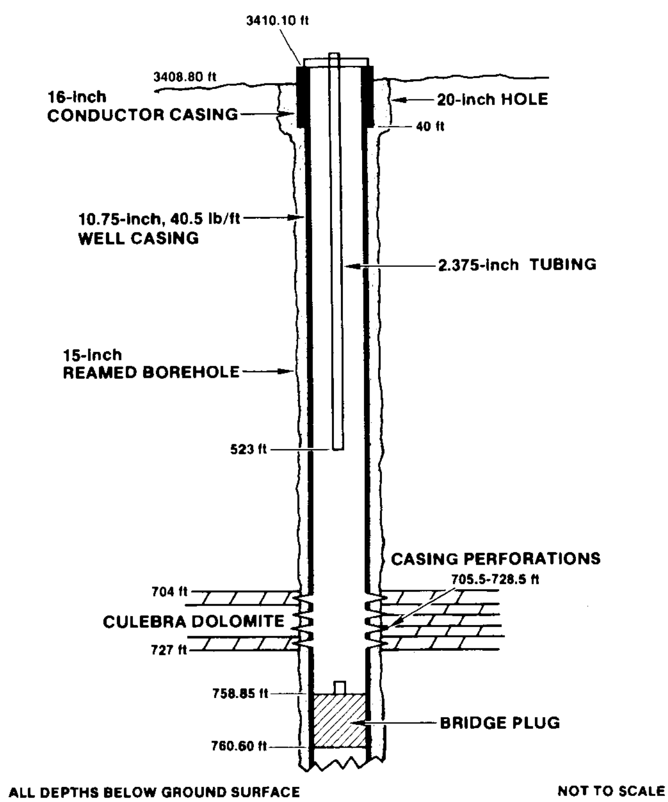

Figure 3-4. Well Configuration for ERDA-9

WIPP-18 (Figure 3-5), WIPP-19 (Figure 3-6), WIPP-21 (Figure 3-7), and WIPP-22 (Figure 3-8) are cased to their total depths or to cement plugs and perforated across the Culebra intervals. WIPP-25 (Figure 3-9), WIPP-30 (Figure 3-10), and H-1 (Figure 3-11) are cased to their total depths; perforated across the Rustler-Salado contact zone, the Culebra, and the Magenta; have bridge plugs below the Culebra; and have production-injection packers (PIPs) set on 2.375-in. tubing between the Culebra and Magenta. H-2b2 (Figure 3-12), H-3b2 (Figure 3-13), H-5b (Figure 3-14), H-6b (Figure 3-15), and H-15 (Figure 3-16) are cased from the surface to the lower Tamarisk and are open through the Culebra to their total depths in the upper part of the unnamed lower member. For the test, a PIP on 1.5-in. galvanized pipe was temporarily placed in H-6b above the Culebra to reduce wellbore-storage effects. H-6a is cased from the surface to the Forty-niner and is an open hole below to the unnamed lower member, with a PIP set on 1.5-in. galvanized pipe between the Magenta and Culebra (Figure 3-17). P-14 is cased from the surface to a cement plug in the upper Salado, is perforated across the Rustler-Salado contact zone and the Culebra, and has a bridge plug set below the Culebra (Figure 3-18). Thus, water levels were measured in the open casing in WIPP-12, WIPP-18, WIPP-19, WIPP-21, WIPP-22, H-2b2, H-3b2, H-5b, H-15, DOE-2, and P-14, through tubing or pipe attached to PIPs in WIPP-25, WIPP-30, H-1, H-6a, and H-6b, and through an inner tubing string hung in the open casing in ERDA-9.

The WIPP Management and Operating Contractor (MOC) collects pressure data on a regular basis from three piezometers (transducers) installed within the liner in the exhaust shaft opposite the Culebra. These piezometers are designated #210, #211, and #212 by the MOC. Details on the piezometer installations are presented in Bechtel National (1986) and Haug et al. (1987). These piezometers were monitored 5 to 7 times a week during the WIPP-13 multipad test to provide relatively continuous data over that period. These piezometers do not provide a continuous range of pressure values, however, but instead show pressure changes in discrete steps of 0.5 to 0.7 psi, depending on the individual instrument calibration.

Water levels in two wells completed in the Magenta dolomite were monitored on a regular basis during the test: H-1 (Figure 3-11) and H-6c (Figure 3-19). Neither showed any response to the WIPP-13 pumping.

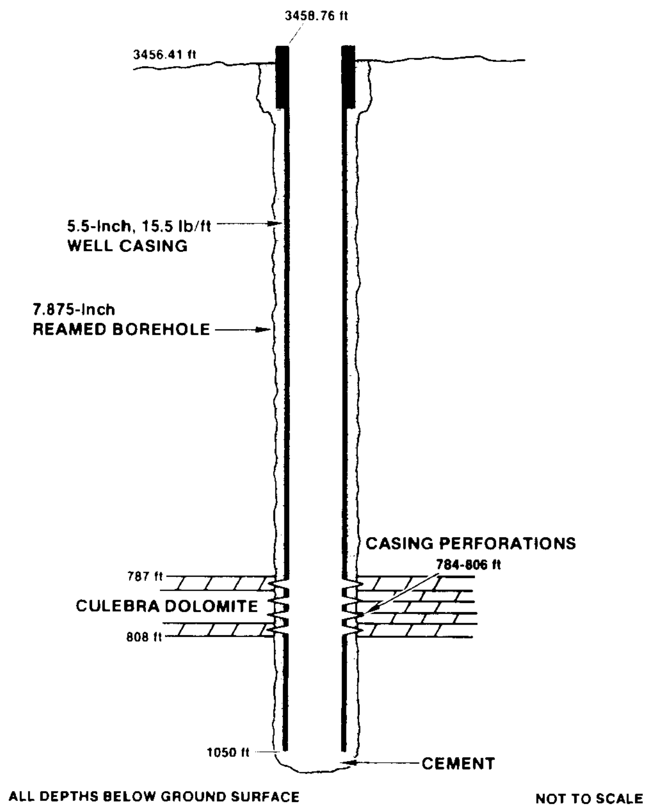

Figure 3-5. Well Configuration for WIPP-18

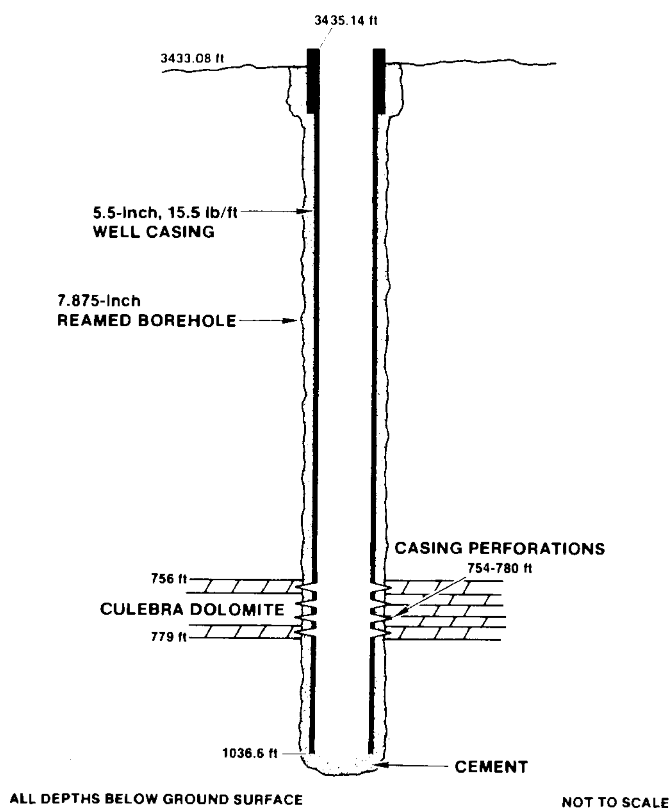

Figure 3-6. Well Configuration for WIPP-19

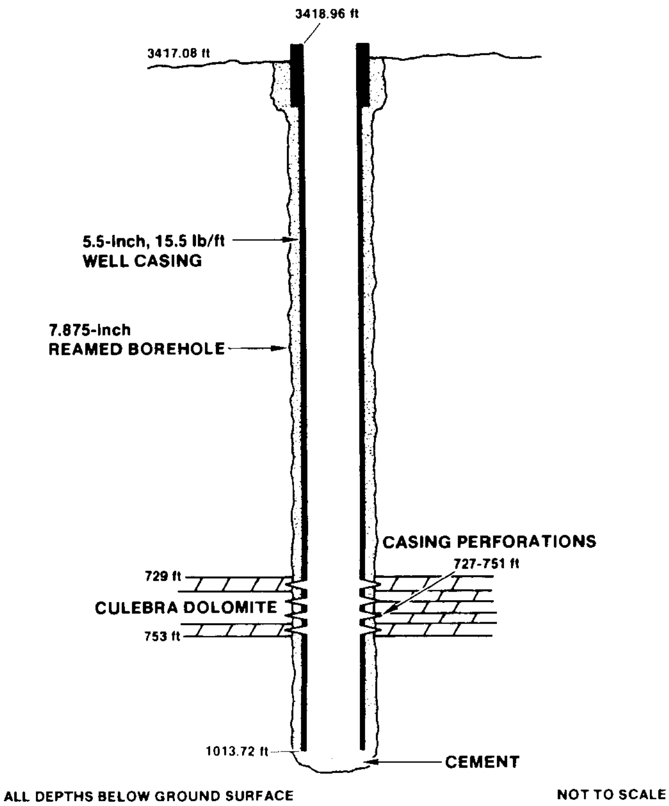

Figure 3-7. Well Configuration for WIPP-21

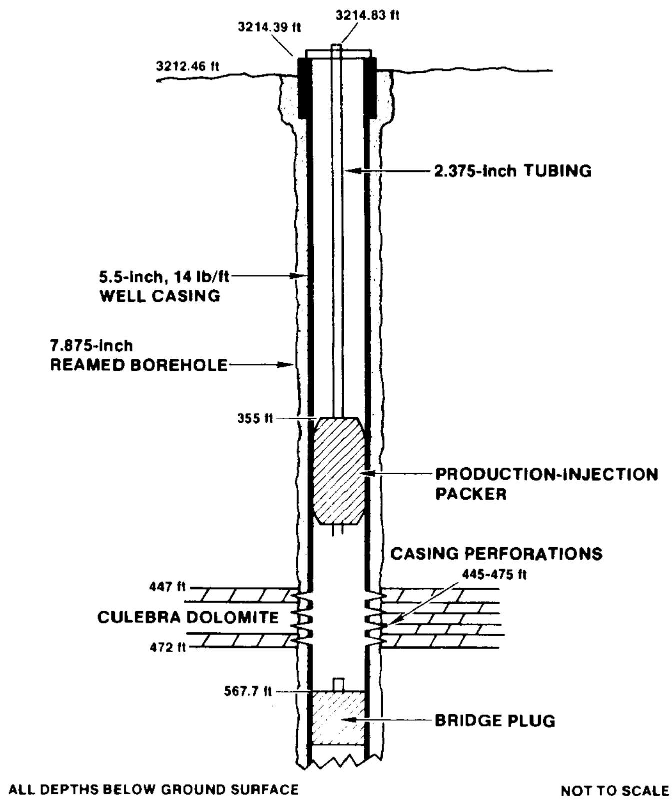

Figure 3-9. Well Configuration for WIPP-25

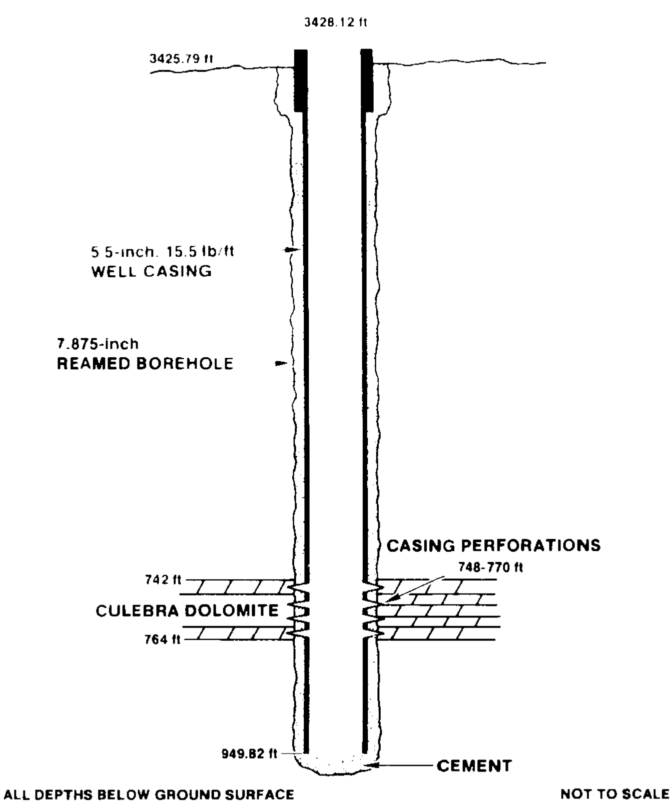

Figure 3-8. Well Configuration for WIPP-22

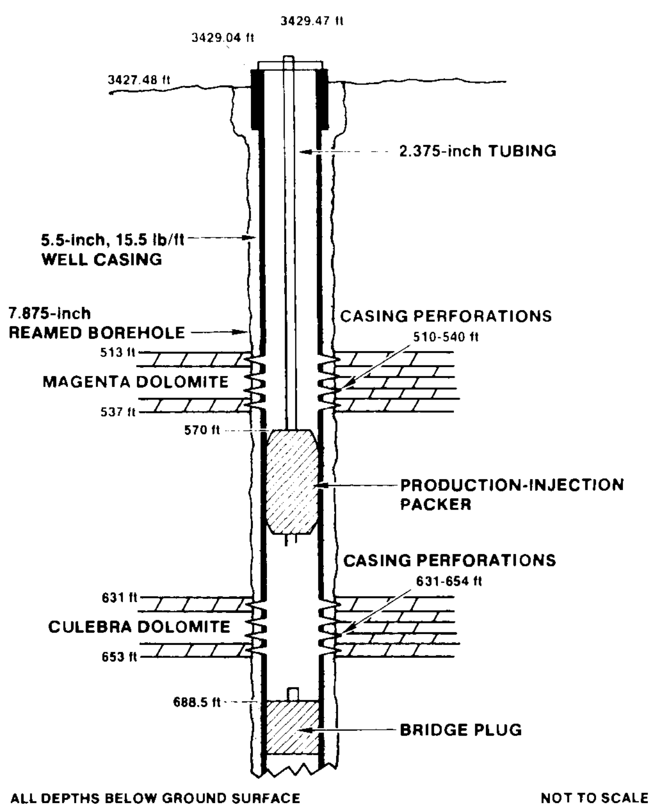

Figure 3-10. Well Configuration for WIPP-30

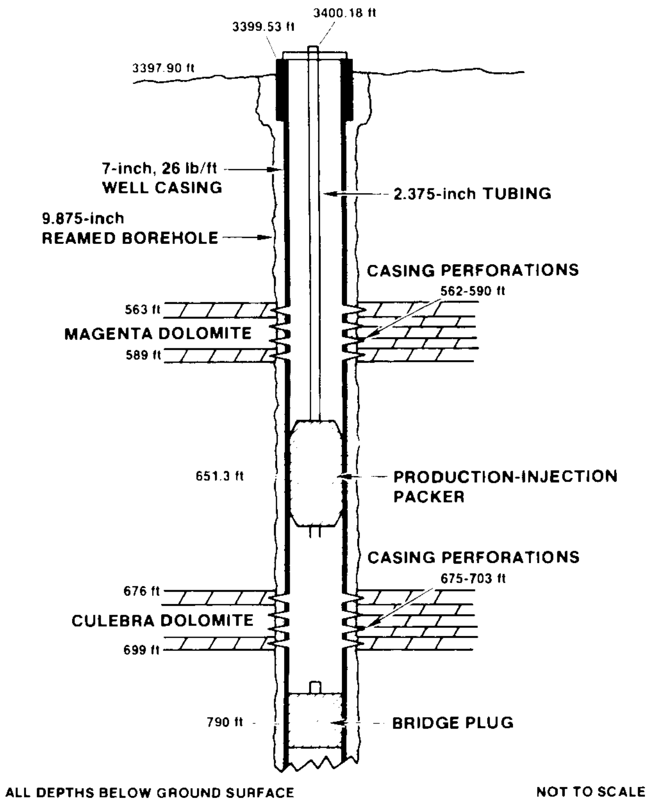

Figure 3-11. Well Configuration for H-1

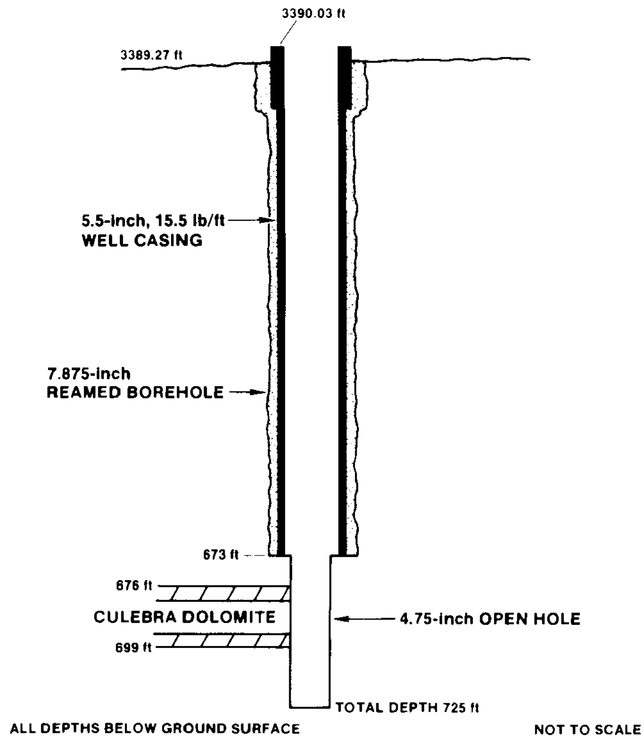

Figure 3-13. Well Configuration for H-3b2

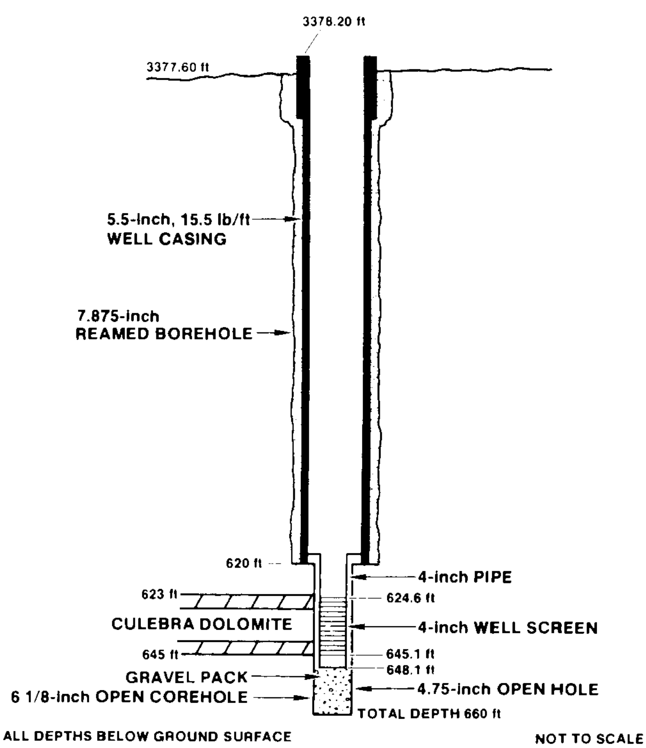

Figure 3-12. Well Configuration for H-2b2

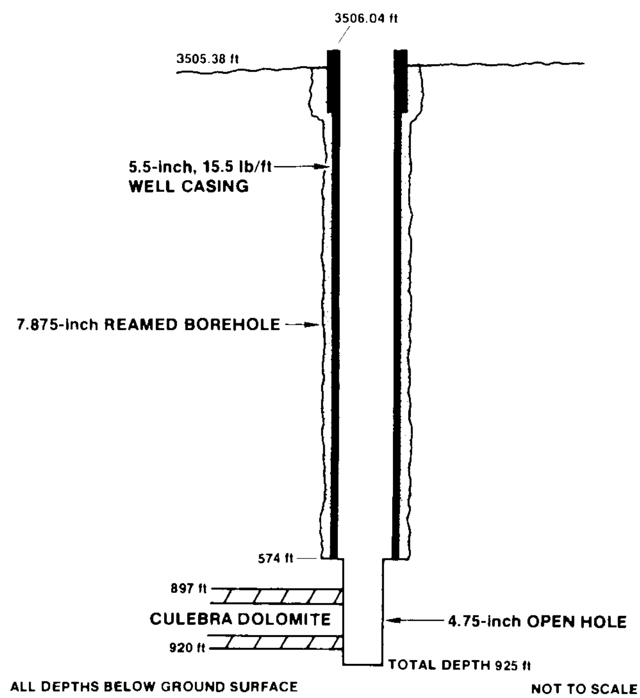

Figure 3-14. Well Configuration for H-5b

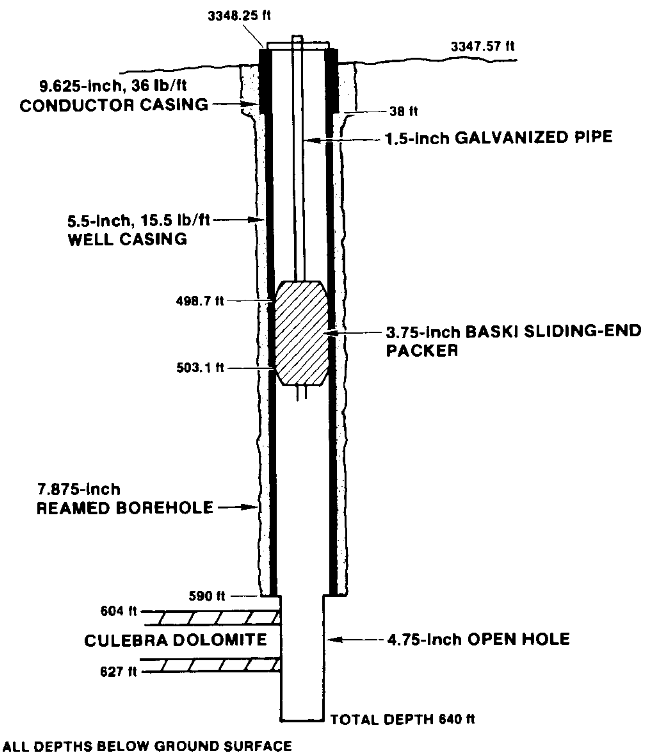

Figure 3-15. Well Configuration for H-6b

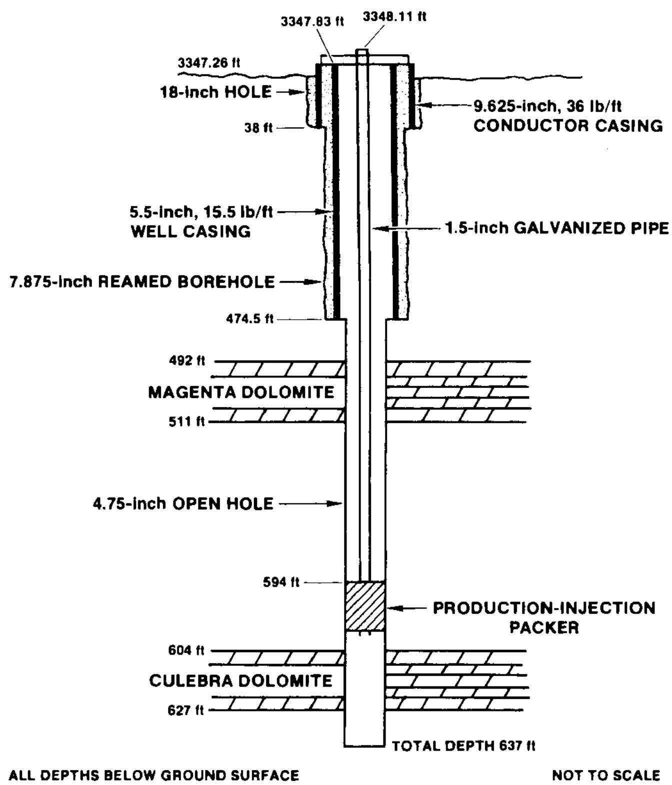

Figure 3-17. Well Configuration for H-6a

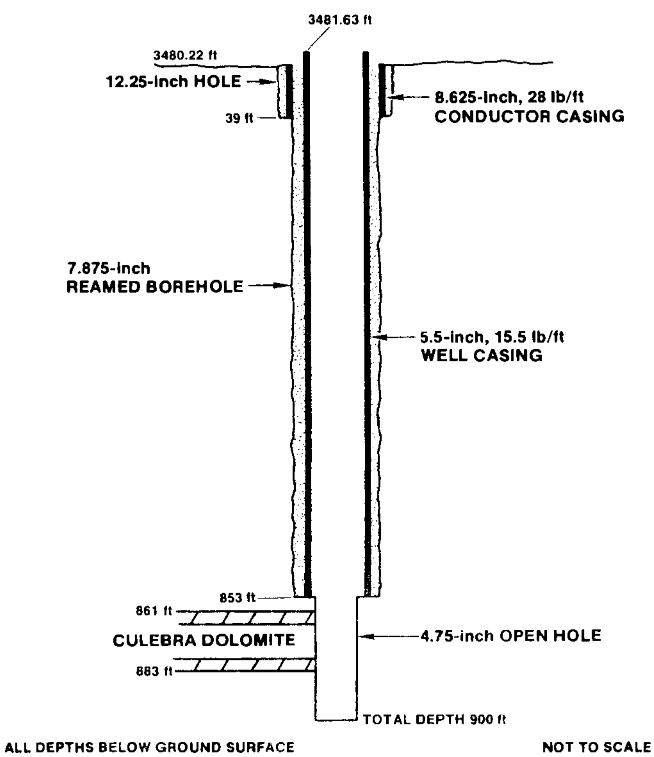

Figure 3-16. Well Configuration for H-15

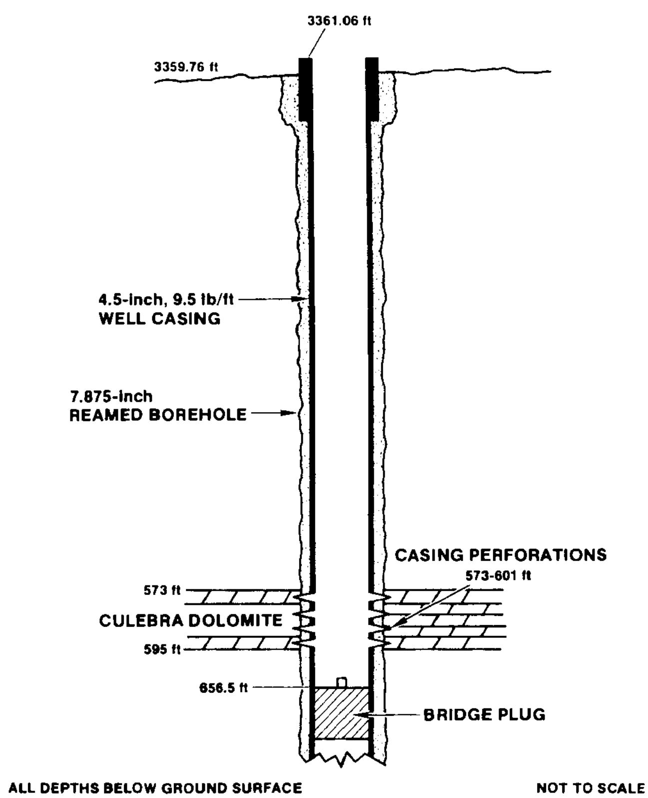

Figure 3-18. Well Configuration for P-14

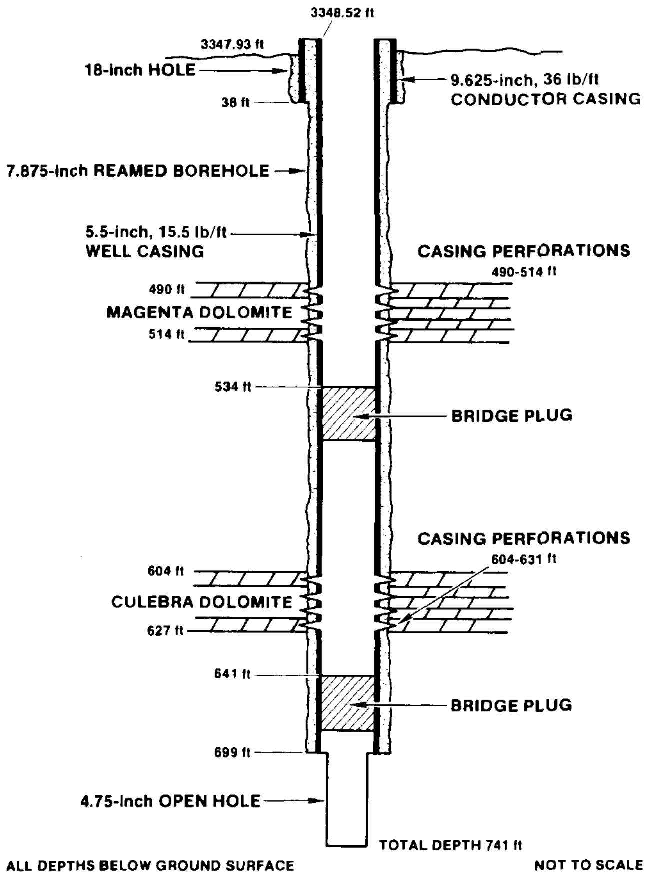

Figure 3-19. Well Configuration for H-6c

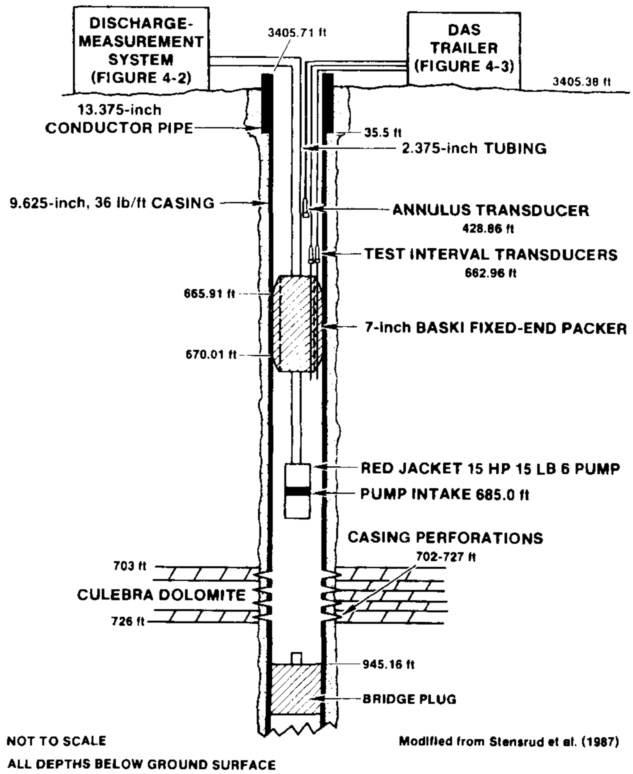

Figure 4-1. Configuration of WIPP-13 for the WIPP-13 Multipad Pumping Test

4. Test Instrumentation

The instrumentation used for the WIPP-13 multipad test is described in detail in Stensrud et al. (1987). A brief discussion is also presented below.

NOTE: The use of brand names in this report is for identification only and does not imply endorsement of specific products by Sandia National Laboratories.

4.1 WIPP-13

The downhole equipment at WIPP-13 consisted of a 15-hp Red Jacket 15LB6 pump suspended below a Baski air-inflatable packer on 2.375-in. tubing, with three Druck PDCR-10/D strain-gage pressure transducers strapped to the tubing above the packer (Figure 4-1). Two of the transducers were connected to the test interval below the packer by feed-through lines through the packer. One of these was the primary transducer used to monitor the test-interval pressure during the test, while the second served as a backup transducer. The third transducer measured the fluid pressure in the well annulus above the packer.

The uphole equipment consisted of a backpressure ball valve, a Flow Technology FT-12 analog flow meter wired to the DAS, a Precision totalizing flow meter, a Dole orifice valve, and a calibrated standpipe to provide a backup means of estimating the pumping rate (Figure 4-2). A Weathertronics Model 7105-A analog-output barometer was also connected to the DAS and provided barometric-pressure data at the WIPP-13 pad for the duration of the test.

The DAS at the surface at WIPP-13 consisted of Tektronix PS503A dual power supplies to provide power to the transducers, a Hewlett Packard (HP) 3495A signal scanner for channel switching, an HP-3456A digital voltmeter (DVM) to measure the transducer output, an HP-9845B desktop computer for system control, and HP-9885M and S floppy disk drives for data storage (Figure 4-3). The HP-3456A DVM is calibrated by the Sandia Standards Laboratory every six months, and the transducers were calibrated in the field by using a Heise pressure gage before installation in the wells. The data-acquisition software was written and is maintained by Sandia National Laboratories. Additional information on this data-acquisition system can be found in INTERA Technologies and HydroGeoChem (1985).

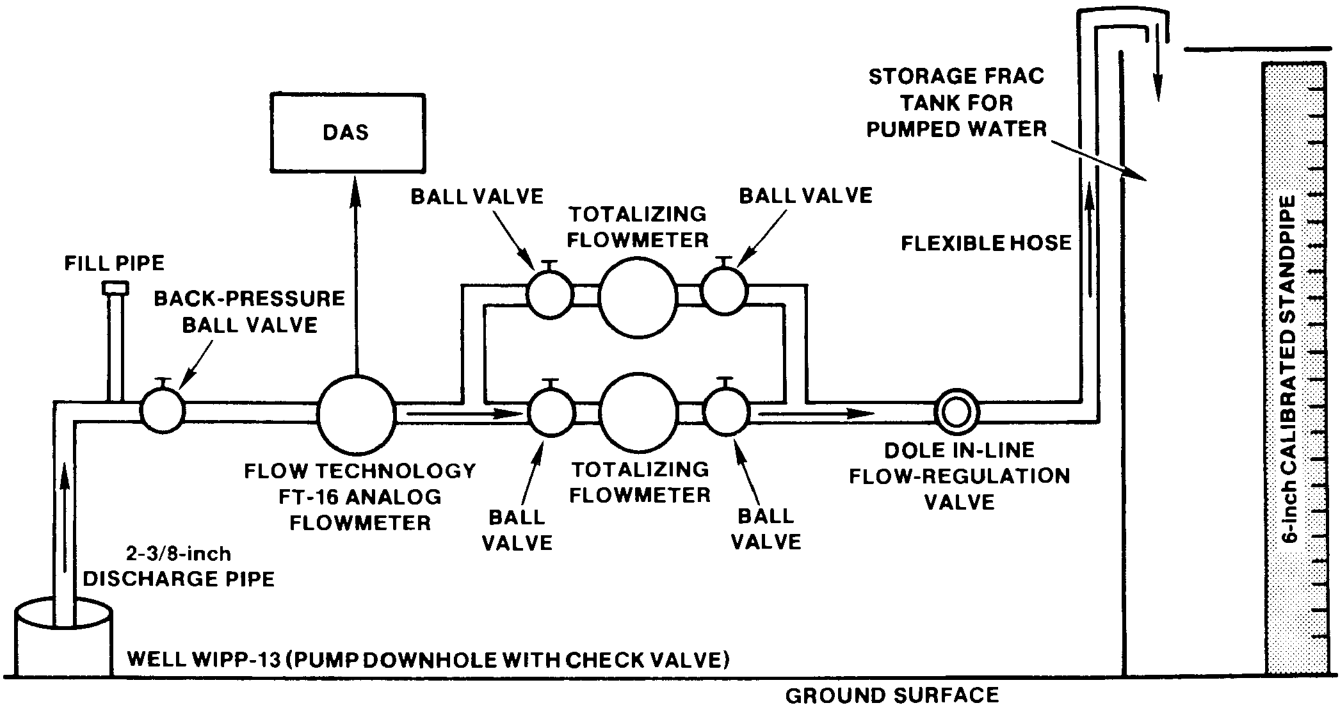

Figure 4-2. WIPP-13 Discharge-Measurement and Flow-Regulation System

4.2 Observation Wells

Water levels in observation wells were measured by using a variety of instruments during the test. Dedicated Solinst water-level meters were mounted in boxes on the WIPP-12, WIPP-18, WIPP-21, WIPP-30, H-1, H-2b2, DOE-2, P-14, and ERDA-9 wellheads for the duration of the test (INTERA Technologies and HydroGeoChem, 1985). The probes were kept in the wells a few feet above the water surfaces between readings. Another Solinst meter was used to measure water levels in H-6a and H-6b. The Iron Horse was used to make water-level measurements in wells WIPP-19, WIPP-22, WIPP-25, H-3b2, H-5b, and H-15 and also to make the less-frequent, regional water-level measurements in more-distant wells (INTERA Technologies and HydroGeoChem, 1985). In this manner, a single instrument was used consistently at each well throughout the test.

5. Test Data

Extensive fluid-pressure and/or water-level data were collected from the pumping well and key observation wells before the WIPP-13 multipad pumping test began, during the 864-hr pumping period, and for up to 2100 hr of recovery. In many instances, the observed data were affected not only by the pumping test, but also by residual hydraulic stresses from earlier hydraulic tests at other locations, well completions, shaft drainage, and/or other factors. Barometric-pressure changes also caused discernible water-level fluctuations in some wells. Consequently, some of the data required modifications to remove the effects of water-level trends existing at the beginning of the test and to compensate for barometric effects. Additionally, because the analysis techniques used to interpret the data require the use of pressures rather than water levels, water-level data were converted to pressure data. The observed data, extraneous trends in the data, and modifications made to the data to aid analysis are discussed below. Tabulations of the observed and modified data are presented in Appendix A.

5.1 WIPP-13

At the pumping well, WIPP-13, the DAS collected more data than were necessary for analysis. Hence, an abridged data set was created by selecting points to give an adequate distribution of data through time for analysis. No other criteria were involved in the data abridgment. The abridged WIPP-13 data set used in the analyses presented in this report is tabulated in Appendix A, Table A-1, and shown graphically in Figure 5-1. A more extensive tabulation of the data collected is contained in Stensrud et al. (1987).

One modification of the data from the pumping well was required for analysis. When a pump is turned on, particularly in a packer-isolated interval, an initial instantaneous pressure drop may occur. This pressure drop is probably related to turbulence in the wellbore caused by the pump and/or to the discontinuity at the rock/well interface rather than to the aquifer response. This pressure drop may be maintained for the duration of pumping, and an instantaneous recovery may be observed when the pump is turned off. Analyses using pressure-change data must compensate for these pressure surges.

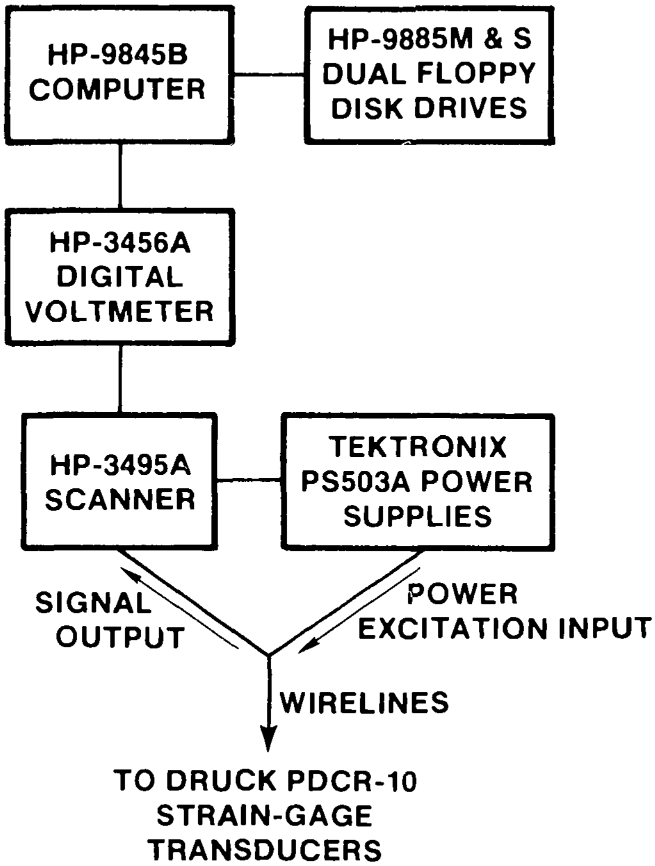

Figure 4-3. WIPP-13 Data-Acquisition System

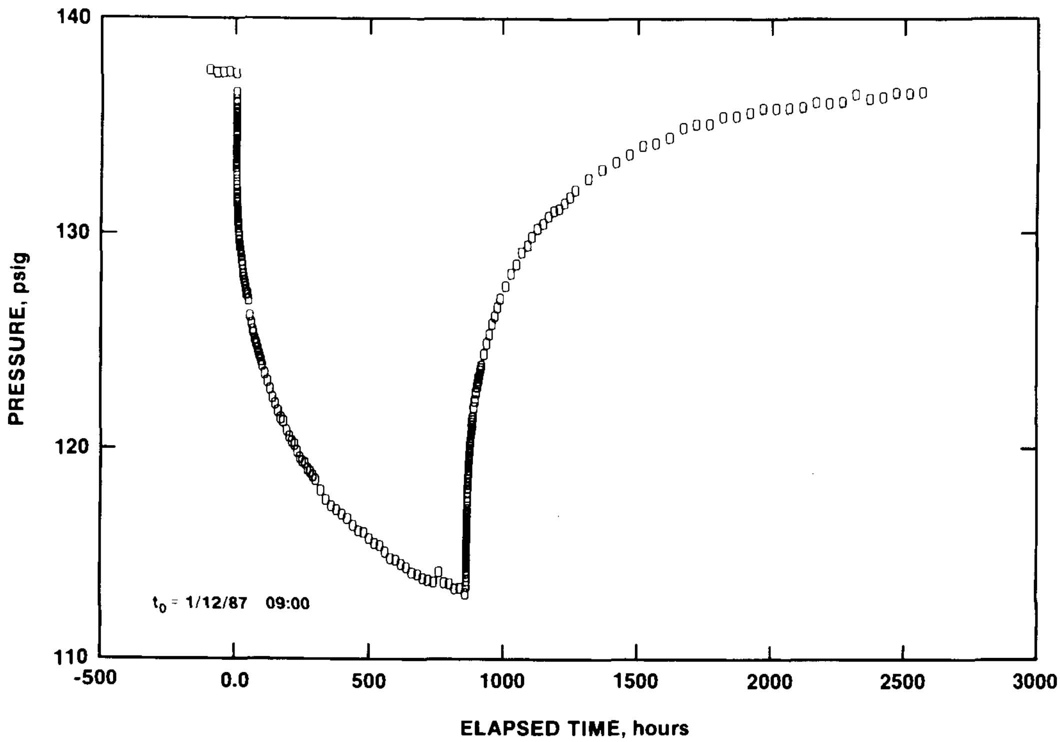

Figure 5-1. WIPP-13 Fluid-Pressure Record

At the beginning of pumping at WIPP-13, the observed pressure drop of 0.9 psi was subtracted from the prepumping pressure to provide the starting point used to calculate test-related drawdowns. Late in the pumping period, the packer that had been isolating the test interval deflated. Thus, when the pump was turned off, the test-interval pressure surged momentarily and then dropped back toward its final pumping value. This surge was ignored, and the average pressure during the last minute of pumping was used as the starting point for calculating recovery. No other modifications were made to the WIPP-13 data.

5.2 WIPP-12

The water-level record for well WIPP-12 leading up to and during the WIPP-13 multipad test is shown in Figure 5-2. The data from the 1000-hr period preceding the test show that the water level was rising at a rate of ~0.148 ft/10 days until ~52 hr after pumping began at WIPP-13. This rise was probably, in part, a recovery response from well development and water-quality sampling at nearby wells such as WIPP-13, WIPP-18, and DOE-2 in August 1986 (Saulnier et al., 1987) and may also be related to the long-term recovery from shaft drainage discussed by Haug et al. (1987), among others. For analysis purposes, the water-level data were modified by subtracting the effects of the pretest trend, assuming that the trend continued linearly throughout the period of interest. The rationale for using a linear compensation of this type is discussed in Section 5.20.

The modified water-level data were converted to pressures by subtracting the depths to water from an arbitrary datum of 500 ft below the water-level reference point and multiplying the remainders by 0.433 psi/ft, the conversion factor for freshwater with a specific gravity (SG) of 1.0. A freshwater conversion was used because the actual specific gravity of the Culebra water at WIPP-12 is unknown. The conversion factor used has no effect on the analysis because a final conversion of the analysis results from oilfield to groundwater units (Appendix B) exactly cancels whatever value is used. The observed water-level data, modified water-level data, and calculated pressure data are tabulated in Appendix A, Table A-2. A plot of the pressure data is included with the final analytical simulation in Section 6.2.

5.3 WIPP-18

Figure 5-3 shows the WIPP-18 water-level record from 1000 hr before the WIPP-13 test through ~2100 hr of recovery. The data up to ~62 hr after the start of pumping at WIPP-13 show a rising trend of ~0.119 ft/10 days. This rise was, in part, a recovery response from well-development bailing performed in WIPP-18 on August 27, 1986 (Saulnier et al., 1987), and may also be related to the long-term recovery from shaft drainage discussed by Haug et al. (1987), among others. For analysis purposes, the water-level data were modified by subtracting the effects of the pretest trend, assuming that the trend continued linearly throughout the drawdown and recovery periods of the WIPP-13 test.

The modified water-level data were converted to pressures by subtracting the depths to water from an arbitrary datum of 500 ft and multiplying the remainders by 0.479 psi/ft (SG = 1.105). This conversion factor was determined from the results of a pressure-density survey of the fluid in the well (between the depths of 500 and 810 ft) on May 12, 1987 (Crawley, 1987). The observed water-level data, modified water-level data, and calculated pressure data are tabulated in Appendix A, Table A-3. A plot of the pressure data is included with the final analytical simulation in Section 6.2.

5.4 WIPP-19

The WIPP-19 water-level record leading up to and during the WIPP-13 multipad test is shown in Figure 5-4. Water levels were rising at an approximate rate of 0.249 ft/10 days during the 1000-hr period preceding the test and the first 53 hr of pumping. This rise was, in part, a recovery response from well-development bailing performed in WIPP-19 on August 22, 1986 (Saulnier et al., 1987), and may also be related to the long-term recovery from shaft drainage discussed by Haug et al. (1987), among others. The water-level data were modified by subtracting the effects of the pretest rising trend, assuming that the trend continued linearly throughout the multipad test.

For analysis, the modified WIPP-19 water levels were converted to equivalent pressures. The conversion was performed by subtracting the modified depths to water from an arbitrary datum of 500 ft and multiplying the remainders by 0.491 psi/ft (SG = 1.133), the conversion factor determined by a pressure-density survey of the fluid in the WIPP-19 wellbore (between the depths of 500 and 781 ft) on May 14, 1987 (Crawley, 1987). The observed water-level data, modified water-level data, and calculated pressure data are tabulated in Appendix A, Table A-4. A plot of the pressure data is included with the final analytical simulation in Section 6.2.

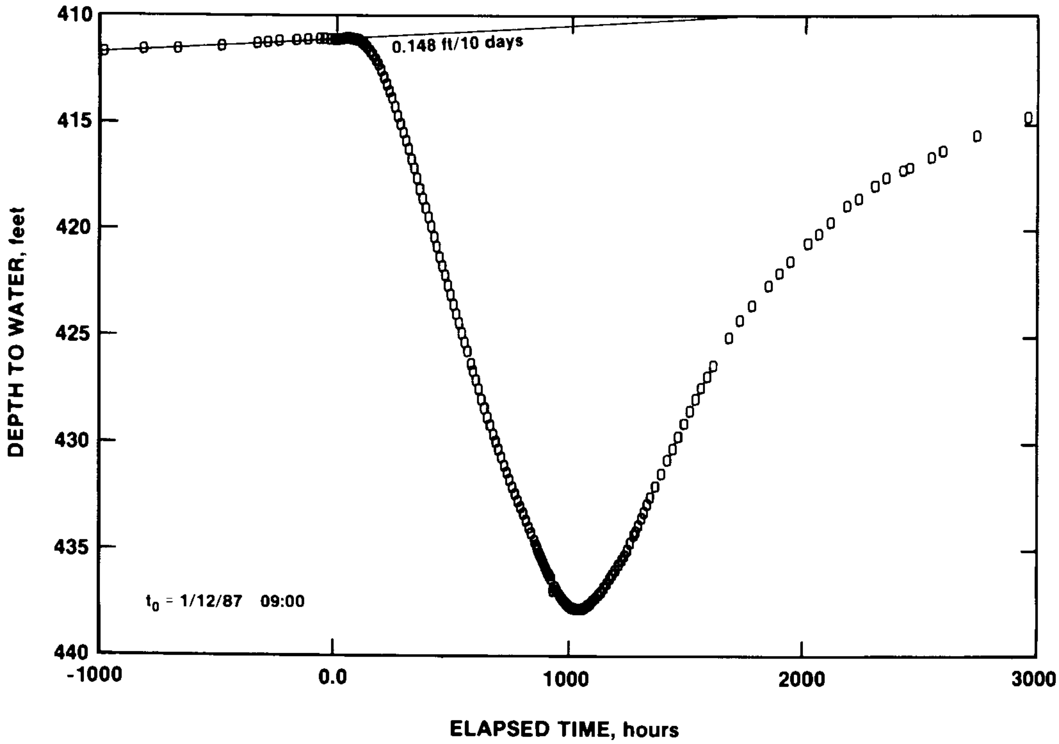

Figure 5-2. WIPP-12 Water-Level Record

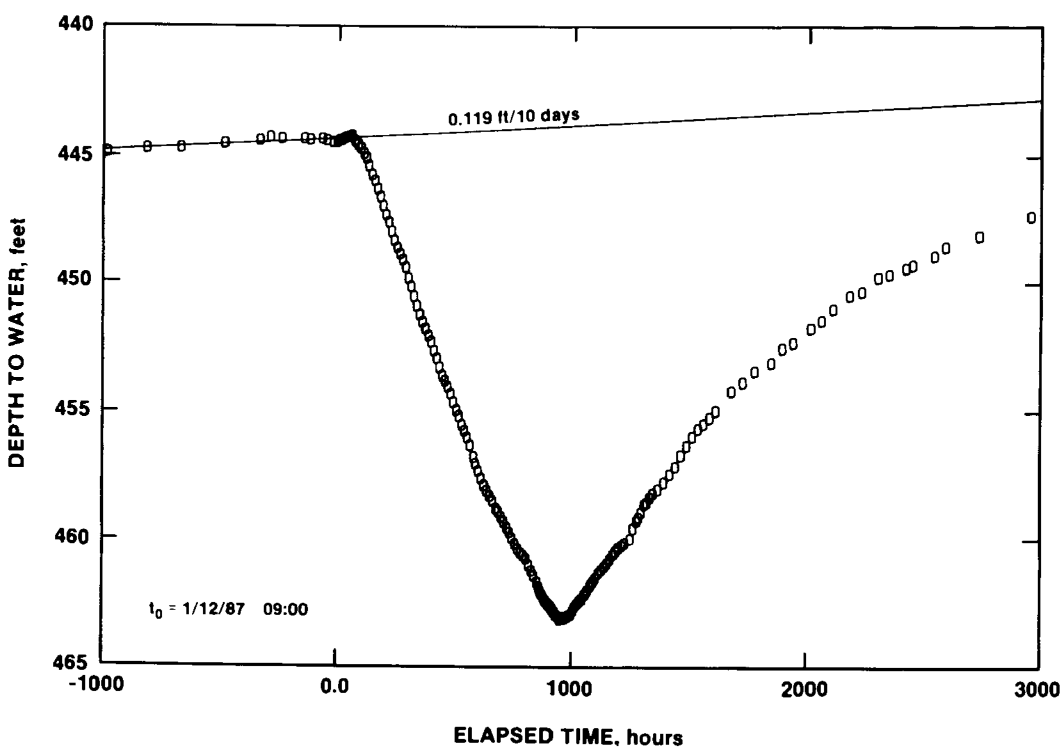

Figure 5-3. WIPP-18 Water-Level Record

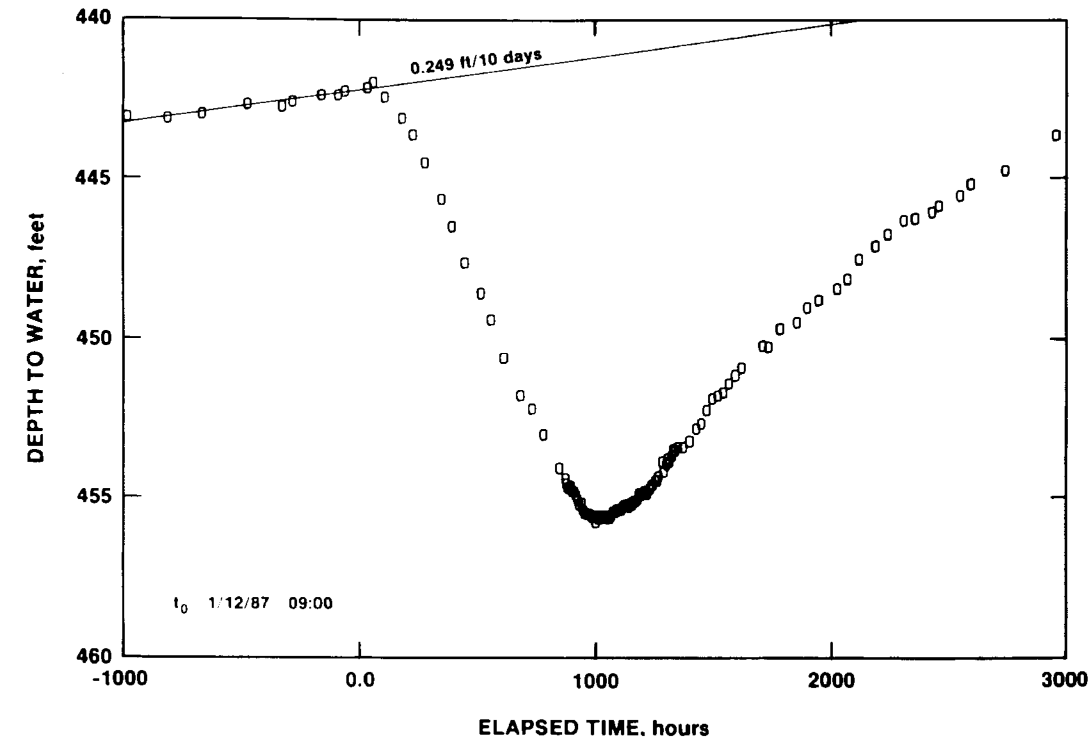

Figure 5-4. WIPP-19 Water-Level Record

5.5 WIPP-21

The water-level record for well WIPP-21 leading up to and during the WIPP-13 multipad test is shown in Figure 5-5. The Culebra water level was rising at an approximate rate of 0.553 ft/10 days from ~1000 hr before the WIPP-13 multipad test until ~122 hr after the pump was turned on. This rise was a combined recovery response to well-development bailing in WIPP-21 on August 27, 1986 (Saulnier et al., 1987), and well-development pumping at ERDA-9 between October 27 and November 14, 1986 (Stensrud et al., 1987), and may also be related to the long-term recovery from shaft drainage discussed by Haug et al. (1987), among others.

For analysis, the observed WIPP-21 water levels were first modified to eliminate the pretest trend, using a linear correction. The corrected values were then converted to equivalent pressures. The conversion was performed by subtracting the depths to water from an arbitrary datum of 500 ft and multiplying the remainders by 0.433 psi/ft, the conversion factor for freshwater. A freshwater conversion was used because the actual specific gravity of the water in the WIPP-21 wellbore is unknown. As discussed earlier, the conversion factor used has no effect on the analysis.

Some of the water-level changes observed at WIPP-21, such as the apparently abrupt transition at ~1240 hr from drawdown to recovery in Figure 5-5, appeared to be related to barometric-pressure fluctuations. Hence, the barometric efficiency of the well was evaluated to allow compensation for these effects. The evaluation was performed by using the barometric-pressure data recorded by the WIPP-13 DAS (Appendix C, Table C-1). The changes in barometric pressure during the test were defined by subtracting 13.1 psi (the barometric pressure at the beginning of the test) from all readings. The measured or interpolated barometric-pressure changes at the precise times of the water-level measurements were then multiplied by several decimal fractions, such as 0.3, 0.5, and 0.7, and added to the pressure data already calculated from the modified water-level data.

The added fractional barometric-pressure change that produced the smoothest pressure curve, 0.5, was judged to represent the best estimate of the barometric efficiency of the well, and that modified pressure data set was used in the analysis. The observed water-level data, modified water-level data, and final pressure data compensated for barometric-pressure effects are tabulated in Appendix A, Table A-5. A plot of the pressure data is included with the final analytical simulation in Section 6.2.

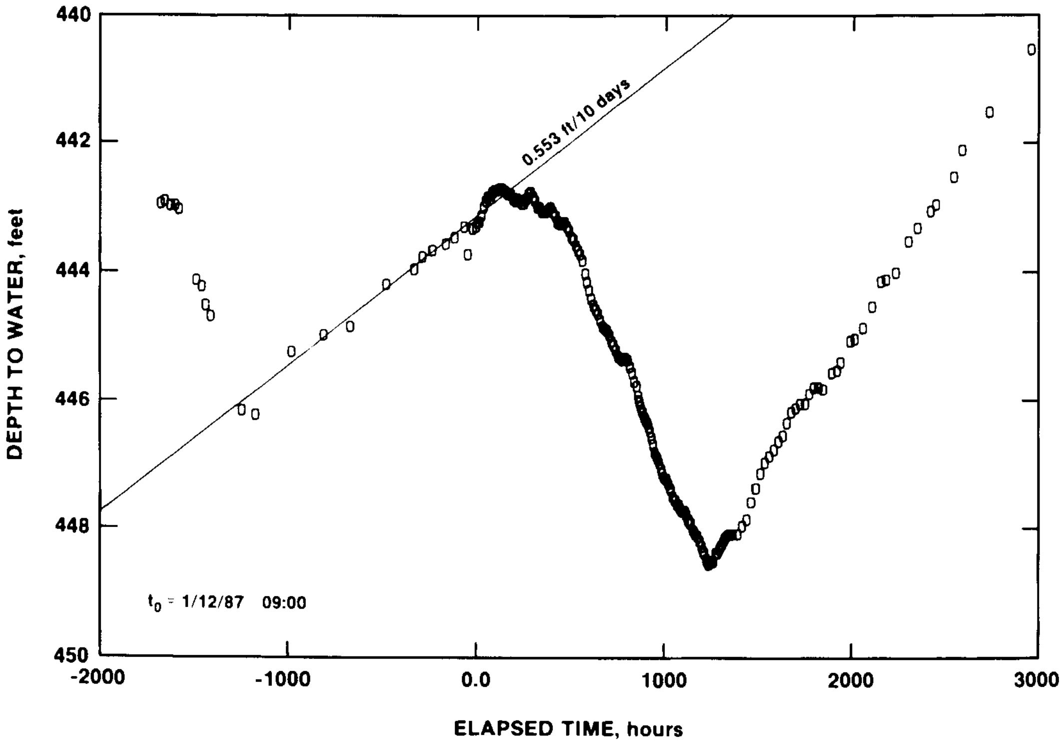

Figure 5-5. WIPP-21 Water-Level Record

5.6 WIPP-22

Figure 5-6 shows the WIPP-22 water-level record preceding and during the WIPP-13 multipad test. During the 1000 hr before the test and the first 53 hr of pumping, water levels in WIPP-22 were rising at a rate of ~0.269 ft/10 days. This rise may have been related to a variety of factors, including well-development bailing in WIPP-22 performed on August 26, 1986 (Saulnier et al., 1987), well-development pumping at ERDA-9 between October 27 and November 14, 1986 (Stensrud et al., 1987), and long-term recovery from shaft drainage (Haug et al., 1987).

For analysis, the observed WIPP-22 water levels were first modified to eliminate the pretest trend, using a linear correction. The corrected values were then converted to equivalent pressures. The conversion was performed by subtracting the depths to water from an arbitrary datum of 500 ft and multiplying the remainders by 0.495 psi/ft (SG = 1.142), the conversion factor derived for the final water produced during well-development pumping on June 17, 1986 (Saulnier et al., 1987). This value may not be entirely representative of the fluid in the wellbore during the WIPP-13 test, but it is the best value available and has no effect on the final analysis. The observed water-level data, modified water-level data, and calculated pressure data are tabulated in Appendix A, Table A-6. A plot of the pressure data is included with the final analytical simulation in Section 6.2.

5.7 WIPP-25

The pretest water-level data at WIPP-25 are relatively sparse, as shown in Figure 5-7. No particular trend is evident in the pretest data and, therefore, no corrections for pretest conditions were required. For analysis, the water-level data were converted to pressures by subtracting the depths to water from an arbitrary datum of 200 ft and multiplying the remainders by 0.4377 psi/ft, a conversion factor derived from the specific-gravity value of 1.01 reported for WIPP-25 Culebra water by Uhland and Randall (1986).

The scatter seen in the data in Figure 5-7 is suggestive of water-level changes caused by fluctuations in barometric pressure. Thus, an attempt was made to determine the barometric efficiency of WIPP-25 and correct the water-level data for barometric fluctuations, using the technique described earlier in Section 5.5. The smoothest data set was produced by using a barometric efficiency of 0.3. The observed water-level data and final pressure data compensated for barometric-pressure effects are tabulated in Appendix A, Table A-7. A plot of the pressure data is included with the final analytical simulation in Section 6.2.

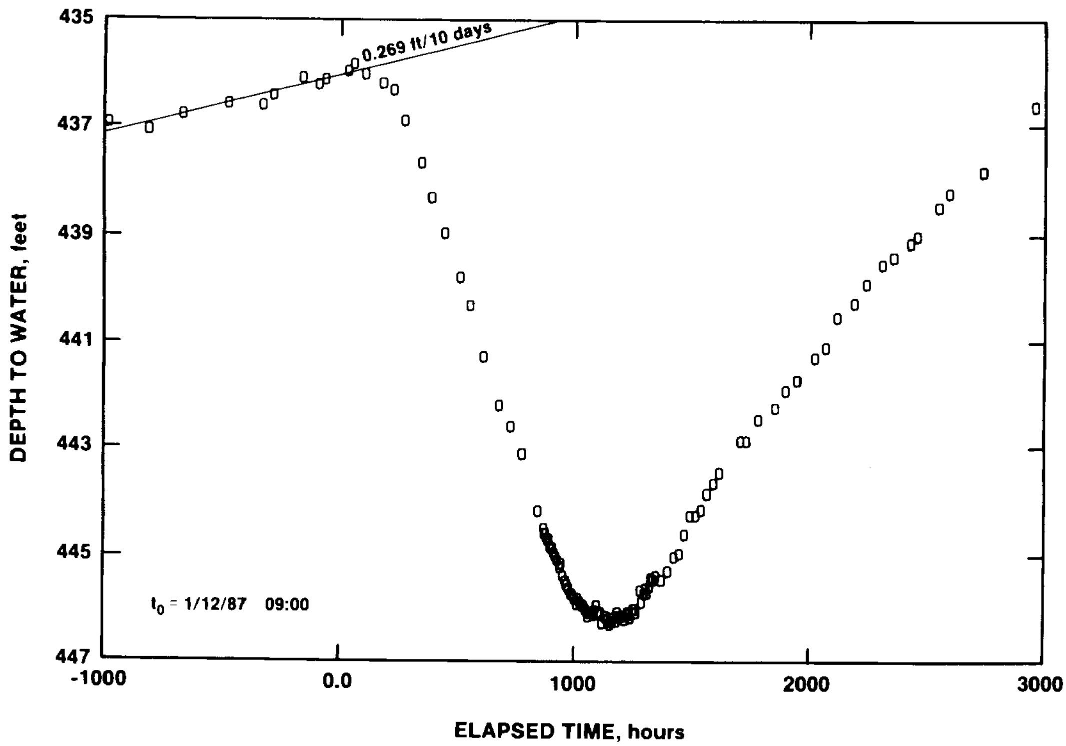

Figure 5-6. WIPP-22 Water-Level Record

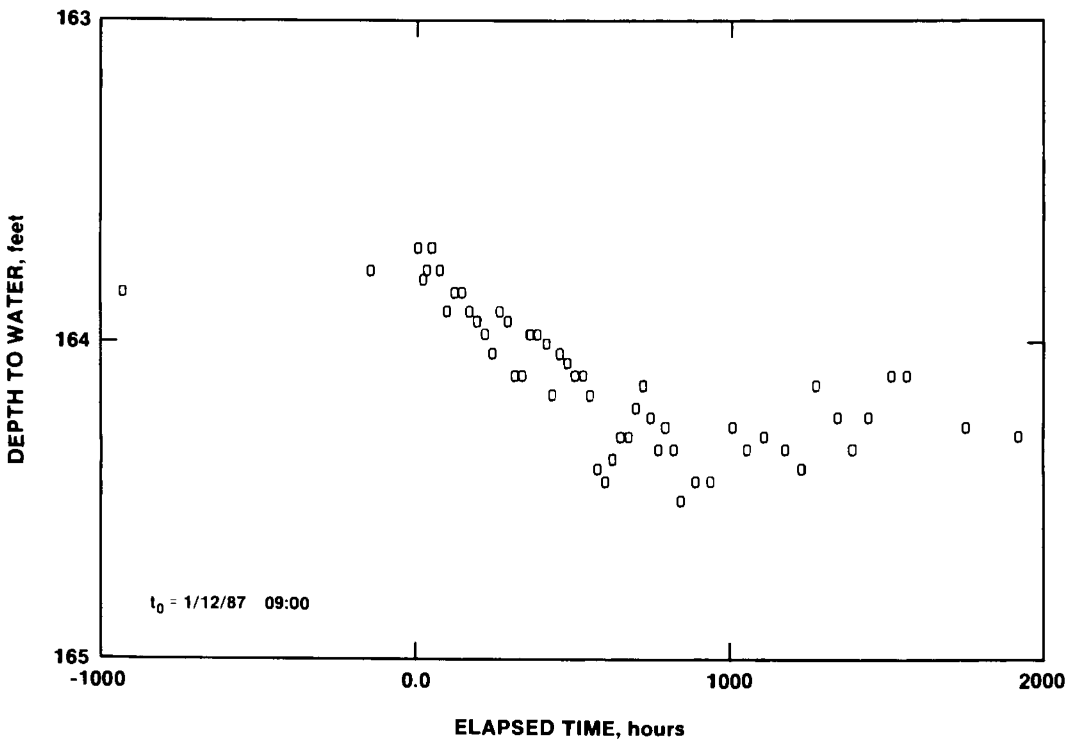

Figure 5-7. WIPP-25 Water-Level Record

5.8 WIPP-30

The water-level record for well WIPP-30 leading up to and during the WIPP-13 multipad test period is shown in Figure 5-8. As shown in the figure, the water level was rising ~0.175 ft/10 days from ~1583 hr before the start of the test to ~51 hr after the start of pumping. While water levels had been rising steadily in WIPP-30 since its last recompletion in August 1983, this rate of rise was significantly greater than the rate observed from mid-1985 through mid-1986 (Haug et al., 1987). Pumping at DOE-2 in July and August 1986 drew down the water level at WIPP-30 by ~1.5 ft (Saulnier et al., 1987). The subsequent recovery was relatively rapid and sustained and brought the WIPP-30 water level higher than was ever measured in the past. No explanation for this seemingly anomalous rise is apparent, and none of the nearest wells (DOE-2, H-6, and WIPP-28) have shown parallel behavior.

For analysis, the observed WIPP-30 water levels were first modified to eliminate the pretest trend, using a linear correction. The modified values were then converted to equivalent pressures by subtracting the depths to water from an arbitrary datum of 400 ft and multiplying the remainders by 0.462 psi/ft (SG = 1.065), the conversion factor determined by a pressure-density survey of the fluid in the well (between the depths of 400 and 570 ft) on May 6, 1987 (Crawley, 1987). The observed water-level data, modified water-level data, and calculated pressure data are tabulated in Appendix A, Table A-8. A plot of the pressure data is included with the final analytical simulation in Section 6.2.

5.9 H-1

The water-level record for the Culebra at H-1 preceding and during the WIPP-13 multipad test is shown in Figure 5-9. A number of trends are evident in the data, reflecting the influence of numerous hydraulic stresses. As discussed by Stevens and Beyeler (1985) and Haug et al. (1987), water levels at H-1 are strongly influenced by drainage of Culebra water into the shafts at the WIPP site. The H-1 water level was ~380 ft below ground surface in July 1981 before the first shaft construction began (Richey, 1987) and reached a low of ~450 ft below ground surface in September 1984 (HydroGeoChem, 1985) following the enlargement and conversion of the ventilation shaft into the waste-handling shaft. In general, H-1 water levels have been rising since that time, particularly since the grouting and sealing of the Culebra in the exhaust shaft in July 1985. The H-1 water level peaked at ~416 ft below ground surface in November 1985 before the pumping associated with the H-3 multipad test drew it down by ~24 ft (INTERA Technologies, 1986).

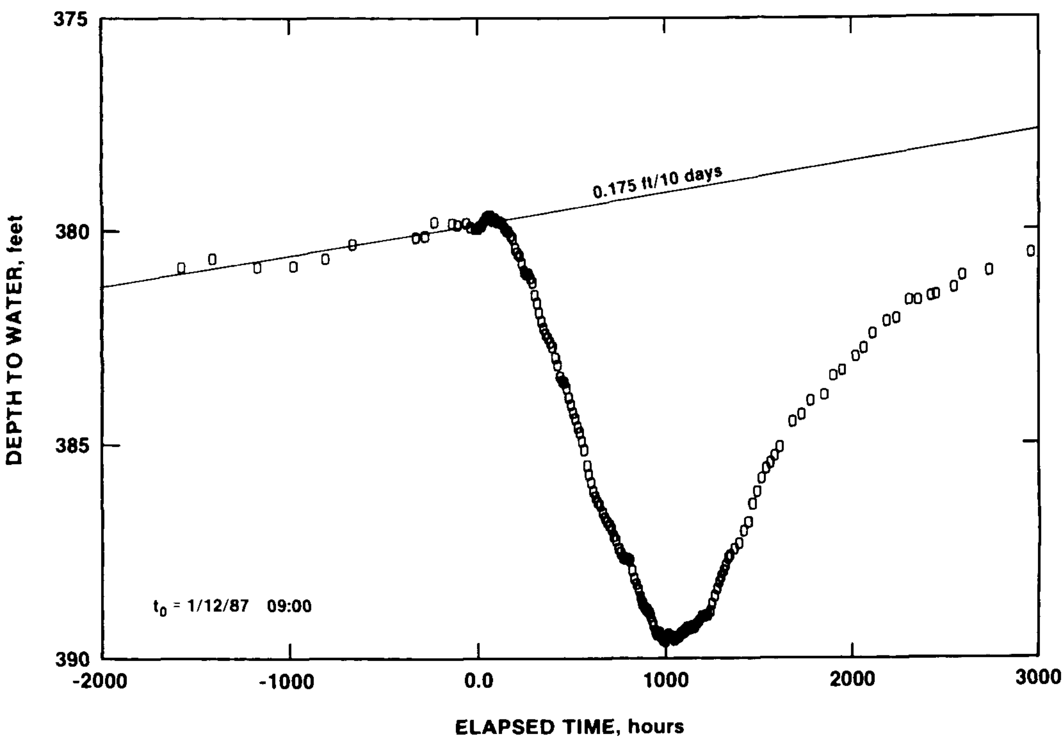

Figure 5-8. WIPP-30 Water-Level Record

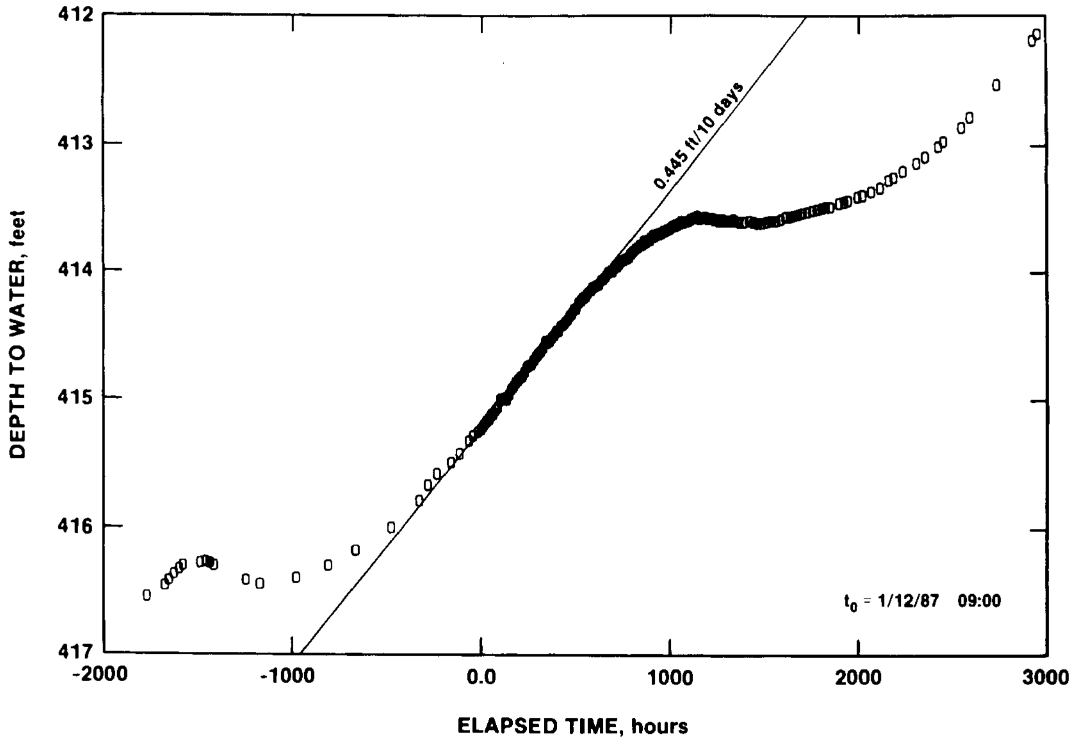

Figure 5-9. H-1 Water-Level Record

Following the H-3 multipad test, H-1 water levels rose monotonically until November 1986, when the effects of well-development pumping at ERDA-9 were felt. These effects are shown in Figure 5-9 by the slight decline in the water level from ~1460 to 1170 hr before the beginning of pumping at WIPP-13. The water level then began rising again, establishing a linear rate of 0.445 ft/10 days between ~8 and 530 hr after the beginning of pumping at WIPP-13. The effects of WIPP-13 pumping began to be manifested after 530 hr of pumping, causing a stabilization of the water level, followed by a very slight decline. Roughly 625 hr after the pump was turned off at WIPP-13, the H-1 water level began to rise again. This rise continued at an ever-increasing rate throughout the remainder of the monitoring period.

To provide drawdown data for analysis, the observed water-level data were modified by subtracting the effects of the 0.445 ft/10 days rising trend observed early in the test, assuming that that trend continued linearly throughout the remainder of the test. The modified water-level data were then converted to pressures by subtracting the modified depths to water from an arbitrary datum of 500 ft and multiplying the remainders by 0.4403 psi/ft, the conversion factor for H-1 Culebra water with a specific gravity of 1.016 (Mercer, 1983). This value may not be entirely representative of the fluid in the tubing at H-1 during the WIPP-13 test, but it is the best value available and has no effect on the final analysis. The observed water-level data, modified water-level data, and calculated pressure data are tabulated in Appendix A, Table A-9. A plot of the pressure data is included with the final analytical simulation in Section 6.2.

5.10 H-2b2

Figure 5-10 shows the H-2b2 water-level record from 1000 hr before the WIPP-13 multipad test through ~2100 hr of recovery. An initial rising trend is evident that lasted through about the first 420 hr of pumping at WIPP-13. This rise was largely a recovery response from shaft leakage, as discussed by Haug et al. (1987), but also includes superimposed recovery components from the H-3 multipad test and WIPP Water Quality Sampling Program (WQSP) sampling exercises on both the H-2 and H-3 hydropads. The trend cannot be clearly defined in Figure 5-10 because of the degree of scatter in the data caused by changes in barometric pressure. Consequently, barometric corrections were performed before defining and correcting for the pretest trend.

The observed water-level data were first converted to pressures by subtracting the depths to water from an arbitrary datum of 400 ft and multiplying the remainders by 0.436 psi/ft, the conversion factor for H-2b2 water with a specific gravity of 1.006 (INTERA and HydroGeoChem, 1985). Next, using the technique described earlier in Section 5.5, a barometric efficiency of ~0.6 was established for H-2b2. The resulting corrected pressure data are shown in Figure 5-11. The pretest rising trend is clearer on this plot than on the water-level plot (Figure 5-10) and is estimated at ~0.086 psi/10 days (0.197 ft/10 days).

The final pressure data used for analysis were then derived by subtracting the effects of this trend, assuming that the trend continued linearly for the duration of the test. The observed water-level data, calculated pressure data compensated for barometric-pressure effects, and final calculated pressure data corrected for the pretest trend are tabulated in Appendix A, Table A-10. A plot of the final pressure data is included with the final analytical simulation in Section 6.2.

5.11 H-3b2

The H-3b2 water-level record before and during the WIPP-13 multipad test is shown in Figure 5-12. A rising trend is evident for the duration of the data record. This rise is a combined recovery response from shaft leakage, the H-3 multipad test pumping from October to December 1985, and WQSP sampling at H-3 in April and May 1986 (Saulnier et al., 1987). A slight decrease in the rate of water-level rise is apparent in the data from the last 2000 hr in Figure 5-12; whether or not this is a response to WIPP-13 pumping or simply a natural slowing of the recovery from the other stresses mentioned earlier is problematic. The observed water-level data are tabulated in Appendix A, Table A-11.

5.12 H-5b

Figure 5-13 presents the H-5b water-level record before and during the WIPP-13 multipad test. A slight rising trend is evident until ~1500 hr after the start of the test. This rise is a long-term recovery response from the WQSP sampling performed in H-5b in May 1986 (Uhland et al., 1987). The last few data points in Figure 5-13 appear to show a slight decline in the water level, but this decline may be due to the removal of a small quantity of fluid from the well during a pressure-density survey performed on April 15, 1987 (the day before the third-to-last point on the plot; Crawley, 1987). The observed water-level data are listed in Appendix A, Table A-12.

5.13 H-6a and H-6b

The water-level data from both wells H-6a and H-6b for the period before and during the WIPP-13 multipad test are shown in Figure 5-14. The pretest water levels appear to be relatively static and, therefore, no corrections for pretest conditions were required. For analysis, the water-level data were converted to pressures by subtracting the depths to water from an arbitrary datum of 400 ft and multiplying the remainders by 0.4515 psi/ft, a conversion factor derived from the specific-gravity value of 1.042 reported for H-6b Culebra water by Uhland and Randall (1986). The observed water-level data and calculated pressure data for H-6a and H-6b are listed in Appendix A, Tables A-13 and A-14, respectively.

5.14 H-15

The water-level record for well H-15 before and during the WIPP-13 multipad test is shown in Figure 5-15. A fairly uniform (ignoring the data scatter) rising trend is evident for the duration of the data record. This rise represents equilibration of the water level in the well with the surrounding formation pressure following well construction in November 1986 (Stensrud et al., 1987). The data provide no indication that H-15 responded to the WIPP-13 multipad test. The observed water-level data are listed in Appendix A, Table A-15.

5.15 DOE-2

The record of DOE-2 water levels before and during the WIPP-13 multipad test is shown in Figure 5-16. The pretest water level appears to be relatively static and, therefore, no corrections for pretest conditions were required. For analysis, the water-level data were converted to pressures by subtracting the depths to water from an arbitrary datum of 500 ft and multiplying the remainders by 0.451 psi/ft, a conversion factor derived from the specific-gravity value of 1.04 reported for DOE-2 Culebra water by Saulnier et al. (1987). The observed water-level data and calculated pressure data are listed in Appendix A, Table A-16.

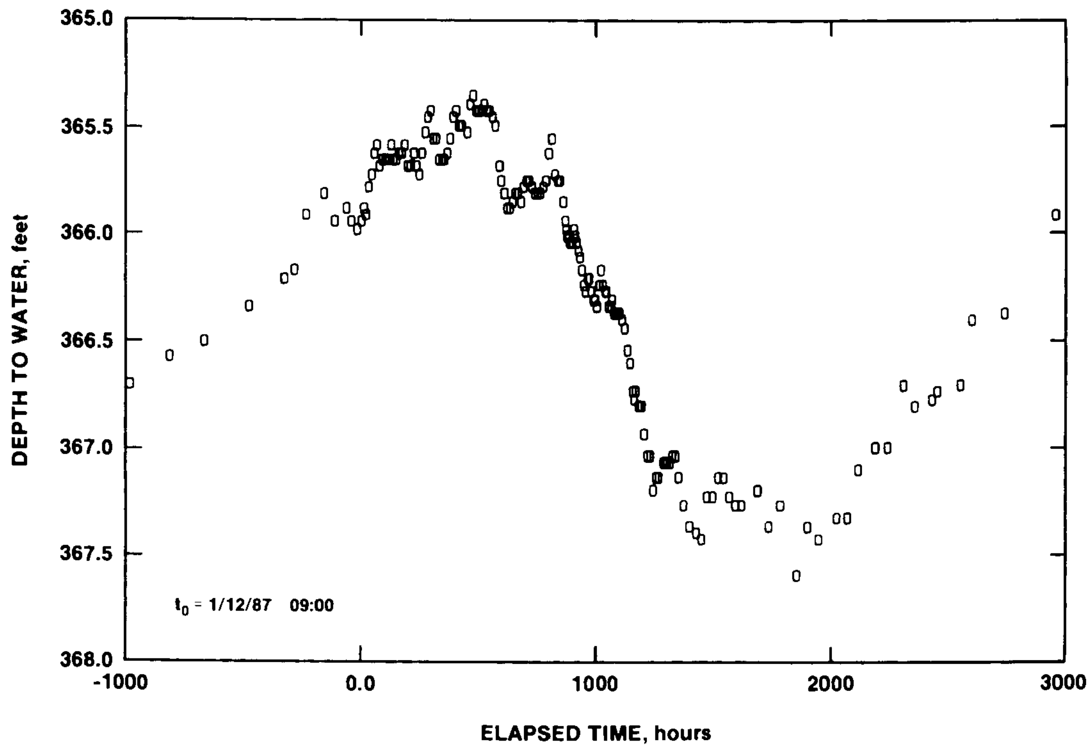

Figure 5-10. H-2b2 Water-Level Record

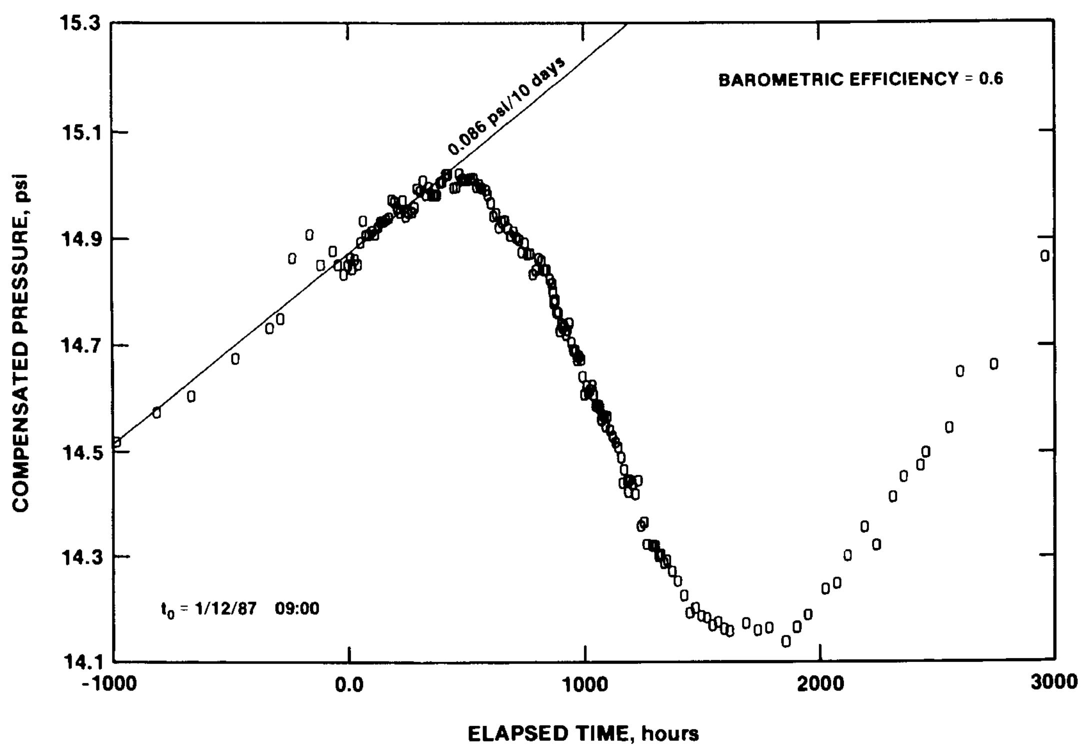

Figure 5-11. H-2b2 Fluid-Pressure Record Compensated for Barometric Effects

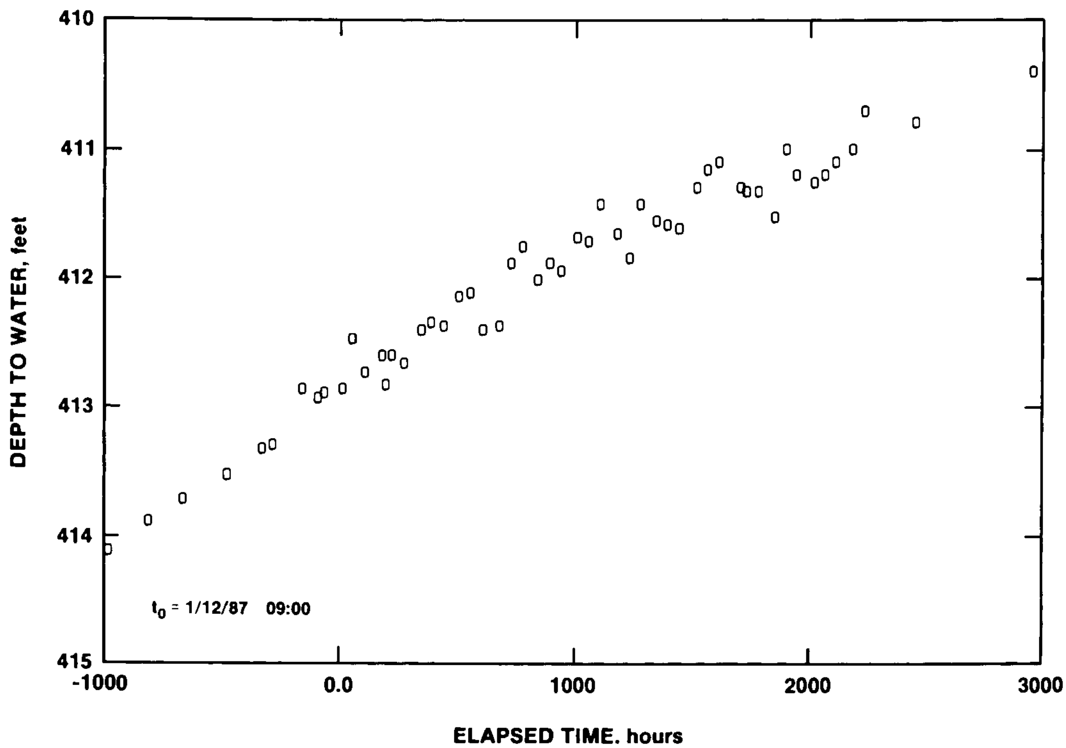

Figure 5-12. H-3b2 Water-Level Record

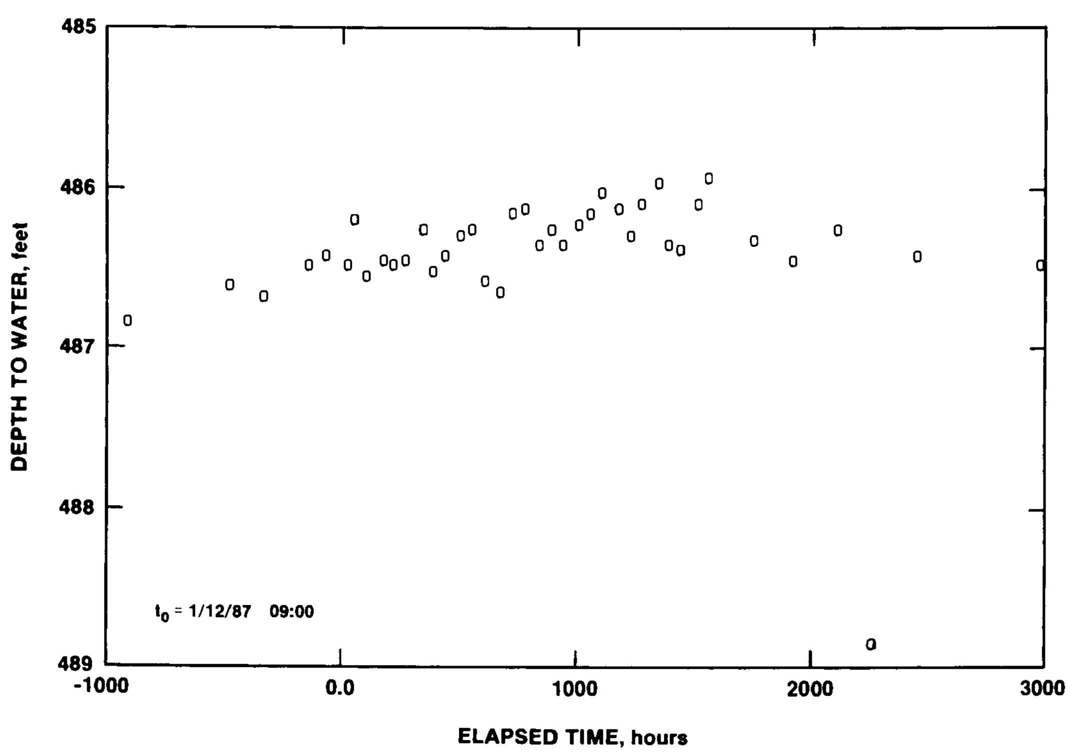

Figure 5-13. H-5b Water-Level Record

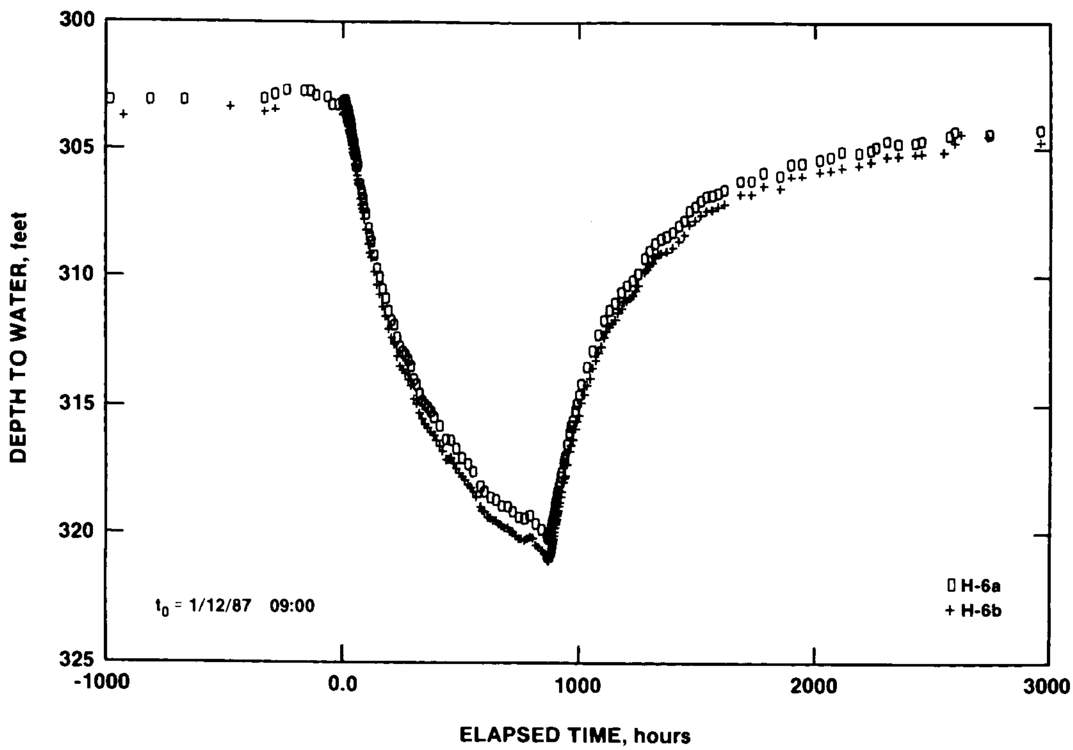

Figure 5-14. H-6a and H-6b Water-Level Records

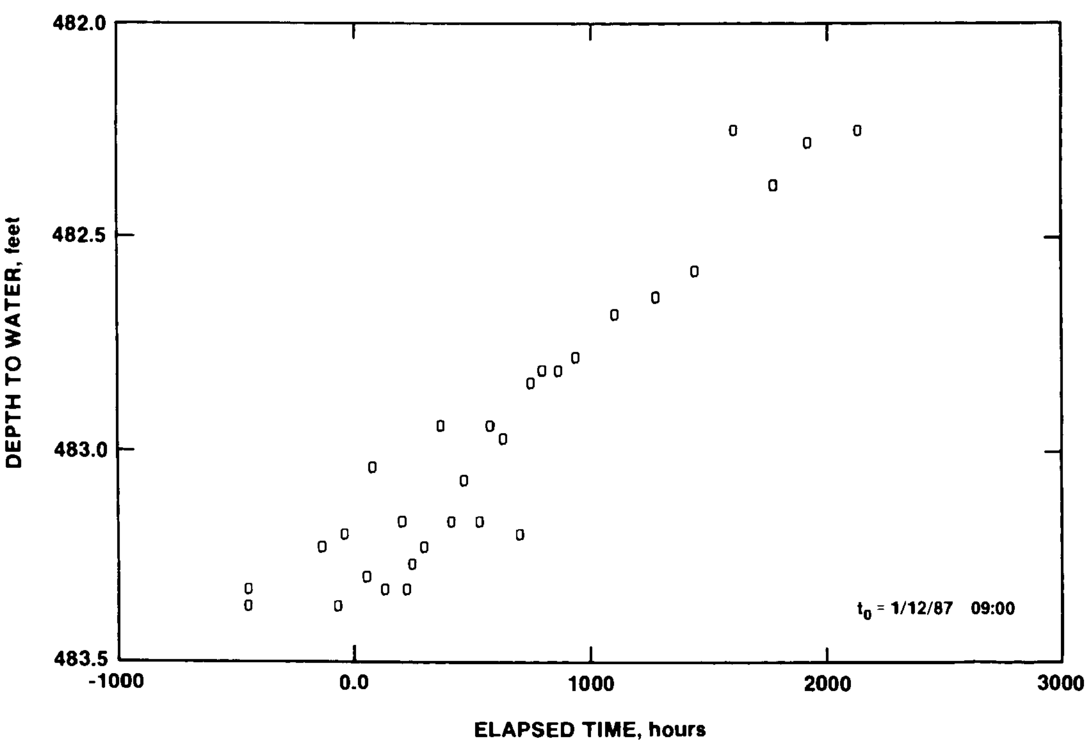

Figure 5-15. H-15 Water-Level Record

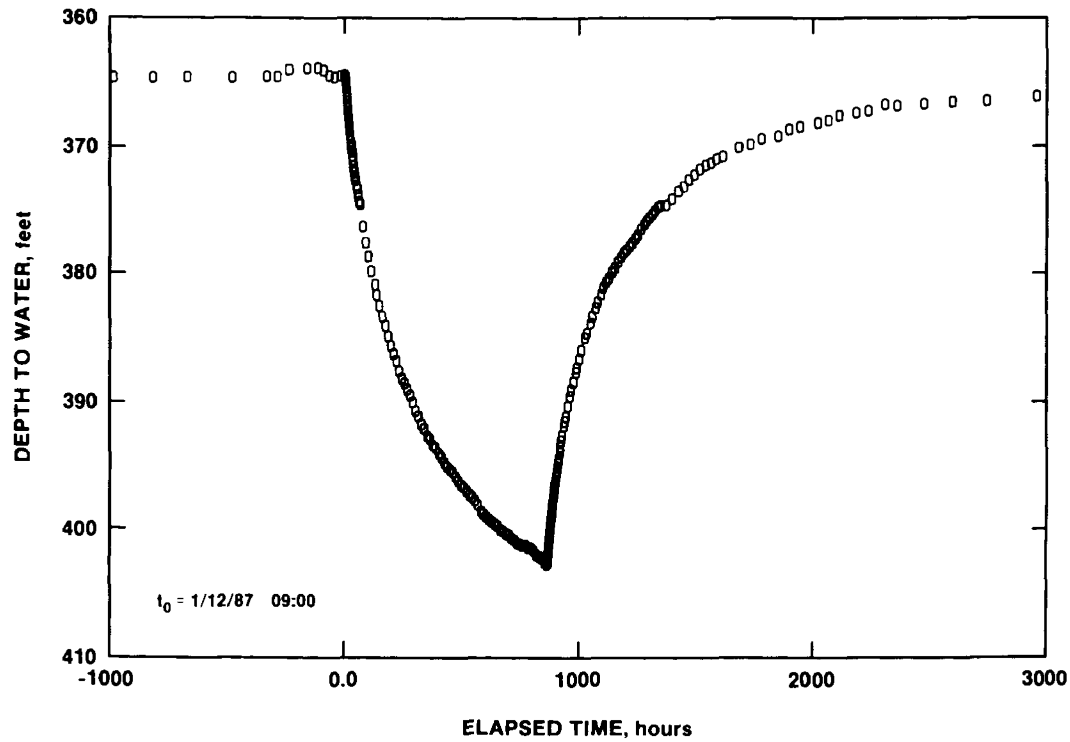

Figure 5-16. DOE-2 Water-Level Record

5.16 P-14

Figure 5-17 shows the water-level record for well P-14 leading up to and during the WIPP-13 multipad test. No particular trend is evident in the pretest data and, therefore, no corrections for pretest conditions were required. The data are fairly noisy, however, apparently in response to barometric-pressure fluctuations. Thus, after converting the water levels to pressures, the data were compensated for barometric effects by using the technique described in Section 5.5.

The water-level data were converted to pressures by subtracting the depths to water from an arbitrary datum of 400 ft and multiplying the remainders by 0.442 psi/ft, a conversion derived from the specific-gravity value of 1.02 reported for P-14 Culebra water by Uhland and Randall (1986). Different barometric corrections were then applied to the pressure data, with the correction using a barometric efficiency of 0.7 providing the smoothest data set. This data set was used for the analysis. The observed water-level data and calculated pressure data compensated for barometric-pressure effects are tabulated in Appendix A, Table A-17. A plot of the final pressure data is included with the final analytical simulation in Section 6.2.

5.17 ERDA-9

Figure 5-18 presents the water-level record for well ERDA-9 leading up to and during the WIPP-13 multipad test. The water level was rising at an approximate rate of 0.52 ft/10 days from ~480 hr before to ~530 hr after the start of pumping at WIPP-13. This rise was largely a recovery response following well-development pumping that occurred at ERDA-9 between October 27 and November 14, 1986 (Stensrud et al., 1987), although some component of it may also be related to drainage into the nearby WIPP shafts.

For analysis, the water-level data were modified by subtracting the effects of the pretest rising trend, assuming that the trend continued linearly for the duration of the multipad test. The modified water levels were then converted to pressures by subtracting the depths to water from an arbitrary datum of 500 ft and multiplying the remainders by 0.459 psi/ft, the conversion factor derived from the specific gravity (1.059) of the final water produced during the ERDA-9 developmental pumping (Stensrud et al., 1987).

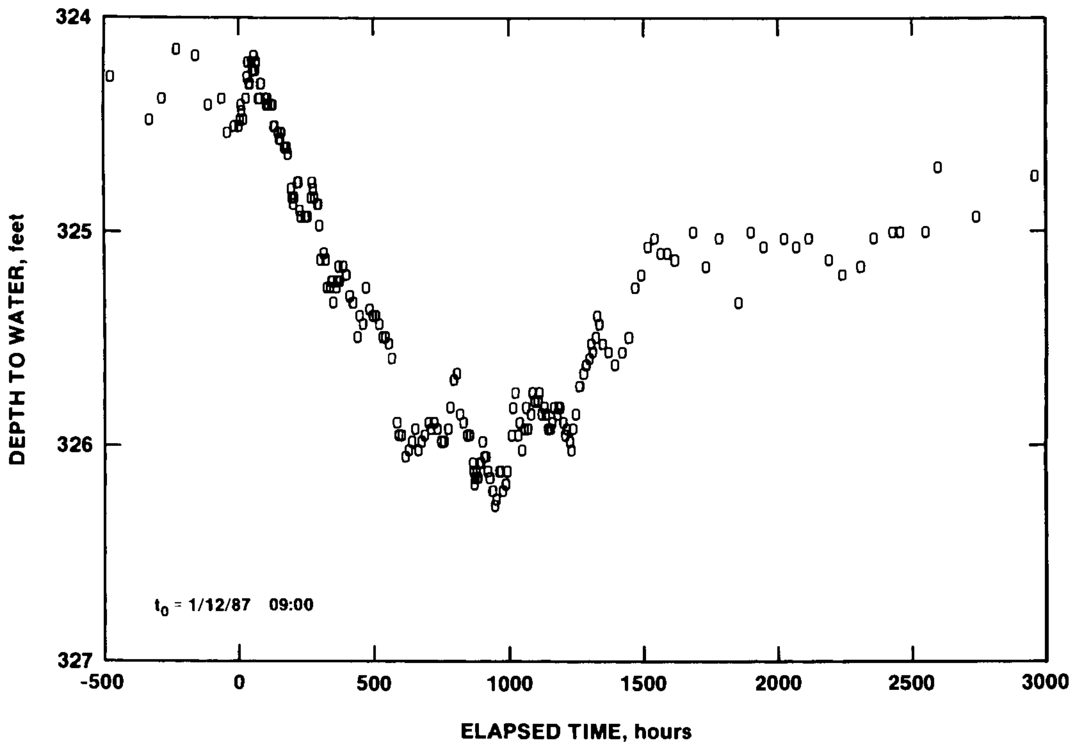

Figure 5-17. P-14 Water-Level Record

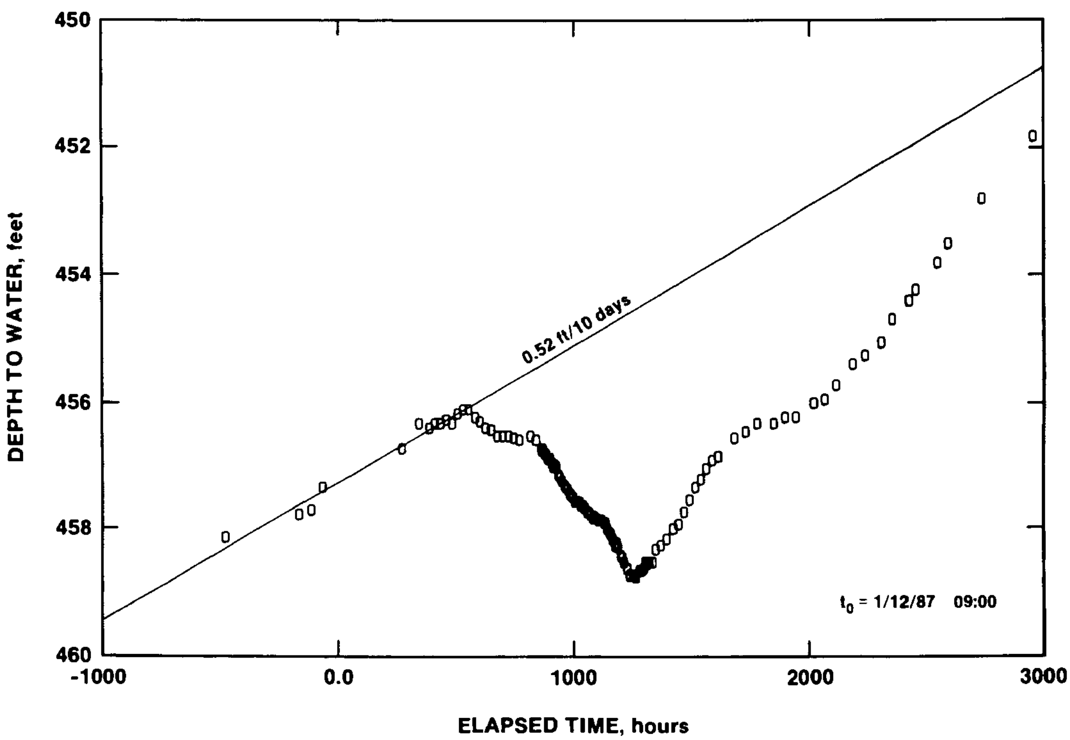

Figure 5-18. ERDA-9 Water-Level Record

Attempts were made to compensate the data for possible barometric effects by using barometric efficiencies of 0.3, 0.5, and 0.7. None of the resulting data sets were significantly smoother than the uncompensated data and, hence, the uncompensated data were used for analysis. The observed water-level data, modified water-level data, and calculated pressure data are tabulated in Appendix A, Table A-18. A plot of the pressure data is included with the final analytical simulation in Section 6.2.

5.18 Exhaust Shaft

The pressure record from the three exhaust shaft Culebra piezometers, #210, #211, and #212, for the period before and during the WIPP-13 multipad test is shown in Figure 5-19. As discussed in Section 3, these piezometers show pressure changes in discrete steps of 0.5 to 0.7 psi. Inasmuch as the pressure changes recorded from all three piezometers are quite similar, only the data from #212 were used for analysis.

Before the test began, the Culebra pressure at the exhaust shaft was rising at an approximate rate of 0.431 psi/10 days (0.939 ft/10 days, using the specific gravity of 1.059 from nearby ERDA-9) following remedial grouting of the Culebra in October 1986 (Saulnier et al., 1987) and the well-development pumping of ERDA-9. This rise appears to have halted ~450 hr after the beginning of pumping at WIPP-13. For analysis, the pressure data were modified by subtracting the effects of the pretest rising trend, assuming that the trend continued linearly for the balance of the monitoring period. The observed and modified pressure data are listed in Appendix A, Table A-19. A plot of the modified pressure data is included with the final analytical simulation in Section 6.2.

5.19 Magenta Observation Wells

Water levels in two Magenta observation wells were monitored specifically as part of the WIPP-13 multipad test: H-1 and H-6c. The data from these two wells are discussed below. Other Magenta wells in the vicinity of the WIPP site were monitored less frequently over this same time period as part of the regular WIPP regional water-level monitoring. None of these wells showed apparent responses to the WIPP-13 test. Data and plots for these other Magenta wells can be found in Stensrud et al. (1987).

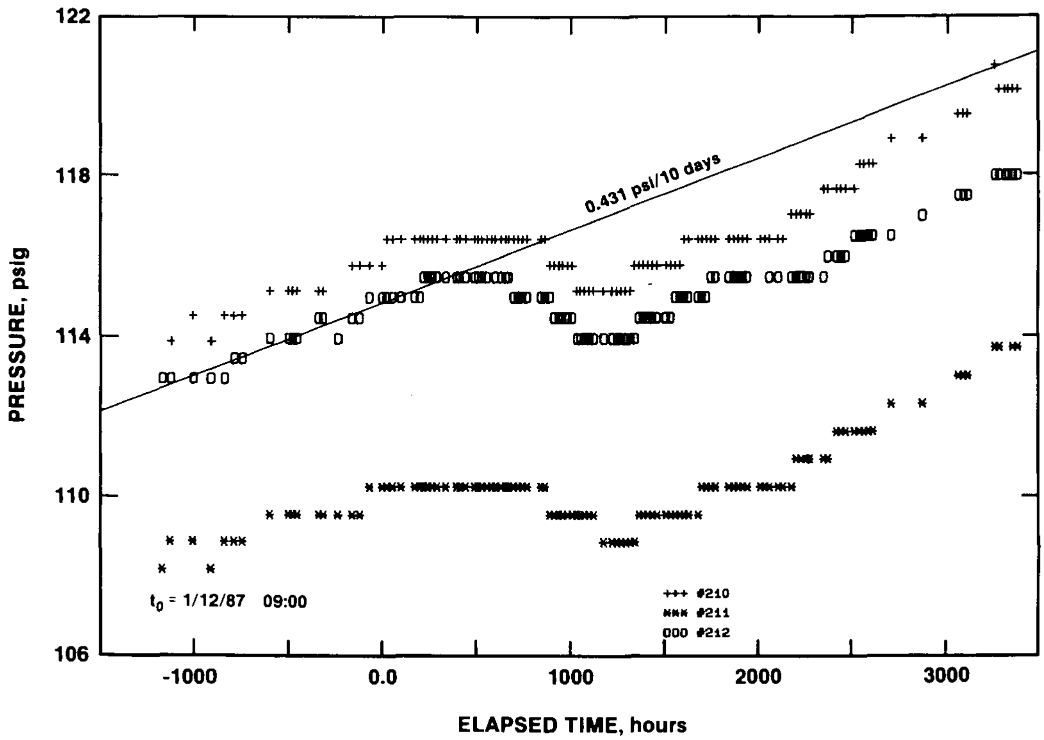

Figure 5-19. Exhaust Shaft Culebra Piezometer Fluid-Pressure Record

5.19.1 H-1

Figure 5-20 shows the Magenta water levels measured at H-1 before and during the WIPP-13 multipad test. Significant fluctuations in the water level occurred, but their causes are unclear. The depth to Magenta water at H-1 was very constant at ~275 ft between August 1985 and July 1986 (INTERA Technologies and HydroGeoChem, 1985; INTERA Technologies, 1986; Saulnier et al., 1987). The water level began rising sharply in July 1986 and continued to rise, albeit with several significant downward fluctuations, through February 1987, after which the drop seen in Figure 5-20 began. These responses may be related to changes in seepage rates from the Magenta into the nearby WIPP shafts. Because the magnitudes of the Magenta responses are much higher than, and their directions do not parallel, Culebra responses over the same period (see Figure 5-9, and Saulnier et al., 1987), no reason for attributing any of these responses to the WIPP-13 test is evident. The H-1 Magenta water-level data are listed in Appendix A, Table A-20.

5.19.2 H-6c

Magenta water levels in well H-6c before and during the WIPP-13 multipad test are shown in Figure 5-21. Water levels rose steadily throughout the period of record as a continuing recovery response to Magenta water-quality sampling performed by the MOC at H-6c in late September 1986 (Uhland et al., 1987). No response attributable to the WIPP-13 pumping is evident in the data. The H-6c Magenta water-level data are listed in Appendix A, Table A-21.

5.20 Discussion and Summary

Pretest rising trends, interpreted as recovery responses to various hydraulic stresses, were observed in the water-level data from WIPP-12, WIPP-18, WIPP-19, WIPP-21, WIPP-22, WIPP-30, H-1, H-2b2, H-3b2, H-5b, H-15, ERDA-9, and the exhaust shaft. To provide data for analysis of responses to the WIPP-13 multipad test, the observed water-level data were modified by using linear correction factors to remove the effects of these preexisting trends. In most hydrologic systems, recovery responses follow logarithmic curves, decaying with time. Hence, applying a linear correction derived from pretest behavior to the observed test data from a well probably represents some degree of overcompensation, particularly at late time.

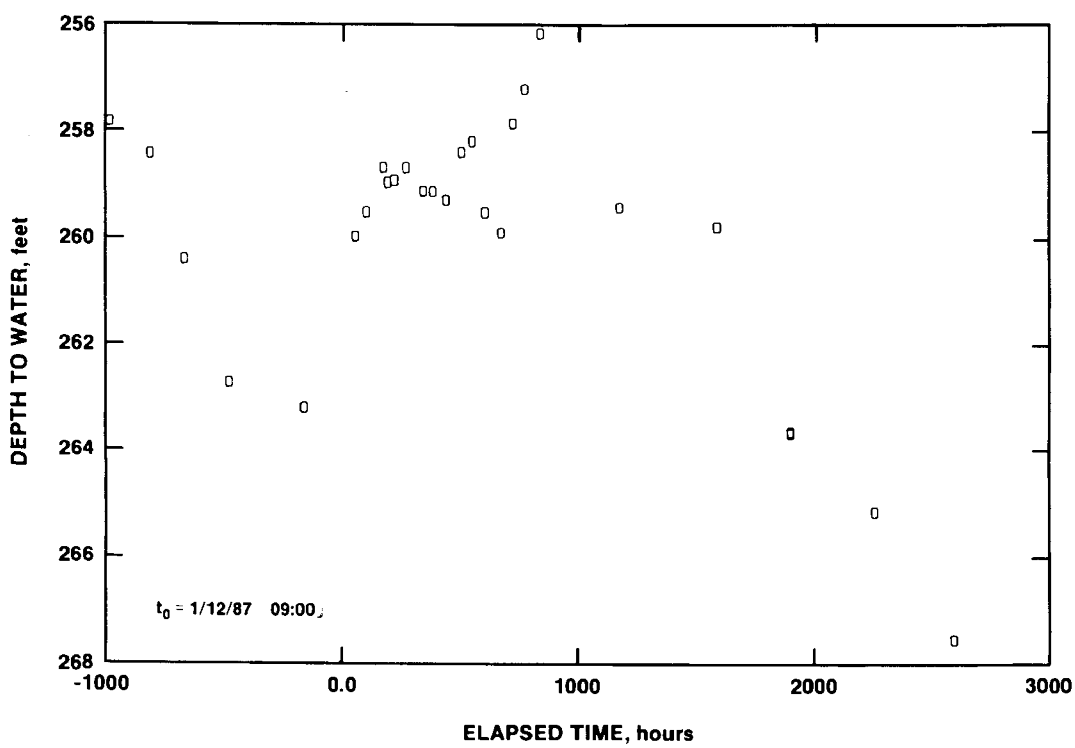

Figure 5-20. H-1 Magenta Water-Level Record

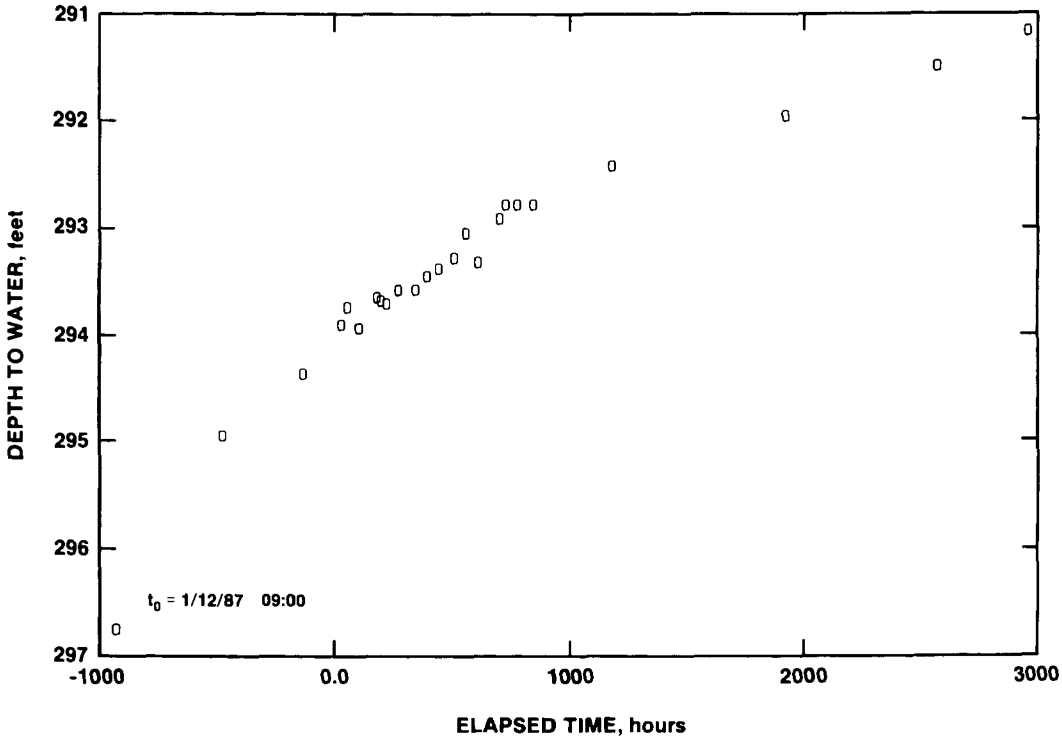

Figure 5-21. H-6c Magenta Water-Level Record

Whether or not this overcompensation is significant depends on a number of factors. Almost any curve can be reasonably approximated as linear over some fraction of its length, however short that length may be. Logarithmic curves, in particular, tend to become more linear with increasing time. In practical terms, this means that as the time since the end of the causative hydraulic stress increases, the observed recovery data should become increasingly linear.

The last hydraulic stress known to have affected some of the key observation wells before the WIPP-13 multipad test was the developmental pumping of ERDA-9 that ended on November 14, 1986 (Stensrud et al., 1987), over 1400 hr before pumping began at WIPP-13. Before that, well development occurred at WIPP-18, WIPP-19, WIPP-21, and WIPP-22 in August 1986 (Saulnier et al., 1987), over 3300 hr before the beginning of the WIPP-13 multipad test. The earliest data used to define any of the pretest trends came from WIPP-21 and WIPP-22 ~980 hr before the start of the WIPP-13 test, over 420 hr since the end of pumping at ERDA-9. Thus, the early portions of the recovery periods from all known hydraulic stresses, during which recovery curves change slope most rapidly, had passed before pretest trends were evaluated.

Further evidence that the errors involved in making linear water-level corrections might not be too severe is provided by the long-term water-level data provided in Haug et al. (1987) and Richey (1987). Many of the wells near the WIPP site have historically exhibited approximately linear rising trends lasting for one or more years, including H-1, H-3b1, H-4b, P-14, P-15, P-17, P-18, and WIPP-30. Considering that the longest extrapolation period used for the multipad test data corrections was only 4 months, linear behavior seems a reasonable assumption, particularly for wells such as WIPP-30 that are far from any known recent hydraulic stress.

The final rationale for using a linear correction to compensate for pretest trends is that the direction, if not the magnitude, of the possible error is known. In the absence of additional stresses on the system, recovery curves can reliably be predicted to decrease in slope with time. Hence, using a linear correction factor will always cause drawdown to be overestimated. Attempting a logarithmically decaying correction for the pretest trends might produce more accurate results, but the direction of the residual error would be unknown.

For each of the wells at which responses to the WIPP-13 multipad test were observed, the maximum interpreted drawdowns, the times at which drawdown responses were first observed, and the times at which maximum drawdowns were observed are summarized in Table 5-1. Several qualifications must be noted with regard to the information in this table. First, because of data noise, a degree of subjectivity is involved in defining response times for the various wells. Second, for those wells exhibiting rising water-level trends before the test, drawdown was considered to begin when the data first appeared to deviate from the trend, a somewhat subjective assessment. Third, the maximum drawdowns presented were calculated by following linear compensations for pretest trends. Consequently, the drawdowns are overestimated to whatever degree the linear compensations are in error. In summary, the times and drawdowns presented in this table enable only qualitative comparisons and should be considered as approximations only.

Table 5-1. Response Times and Maximum Drawdowns at Observation Wells

Observation Well	Time After Pump on Until First Drawdown Observed (hr)	Time After Pump on Until Maximum Drawdown Observed (hr)*	Maximum Drawdown Observed (psi)
WIPP-12	74	1050	11.9
WIPP-18	74	950	9.3
WIPP-19	102	1050	7.2
WIPP-21	133	1260	3.6
WIPP-22	102	1150	5.7
WIPP-25	76	890	0.3
WIPP-30	61	1000	4.9
H-1	600	2950(?)	1.1
H-2b2	445	1850	1.4
H-6a	8	869	7.7
H-6b	8	869	7.9
DOE-2	1	865	17.3
P-14	71	920	0.8
ERDA-9	550	1260	2.0
Exhaust Shaft	400	1200	3

*Pump was turned off after 864 hr

6. Analytical Interpretations

The test data from the pumping and observation wells were interpreted by using analytical techniques developed for tests in homogeneous, porous media. These techniques readily, and rigorously, accommodate such factors as double-porosity, anisotropy, and discrete boundaries. Large-scale heterogeneities, however, such as progressive changes in transmissivity and storativity with distance and direction, are not treated rigorously by using these analytical techniques. In this situation, the most information that can be gained is a qualitative understanding of the nature of the heterogeneities and nonunique quantitative evaluations of average hydraulic properties over the distances of the observations. These concepts will be discussed more fully in connection with individual well responses.

Given these limitations, the analytical interpretations of the WIPP-13 multipad test data had the following objectives:

- Determine the most appropriate conceptualization of the nature of the Culebra flow system around WIPP-13
- Quantify the hydraulic properties of the Culebra dolomite in the vicinity of WIPP-13
- Determine the nature and distribution of heterogeneities in the Culebra dolomite within the area influenced by the test
- Determine average hydraulic properties of the Culebra dolomite between WIPP-13 and observation wells

The analytical methods used to meet these objectives, and the nomenclature and symbols used in the following text and figures, are discussed in Appendix B. All analyses were performed with the INTERPRET well-test interpretation code developed by A. C. Gringarten and Scientific Software-Intercomp, which is described briefly in Appendix B. Familiarity on the part of the reader with the material in Appendix B is assumed in the following chapter.

6.1 WIPP-13

The pressure response observed at WIPP-13 during the multipad test appears to be that of a well completed in a heterogeneous, double-porosity medium. Double-porosity media have two porosity sets that differ in terms of storage volume and permeability. Typically, the two porosity sets are a fracture network with higher permeability and lower storage, and the primary porosity of the rock matrix with lower permeability and higher storage. Double-porosity media are discussed more fully in Appendix B.

Figure 6-1 shows a log-log plot of the WIPP-13 drawdown data along with the best-fit simulation of those data generated with the INTERPRET well-test-analysis code (see Appendix B). The simulation shown uses a formulation for a double-porosity system with slab-shaped matrix blocks, unrestricted interporosity flow, a transmissivity of 69 ft^2/day, and includes the effects of an image discharge well relatively close (6800 ft) to WIPP-13 and three image recharge wells much farther (27 700, 35 100, and 39 200 ft) from WIPP-13 (Table 6-1).

The image discharge well represents a no-flow (low-permeability) boundary 3400 ft (half the distance to the image well) from WIPP-13, and the image recharge wells represent constant-pressure (high-permeability) boundaries 13 900, 17 600, and 19 600 ft from WIPP-13. The storativity ratio, ω, for this simulation is 0.001, which is an approximate measure of the percentage of water produced from the fractures versus that produced from the matrix.

Assuming that the matrix porosity of the Culebra is ~20%, that the fluid viscosity is ~1.0 cp, and that the total-system compressibility is $\sim 1.0 \times 10^{-5}$ psi^{-1}, the skin factor (s) for WIPP-13 is ~−7.7. A highly negative skin factor such as this indicates that the wellbore is directly intersected by fractures, an indication supported by examination of the core obtained from WIPP-13. High-permeability fractures in direct communication with a wellbore may act as additional production surfaces to the well in addition to the wellbore itself.

Jenkins and Prentice (1982) term this type of wellbore-fracture system an "extended" well. Earlougher (1977) relates skin factor to an "effective" wellbore radius quantitatively by the following equation:

$$r_e = r_w e^{-s} \quad \textbf{(6.1)}$$

where

r_e = effective wellbore radius
r_w = actual wellbore radius
s = skin factor

This equation indicates that a well with a positive skin factor (wellbore damage) behaves hydraulically like a well with a smaller radius. Conversely, a well with a negative skin factor should behave like a well with a larger radius.

Application of Eq (6.1) indicates that WIPP-13, with a skin factor of ~−7.7 and an actual radius of 0.372 ft, behaves like a well with a radius of ~800 ft. Extremely negative skin factors, however, are better viewed qualitatively than quantitatively. Instead of attaching too much significance to a calculated effective well radius, WIPP-13 should be viewed simply as a well intersected by fractures that increase its production surface.

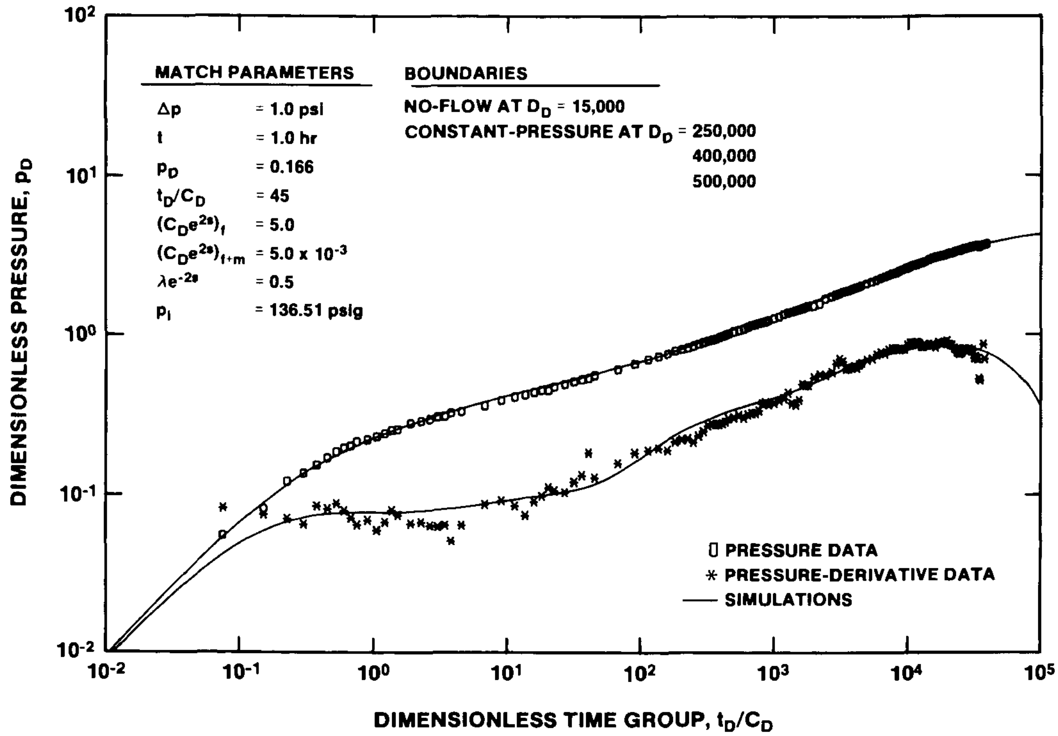

Figure 6-1. WIPP-13 Drawdown Log-Log Plot With INTERPRET Simulation

Table 6-1. Summary of Well-Response Interpretations

For Flowpath Between WIPP-13 and Well	Data Modifications: Trend (ft/10 days)	Data Modifications: Barometric Efficiency	Apparent Trans-missivity (ft^2/day)	Apparent Stora-tivity	Distances to Image Wells: Discharge (ft)	Distances to Image Wells: Recharge (ft)
WIPP-13						
Drawdown	NA	NA	69*	—	6 800	27 700 35 100 39 200
Recovery	NA	NA	69*	—	6 300	25 600 32 300 36 200
WIPP-12	0.148	NA	7.9	3.6×10^{-5}	—	7 300
WIPP-18	0.119	NA	23	4.0×10^{-5}	—	18 700
WIPP-19	0.249	NA	24	4.0×10^{-5}	—	23 200
WIPP-21	0.553	0.5	22	5.3×10^{-5}	—	19 200
WIPP-22	0.269	NA	19	4.7×10^{-5}	—	14 200
WIPP-25	NA	0.3	650	6.4×10^{-5}	—	—
WIPP-30	0.175	NA	28	5.6×10^{-6}	—	40 900
H-1	0.445 0.445	NA NA	20 20	1.3×10^{-4} 1.3×10^{-4}	— —	— 17 600
H-2b2	0.197	0.6	16	7.3×10^{-5}	—	12 000
H-6a	NA	NA	71	8.2×10^{-6}	—	50 800
H-6b	NA	NA	69	7.9×10^{-6}	—	50 800
DOE-2	NA	NA	57	5.1×10^{-6}	15 300	34 200 48 400
P-14	NA	0.7	265	5.2×10^{-5}	—	43 900
ERDA-9	0.520	NA	22	5.4×10^{-5}	—	11 700
Exhaust Shaft	0.939	NA	28	5.5×10^{-5}	—	—

*True (not apparent) value

The interpretation of unrestricted interporosity flow and the low storativity ratio at WIPP-13 further attest to the role of fractures as production surfaces. As mentioned earlier, the WIPP-13 data were best matched by using a model incorporating unrestricted interporosity flow. This means that the water stored in the matrix pores communicates readily with the fractures. The very early stabilization of the pressure derivative in Figure 6-1 shows that the transition from fluid being produced to the well only from fractures to fluid being produced from both fractures and the matrix began almost immediately after the pump was turned on. The low storativity ratio, which indicates that the vast majority of the water produced came from the matrix, provides additional evidence that the primary role of the fractures is to move water produced from the matrix to the wellbore.

The hydraulic boundaries included in the simulation in Figure 6-1 must be viewed qualitatively. Boundaries within the Culebra are not absolute, as is assumed by the analysis technique. The apparent boundaries are caused by variations in transmissivity over the area stressed by the pumping test. Thus, the meaning of the distances to the boundaries derived from the simulations is unclear. The apparent no-flow boundary revealed by the analysis probably indicates a decrease in Culebra transmissivity fairly close to WIPP-13. This correlates with the known area of low transmissivity to the east of WIPP-13, which includes, among others, wells WIPP-12, WIPP-18, WIPP-19, and H-5 (Mercer, 1983; Beauheim, 1987b). The three constant-pressure boundaries indicated by the simulation can be related to the very high transmissivities found to the west of WIPP-13 in Nash Draw, such as at wells P-14, WIPP-25, and WIPP-26 (Mercer, 1983).

Figure 6-2 shows a dimensionless Horner plot of the WIPP-13 drawdown data, along with the simulation generated by INTERPRET using the same model as in Figure 6-1. The simulation fits the data very well, indicating the model is a reasonable approximation of the physical situation. Figure 6-3 is a linear-linear plot of the drawdown data and simulation, again indicating close agreement.

Approximately 750 hr after the start of the 864-hr pumping period, the packer isolating the test interval in WIPP-13 (Figure 4-1) began to deflate. By the beginning of the recovery period, the packer was entirely deflated. Thus, the recovery of the well entailed an actual *water-level* change in the well casing, as opposed to the *pressure* change that occurred during the drawdown period when the packer was inflated. One consequence of this difference was that more wellbore storage was evident in the recovery data than in the drawdown data.

This is seen most clearly in the log-log plot of the recovery data (Figure 6-4). The best-fit simulation of these data used an initial C_De^{2s} type curve with a value of 100, as opposed to the value of 5.0 used for the drawdown simulation, indicating more wellbore storage during recovery. The pressure derivative shows an initial maximum early in the recovery curve, also indicating more wellbore storage than was present during drawdown.

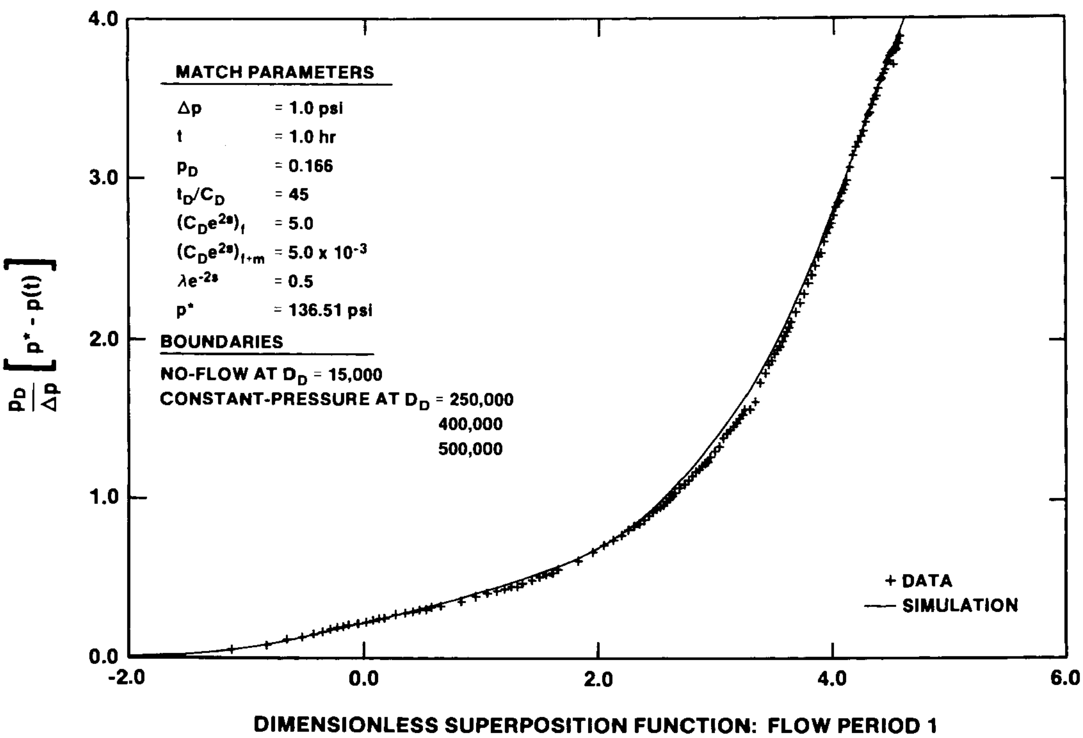

Figure 6-2. WIPP-13 Drawdown Dimensionless Horner Plot With INTERPRET Simulation

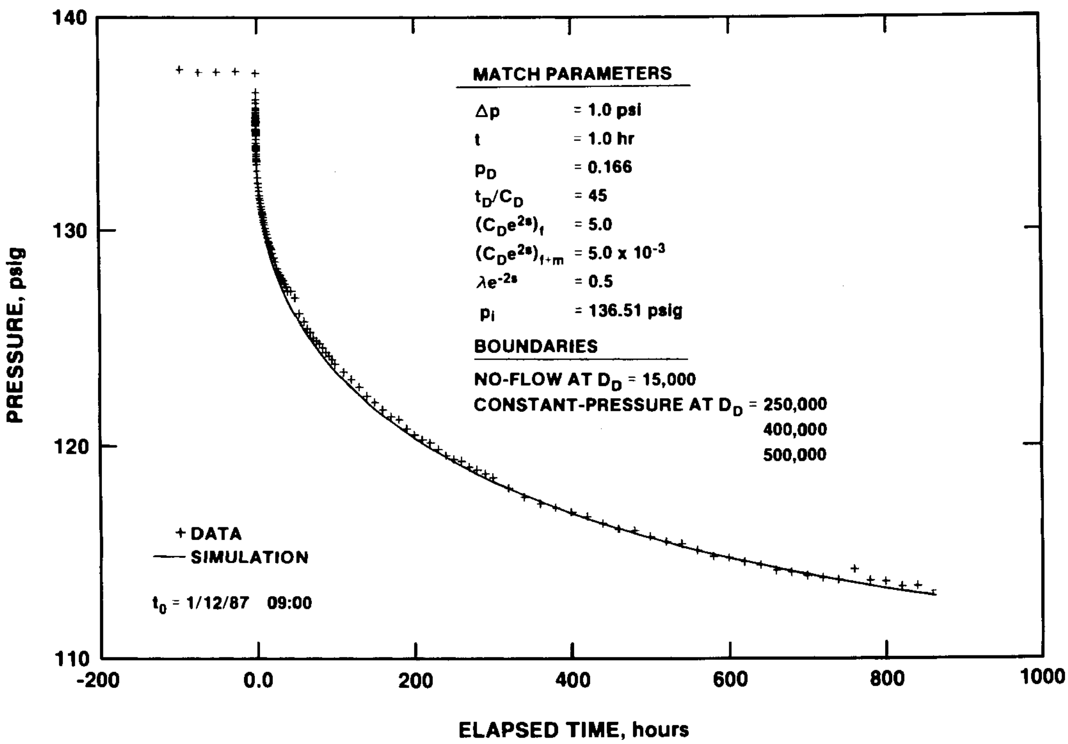

Figure 6-3. WIPP-13 Drawdown Linear-Linear Sequence Plot With INTERPRET Simulation

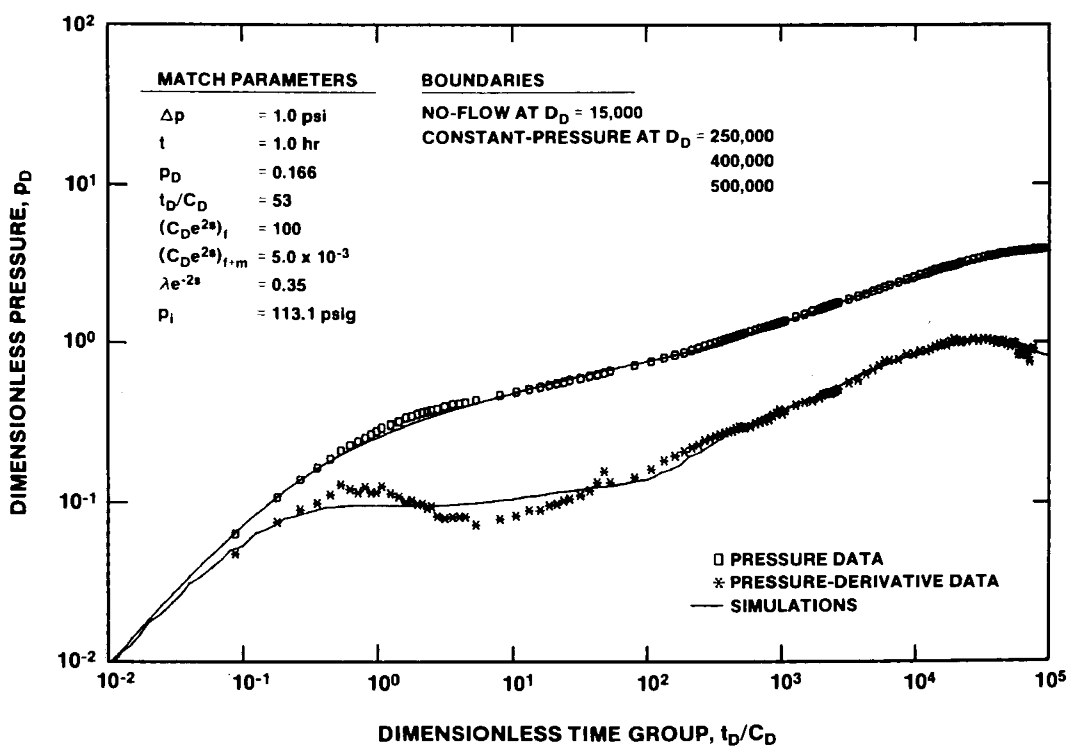

Figure 6-4. WIPP-13 Recovery Log-Log Plot With INTERPRET Simulation

The model used for the simulation in Figure 6-4 is very similar to that used for the drawdown simulations (Figures 6-1 through 6-3). The model is of a double-porosity system with slab-shaped matrix blocks, unrestricted interporosity flow, a transmissivity of 69 ft^2/day, and includes the effects of a no-flow (low-permeability) boundary relatively close (3100 ft) to WIPP-13 and three constant-pressure (high-permeability) boundaries much farther (12 800, 16 200, and 18 100 ft) from the well (corresponding distances to image wells listed in Table 6-1). The boundaries in the recovery simulation are 300 to 1500 ft (8% to 9%) closer than they are in the drawdown simulation, providing a measure of the uncertainty associated with distance determinations made by using INTERPRET. As discussed earlier, however, these boundaries should be considered qualitatively rather than quantitatively.

A dimensionless Horner plot of the recovery data and the INTERPRET simulation is shown in Figure 6-5. The agreement between the simulation and data is excellent. Figure 6-6 shows the fit between the model derived from the recovery analysis and both the drawdown and recovery data on a linear-linear plot; again, the fit is excellent.

6.2 Observation Wells

The observation-well data from the WIPP-13 multipad test were interpreted by fitting them to the line-source solution of Theis (1935) for flow in a confined porous medium, as implemented in INTERPRET (Appendix B). The line-source solution describes the response observed at an observation well sufficiently far from a pumping well that the pumping well can be approximated as a line source (or sink). The values obtained from this solution describe the properties of the aquifer between the pumping well and the observation well.

Several assumptions are implicit in the use of the line-source solution to simulate observation-well responses. One assumption is that the aquifer is areally homogeneous. This means that water is contributed to the pumping well equally from all directions. In a nonhomogeneous aquifer, less permeable regions will contribute less water, and more permeable regions will contribute more water. In a nonhomogeneous aquifer with smoothly and monotonically varying properties, this will cause more drawdown in the more permeable regions than would result from pumping at the same rate in a homogeneous system and less drawdown in the less permeable regions.

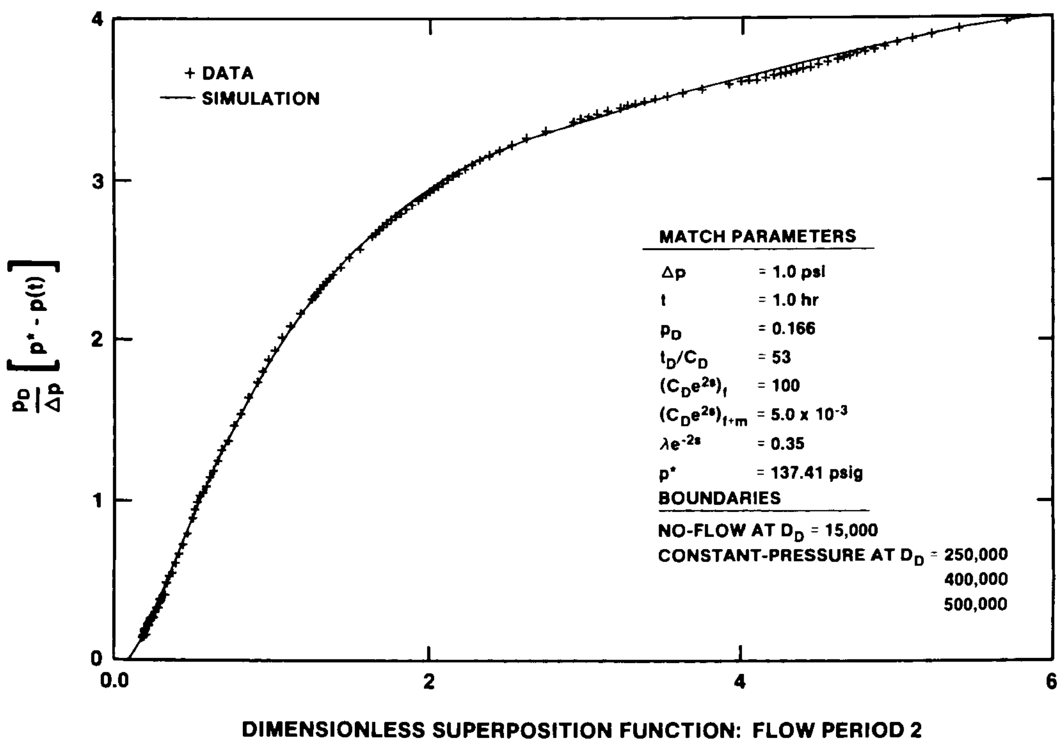

Figure 6-5. WIPP-13 Recovery Dimensionless Horner Plot With INTERPRET Simulation

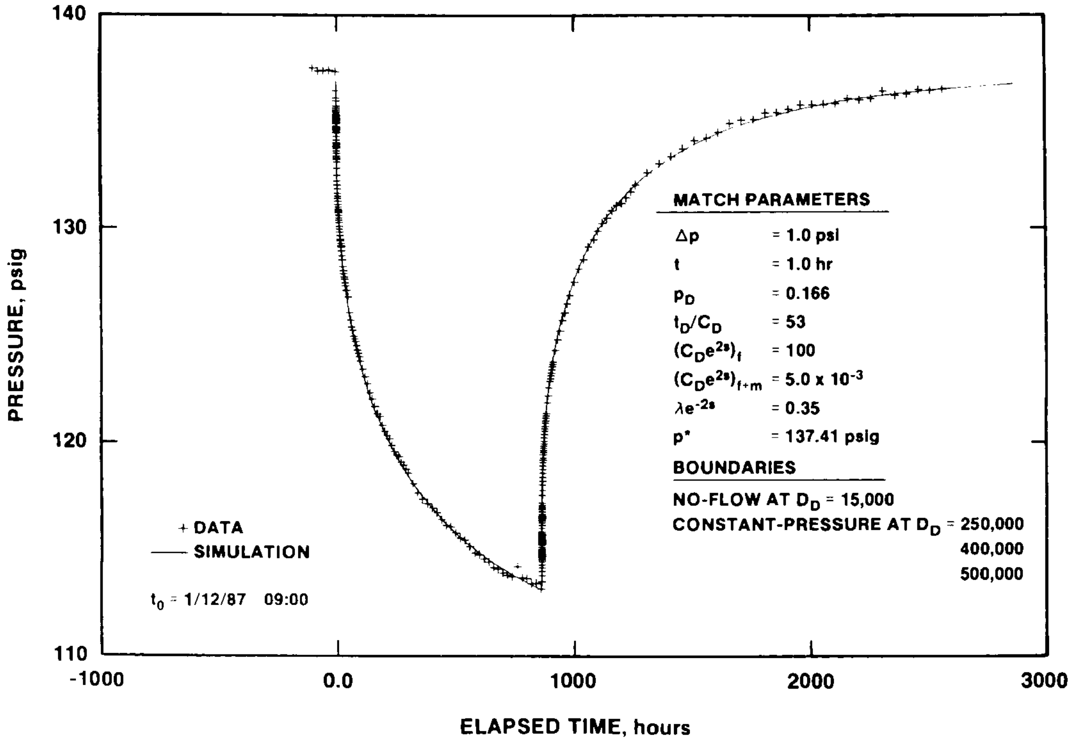

Figure 6-6. WIPP-13 Linear-Linear Sequence Plot With INTERPRET Simulation

As a result, estimates of the transmissivity between the pumping well and an observation well in a more permeable region will be too low, and estimates of the transmissivity between the pumping well and an observation well in a less permeable region will be too high. In a more complex, nonhomogeneous aquifer with an irregular distribution of properties, responses are more difficult to predict and could result in estimated hydraulic properties that are either too high or too low. Thus, the solution obtained from a single test in a nonhomogeneous aquifer is in no sense a unique description of the average hydraulic properties between any two points.

Numerical rather than analytical modeling is required to define the distribution of hydraulic properties that will best simulate the responses observed when a number of wells in a nonhomogeneous system are pumped concurrently or in succession. In this report, the transmissivity and storativity values derived by using an analytical approach are termed the "apparent" values.

A second assumption underlying the use of a line-source solution is that, on the areal scale of the observations, the aquifer behaves like a single-porosity medium. In a double-porosity medium, this assumption is justified when an observation well is far enough from the pumping well that only total-system responses are observed (Appendix B). With the nearest observation well (WIPP-12) being 4210 ft from the pumping well (Table 3-1), no measurable double-porosity effects were expected and, in fact, none were detected at any of the observation wells.

A final cautionary note is appropriate with regard to the hydraulic boundaries (image wells) used in the simulations presented below. The INTERPRET analysis code uses image wells at specific distances from the pumping and observation wells to simulate the effects of hydraulic boundaries. If these boundaries were in fact discrete hydrogeologic features such as faults or rivers intersecting the aquifer, the uncertainty in the distances presented would be, at best, $\sim \pm 10\%$. In the case of the Culebra, the boundaries are believed to represent a heterogeneous distribution of transmissivity, and the significance of the distances provided by the simulations is unclear. Consequently, the boundaries used in the simulations should not be viewed quantitatively, but should be regarded as indicators of the types of transmissivity changes occurring in different regions.

6.2.1 WIPP-12

Figure 6-7 presents the WIPP-12 pressure data modified to compensate for the pretest trend (Section 5.2), along with an INTERPRET-generated simulation of those data. The simulation shown is a line-source solution using an apparent transmissivity of

7.9 ft^2/day, an apparent storativity of 3.6 × 10^{-5}, and an image recharge well at a distance of ~7300 ft from WIPP-12 (Table 6-1). The image recharge well was necessary to make the recovery simulation rise as rapidly as the data. To whatever extent the linear compensation for the pretest trend is an overcompensation, it serves to slow the rise of the recovery data. Hence, the actual recovery might have been somewhat *more* rapid, requiring that the image recharge well be moved *closer* to WIPP-12.

Figure 6-8 shows a dimensionless Horner plot of the WIPP-12 drawdown data as well as the simulation generated by INTERPRET. The excellent fit of the simulation to the data indicates that an appropriate model has been selected. The response at WIPP-12 (and most of the other observation wells) to pumping at WIPP-13 was not sufficiently developed to make log-log data plotting and curve matching particularly informative or definitive. That is to say, no period of infinite-acting radial flow, as indicated by a stabilized pressure derivative, was reached during the test. Therefore, no log-log plots are presented of the WIPP-12 (and most other observation wells') data.

The apparent transmissivity of 7.9 ft^2/day derived from the INTERPRET simulations of the WIPP-12 data is considerably lower than the 69 ft^2/day determined for WIPP-13. As discussed earlier, this value represents an average transmissivity for the Culebra between WIPP-13 and WIPP-12. It is lower than the value for WIPP-13 because WIPP-12 lies in a low-permeability region of the Culebra. The local Culebra transmissivity derived from tests at WIPP-12 is ~0.1 ft^2/day (Beauheim, 1987b). The image recharge well used in the simulation should not be viewed quantitatively, but should be regarded as a qualitative indication of the higher permeability region lying to the west of WIPP-12.

6.2.2 WIPP-18

The WIPP-18 pressure data, modified to compensate for the pretest trend (Section 5.3), are presented in Figure 6-9 along with an INTERPRET-generated simulation of those data. The simulation shown is a line-source solution using an apparent transmissivity of 23 ft^2/day, an apparent storativity of 4.0 × 10^{-5}, and an image recharge well at a distance of ~18 700 ft (Table 6-1). As was the case with the WIPP-12 data (Section 6.2.1), the image recharge well was necessary to make the recovery simulation rise as rapidly as the data. If the linear compensation for the pretest trend is an overcompensation, the actual recovery was somewhat *more* rapid, requiring that the image recharge well be moved *closer* to WIPP-18.

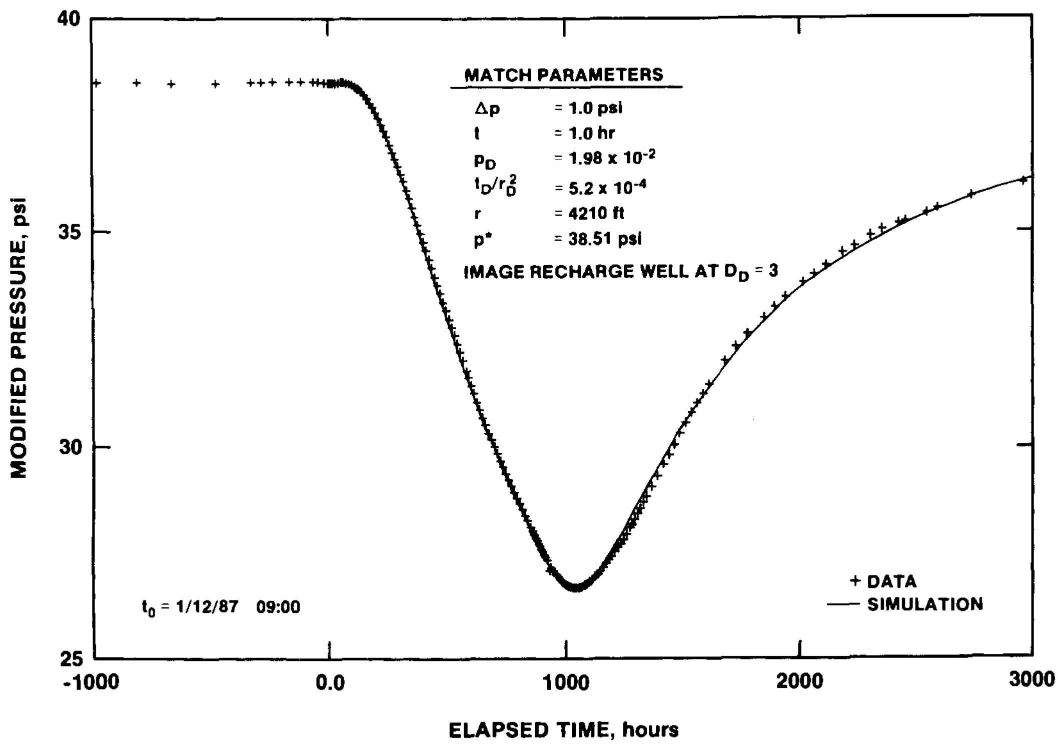

Figure 6-7. WIPP-12 Modified Pressure Response With INTERPRET Simulation

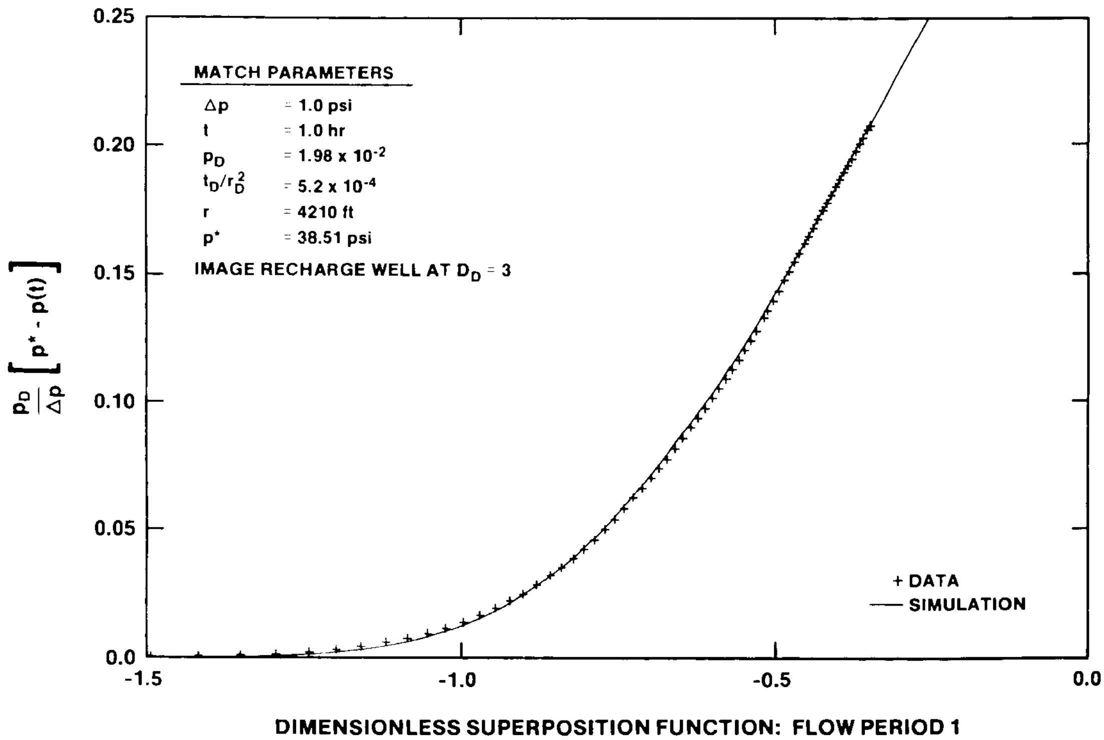

Figure 6-8. WIPP-12 Drawdown Dimensionless Horner Plot With INTERPRET Simulation

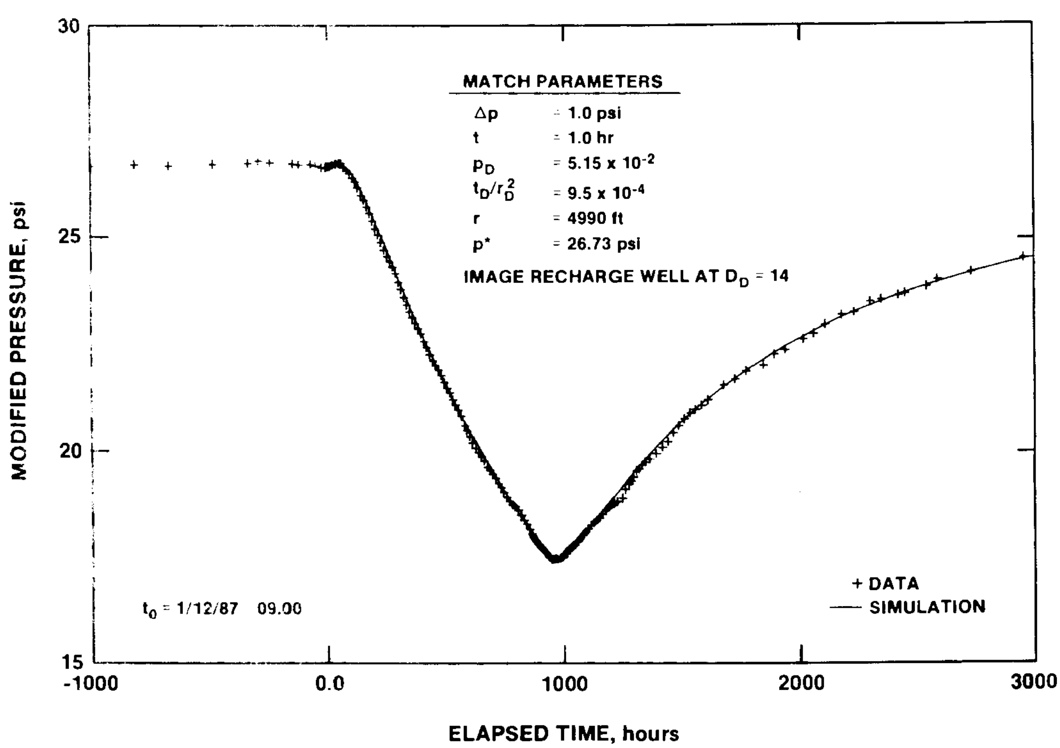

Figure 6-9. WIPP-18 Modified Pressure Response With INTERPRET Simulation

A dimensionless Horner plot of the WIPP-18 data is presented in Figure 6-10 along with the INTERPRET-generated simulation. The data and simulation agree very well. The apparent transmissivity of 23 ft^2/day obtained from the simulations is lower than the 69 ft^2/day determined for WIPP-13, but higher than the 7.9 ft^2/day determined for WIPP-12. As discussed earlier, this value represents an average transmissivity for the Culebra between WIPP-13 and WIPP-18. It is lower than the value for WIPP-13 because WIPP-18 lies in a low-permeability region of the Culebra, but it is higher than the value for WIPP-12 because the local Culebra transmissivity at WIPP-18, 0.3 ft^2/day, is higher than that at WIPP-12 (Beauheim, 1987b). The image recharge well used in the simulation should not be viewed quantitatively, but should be regarded as a qualitative indication of the higher permeability region lying to the northwest of WIPP-18.

6.2.3 WIPP-19

Figure 6-11 presents the WIPP-19 pressure data modified to compensate for the pretest trend (Section 5.4), along with an INTERPRET-generated simulation of those data. The simulation shown is a line-source solution using an apparent transmissivity of 24 ft^2/day, an apparent storativity of 4.0×10^{-5}, and an image recharge well at a distance of ~23 200 ft (Table 6-1). A dimensionless Horner plot of the drawdown data is shown in Figure 6-12 with the simulation generated using INTERPRET. As with the linear-linear plot (Figure 6-11), the data and simulation are in close agreement.

The apparent transmissivity of 24 ft^2/day used in the WIPP-19 simulations is lower than the 69 ft^2/day determined for WIPP-13 because WIPP-19 lies in a low-permeability region of the Culebra (Beauheim, 1987b). The image recharge well used in the simulation should not be interpreted as a quantitative measure of the distance to a boundary, but should be viewed as a qualitative indication of the higher permeability region lying to the northwest of WIPP-19. Note also that the simulated distance to the image recharge well is partly dependent on the pretest-trend compensation used for the WIPP-19 data.

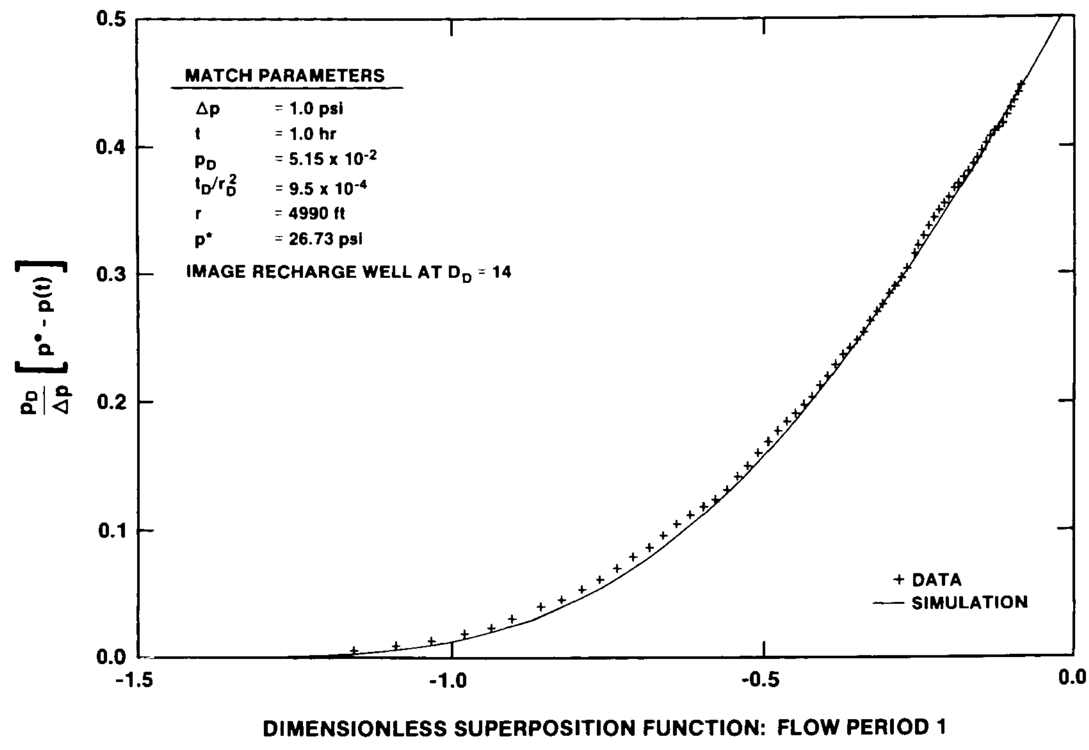

Figure 6-10. WIPP-18 Drawdown Dimensionless Horner Plot With INTERPRET Simulation

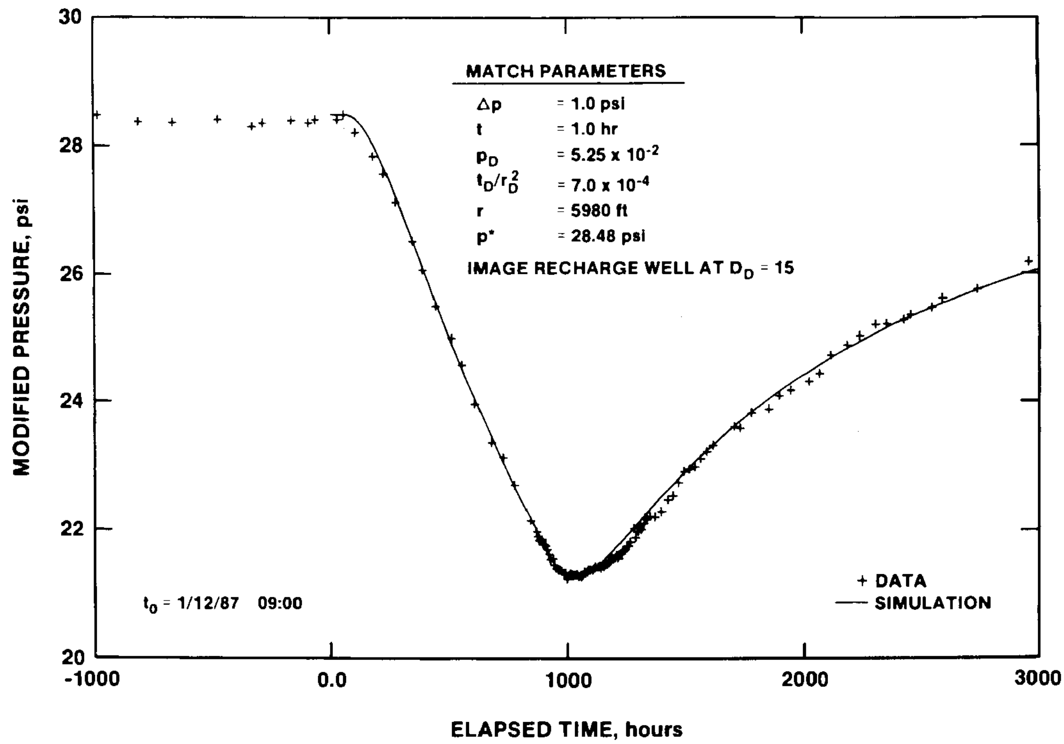

Figure 6-11. WIPP-19 Modified Pressure Response With INTERPRET Simulation

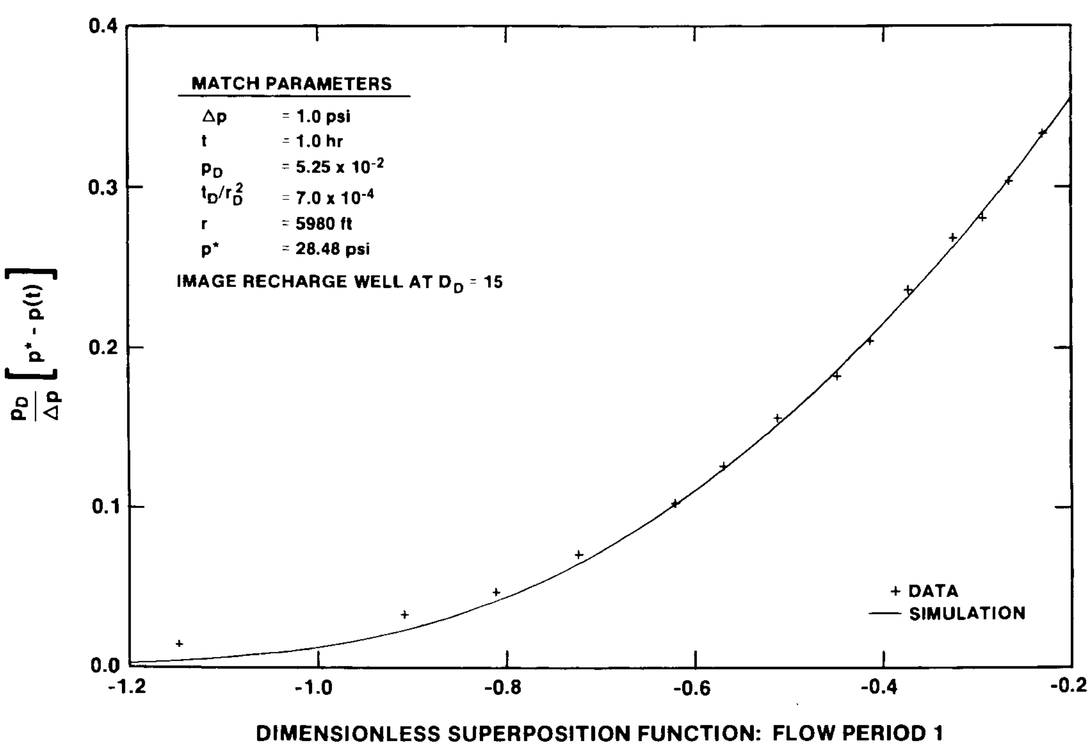

Figure 6-12. WIPP-19 Drawdown Dimensionless Horner Plot With INTERPRET Simulation

6.2.4 WIPP-21

Figure 6-13 presents the WIPP-21 pressure data compensated for barometric effects and the pretest trend (Section 5.5), along with the best-fit simulation of those data generated by INTERPRET. The simulation employs a line-source solution with an apparent transmissivity of 22 ft^2/day, an apparent storativity of 5.3×10^{-5}, and an image recharge well at a distance of ~19 200 ft (Table 6-1). The simulation does not fit the data quite as well as do the simulations for WIPP-12 (Figure 6-7), WIPP-18 (Figure 6-9), and WIPP-19 (Figure 6-11), primarily because the plotted WIPP-21 data are not as regular as are the data from those other wells. The more irregular behavior of the WIPP-21 data may reflect pressure changes in the Culebra caused by leakage from the Culebra into one or more of the nearby shafts at the WIPP site (see Sections 6.2.13 and 6.2.14).

Regardless of any potential minor shaft influences on the WIPP-21 data, the best-fit simulation is very consistent with those for WIPP-18 and WIPP-19. The apparent transmissivity of 22 ft^2/day derived from the WIPP-21 data is similar in magnitude to the values determined from the WIPP-18 and WIPP-19 data (Table 6-1) and is lower than the 69 ft^2/day determined for WIPP-13 because WIPP-21 lies in a low-permeability region of the Culebra (Beauheim, 1987b). The image recharge well used in the simulation (whose modeled location is dependent in part on the pretest trend compensation used) should not be interpreted as a quantitative measure of the distance to a boundary, but should be viewed as a qualitative indication of the higher permeability region lying to the northwest of WIPP-21.

6.2.5 WIPP-22

The WIPP-22 pressure data, modified to compensate for the pretest trend (Section 5.6), are presented in Figure 6-14 along with an INTERPRET-generated simulation of those data. The simulation shown is a line-source solution using an apparent transmissivity of 19 ft^2/day, an apparent storativity of 4.7×10^{-5}, and an image recharge well at a distance of ~14 200 ft (Table 6-1). The apparent transmissivity of 19 ft^2/day is lower than the 69 ft^2/day determined for WIPP-13 because WIPP-22 lies in the same low-permeability region of the Culebra as WIPP-18, WIPP-19, and WIPP-21 (Beauheim, 1987b). The image recharge well used in the simulation (whose modeled location is dependent in part on the pretest trend compensation used) should not be interpreted as a quantitative measure of the distance to a boundary, but should be viewed as a qualitative indication of the higher permeability region lying to the northwest of WIPP-22.

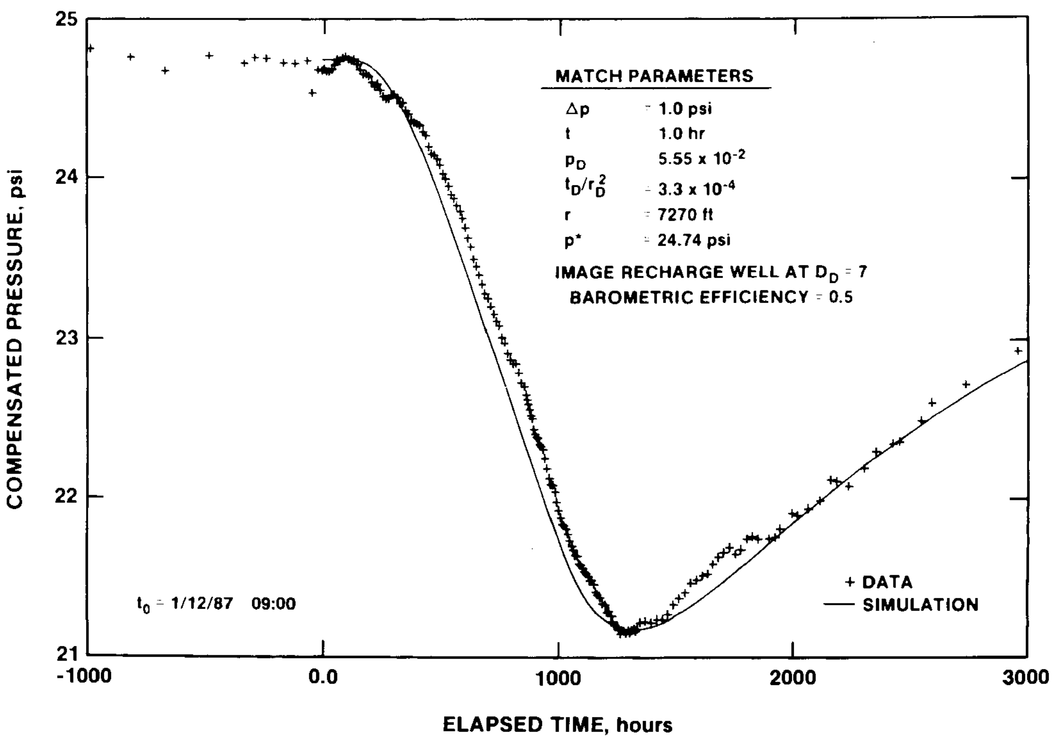

Figure 6-13. WIPP-21 Compensated Pressure Response With INTERPRET Simulation

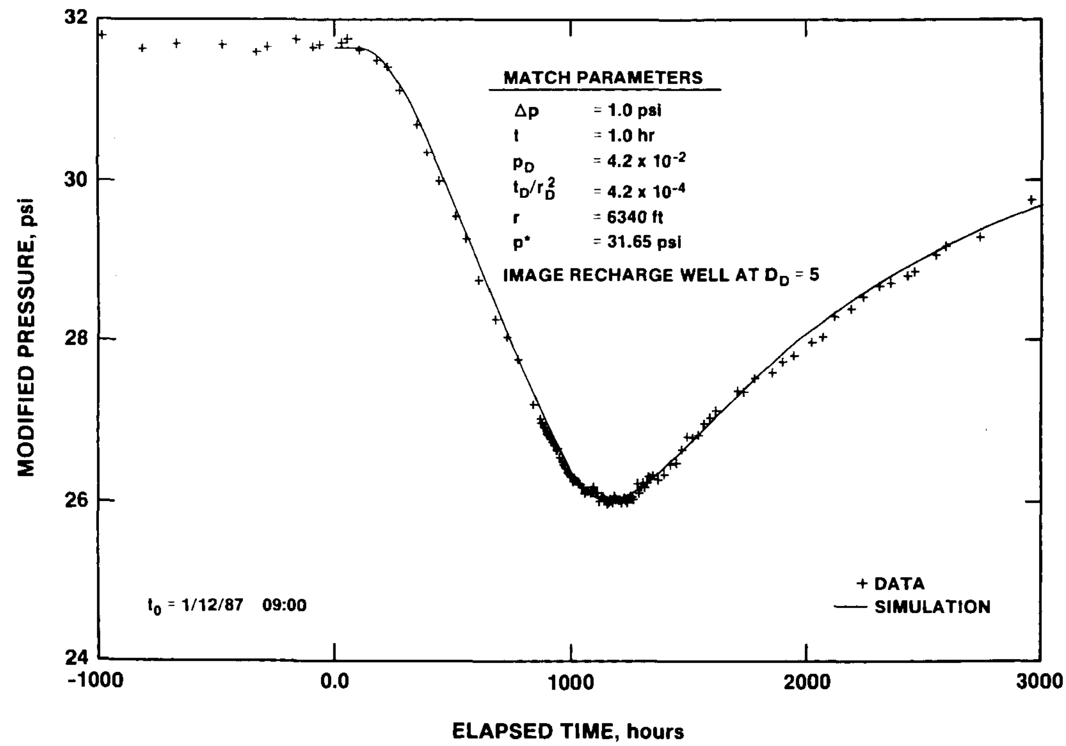

Figure 6-14. WIPP-22 Modified Pressure Response With INTERPRET Simulation

6.2.6 WIPP-25

Figure 6-15 presents the WIPP-25 pressure data compensated for barometric effects (Section 5.7), along with a simulation of those data generated by INTERPRET. The simulation uses a line-source solution with an apparent transmissivity of 650 ft^2/day and an apparent storativity of 6.4×10^{-5} (Table 6-1). Even with the barometric correction, the data are somewhat scattered, resulting in a moderate degree of uncertainty in the fit of the simulation to the data. No specific need for any type of hydraulic boundary was indicated by the simulation.

The apparent transmissivity of 650 ft^2/day is considerably higher than both the 69 ft^2/day determined for WIPP-13 alone and the local Culebra transmissivity at WIPP-25 of 270 ft^2/day reported by Mercer (1983). This may reflect either the presence of a zone with extremely high transmissivity between WIPP-13 and WIPP-25, similar to the areas around WIPP-26 and WIPP-27 (Mercer, 1983), or a general diminution of the magnitude of the pressure front from WIPP-13 as it began to expand westward into the high-transmissivity region represented by Nash Draw.

6.2.7 WIPP-30

The WIPP-30 pressure data, compensated for the pretest trend (Section 5.8), are shown in Figure 6-16 along with a simulation of those data generated by INTERPRET. The simulation is a line-source solution using an apparent transmissivity of 28 ft^2/day, an apparent storativity of 5.6×10^{-6}, and an image recharge well at a distance of ~40 900 ft (Table 6-1). A dimensionless Horner plot of the WIPP-30 drawdown data and simulation is shown in Figure 6-17. The simulation fits the data as well by using this plotting technique as it does on the linear-linear plot (Figure 6-16), indicating that an appropriate model has been selected. As discussed in reference to WIPP-12 and other wells, the modeled location of the image recharge well used in these simulations is dependent in part on the pretest trend compensation used. Furthermore, the need for this image well in the simulations should be interpreted only as a qualitative indication of the WIPP-30 response being affected by a higher permeability region.

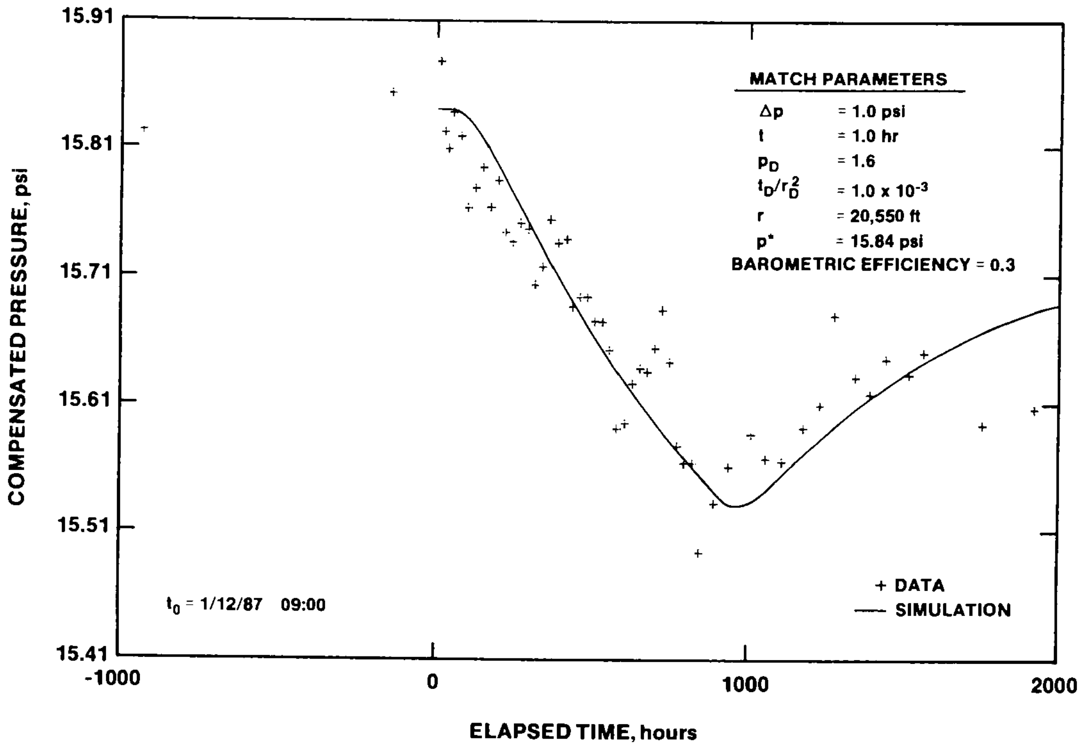

Figure 6-15. WIPP-25 Compensated Pressure Response With INTERPRET Simulation

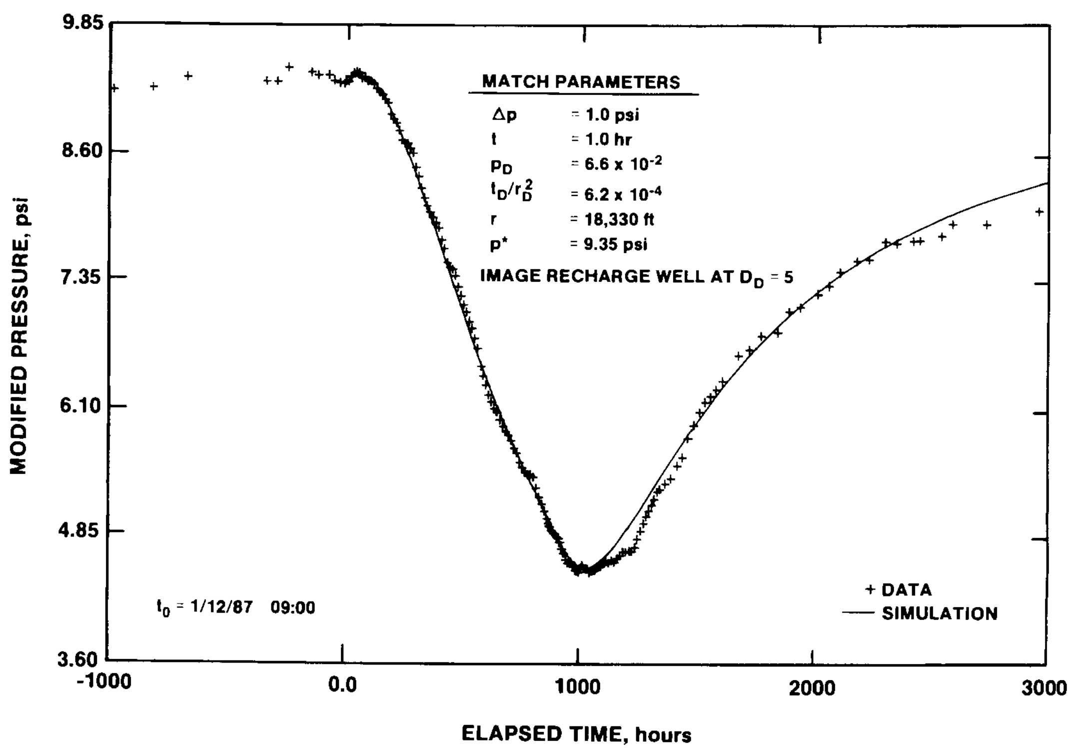

Figure 6-16. WIPP-30 Modified Pressure Response With INTERPRET Simulation

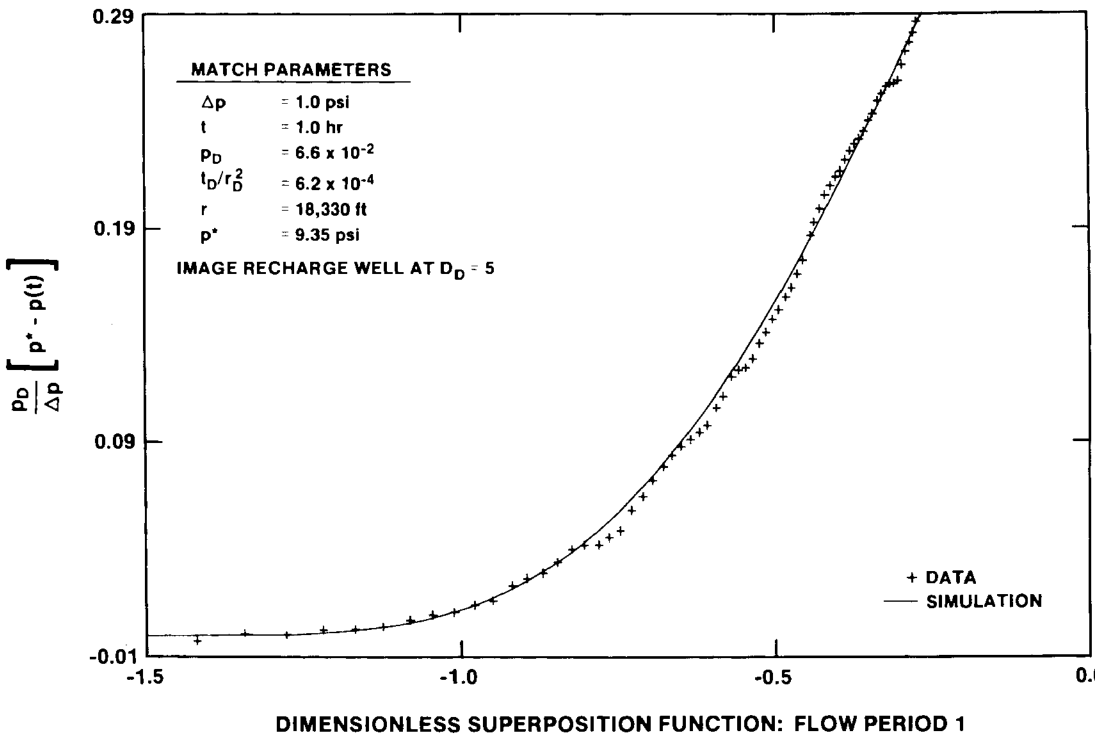

Figure 6-17. WIPP-30 Drawdown Dimensionless Horner Plot With INTERPRET Simulation

The WIPP-30 response and simulations are interesting for several reasons. First, a higher magnitude drawdown response was observed at WIPP-30 than at other observation wells closer to WIPP-13 (Table 5-1) with comparably low local values of transmissivity (Beauheim, 1987b; Mercer, 1983). Second, the apparent storativity indicated by the simulations, 5.6×10^{-6}, is about an order of magnitude lower than the values used in the simulations of the data from the WIPP-series wells to the southeast of WIPP-13 (Table 6-1). Given these observations, the high-transmissivity fractured region known to exist in the area of WIPP-13, H-6, and DOE-2 must extend closer to WIPP-30 to the north than it does to the wells such as WIPP-21, ERDA-9, H-1, and H-2 to the south (Figure 1-1).

6.2.8 H-1

Figure 6-18 presents the H-1 pressure data, compensated for the pretest trend (Section 5.9), along with an INTERPRET-generated simulation of those data. An important feature of this plot is that, after the pretest trend compensation was made, no actual recovery (i.e., pressure rise) was evident by the end of the monitoring period. The lack of a recovery limb on the data curve decreases the uniqueness of any simulation. For example, the simulation shown in Figure 6-18 is of a line-source solution using an apparent transmissivity of 20 ft^2/day, an apparent storativity of 1.3×10^{-4}, and no image wells (Table 6-1). Figure 6-19 shows an alternative simulation that fits the data equally well by using the same line-source solution and similar hydraulic properties, but with an image recharge well at a distance of ~17 600 ft (Table 6-1). The presence or absence of such an image well is most conclusively manifested during recovery, but as noted earlier, recovery data are lacking in this instance.

The apparent transmissivity and storativity values do not change appreciably between the two H-1 simulations presented, indicating that they are reliable estimates of the average properties between WIPP-13 and H-1 for this test configuration. The existence of some type of recharge boundary is more problematic; it cannot be conclusively supported by the H-1 data alone, but its effects are evident in the data from other nearby wells such as WIPP-21 (Section 6.2.4), H-2b2 (Section 6.2.9), and ERDA-9 (Section 6.2.13).

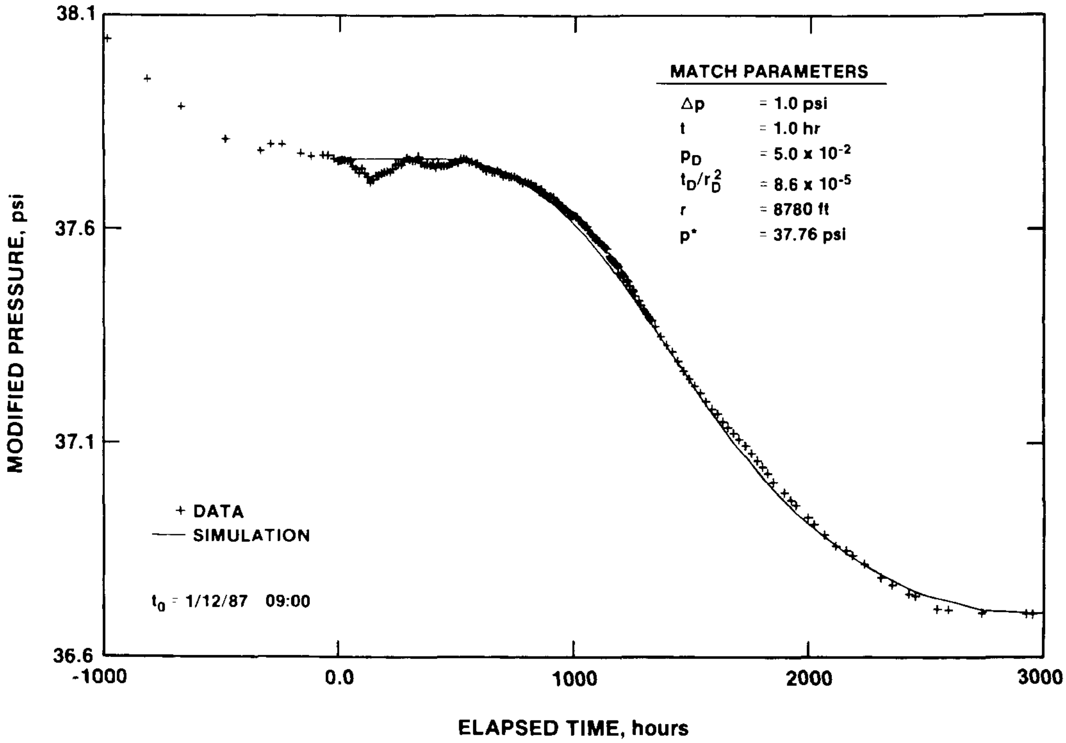

Figure 6-18. H-1 Modified Pressure Response With INTERPRET Simulation Incorporating No Boundaries

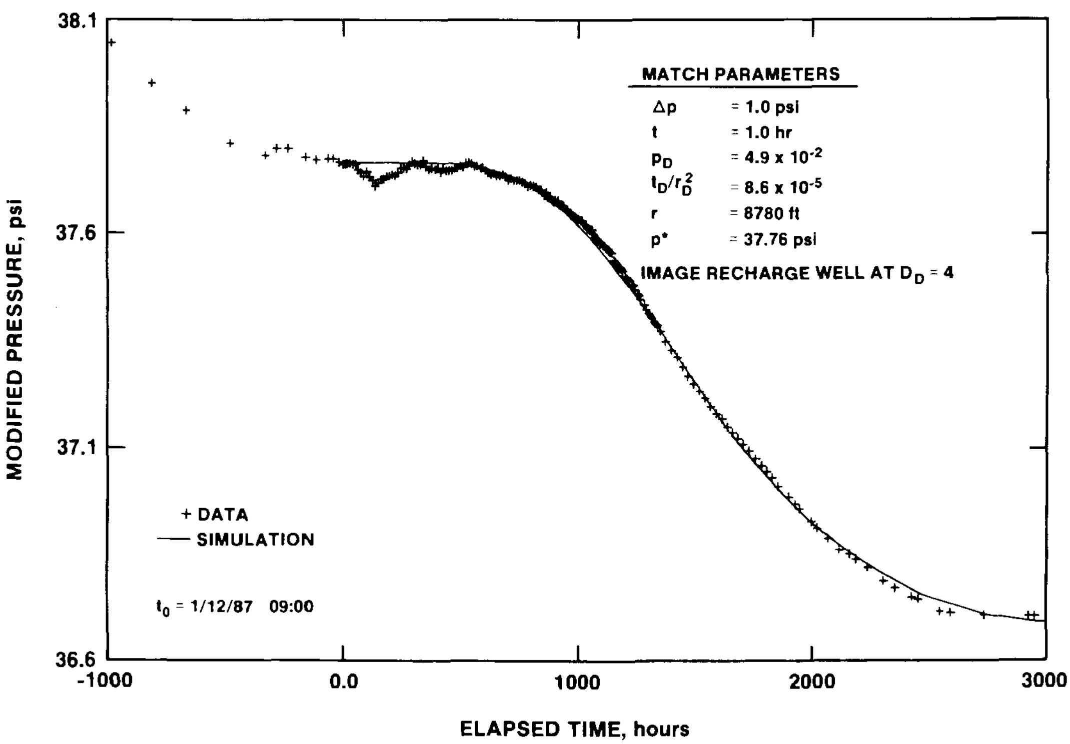

Figure 6-19. H-1 Modified Pressure Response With INTERPRET Simulation Incorporating a Recharge Boundary

6.2.9 H-2b2

Figure 6-20 presents the H-2b2 pressure data compensated for barometric effects and the pretest trend (Section 5.10), along with the best-fit simulation of those data generated by INTERPRET. The simulation uses a line-source solution with an apparent transmissivity of 16 ft^2/day, an apparent storativity of 7.3×10^{-5}, and an image recharge well at a distance of ~12 000 ft (Table 6-1). This apparent transmissivity is the lowest value obtained for any of the wells south and southeast of WIPP-13. The reason for this is unclear, but may be related to the distribution of heterogeneity within the Culebra. As discussed earlier with reference to the responses of the WIPP-series wells lying southeast of WIPP-13, the image recharge well used in the H-2b2 simulation should be viewed as a qualitative indication of the higher permeability regions of the Culebra lying north and west of H-2b2.

6.2.10 H-6a and H-6b

The H-6a pressure data and an INTERPRET-generated simulation of those data are presented in Figure 6-21. The simulation is based on a line-source solution with an apparent transmissivity of 71 ft^2/day, an apparent storativity of 8.2×10^{-6}, and an image recharge well at a distance of ~50 800 ft (Table 6-1). The H-6a response to pumping was sufficiently well developed to allow a reasonably definitive log-log simulation match to the data. Figure 6-22 shows a log-log plot of the H-6a drawdown data along with the line-source solution simulation discussed earlier. The fit of the simulation to the pressure data is excellent.

The pressure-derivative data are fairly noisy, but the simulation shows that the effects of the recharge well or boundary (indicated by the declining derivative in the simulation) were not significantly manifested by the end of the drawdown period. The effects of the boundary were more evident in the recovery data. This is shown in Figure 6-21 by an alternative simulation lacking a boundary that fits the drawdown data well, but falls below the recovery data at late time.

Figure 6-23 shows a linear-linear plot of the H-6b pressure data and simulation. This simulation is very similar to that for H-6a, using a line-source solution with an apparent transmissivity of 69 ft^2/day, an apparent storativity of 7.9×10^{-6}, and an image recharge well at a distance of ~50 800 ft (Table 6-1).

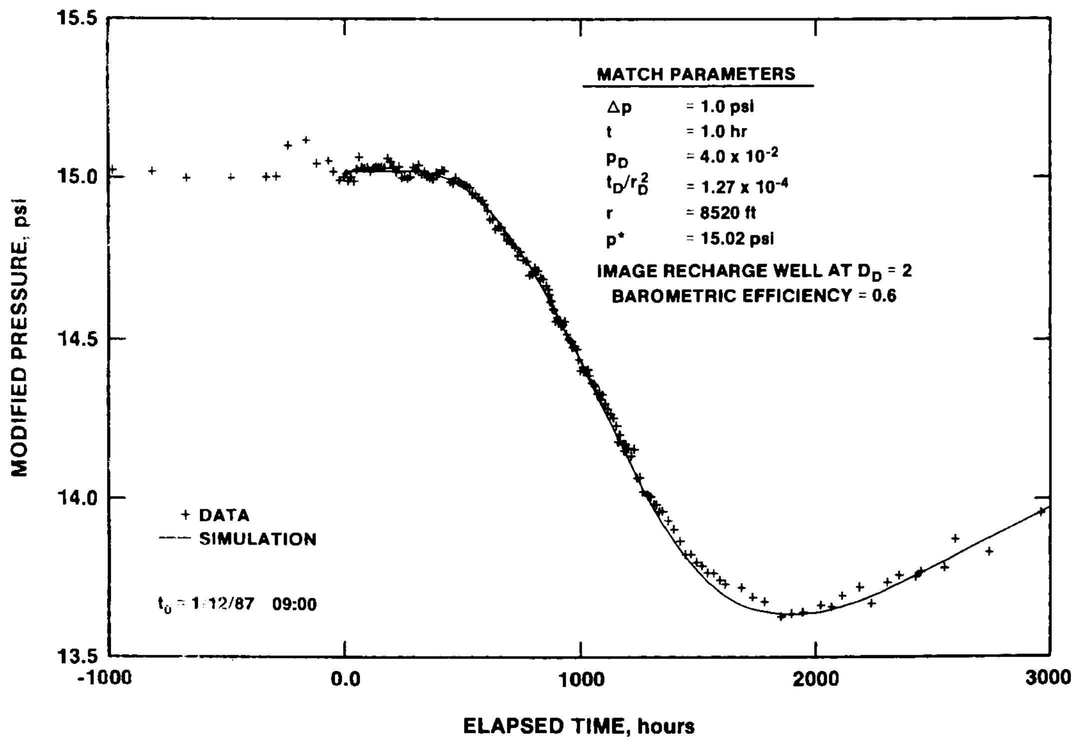

Figure 6-20. H-2b2 Modified Pressure Response With INTERPRET Simulation

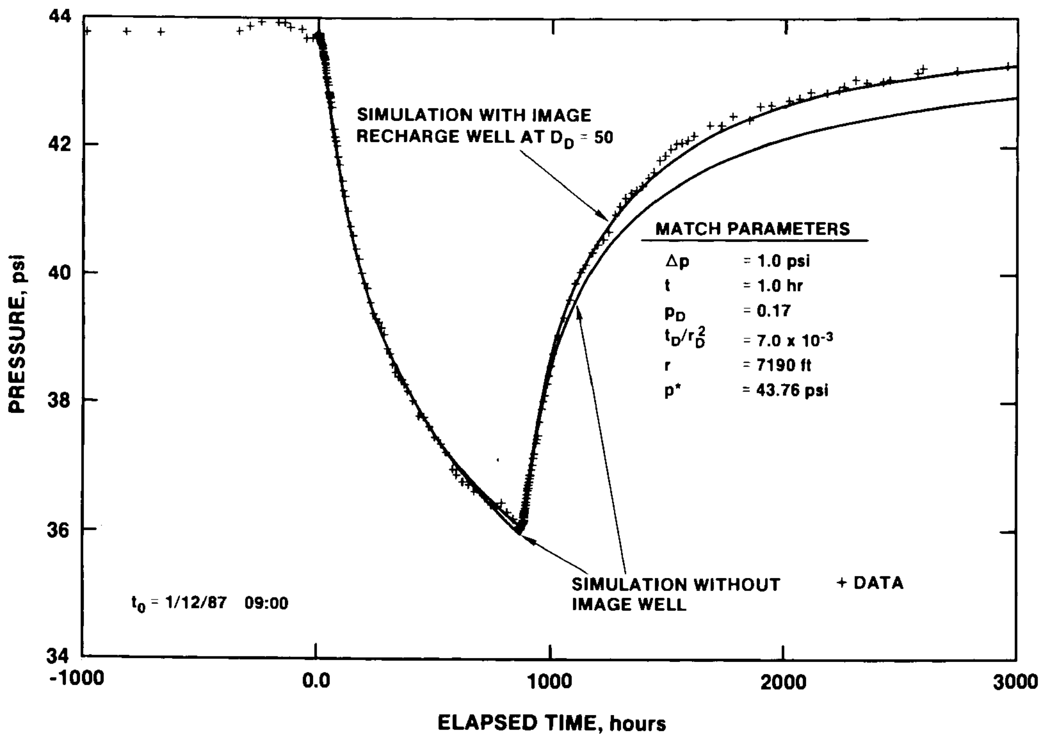

Figure 6-21. H-6a Pressure Response With INTERPRET Simulation

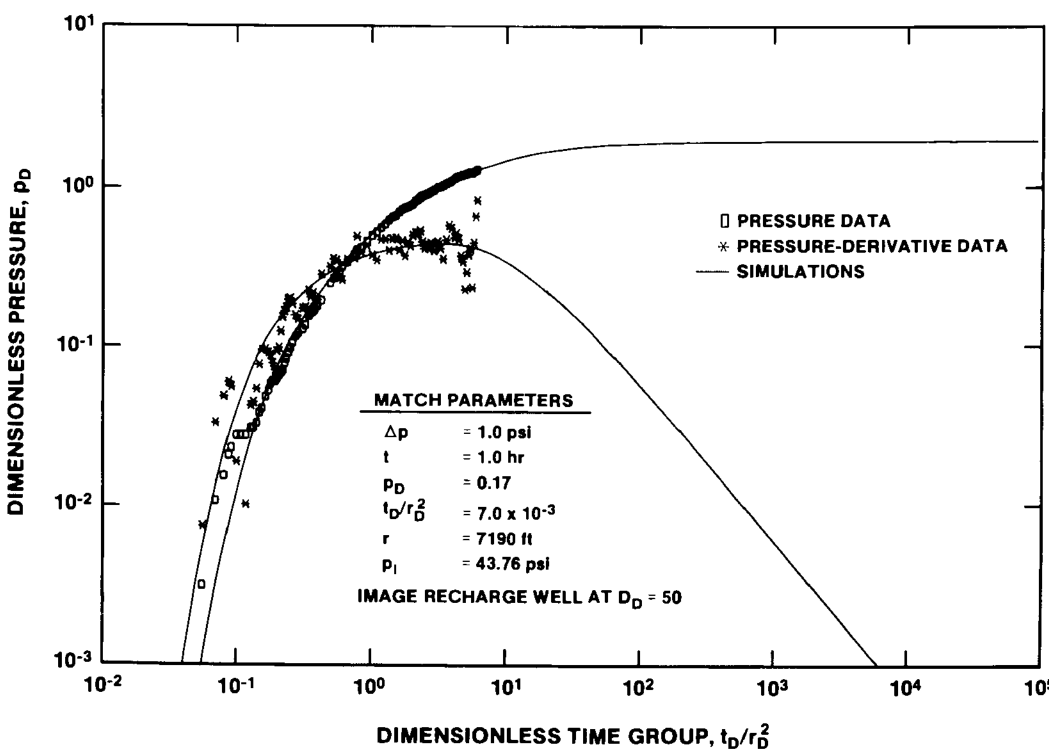

Figure 6-22. H-6a Drawdown Log-Log Plot With INTERPRET Simulation

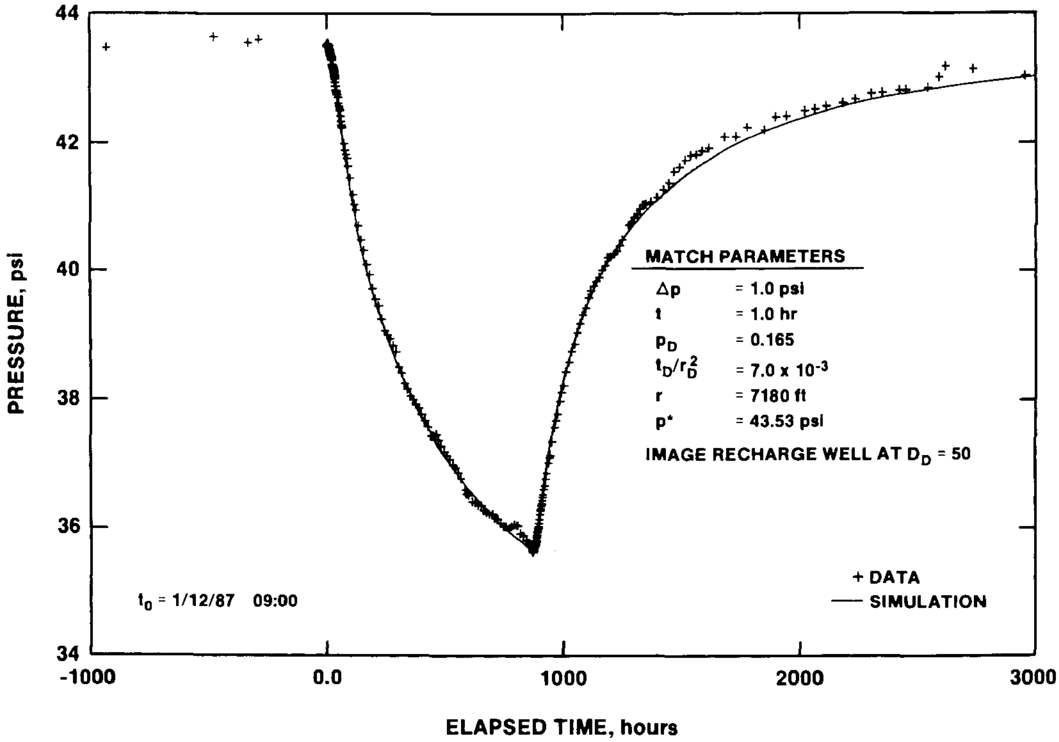

Figure 6-23. H-6b Pressure Response With INTERPRET Simulation

The close agreement between the two H-6 apparent transmissivity values and the transmissivity obtained for WIPP-13 indicates that the Culebra is reasonably homogeneous between WIPP-13 and H-6. These apparent transmissivity values are also in close agreement with the local H-6b transmissivity of 73 ft^2/day reported by Mercer (1983), again indicating relative homogeneity in this region. The image recharge well used in the H-6 simulations probably reflects an increase in Culebra transmissivity toward Nash Draw to the west.

6.2.11 DOE-2

DOE-2 was the first well at which a response to pumping at WIPP-13 was observed (Table 5-1). The continued response at DOE-2 was also more developed than those observed at other wells in terms of approaching late-time behavior representative of infinite-acting radial flow and providing a clearer definition of boundary effects. Figure 6-24 shows a linear-linear plot of the DOE-2 pressure data, as well as the best-fit simulation of those data generated with INTERPRET.

This simulation is a line-source solution with an apparent transmissivity of 57 ft^2/day, an apparent storativity of 5.1×10^{-6}, an image discharge well at a distance of ~15 300 ft, and image recharge wells at distances of ~34 200 and ~48 400 ft (Table 6-1). The log-log plot of the DOE-2 drawdown data (Figure 6-25) shows a reasonably definitive match to the simulation curves, except at early time. The early-time difference between the data and the simulation is probably related to wellbore-storage effects not accounted for in the line-source solution.

The image wells used in the DOE-2 simulation are similar to those used in the WIPP-13 simulation (Section 6.1). The relatively close image discharge well probably relates to the several-orders-of-magnitude decrease in transmissivity known to occur between DOE-2 and H-5 to the east (Mercer, 1983) and WIPP-12 to the south (Beauheim, 1987b). The more-distant image recharge wells probably relate to the increase in Culebra transmissivity that occurs to the west toward Nash Draw (Mercer, 1983). The relative consistency between the transmissivity value obtained for WIPP-13 (69 ft^2/day, Table 6-1) and the apparent transmissivity of 57 ft^2/day obtained from the DOE-2 data indicates greater Culebra homogeneity between WIPP-13 and DOE-2 than between WIPP-13 and the WIPP-series wells to the southeast of WIPP-13.

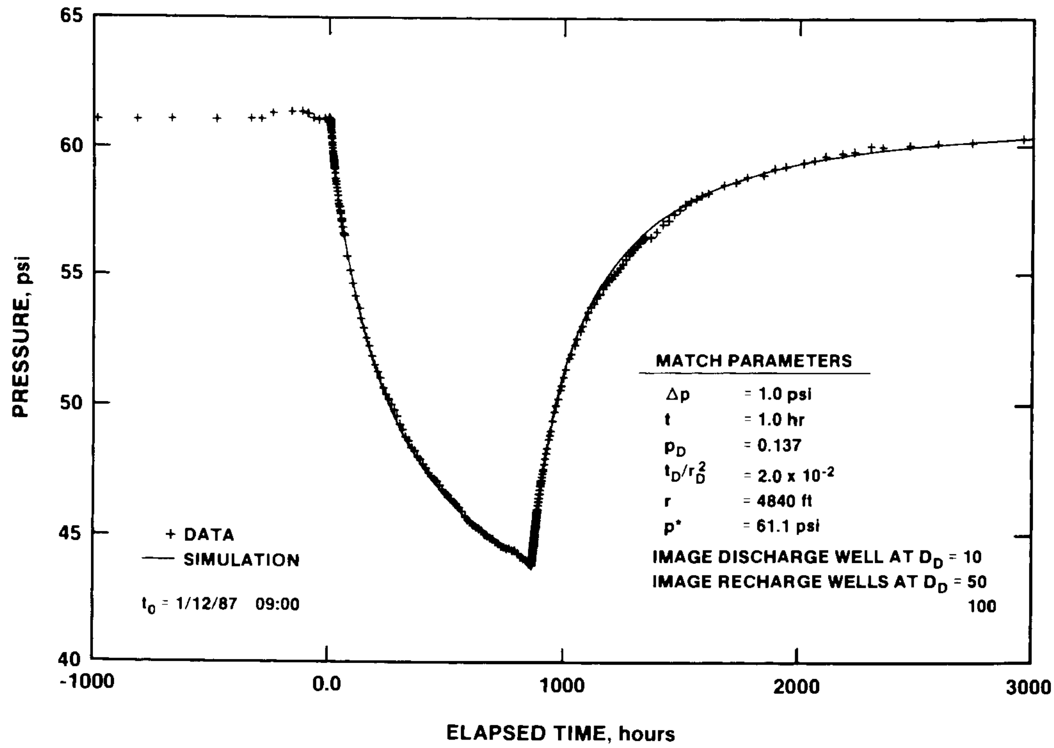

Figure 6-24. DOE-2 Pressure Response With INTERPRET Simulation

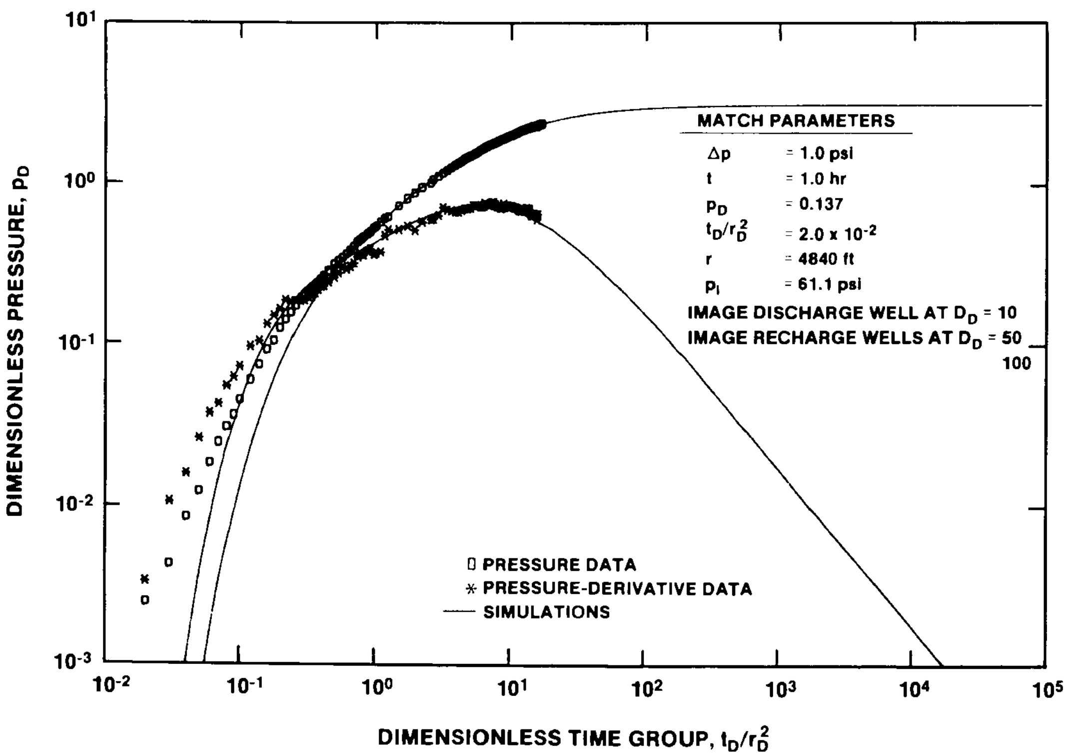

Figure 6-25. DOE-2 Drawdown Log-Log Plot With INTERPRET Simulation

6.2.12 P-14

Figure 6-26 shows the P-14 pressure data compensated for barometric-pressure effects (Section 5.16), as well as the best-fit simulation of those data generated using INTERPRET. The simulation uses a line-source solution with an apparent transmissivity of 265 ft^2/day, an apparent storativity of 5.2 $\times$ 10^{-5}, and an image recharge well at a distance of ~43 900 ft (Table 6-1). The simulation fits the data very well throughout most of the test period. Beginning ~2000 hr after pumping began, however, the pressure data show a sharp decline for an unknown reason for several hundred hours before resuming recovery (Figure 6-26).

Figure 6-27 shows a dimensionless Horner plot of the P-14 drawdown data and simulation. The simulation fits the data as well by using this plotting technique as it does on the linear-linear plot (Figure 6-26), indicating that an appropriate model has been selected. The apparent transmissivity of 265 ft^2/day used in the P-14 simulations is almost twice as great as the local transmissivity of 140 ft^2/day reported by Mercer and Orr (1979) for P-14. This high apparent transmissivity and the need for an image recharge well in the simulation both are indicative of increasing transmissivity from WIPP-13 toward P-14 and Nash Draw.

6.2.13 ERDA-9

The ERDA-9 pressure data, compensated for the pretest trend (Section 5.17), are shown in Figure 6-28 along with the best-fit simulation obtained by using INTERPRET. The simulation is a line-source solution with an apparent transmissivity of 22 ft^2/day, an apparent storativity of 5.4 $\times$ 10^{-5}, and an image recharge well at a distance of ~11 700 ft (Table 6-1). The simulation does not fit the data particularly well, but does duplicate the total amount of drawdown measured and the time at which recovery began. The parameters used in the simulation are also very consistent with those used in the simulations of the responses of the WIPP-series wells located north of ERDA-9 (Table 6-1).

Several features of the ERDA-9 response shown in Figure 6-28 appear anomalous. First, drawdown appears to begin very sharply several hundred hours after the simulation indicates it should have begun. Second, recovery also appears to begin quite sharply, with little transition from the drawdown response, and initially proceeds more rapidly than the simulation. Third, ~1700 hr after the beginning of pumping (~800 hr since the pump was turned off), the ERDA-9 pressure stopped rising and began to drop for ~300 hr before recovery resumed. Slight decreases in the rates of pressure recovery at WIPP-21 (Figure 6-13) and the exhaust shaft (Figure 5-19) were also noted at about this same time.

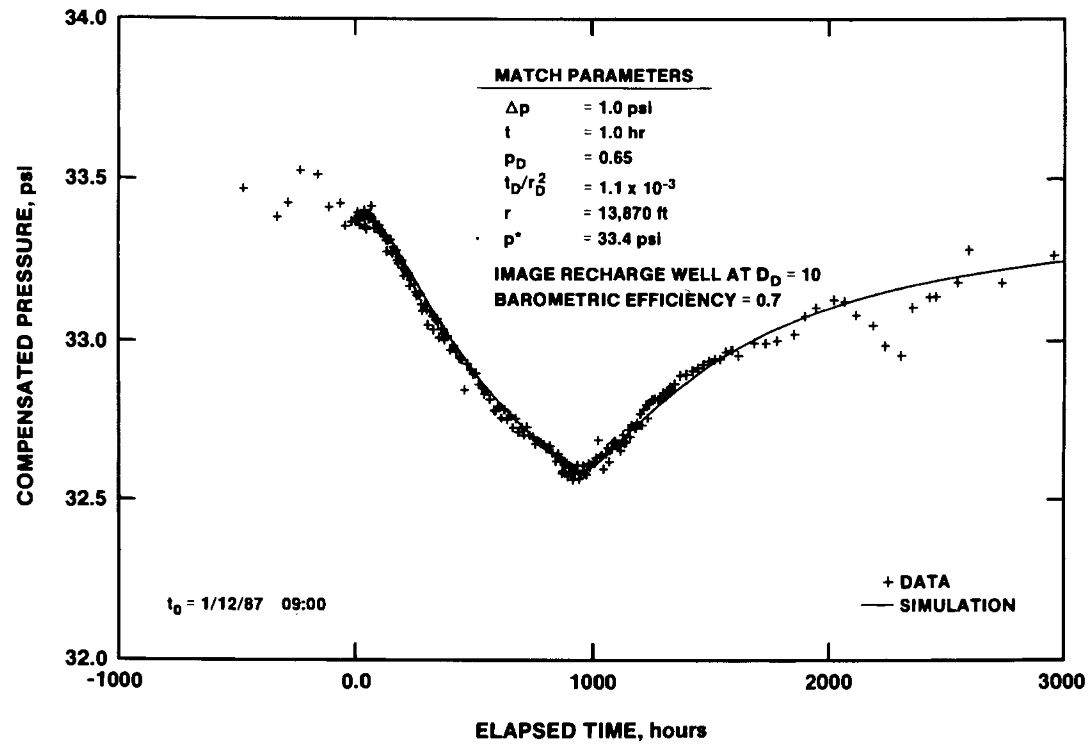

Figure 6-26. P-14 Compensated Pressure Response With INTERPRET Simulation

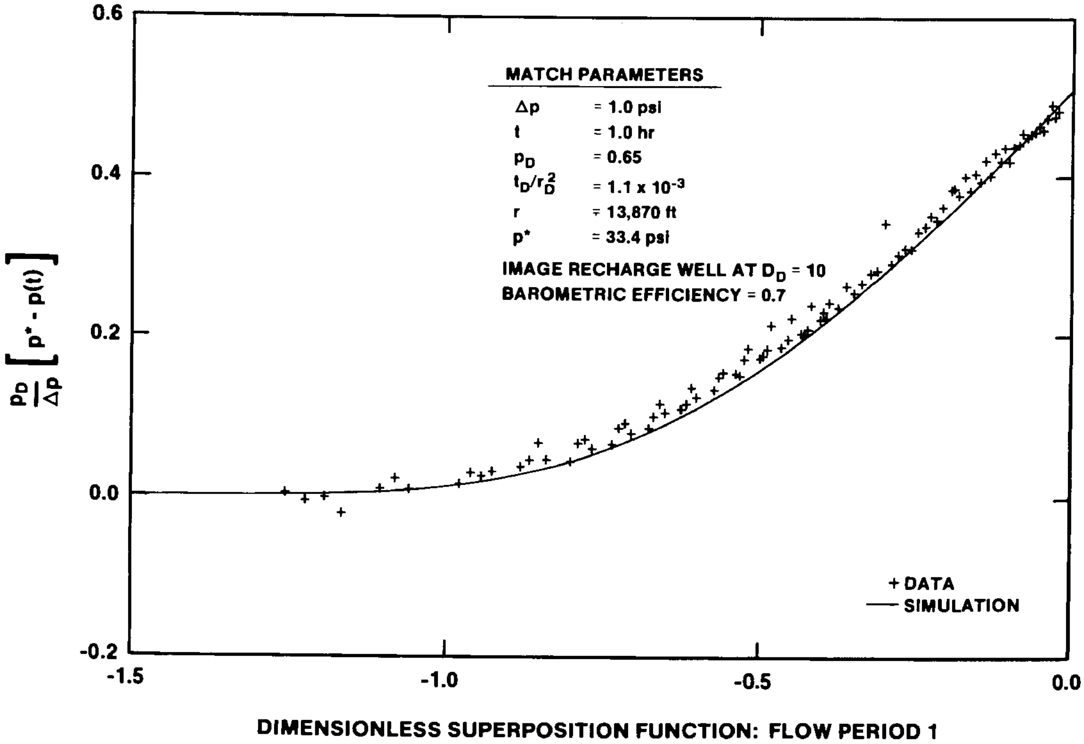

Figure 6-27. P-14 Drawdown Dimensionless Horner Plot With INTERPRET Simulation

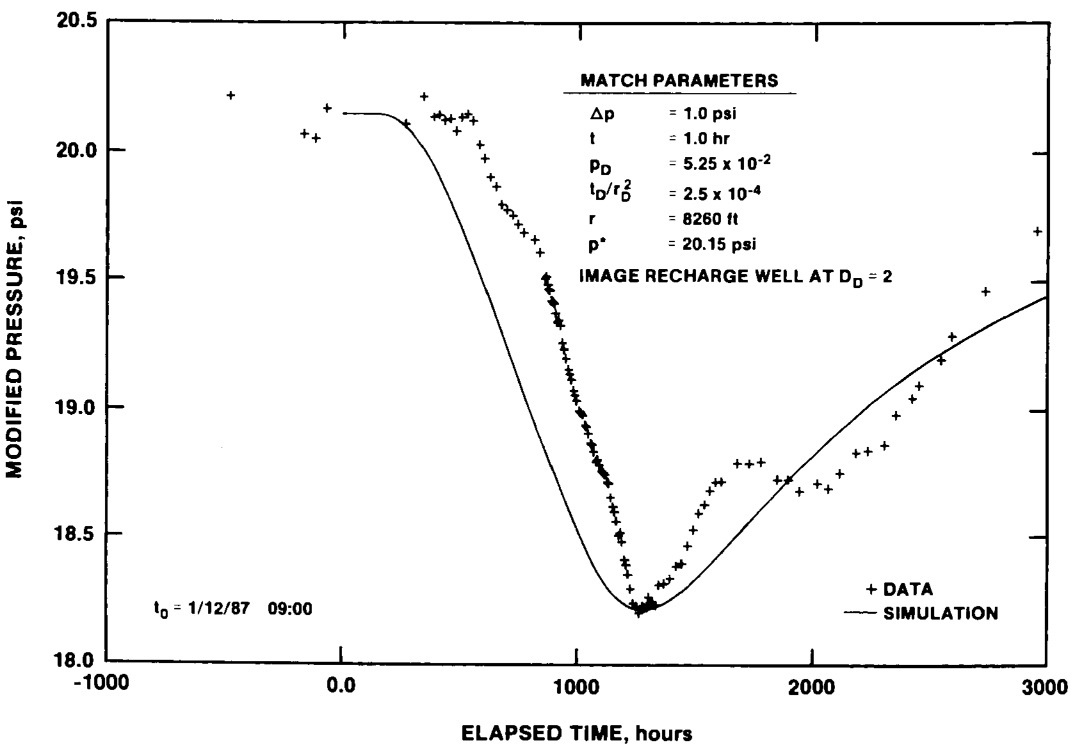

Figure 6-28. ERDA-9 Modified Pressure Response With INTERPRET Simulation

These observations indicate that ERDA-9 may not have been responding only to the pumping of WIPP-13. The drawdown in the middle of the recovery period in particular appears to be a response to a separate event. No nearby wells were pumped during this period (Stensrud et al., 1987), leaving only the WIPP-site shafts as potential candidates for the source of this response. The exhaust shaft response (Figure 5-19) appears to be too small to be a direct measure of an event that could have caused the response observed at ERDA-9. No pressure or leakage data are available from the C&SH shaft over this period, but that shaft has no history of significant leakage from the Culebra. The waste-handling shaft, for which leakage from the Culebra is better documented (Haug et al., 1987), is the most likely source of a separate drawdown event. The lack of data from that shaft over this period, however, leaves this argument speculative at best.

6.2.14 Exhaust Shaft

The pressure data from exhaust shaft piezometer #212, compensated for the pretest trend, are shown in Figure 6-29, along with a simulation generated by INTERPRET. Because this piezometer indicates pressure changes in discrete steps of 0.5 psi rather than over a continuous range, the linear compensation applied to correct for the pretest trend created an apparent en echelon pattern in the data, with each group of points corresponding to a plateau between steps in the data. The goal of the simulation was to match the midpoint of each group of data as well as possible. This goal was met with only modest success in the best-fit simulation obtained (Figure 6-29). This simulation uses a line-source solution with an apparent transmissivity of 28 ft^2/day, an apparent storativity of 5.5×10^{-5}, and no hydraulic boundaries (Table 6-1).

The data and the simulation shown in Figure 6-29 differ in several important respects. First, drawdown began later than predicted by the model, as was the case with ERDA-9 (Section 6.2.13). Second, ~2000 hr after the beginning of pumping (~1100 hr after the pump was turned off), the pressure stopped rising (i.e., stayed on a specific step) for several hundred hours before recovery resumed, as if a withdrawal of fluid from the Culebra at some location temporarily caused drawdown at the exhaust shaft. Again, this behavior parallels that observed at ERDA-9 (Figure 6-28).

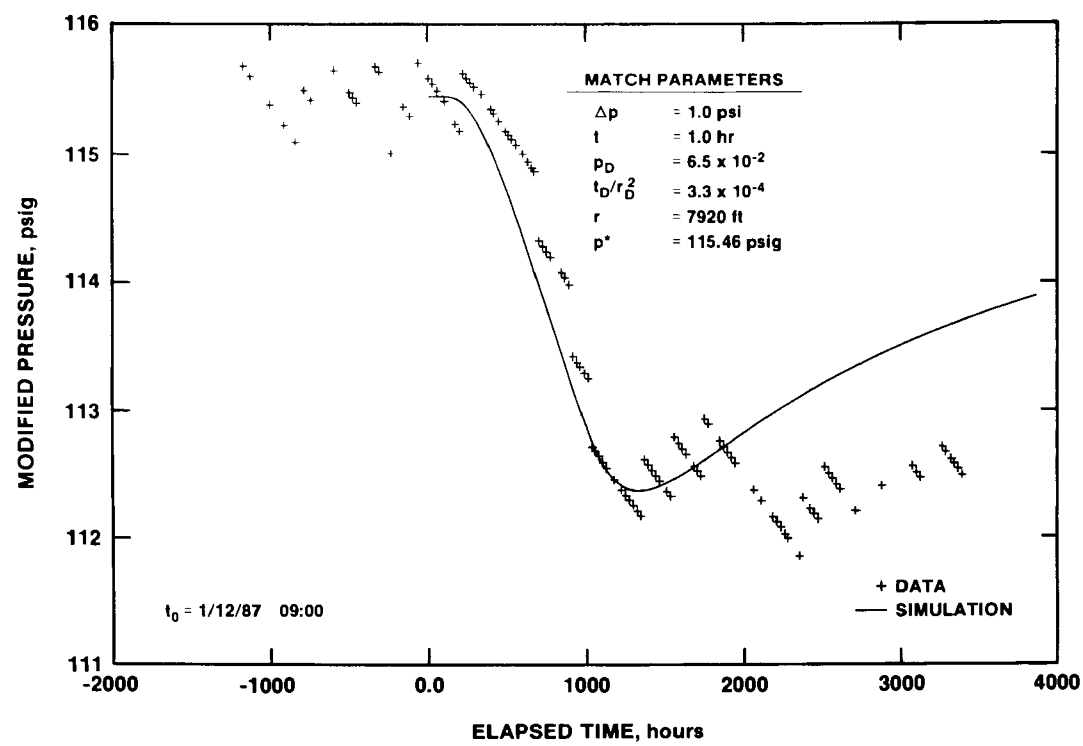

Figure 6-29. Exhaust Shaft Piezometer #212 Modified Pressure Response With INTERPRET Simulation

The anomalous drawdown response at the exhaust shaft appears to lag behind that seen at ERDA-9, although the low resolution of the exhaust shaft pressure data makes identification of inflection points difficult. If leakage into the waste-handling shaft were the cause of the drawdowns seen at the exhaust shaft and ERDA-9, the response at the exhaust shaft should have been noted before that at ERDA-9 because the exhaust shaft is slightly closer to the waste-handling shaft than is ERDA-9. However, heterogeneity in the Culebra could be responsible for the response being observed at ERDA-9 first.

No image recharge wells were used in the simulation of the exhaust shaft data, even though they were used in the simulations of the data from all of the other wells southeast of WIPP-13. The short duration of the recovery period before the anomalous drawdown mentioned earlier, however, causes the simulation to be nondefinitive. Had recovery continued longer without interruption, the inclusion of an image recharge well in the simulation might have been indicated. Inclusion of an image recharge well would have caused the apparent transmissivity between WIPP-13 and the exhaust shaft to decrease slightly. In general, the apparent hydraulic parameters used in the exhaust shaft simulation are in good agreement with those used in the simulations of the data from nearby wells (Table 6-1).

6.3 Discussion

From the analysis of the pumping-well data, the Culebra was determined to behave hydraulically like a double-porosity medium with unrestricted interporosity flow, having a transmissivity of 69 ft^2/day at WIPP-13. The presence of large, open fractures in the Culebra core from WIPP-13 indicates that the two porosity sets identified by the analysis probably consist of the fractures and the primary porosity of the rock matrix, which includes a large component of vugs.

The unrestricted interporosity flow, highly negative skin factor, and low storativity ratio determined from the WIPP-13 data indicate that the fractures and the rock matrix in the Culebra around WIPP-13 communicate readily and that the fractures act as the principal transport medium for water in storage in the matrix. Both low-transmissivity and high-transmissivity boundaries were indicated by the analysis of the WIPP-13 data; these correlate with a region of decreased Culebra transmissivity east of WIPP-13 and a region of increased Culebra transmissivity west of WIPP-13.

The wells to the south and southeast of WIPP-13 that responded during the test all lie in a region of the Culebra having a transmissivity <1 ft^2/day (Beauheim, 1987b; Mercer, 1983). No pervasive, open fractures are evident in the existing Culebra core from these holes. Similar responses to the pumping test were observed at all of these wells, and the apparent hydraulic parameters derived from the simulations of these responses are in reasonably good agreement.

With the exception of WIPP-12, apparent transmissivities ranged from 16 to 28 ft^2/day (Table 6-1). The apparent transmissivity determined from the WIPP-12 data was only 7.9 ft^2/day (Table 6-1), probably reflecting the fact that the local transmissivity around WIPP-12 is lower than that around the other wells farther south (Beauheim, 1987b). The apparent storativities among this group of wells are also consistent, with values ranging generally from 3.6×10^{-5} to 5.5×10^{-5} (Table 6-1). The apparent storativities derived from the H-1 and H-2b2 data are slightly higher, being 1.3×10^{-4} and 7.3×10^{-5}, respectively (Table 6-1). Why these two values are higher remains unknown.

Similar types of hydraulic boundaries were also indicated by the simulations of the data from this group of wells. With the exception of H-1 and the exhaust shaft, all simulations included the presence of a recharge (or high-transmissivity) boundary. The H-1 and exhaust shaft simulations did not *require* recharge boundaries (although equally good fits were obtainable with recharge boundaries as without), primarily because of low degrees of measured recovery. Additional recovery data could have provided definitive indications of the presence of a recharge boundary.

The recharge boundary probably represents the effects of the higher transmissivity region of the Culebra lying to the west of these wells. If the actual boundary were a discrete hydrologic feature, such as a stream intersecting the Culebra, rather than a gradational change in transmissivity, its precise location could be identified by using the distances to the boundary given by each of the simulations and the graphical techniques presented in Ferris et al. (1962). In this instance, these techniques produced no meaningful results, indicating that gradual changes in Culebra transmissivity and not a discrete hydrologic feature were responsible for the apparent boundary effects.

A second group of wells that exhibited similar behavior includes H-6a, H-6b, and DOE-2. The Culebra core from the H-6 wells and DOE-2 shows extensive fracturing, similar to that at WIPP-13. The area encompassing H-6, DOE-2, and WIPP-13 appears to be an area of relative Culebra homogeneity. The apparent transmissivities derived from the simulations of the responses at H-6 and DOE-2 are high and are in reasonable agreement with the value derived from the WIPP-13 data (Table 6-1). The apparent storativities are similar among this group of wells, ranging from 5.1×10^{-6} to 8.2×10^{-6} (Table 6-1), and are approximately one order of magnitude lower than the apparent storativities derived for the wells to the south and southeast of WIPP-13. The fastest responses to the WIPP-13 pumping were observed at these wells; DOE-2 responded within 1 hr to the start of pumping at WIPP-13, and the H-6 wells responded in 8 hr (Table 5-1).

The high apparent transmissivities, low apparent storativities, and rapid responses noted at these wells all indicate that the Culebra exhibits well-developed hydraulic communication and relatively homogeneous hydraulic properties within this region. These observations are consistent with the presence of an extensive, well-developed fracture system within the Culebra over this portion of the WIPP site.

The simulations of the DOE-2 data incorporated boundaries very similar to those used in the WIPP-13 simulations, including a discharge (low-transmissivity) boundary and two recharge (high-transmissivity) boundaries. No other observation-well simulations included discharge boundaries. The justification for a discharge boundary in the DOE-2 simulation is clear, however, as DOE-2 is the only well in an area of high Culebra transmissivity that is between WIPP-13 and the low-transmissivity region to the east. The recharge boundaries used in the DOE-2 and H-6 simulations probably reflect the increased Culebra transmissivities found to the west toward Nash Draw.

Culebra core from WIPP-30 (Sandia and USGS, 1980b) is similar to that from such wells as WIPP-19 (Sandia and USGS, 1980a) in that no pervasive, open fractures are evident. The local Culebra transmissivity at WIPP-30, 0.2 ft^2/day, is also similar to the values measured at the wells southeast of WIPP-13 (Beauheim, 1987b). The WIPP-13 multipad test response at WIPP-30 and its simulation bear resemblances both to those at the wells southeast of WIPP-13 and to those at DOE-2 and H-6. Similarities between the WIPP-30 and southeastern wells' responses and simulations include similar apparent transmissivities and the need for single recharge boundaries in the simulations. Similarities to the DOE-2 and H-6 responses and simulations include a short response time (Table 5-1) considering WIPP-30's distance from WIPP-13 (18 330 ft) and a low apparent storativity of 5.6×10^{-6} (Table 6-1). Together, these observations indicate that, while WIPP-30 itself lies in a region of relatively low Culebra transmissivity similar in magnitude to that to the southeast of WIPP-13, the high-transmissivity region incorporating DOE-2 must come relatively closer to WIPP-30 than to the WIPP-series wells to the southeast.

The Culebra core from WIPP-25 shows extensive fracturing (Sandia and USGS, 1979b). The Culebra was not cored at P-14, but based on the apparent dissolution of halite from the unnamed lower member of the Rustler beneath the Culebra at P-14 (Snyder, 1985) and the high productivity of the Culebra during testing at P-14 (Mercer and Orr, 1979), fractures can be predicted to be present in the Culebra at that location. The WIPP-13 multipad test responses observed at P-14 and WIPP-25 had similar differences from those observed at the other wells. Responses to pumping were observed at both P-14 and WIPP-25 sooner than at some other wells closer to WIPP-13, but the magnitudes of the drawdowns observed were lower than at those other wells (Table 5-1).

The apparent transmissivities obtained from the simulations of the responses at P-14 and WIPP-25 are very high, particularly that from WIPP-25, reflecting the high transmissivities found in Nash Draw (Mercer, 1983). The apparent storativities are in close agreement and are similar to those obtained from the wells to the southeast of WIPP-13 (Table 6-1). The P-14 simulation included a recharge (high-transmissivity) boundary, probably indicating the higher transmissivity toward Nash Draw, while that for WIPP-25 (which is *in* Nash Draw) did not.

In summary, the geologic data, individual well-test results, and the simulations of the WIPP-13 multipad test responses provide a picture of a heterogeneous, water-bearing unit. The Culebra appears to be a fractured unit, exhibiting double-porosity hydraulic behavior on the local pad scale, in the vicinity of WIPP-13, H-6, and DOE-2. This system appears to extend further to the north toward WIPP-30, although WIPP-30 itself lies in an apparently unfractured, lower transmissivity zone. To the south and southeast, fracturing decreases as the apparent transmissivity decreases and the apparent storativity increases. Toward Nash Draw to the west, the apparent transmissivity increases, indicating increased fracturing in that direction.

As discussed in the introduction to this chapter, the quantitative information obtained from the analytic techniques applied to the observation-well data is nonunique. However, these analyses provide a qualitative conceptualization of that part of the Culebra affected by the WIPP-13 multipad pumping test. This conceptualization is being refined by using numerical-modeling techniques to simulate the WIPP-13 multipad test and other tests at the WIPP site in an attempt to define the distribution of hydraulic properties that will reproduce the responses observed.

7. Summary and Conclusions

A large-scale pumping test of the Culebra Dolomite Member of the Rustler Formation was performed in early 1987 at the WIPP site in southeastern New Mexico. This test, known as the WIPP-13 (or northern) multipad test, complemented the H-3 (or southern) multipad test (Beauheim, 1987a) by creating a hydraulic stress that could be measured over the northern portion of the WIPP site. The test was performed by pumping well WIPP-13 at a rate of 30 gpm for 36 days and monitoring drawdown and recovery responses in 17 observation wells and one WIPP shaft. Responses were observed in 14 of these wells, including WIPP-25, 20 500 ft from WIPP-13, and in the WIPP exhaust shaft. Responses to both the WIPP-13 and H-3 multipad tests were observed in 5 wells: WIPP-19, WIPP-21, WIPP-22, H-1, and H-2b2 (Beauheim, 1987a).

Individual well tests at various locations around the WIPP site have demonstrated that the Culebra is a heterogeneous, water-bearing unit. The responses measured in observation wells to pumping tests in heterogeneous systems cannot be rigorously interpreted by using the standard analytical (as opposed to numerical) techniques developed for tests in homogeneous porous media. Application of analytical techniques to data from heterogeneous media results in quantitative evaluations of average hydraulic properties between pumping and observation wells that are nonunique in the sense that they are representative only of the responses observed when a hydraulic stress is imposed at a certain location. These "apparent" hydraulic properties do, however, provide a qualitative understanding of the nature and distribution of both hydraulic properties and heterogeneities or boundaries within the tested area.

The analytical interpretations of the test responses presented in this report had four principal objectives.

The first objective was to determine the most appropriate conceptualization of the nature of the Culebra flow system around WIPP-13. The response of the pumping well, WIPP-13, during the test appears to be that of a well completed in a bounded, double-porosity medium with unrestricted interporosity flow. In such a system, fractures provide the bulk of the permeability, matrix pores provide the majority of the storage capacity, and little impediment exists to flow between the fractures and pores. Both low-transmissivity and high-transmissivity boundaries are evident in the WIPP-13 response, reflecting an area of lower Culebra transmissivity lying east and south of WIPP-13 and an area of higher Culebra transmissivity lying to the west.

The second objective was to quantify the hydraulic properties of the Culebra in the vicinity of WIPP-13. The transmissivity of the Culebra at WIPP-13 is 69 ft^2/day. The ratio of the fracture storativity to the total-system (i.e., fractures + matrix) storativity derived from the drawdown data is 0.001. This latter value indicates the importance of matrix pores as the primary fluid-storage medium.

The third objective was to determine the nature and distribution of heterogeneities within the area of Culebra influenced by the test. The wells to the southeast and south of WIPP-13 lie in a region where the Culebra is largely unfractured and has a lower transmissivity than at WIPP-13. The simulations of the responses observed at these wells indicate the presence of a recharge boundary, which is probably the high-transmissivity region of the Culebra lying west of these wells. WIPP-13, H-6 (to the northwest), and DOE-2 (to the northeast) lie in a relatively homogeneous region of the Culebra characterized by fracturing, high transmissivity, and low storativity.

The simulation of the response observed at DOE-2 includes both recharge and discharge boundaries, while the H-6 simulations include only a recharge boundary. The recharge boundaries probably reflect the higher transmissivity found toward Nash Draw to the west, while the discharge boundary probably represents the low-transmissivity region lying to the east of DOE-2.

Farther to the north, WIPP-30 lies in an area of low transmissivity where the Culebra is unfractured. The WIPP-30 response, however, shows the presence of a recharge boundary and indicates that the region of high transmissivity and low storativity around WIPP-13 and DOE-2 extends close to WIPP-30. To the west of WIPP-13, wells P-14 and WIPP-25 lie in a region where the Culebra is fractured and has a higher transmissivity than at WIPP-13. The P-14 response shows the effects of a recharge boundary, probably the higher transmissivity found in Nash Draw to the west, whereas no hydraulic boundary effects are evident in the response observed at WIPP-25.

The fourth objective was to determine the apparent hydraulic properties of the Culebra between WIPP-13 and responding observation wells. The results are listed in Table 6-1 and summarized below. The apparent transmissivities between WIPP-13 and the wells to the southeast and south generally range from 16 to 28 ft^2/day, while the apparent storativities range from 3.6×10^{-5} to 5.5×10^{-5}. The apparent transmissivity between WIPP-13 and WIPP-12 (7.9 ft^2/day) is slightly lower, reflecting the lower local transmissivity at WIPP-12, while the apparent storativities between WIPP-13 and H-1 (1.3×10^{-4}) and H-2b2 (7.3×10^{-5}) are slightly higher.

All of these apparent transmissivities are intermediate between the local value determined for WIPP-13 and those determined for the individual wells from single-well tests. Between WIPP-13 and DOE-2 and H-6, apparent transmissivities are higher (~57 and 70 ft^2/day, respectively) and apparent storativities are lower ($\sim 5 \times 10^{-6}$ and 8×10^{-6}, respectively). The apparent transmissivity between WIPP-13 and WIPP-30, 28 ft^2/day, is similar to those found to the southeast, while the apparent storativity of 5.6×10^{-6} is similar to that between WIPP-13 and DOE-2 and H-6. Finally, the apparent transmissivities between WIPP-13 and P-14 and WIPP-25 to the west are considerably higher (265 and 650 ft^2/day, respectively) than in any other region affected by the test, while the apparent storativities (5.2×10^{-5} and 6.4×10^{-5}, respectively) are similar to those found to the southeast of WIPP-13.

In summary, the analyses of the observed responses to the WIPP-13 multipad pumping test provide a qualitative conceptualization of three distinct domains with a heterogeneous portion of the Culebra dolomite north of the center of the WIPP site. The Culebra is a fractured, high-transmissivity system around WIPP-13, H-6, and DOE-2. This system appears to extend further to the north toward WIPP-30, although WIPP-30 itself lies in an unfractured, lower transmissivity zone.

Toward the center of the WIPP site to the south and east, fracturing and the apparent transmissivity decrease, and the apparent storativity increases. To the west of WIPP-13 toward Nash Draw, apparent transmissivity increases, probably as a result of increased fracturing in that direction. This conceptualization is being refined by using numerical-modeling techniques to simulate the WIPP-13 multipad test and other tests at the WIPP site in an attempt to define the distribution of hydraulic properties that will reproduce the responses observed. The full numerical simulation of Culebra hydrology near the center of the WIPP site is guided by, and must be consistent with, the interpretations presented here.

APPENDIX A

Water-Level and Fluid-Pressure Data

Table A-1. Pressure in Pumping Well WIPP-13 During the WIPP-13 Multipad Pumping Test

Day	Hr	Min	S	Elapsed Time (hr)	Pressure (psig)	
8	8	51	0	-96.150000	137.58	
9	9	0	0	-72.000000	137.44	
10	7	40	0	-49.333333	137.45	
11	8	0	0	-25.000000	137.49	
12	8	59	54	-0.001667	137.41	
12	9	0	0	0.000000	136.51	pump on
12	9	0	6	0.001667	136.18	
12	9	0	12	0.003333	136.02	
12	9	0	18	0.005000	135.78	
12	9	0	24	0.006667	135.69	
12	9	0	30	0.008333	135.58	
12	9	0	36	0.010000	135.48	
12	9	0	42	0.011667	135.38	
12	9	0	48	0.013333	135.32	
12	9	0	54	0.015000	135.28	
12	9	1	0	0.016667	135.21	
12	9	1	12	0.020000	135.17	
12	9	1	24	0.023333	135.11	
12	9	1	36	0.026667	135.04	
12	9	1	48	0.030000	134.98	
12	9	2	0	0.033333	134.96	
12	9	2	30	0.041667	134.81	
12	9	3	0	0.050000	134.76	
12	9	3	30	0.058333	134.71	
12	9	4	0	0.066667	134.64	
12	9	4	30	0.075000	134.62	
12	9	5	0	0.083333	134.54	
12	9	6	0	0.100000	134.50	
12	9	9	0	0.150000	134.32	
12	9	12	0	0.200000	134.15	
12	9	15	0	0.250000	134.03	
12	9	18	0	0.300000	133.94	
12	9	21	0	0.350000	133.86	
12	9	24	0	0.400000	133.77	
12	9	27	0	0.450000	133.78	
12	9	30	0	0.500000	133.64	
12	9	36	0	0.600000	133.53	
12	9	42	0	0.700000	133.41	
12	9	48	0	0.800000	133.32	
12	9	54	0	0.900000	133.25	
12	10	0	0	1.000000	133.12	

(continued)

Table A-1. (continued)

Day	Hr	Min	S	Elapsed Time (hr)	Pressure (psig)
12	10	30	0	1.500000	132.81
12	11	0	0	2.000000	132.50
12	11	30	0	2.500000	132.23
12	12	0	0	3.000000	132.03
12	12	30	0	3.500000	131.86
12	13	0	0	4.000000	131.65
12	13	30	0	4.500000	131.52
12	14	0	0	5.000000	131.42
12	14	30	0	5.500000	131.28
12	15	0	0	6.000000	131.13
12	15	30	0	6.500000	131.00
12	16	0	0	7.000000	130.89
12	16	30	0	7.500000	130.80
12	17	0	0	8.000000	130.73
12	17	30	0	8.500000	130.60
12	18	0	0	9.000000	130.50
12	18	30	0	9.500000	130.39
12	19	0	0	10.000000	130.28
12	20	0	0	11.000000	130.09
12	21	0	0	12.000000	129.97
12	22	0	0	13.000000	129.82
12	23	0	0	14.000000	129.66
13	0	0	0	15.000000	129.48
13	1	0	0	16.000000	129.40
13	2	0	0	17.000000	129.28
13	3	0	0	18.000000	129.18
13	4	0	0	19.000000	129.12
13	5	0	0	20.000000	128.95
13	7	0	0	22.000000	128.73
13	9	0	0	24.000000	128.55
13	11	0	0	26.000000	128.24
13	13	0	0	28.000000	128.05
13	15	0	0	30.000000	127.92
13	17	0	0	32.000000	127.76
13	19	0	0	34.000000	127.65
13	21	0	0	36.000000	127.49
13	23	0	0	38.000000	127.35
14	1	0	0	40.000000	127.16
14	5	0	0	44.000000	127.15
14	10	0	0	49.000000	126.86
14	15	0	0	54.000000	126.13

(continued)

Table A-1. (continued)

Day	Hr	Min	S	Elapsed Time (hr)	Pressure (psig)
14	21	0	0	60.000000	125.77
15	1	0	0	64.000000	125.45
15	5	0	0	68.000000	125.30
15	9	0	0	72.000000	125.04
15	13	0	0	76.000000	124.89
15	17	0	0	80.000000	124.77
15	21	0	0	84.000000	124.58
16	1	0	0	88.000000	124.36
16	5	0	0	92.000000	124.21
16	9	0	0	96.000000	124.05
16	13	0	0	100.000000	123.84
16	23	0	0	110.000000	123.47
17	9	0	0	120.000000	123.12
17	19	0	0	130.000000	122.77
18	5	0	0	140.000000	122.36
18	15	0	0	150.000000	122.06
19	1	0	0	160.000000	121.73
19	11	0	0	170.000000	121.39
19	21	0	0	180.000000	121.25
20	7	0	0	190.000000	120.82
20	17	0	0	200.000000	120.54
21	3	0	0	210.000000	120.31
21	13	0	0	220.000000	120.17
21	23	0	0	230.000000	119.86
22	9	0	0	240.000000	119.57
22	19	0	0	250.000000	119.40
23	5	0	0	260.000000	119.32
23	15	0	0	270.000000	119.04
24	1	0	0	280.000000	118.91
24	11	0	0	290.000000	118.73
24	21	0	0	300.000000	118.55
25	17	0	0	320.000000	118.06
26	13	0	0	340.000000	117.61
27	9	0	0	360.000000	117.31
28	5	0	0	380.000000	117.12
29	1	0	0	400.000000	116.91
29	21	0	0	420.000000	116.70
30	17	0	0	440.000000	116.37
31	13	0	0	460.000000	116.11
32	9	0	0	480.000000	116.04
33	5	0	0	500.000000	115.74

(continued)

Table A-1. (continued)

Day	Hr	Min	S	Elapsed Time (hr)	Pressure (psig)	
34	1	0	0	520.000000	115.50	
34	21	0	0	540.000000	115.40	
35	17	0	0	560.000000	115.11	
36	13	0	0	580.000000	114.80	
37	9	0	0	600.000000	114.73	
38	5	0	0	620.000000	114.53	
39	1	0	0	640.000000	114.38	
39	21	0	0	660.000000	114.12	
40	17	0	0	680.000000	114.04	
41	13	0	0	700.000000	113.87	
42	9	0	0	720.000000	113.76	
43	5	0	0	740.000000	113.68	
44	1	0	0	760.000000	114.17	
44	21	0	0	780.000000	113.65	
45	17	0	0	800.000000	113.60	
46	13	0	0	820.000000	113.37	
47	9	0	0	840.000000	113.40	
48	5	0	0	860.000000	113.14	
48	9	0	0	864.000000	114.68	pump off
48	9	0	6	864.001667	113.48	
48	9	0	12	864.003333	113.75	
48	9	0	18	864.005000	113.95	
48	9	0	24	864.006667	114.11	
48	9	0	30	864.008333	114.25	
48	9	0	36	864.010000	114.41	
48	9	0	42	864.011667	114.51	
48	9	0	48	864.013333	114.60	
48	9	0	54	864.015000	114.67	
48	9	1	0	864.016667	114.76	
48	9	1	6	864.018333	114.83	
48	9	1	12	864.020000	114.91	
48	9	1	24	864.023333	115.00	
48	9	1	36	864.026667	115.09	
48	9	1	48	864.030000	115.19	
48	9	2	0	864.033333	115.24	
48	9	2	12	864.036667	115.30	
48	9	2	24	864.040000	115.34	
48	9	2	36	864.043333	115.39	
48	9	2	48	864.046667	115.43	
48	9	36	6	864.601667	115.47	
48	9	3	30	864.058333	115.56	

(continued)

Table A-1. (continued)

Day	Hr	Min	S	Elapsed Time (hr)	Pressure (psig)
48	9	4	0	864.066667	115.64
48	9	4	30	864.075000	115.66
48	9	5	0	864.083333	115.70
48	9	6	0	864.100000	115.80
48	9	9	0	864.150000	115.99
48	9	12	0	864.200000	116.13
48	9	15	0	864.250000	116.25
48	9	18	0	864.300000	116.34
48	9	21	0	864.350000	116.43
48	9	24	0	864.400000	116.50
48	9	27	0	864.450000	116.57
48	9	30	0	864.500000	116.66
48	9	36	0	864.600000	116.76
48	9	42	0	864.700000	116.87
48	9	48	0	864.800000	116.96
48	9	54	0	864.900000	117.05
48	10	0	0	865.000000	117.16
48	10	30	0	865.500000	117.49
48	11	0	0	866.000000	117.76
48	11	30	0	866.500000	118.01
48	12	0	0	867.000000	118.20
48	12	30	0	867.500000	118.39
48	13	0	0	868.000000	118.56
48	13	30	0	868.500000	118.73
48	14	0	0	869.000000	118.91
48	14	30	0	869.500000	119.05
48	15	0	0	870.000000	119.17
48	15	30	0	870.500000	119.28
48	16	0	0	871.000000	119.43
48	16	30	0	871.500000	119.54
48	17	0	0	872.000000	119.64
48	17	30	0	872.500000	119.75
48	18	0	0	873.000000	119.86
48	18	30	0	873.500000	119.96
48	19	0	0	874.000000	120.08
48	20	0	0	875.000000	120.25
48	21	0	0	876.000000	120.40
48	22	0	0	877.000000	120.57
48	23	0	0	878.000000	120.68
49	0	0	0	879.000000	120.80
49	1	0	0	880.000000	120.93

(continued)

Table A-1. (continued)

Day	Hr	Min	S	Elapsed Time (hr)	Pressure (psig)
49	2	0	0	881.000000	121.06
49	3	0	0	882.000000	121.18
49	4	0	0	883.000000	121.31
49	5	0	0	884.000000	121.42
49	9	0	0	888.000000	121.91
49	13	0	0	892.000000	122.23
49	17	0	0	896.000000	122.61
49	21	0	0	900.000000	122.90
49	23	0	0	902.000000	123.03
50	1	0	0	904.000000	123.18
50	3	0	0	906.000000	123.31
50	5	0	0	908.000000	123.46
50	7	0	0	910.000000	123.60
50	9	0	0	912.000000	123.71
50	11	0	0	914.000000	123.82
50	21	0	0	924.000000	124.37
51	7	0	0	934.000000	124.86
51	17	0	0	944.000000	125.27
52	3	0	0	954.000000	125.76
52	13	0	0	964.000000	126.11
52	23	0	0	974.000000	126.54
53	9	0	0	984.000000	126.94
54	5	0	0	1004.000000	127.53
55	1	0	0	1024.000000	128.13
55	21	0	0	1044.000000	128.57
56	17	0	0	1064.000000	129.14
57	17	20	6	1088.335000	129.47
58	9	0	3	1104.000833	129.88
59	5	0	0	1124.000000	130.25
60	1	0	0	1144.000000	130.49
60	21	0	0	1164.000000	130.84
61	17	0	0	1184.000000	131.08
62	13	0	0	1204.000000	131.19
63	9	0	0	1224.000000	131.45
64	5	0	0	1244.000000	131.74
65	1	0	0	1264.000000	132.05
67	3	0	0	1314.000000	132.61
69	5	0	0	1364.000000	133.04
71	7	0	0	1414.000000	133.38
73	9	0	0	1464.000000	133.75
75	11	0	0	1514.000000	134.13

(continued)

Table A-1. (concluded)

Day	Hr	Min	S	Elapsed Time (hr)	Pressure (psig)
77	13	0	0	1564.000000	134.25
79	15	0	0	1614.000000	134.51
81	17	0	0	1664.000000	134.94
83	19	0	0	1714.000000	135.10
85	21	0	0	1764.000000	135.13
87	23	0	0	1814.000000	135.44
90	1	0	0	1864.000000	135.45
92	3	0	0	1914.000000	135.62
94	5	0	0	1964.000000	135.81
96	7	0	0	2014.000000	135.83
98	9	0	0	2064.000000	135.84
100	11	0	0	2114.000000	135.88
102	13	0	0	2164.000000	136.11
104	15	0	0	2214.000000	136.05
106	17	0	0	2264.000000	136.12
108	19	0	0	2314.000000	136.46
110	21	0	0	2364.000000	136.26
112	23	0	0	2414.000000	136.34
115	1	0	0	2464.000000	136.53
117	3	0	0	2514.000000	136.50
119	5	0	0	2564.000000	136.57

Table A-2. Water Levels and Pressures in Observation Well WIPP-12 During the WIPP-13 Multipad Pumping Test

Day	Hr	Min	Elapsed Time (hr)	Depth to Water (ft)	Pressure* (psi)	Modified+ Pressure (psi)
336	10	28	-982.533	411.71	38.23	38.51
343	11	14	-813.767	411.58	38.29	38.52
349	11	30	-669.500	411.55	38.30	38.49
357	8	53	-480.117	411.42	38.35	38.50
363	14	4	-330.933	411.29	38.41	38.51
365	10	39	-286.350	411.25	38.43	38.52
2	12	20	-236.667	411.19	38.45	38.53
5	12	50	-164.167	411.15	38.47	38.53
7	11	57	-117.050	411.12	38.48	38.53
9	15	10	-65.833	411.09	38.50	38.53
10	11	50	-45.167	411.09	38.50	38.52
11	13	15	-19.750	411.12	38.48	38.50
12	6	50	-2.167	411.12	38.48	38.50
12	16	20	7.333	411.12	38.48	38.50
13	1	7	16.117	411.12	38.48	38.49
13	12	23	27.383	411.12	38.48	38.49
14	1	6	40.100	411.09	38.50	38.50
14	13	3	52.050	411.06	38.51	38.51
14	22	52	61.867	411.06	38.51	38.51
15	10	35	73.583	411.09	38.50	38.49
15	22	50	85.833	411.12	38.48	38.48
16	10	42	97.700	411.15	38.47	38.46
16	23	14	110.233	411.25	38.43	38.41
17	10	42	121.700	411.35	38.38	38.37
17	22	10	133.167	411.48	38.33	38.31
18	11	6	146.100	411.68	38.24	38.22
18	22	48	157.800	411.84	38.17	38.15
19	11	4	170.067	412.07	38.07	38.04
19	22	44	181.733	412.30	37.97	37.94
20	10	33	193.550	412.57	37.86	37.82
20	22	44	205.733	412.89	37.72	37.68
21	11	12	218.200	413.22	37.58	37.53
21	22	40	229.667	413.55	37.43	37.38
22	10	10	241.167	413.85	37.30	37.25
22	22	36	253.600	414.27	37.12	37.07
23	11	10	266.167	414.70	36.94	36.88
23	22	38	277.633	415.06	36.78	36.72
24	11	8	290.133	415.45	36.61	36.55
24	22	40	301.667	415.85	36.44	36.37
25	10	10	313.167	416.24	36.27	36.20
25	22	40	325.667	416.73	36.06	35.98

*Pressure = (500 ft – Depth to Water) × 0.433 psi/ft

+ Modified Pressure = (500 ft – {Depth to Water + [0.148 ft/240 hrs × (Elapsed Time – 52 hrs)]}) × 0.433 psi/ft

(continued)

Table A-2. (continued)

Day	Hr	Min	Elapsed Time (hr)	Depth to Water (ft)	Pressure (psi)	Modified Pressure (psi)
26	10	43	337.717	417.16	35.87	35.79
26	22	37	349.617	417.65	35.66	35.58
27	10	40	361.667	418.14	35.45	35.36
27	22	37	373.617	418.57	35.26	35.17
28	11	7	386.117	419.03	35.06	34.97
28	22	37	397.617	419.46	34.87	34.78
29	10	10	409.167	419.88	34.69	34.60
29	22	37	421.617	420.37	34.48	34.38
30	10	16	433.267	420.83	34.28	34.18
30	22	40	445.667	421.33	34.06	33.96
31	10	35	457.583	421.75	33.88	33.77
31	22	40	469.667	422.18	33.70	33.59
32	11	11	482.183	422.67	33.48	33.37
32	22	35	493.583	423.10	33.30	33.18
33	11	35	506.583	423.56	33.10	32.98
33	22	37	517.617	423.98	32.92	32.79
34	11	33	530.550	424.41	32.73	32.60
34	22	37	541.617	424.87	32.53	32.40
35	10	53	553.883	425.30	32.34	32.21
35	22	37	565.617	425.72	32.16	32.03
36	14	50	581.833	426.31	31.91	31.77
36	22	37	589.617	426.64	31.77	31.62
37	11	1	602.017	427.07	31.58	31.43
37	22	38	613.633	427.49	31.40	31.25
38	10	54	625.900	427.99	31.18	31.03
38	22	38	637.633	428.38	31.01	30.86
39	11	0	650.000	428.81	30.82	30.67
39	22	37	661.617	429.17	30.67	30.51
40	12	18	675.300	429.63	30.47	30.30
40	22	37	685.617	429.95	30.33	30.16
41	10	50	697.833	430.31	30.18	30.00
41	22	37	709.617	430.68	30.02	29.84
42	11	35	722.583	431.07	29.85	29.67
42	22	37	733.617	431.40	29.70	29.52
43	10	10	745.167	431.73	29.56	29.38
43	22	49	757.817	432.09	29.41	29.22
44	10	28	769.467	432.41	29.27	29.07
44	22	37	781.617	432.74	29.12	28.93
45	10	37	793.617	433.04	28.99	28.80
45	22	40	805.667	433.33	28.87	28.67
46	10	45	817.750	433.66	28.73	28.52

(continued)

Table A-2. (continued)

Day	Hr	Min	Elapsed Time (hr)	Depth to Water (ft)	Pressure (psi)	Modified Pressure (psi)
46	22	41	829.683	433.99	28.58	28.38
47	8	50	839.833	434.25	28.47	28.26
47	22	46	853.767	434.61	28.31	28.10
48	6	50	861.833	434.81	28.23	28.01
48	10	35	865.583	434.94	28.17	27.95
48	14	28	869.467	435.04	28.13	27.91
48	20	25	875.417	435.20	28.06	27.84
49	2	30	881.500	435.33	28.00	27.78
49	8	44	887.733	435.50	27.93	27.70
49	14	23	893.383	435.63	27.87	27.65
49	20	12	899.200	435.79	27.80	27.58
50	2	5	905.083	435.93	27.74	27.52
50	8	10	911.167	436.09	27.67	27.44
50	15	5	918.083	436.22	27.62	27.39
50	22	15	925.250	436.38	27.55	27.31
51	7	10	934.167	436.94	27.30	27.07
51	14	34	941.567	436.78	27.37	27.14
51	22	15	949.250	436.94	27.30	27.07
52	9	0	960.000	437.14	27.22	26.98
52	14	38	965.633	437.24	27.18	26.93
52	22	40	973.667	437.37	27.12	26.87
53	9	0	984.000	437.50	27.06	26.81
53	14	35	989.583	437.57	27.03	26.78
53	22	15	997.250	437.66	26.99	26.74
54	8	32	1007.533	437.73	26.96	26.71
54	14	17	1013.283	437.76	26.95	26.69
54	22	30	1021.500	437.80	26.93	26.67
55	9	5	1032.083	437.83	26.92	26.66
55	14	12	1037.200	437.83	26.92	26.66
55	22	35	1045.583	437.83	26.92	26.65
56	9	25	1056.417	437.83	26.92	26.65
56	14	45	1061.750	437.80	26.93	26.66
56	22	31	1069.517	437.76	26.95	26.68
57	9	16	1080.267	437.66	26.99	26.72
57	14	45	1085.750	437.63	27.01	26.73
57	22	25	1093.417	437.57	27.03	26.75
58	8	11	1103.183	437.43	27.09	26.81
58	20	35	1115.583	437.30	27.15	26.86
59	9	10	1128.167	437.14	27.22	26.93
59	20	35	1139.583	437.01	27.27	26.98
60	8	48	1151.800	436.81	27.36	27.07

(continued)

Table A-2. (continued)

Day	Hr	Min	Elapsed Time (hr)	Depth to Water (ft)	Pressure (psi)	Modified Pressure (psi)
60	21	57	1164.950	436.61	27.45	27.15
61	10	31	1177.517	436.38	27.55	27.25
61	20	45	1187.750	436.19	27.63	27.33
62	8	35	1199.583	435.99	27.72	27.41
62	21	40	1212.667	435.73	27.83	27.52
63	9	56	1224.933	435.50	27.93	27.61
63	21	40	1236.667	435.30	28.02	27.70
64	10	5	1249.083	435.04	28.13	27.81
64	22	30	1261.500	434.71	28.27	27.95
65	13	23	1276.383	434.35	28.43	28.10
65	21	45	1284.750	434.19	28.50	28.17
66	8	40	1295.667	433.89	28.63	28.29
66	21	45	1308.750	433.56	28.77	28.43
67	8	40	1319.667	433.27	28.89	28.56
67	21	45	1332.750	432.91	29.05	28.71
68	10	23	1345.383	432.58	29.19	28.85
69	8	20	1367.333	432.05	29.42	29.07
70	10	13	1393.217	431.46	29.68	29.32
71	11	52	1418.867	430.81	29.96	29.59
72	11	44	1442.733	430.28	30.19	29.82
73	10	10	1465.167	429.72	30.43	30.05
74	10	10	1489.167	429.10	30.70	30.32
75	10	10	1513.167	428.51	30.95	30.57
76	10	30	1537.500	427.95	31.20	30.80
77	10	10	1561.167	427.43	31.42	31.02
78	12	29	1587.483	426.90	31.65	31.24
79	14	13	1613.217	426.38	31.88	31.46
82	10	5	1681.083	425.07	32.45	32.01
84	10	35	1729.583	424.28	32.79	32.34
86	11	5	1778.083	423.59	33.09	32.62
89	11	10	1850.167	422.67	33.48	33.00
91	10	15	1897.250	422.08	33.74	33.25
93	9	25	1944.417	421.52	33.98	33.48
96	12	50	2019.833	420.67	34.35	33.82
98	10	10	2065.167	420.21	34.55	34.01
100	11	27	2114.450	419.69	34.77	34.22
103	10	40	2185.667	418.93	35.10	34.53
105	13	45	2236.750	418.57	35.26	34.68
108	10	20	2305.333	417.98	35.52	34.91
110	10	15	2353.250	417.62	35.67	35.06
113	9	20	2424.333	417.26	35.83	35.19

(continued)

Table A-2. (concluded)

Day	Hr	Min	Elapsed Time (hr)	Depth to Water (ft)	Pressure (psi)	Modified Pressure (psi)
114	14	29	2453.483	417.13	35.88	35.24
118	11	5	2546.083	416.63	36.10	35.43
120	9	35	2592.583	416.34	36.23	35.55
126	9	40	2736.667	415.62	36.54	35.82
135	13	35	2956.583	414.76	36.91	36.13

Table A-3. Water Levels and Pressures in Observation Well WIPP-18 During the WIPP-13 Multipad Pumping Test

Day	Hr	Min	Elapsed Time (hr)	Depth to Water (ft)	Pressure* (psi)	Modified+ Pressure (psi)
336	10	34	-982.433	444.88	26.40	26.65
343	11	25	-813.583	444.72	26.48	26.69
349	11	34	-669.433	444.69	26.49	26.67
357	8	57	-480.050	444.52	26.57	26.70
363	14	7	-330.883	444.39	26.64	26.73
365	10	42	-286.300	444.26	26.70	26.78
2	12	35	-236.417	444.32	26.67	26.74
6	10	30	-142.500	444.32	26.67	26.72
7	11	58	-117.033	444.36	26.65	26.69
9	15	13	-65.783	444.32	26.67	26.70
10	11	46	-45.233	444.39	26.64	26.66
11	13	18	-19.700	444.46	26.60	26.62
12	6	46	-2.233	444.46	26.60	26.62
12	16	17	7.283	444.39	26.64	26.65
13	1	4	16.067	444.39	26.64	26.65
13	12	20	27.333	444.32	26.67	26.68
14	1	3	40.050	444.26	26.70	26.70
14	13	0	52.000	444.23	26.71	26.72
14	22	49	61.817	444.19	26.73	26.73
15	10	38	73.633	444.42	26.62	26.62
15	22	47	85.783	444.55	26.56	26.55
16	10	46	97.767	444.69	26.49	26.48
16	23	18	110.300	444.91	26.39	26.38
17	10	48	121.800	445.08	26.31	26.29
17	20	14	131.233	445.37	26.17	26.15
18	11	2	146.033	445.73	26.00	25.98
18	22	53	157.883	445.96	25.89	25.86
19	11	0	170.000	446.29	25.73	25.70
19	22	48	181.800	446.59	25.58	25.55
20	10	36	193.600	446.95	25.41	25.38
20	22	48	205.800	447.31	25.24	25.20
21	11	9	218.150	447.60	25.10	25.06
21	22	44	229.733	447.97	24.92	24.88
22	10	15	241.250	448.33	24.75	24.71
22	22	40	253.667	448.62	24.61	24.57
23	11	13	266.217	448.88	24.49	24.44
23	22	48	277.800	449.11	24.38	24.32
24	11	11	290.183	449.41	24.23	24.18
24	22	50	301.833	449.84	24.03	23.97
25	10	15	313.250	450.16	23.87	23.81
25	22	44	325.733	450.56	23.68	23.62

*Pressure = (500 ft – Depth to Water) × 0.479 psi/ft

+ Modified Pressure = (500 ft – {Depth to Water + [0.119 ft/240 hrs × (Elapsed Time – 62 hrs)]}) × 0.479 psi/ft

(continued)

Table A-3. (continued)

Day	Hr	Min	Elapsed Time (hr)	Depth to Water (ft)	Pressure (psi)	Modified Pressure (psi)
26	10	46	337.767	450.92	23.51	23.44
26	22	39	349.650	451.25	23.35	23.28
27	10	43	361.717	451.54	23.21	23.14
27	22	40	373.667	451.80	23.09	23.01
28	11	10	386.167	452.07	22.96	22.88
28	22	40	397.667	452.30	22.85	22.77
29	10	57	409.950	452.66	22.68	22.59
29	22	40	421.667	452.95	22.54	22.45
30	10	20	433.333	453.31	22.36	22.28
30	22	44	445.733	453.61	22.22	22.13
31	10	39	457.650	453.81	22.12	22.03
31	22	44	469.733	454.04	22.02	21.92
32	11	6	482.100	454.30	21.89	21.79
32	22	38	493.633	454.63	21.73	21.63
33	11	31	506.517	454.92	21.59	21.49
33	22	40	517.667	455.15	21.48	21.38
34	11	36	530.600	455.48	21.32	21.21
34	22	40	541.667	455.71	21.21	21.10
35	10	50	553.833	455.97	21.09	20.97
35	22	40	565.667	456.27	20.95	20.83
36	14	55	581.917	456.73	20.73	20.60
36	22	40	589.667	456.99	20.60	20.48
37	11	5	602.083	457.28	20.46	20.34
37	22	42	613.700	457.58	20.32	20.19
38	10	57	625.950	457.84	20.20	20.06
38	22	42	637.700	458.07	20.08	19.95
39	11	3	650.050	458.27	19.99	19.85
39	22	40	661.667	458.46	19.90	19.75
40	12	21	675.350	458.76	19.75	19.61
40	22	40	685.667	458.89	19.69	19.54
41	10	55	697.917	459.09	19.60	19.45
41	22	40	709.667	459.28	19.50	19.35
42	11	40	722.667	459.51	19.39	19.24
42	22	40	733.667	459.71	19.30	19.14
43	10	13	745.217	459.94	19.19	19.03
43	22	52	757.867	460.17	19.08	18.91
44	10	32	769.533	460.37	18.98	18.82
44	22	40	781.667	460.53	18.91	18.73
45	10	40	793.667	460.63	18.86	18.68
45	22	45	805.750	460.76	18.80	18.62
46	10	48	817.800	461.02	18.67	18.49

(continued)

Table A-3. (continued)

Day	Hr	Min	Elapsed Time (hr)	Depth to Water (ft)	Pressure (psi)	Modified Pressure (psi)
46	22	45	829.750	461.25	18.56	18.38
47	8	53	839.883	461.45	18.46	18.28
47	22	50	853.833	461.71	18.34	18.15
48	6	55	861.917	461.91	18.25	18.05
48	10	33	865.550	462.01	18.20	18.01
48	14	25	869.417	462.11	18.15	17.96
48	20	30	875.500	462.20	18.11	17.91
49	2	33	881.550	462.30	18.06	17.86
49	8	42	887.700	462.40	18.01	17.81
49	14	20	893.333	462.47	17.98	17.78
49	20	10	899.167	462.53	17.95	17.75
50	2	3	905.050	462.60	17.91	17.71
50	8	15	911.250	462.66	17.89	17.68
50	15	10	918.167	462.76	17.84	17.64
50	22	20	925.333	462.86	17.79	17.59
51	7	14	934.233	462.99	17.73	17.52
51	14	37	941.617	463.06	17.69	17.48
51	22	20	949.333	463.16	17.65	17.44
52	9	3	960.050	463.12	17.67	17.45
52	14	41	965.683	463.09	17.68	17.46
52	22	44	973.733	463.12	17.67	17.45
53	9	3	984.050	463.06	17.69	17.48
53	14	38	989.633	463.02	17.71	17.49
53	22	20	997.333	462.99	17.73	17.51
54	8	35	1007.583	462.83	17.80	17.58
54	14	21	1013.350	462.70	17.87	17.64
54	22	37	1021.617	462.60	17.91	17.69
55	9	7	1032.117	462.50	17.96	17.73
55	14	15	1037.250	462.43	18.00	17.76
55	22	37	1045.617	462.37	18.02	17.79
56	9	30	1056.500	462.20	18.11	17.87
56	14	48	1061.800	462.14	18.14	17.90
56	22	35	1069.583	462.04	18.18	17.94
58	8	14	1103.233	461.55	18.42	18.17
57	9	18	1080.300	461.88	18.26	18.02
57	14	50	1085.833	461.78	18.31	18.06
57	22	30	1093.500	461.68	18.36	18.11
58	20	40	1115.667	461.35	18.51	18.26
59	9	12	1128.200	461.22	18.58	18.32
59	20	40	1139.667	461.09	18.64	18.38
60	8	52	1151.867	460.96	18.70	18.44

(continued)

Table A-3. (continued)

Day	Hr	Min	Elapsed Time (hr)	Depth to Water (ft)	Pressure (psi)	Modified Pressure (psi)
60	22	0	1165.000	460.79	18.78	18.52
61	10	35	1177.583	460.60	18.87	18.61
61	20	50	1187.833	460.47	18.93	18.67
62	8	38	1199.633	460.33	19.00	18.73
62	21	45	1212.750	460.24	19.05	18.77
63	9	59	1224.983	460.14	19.09	18.82
64	10	8	1249.133	459.97	19.17	18.89
64	21	35	1260.583	459.55	19.38	19.09
65	13	25	1276.417	459.25	19.52	19.23
65	21	50	1284.833	459.12	19.58	19.29
66	8	43	1295.717	458.92	19.68	19.38
66	21	50	1308.833	458.60	19.83	19.53
67	8	43	1319.717	458.53	19.86	19.57
67	21	50	1332.833	458.33	19.96	19.66
68	10	26	1345.433	458.17	20.04	19.73
69	8	25	1367.417	458.01	20.11	19.80
70	10	16	1393.267	457.74	20.24	19.93
71	11	55	1418.917	457.41	20.40	20.08
72	11	47	1442.783	457.12	20.54	20.21
73	10	13	1465.217	456.66	20.76	20.43
74	10	15	1489.250	456.30	20.93	20.59
75	10	15	1513.250	455.94	21.11	20.76
76	10	35	1537.583	455.64	21.25	20.90
77	10	15	1561.250	455.45	21.34	20.98
78	12	31	1587.517	455.22	21.45	21.09
79	14	10	1613.167	454.95	21.58	21.21
82	10	10	1681.167	454.20	21.94	21.55
84	10	40	1729.667	453.87	22.10	21.70
86	11	7	1778.117	453.44	22.30	21.89
89	11	15	1850.250	453.12	22.46	22.03
91	10	20	1897.333	452.56	22.72	22.29
93	9	30	1944.500	452.33	22.83	22.39
96	12	55	2019.917	451.77	23.10	22.64
98	10	15	2065.250	451.48	23.24	22.77
100	11	30	2114.500	451.02	23.46	22.97
103	10	45	2185.750	450.52	23.70	23.20
105	13	50	2236.833	450.36	23.78	23.26
108	10	23	2305.383	449.80	24.05	23.51
110	10	20	2353.333	449.67	24.11	23.56
113	9	23	2424.383	449.44	24.22	23.66
114	14	32	2453.533	449.31	24.28	23.71

(continued)

Table A-3. (concluded)

Day	Hr	Min	Elapsed Time (hr)	Depth to Water (ft)	Pressure (psi)	Modified Pressure (psi)
118	11	10	2546.167	448.95	24.45	23.86
120	9	40	2592.667	448.59	24.62	24.02
126	9	45	2736.750	448.16	24.83	24.20
135	13	40	2956.667	447.38	25.20	24.52

Table A-4. Water Levels and Pressures in Observation Well WIPP-19 During the WIPP-13 Multipad Pumping Test

Day	Hr	Min	Elapsed Time (hr)	Depth to Water (ft)	Pressure* (psi)	Modified+ Pressure (psi)
336	10	38	-982.367	443.08	27.95	28.48
343	11	30	-813.500	443.11	27.93	28.37
349	11	40	-669.333	442.98	28.00	28.36
357	13	25	-475.583	442.68	28.14	28.41
363	14	20	-330.667	442.75	28.11	28.30
365	10	50	-286.167	442.59	28.19	28.36
5	11	28	-165.533	442.39	28.29	28.40
8	9	50	-95.167	442.39	28.29	28.36
9	15	20	-65.667	442.26	28.35	28.41
13	13	30	28.500	442.16	28.40	28.41
14	14	0	53.000	441.99	28.48	28.48
16	14	49	101.817	442.45	28.26	28.23
19	17	25	176.417	443.11	27.93	27.87
21	13	25	220.417	443.64	27.67	27.59
23	15	15	270.250	444.52	27.24	27.13
26	15	0	342.000	445.67	26.68	26.53
28	10	0	385.000	446.52	26.26	26.09
30	16	12	439.200	447.64	25.71	25.51
33	13	28	508.467	448.59	25.24	25.01
35	8	25	551.417	449.41	24.84	24.59
37	14	22	605.367	450.59	24.26	23.98
40	12	28	675.467	451.77	23.68	23.36
42	15	18	726.300	452.20	23.47	23.13
44	14	46	773.767	453.02	23.07	22.70
47	9	30	840.500	454.07	22.55	22.15
48	12	0	867.000	454.40	22.39	21.98
48	14	40	869.667	454.56	22.31	21.89
48	20	37	875.617	454.69	22.25	21.83
49	2	15	881.250	454.69	22.25	21.82
49	10	10	889.167	454.63	22.28	21.85
49	15	43	894.717	454.79	22.20	21.77
49	20	18	899.300	454.79	22.20	21.77
50	2	12	905.200	454.82	22.18	21.75
50	8	20	911.333	454.92	22.13	21.70
50	15	15	918.250	455.05	22.07	21.63
50	22	30	925.500	455.22	21.99	21.54
51	10	32	937.533	455.18	22.01	21.56
51	14	44	941.733	455.38	21.91	21.46
51	22	30	949.500	455.48	21.86	21.40
52	9	10	960.167	455.51	21.84	21.38
52	14	48	965.800	455.51	21.84	21.38

*Pressure = (500 ft − Depth to Water) × 0.491 psi/ft

+ Modified Pressure = (500 ft − {Depth to Water + [0.249 ft/240 hrs × (Elapsed Time − 53 hrs)]}) × 0.491 psi/ft

(continued)

Table A-4. (continued)

Day	Hr	Min	Elapsed Time (hr)	Depth to Water (ft)	Pressure (psi)	Modified Pressure (psi)
52	22	50	973.833	455.54	21.83	21.36
53	9	10	984.167	455.61	21.80	21.32
53	14	48	989.800	455.58	21.81	21.33
53	22	30	997.500	455.77	21.72	21.24
54	8	45	1007.750	455.64	21.78	21.29
54	14	30	1013.500	455.58	21.81	21.32
54	22	50	1021.833	455.64	21.78	21.29
55	9	17	1032.283	455.61	21.80	21.30
55	14	24	1037.400	455.58	21.81	21.31
55	22	48	1045.800	455.64	21.78	21.27
56	9	35	1056.583	455.64	21.78	21.27
56	14	58	1061.967	455.58	21.81	21.30
56	22	44	1069.733	455.45	21.87	21.36
57	10	45	1081.750	455.45	21.87	21.35
57	14	55	1085.917	455.38	21.91	21.38
57	22	40	1093.667	455.38	21.91	21.38
58	10	0	1105.000	455.38	21.91	21.37
58	15	20	1110.333	455.31	21.94	21.40
58	21	10	1116.167	455.25	21.97	21.43
59	9	24	1128.400	455.25	21.97	21.42
59	14	47	1133.783	455.22	21.99	21.44
59	20	50	1139.833	455.28	21.96	21.40
60	9	0	1152.000	455.22	21.99	21.43
60	15	0	1158.000	455.12	22.04	21.47
60	22	10	1165.167	455.12	22.04	21.47
61	8	20	1175.333	455.05	22.07	21.50
61	15	5	1182.083	454.86	22.16	21.59
61	21	0	1188.000	454.92	22.13	21.56
62	8	50	1199.833	454.89	22.15	21.57
62	15	15	1206.250	454.79	22.20	21.61
62	21	55	1212.917	454.89	22.15	21.56
63	10	12	1225.200	454.72	22.23	21.64
63	15	55	1230.917	454.63	22.28	21.68
63	21	50	1236.833	454.59	22.30	21.69
64	10	15	1249.250	454.46	22.36	21.75
64	16	21	1255.350	454.46	22.36	21.75
64	21	45	1260.750	454.33	22.42	21.81
65	14	45	1277.750	453.87	22.65	22.03
65	22	0	1285.000	454.17	22.50	21.88
66	8	50	1295.833	453.94	22.61	21.98
66	15	0	1302.000	453.77	22.70	22.06

(continued)

Table A-4. (concluded)

Day	Hr	Min	Elapsed Time (hr)	Depth to Water (ft)	Pressure (psi)	Modified Pressure (psi)
66	22	0	1309.000	453.87	22.65	22.01
67	8	50	1319.833	453.67	22.75	22.10
67	14	15	1325.250	453.48	22.84	22.19
67	22	0	1333.000	453.51	22.83	22.18
68	10	35	1345.583	453.41	22.88	22.22
69	8	30	1367.500	453.41	22.88	22.21
70	10	25	1393.417	453.22	22.97	22.29
71	13	32	1420.533	452.82	23.16	22.47
72	11	54	1442.900	452.66	23.24	22.54
73	10	22	1465.367	452.23	23.45	22.74
74	10	25	1489.417	451.87	23.63	22.90
75	10	25	1513.417	451.77	23.68	22.94
76	10	40	1537.667	451.67	23.73	22.97
77	10	25	1561.417	451.38	23.87	23.10
78	12	39	1587.650	451.12	24.00	23.22
79	14	7	1613.117	450.89	24.11	23.32
83	9	20	1704.333	450.20	24.45	23.61
84	10	50	1729.833	450.23	24.44	23.58
86	11	16	1778.267	449.67	24.71	23.83
89	11	20	1850.333	449.48	24.80	23.89
91	8	25	1895.417	449.02	25.03	24.09
93	9	37	1944.617	448.79	25.14	24.18
96	13	0	2020.000	448.43	25.32	24.32
98	10	20	2065.333	448.13	25.47	24.44
100	11	36	2114.600	447.51	25.77	24.72
103	10	50	2185.833	447.11	25.97	24.88
105	14	0	2237.000	446.75	26.15	25.03
108	10	35	2305.583	446.33	26.35	25.20
110	10	30	2353.500	446.26	26.39	25.21
113	9	30	2424.500	446.06	26.48	25.28
114	14	40	2453.667	445.87	26.58	25.36
118	11	20	2546.333	445.54	26.74	25.47
120	7	20	2590.333	445.18	26.92	25.62
126	12	30	2739.500	444.75	27.13	25.76
135	13	50	2956.833	443.64	27.67	26.19

Table A-5. Water Levels and Pressures in Observation Well WIPP-21 During the WIPP-13 Multipad Pumping Test

Day	Hr	Min	Elapsed Time (hr)	Depth to Water (ft)	Pressure* (psi)	Modified+ Pressure (psi)	Compensated@ Pressure (psi)
307	11	25	-1677.583	442.95	24.70	26.50	26.50#
308	8	0	-1657.000	442.91	24.72	26.50	26.50#
309	14	35	-1626.417	442.98	24.69	26.43	26.43#
310	14	25	-1602.583	442.98	24.69	26.41	26.41#
311	10	30	-1582.500	443.04	24.66	26.36	26.36#
315	8	25	-1488.583	444.13	24.19	25.80	25.80#
316	13	50	-1459.167	444.23	24.15	25.73	25.73#
317	10	0	-1439.000	444.52	24.02	25.58	25.58#
318	12	47	-1412.217	444.69	23.95	25.48	25.48#
325	10	35	-1246.417	446.16	23.31	24.68	24.68#
328	10	55	-1174.083	446.23	23.28	24.58	24.58#
336	10	56	-982.067	445.24	23.71	24.81	24.81#
343	11	55	-813.083	444.98	23.82	24.76	24.76#
349	11	25	-669.583	444.85	23.88	24.67	24.67#
357	9	0	-480.000	444.19	24.17	24.77	24.77#
363	14	0	-331.000	443.96	24.27	24.72	24.72#
365	10	35	-286.417	443.77	24.35	24.75	24.76#
2	12	45	-236.250	443.67	24.39	24.75	24.75#
5	13	10	-163.833	443.57	24.43	24.72	24.72#
7	11	50	-117.167	443.47	24.48	24.72	24.72#
9	15	30	-65.500	443.31	24.55	24.73	24.73#
10	11	40	-45.333	443.73	24.36	24.53	24.53#
11	13	21	-19.650	443.34	24.53	24.68	24.68#
12	6	43	-2.283	443.31	24.55	24.67	24.67#
12	16	13	7.217	443.24	24.58	24.69	24.68
13	0	58	15.967	443.24	24.58	24.68	24.67
13	12	16	27.267	443.14	24.62	24.71	24.66
14	0	58	39.967	443.01	24.68	24.76	24.68
14	12	57	51.950	442.91	24.72	24.79	24.71
14	22	44	61.733	442.85	24.75	24.81	24.75
15	10	41	73.683	442.88	24.73	24.78	24.73
15	22	42	85.700	442.78	24.78	24.81	24.75
16	10	49	97.817	442.75	24.79	24.81	24.76
16	23	25	110.417	442.75	24.79	24.80	24.74
17	10	53	121.883	442.72	24.80	24.80	24.73
17	22	17	133.283	442.72	24.80	24.79	24.75
18	10	58	145.967	442.75	24.79	24.77	24.71
18	22	58	157.967	442.78	24.78	24.74	24.68
19	10	57	169.950	442.81	24.76	24.71	24.65
19	22	53	181.883	442.81	24.76	24.70	24.65

*Pressure = (500 ft – Depth to Water) × 0.433 psi/ft
+ Modified Pressure = (500 ft – {Depth to Water + [0.553 ft/240 hrs × (Elapsed Time – 22 hrs)]}) × 0.433 psi/ft
@Compensated Pressure = Modified Pressure + 0.5 (Barometric Pressure – 13.10 psi)
#Not compensated

(continued)

Table A-5. (continued)

Day	Hr	Min	Elapsed Time (hr)	Depth to Water (ft)	Pressure (psi)	Modified Pressure (psi)	Compensated Pressure (psi)
20	10	40	193.667	442.88	24.73	24.66	24.64
20	22	53	205.883	442.91	24.72	24.64	24.60
21	11	7	218.117	442.88	24.73	24.64	24.57
21	22	48	229.800	442.91	24.72	24.61	24.59
22	10	20	241.333	442.95	24.70	24.58	24.55
22	22	44	253.733	442.95	24.70	24.57	24.51
23	11	17	266.283	442.88	24.73	24.59	24.49
23	22	52	277.867	442.81	24.76	24.61	24.50
24	11	15	290.250	442.78	24.78	24.61	24.52
24	22	58	301.967	442.85	24.75	24.57	24.52
25	10	20	313.333	442.91	24.72	24.53	24.50
25	22	48	325.800	443.01	24.68	24.47	24.47
26	10	50	337.833	443.01	24.68	24.46	24.47
26	22	43	349.717	443.08	24.65	24.42	24.42
27	10	48	361.800	443.08	24.65	24.41	24.40
27	22	44	373.733	443.08	24.65	24.39	24.36
28	11	14	386.233	443.04	24.66	24.40	24.35
28	22	44	397.733	443.01	24.68	24.40	24.34
29	10	7	409.117	443.08	24.65	24.36	24.33
29	22	44	421.733	443.14	24.62	24.32	24.29
30	10	25	433.417	443.24	24.58	24.27	24.26
30	22	46	445.767	443.27	24.56	24.24	24.19
31	10	43	457.717	443.24	24.58	24.24	24.15
31	22	46	469.767	443.24	24.58	24.23	24.14
32	11	3	482.050	443.31	24.55	24.19	24.12
32	22	44	493.733	443.37	24.52	24.15	24.08
33	11	28	506.467	443.47	24.48	24.09	24.02
33	22	44	517.733	443.50	24.46	24.07	23.99
34	11	39	530.650	443.60	24.42	24.01	23.95
34	22	44	541.733	443.67	24.39	23.97	23.90
35	10	46	553.767	443.73	24.36	23.93	23.87
35	22	44	565.733	443.83	24.32	23.88	23.83
36	14	58	581.967	444.03	24.23	23.78	23.79
36	22	44	589.733	444.16	24.18	23.71	23.75
37	11	9	602.150	444.29	24.12	23.64	23.69
37	22	48	613.800	444.42	24.07	23.57	23.63
38	11	1	626.017	444.52	24.02	23.52	23.57
38	22	48	637.800	444.59	23.99	23.48	23.50
39	11	7	650.117	444.65	23.97	23.44	23.45
39	22	44	661.733	444.75	23.92	23.39	23.40

(continued)

Table A-5. (continued)

Day	Hr	Min	Elapsed Time (hr)	Depth to Water (ft)	Pressure (psi)	Modified Pressure (psi)	Compensated Pressure (psi)
40	12	13	675.217	444.85	23.88	23.33	23.34
40	22	44	685.733	444.88	23.87	23.30	23.28
41	11	0	698.000	444.91	23.85	23.28	23.25
41	22	44	709.733	444.98	23.82	23.24	23.20
42	11	44	722.733	445.08	23.78	23.18	23.15
42	22	44	733.733	445.14	23.75	23.14	23.11
43	10	17	745.283	445.21	23.72	23.10	23.08
43	22	56	757.933	445.31	23.68	23.05	23.01
44	10	37	769.617	445.34	23.67	23.02	22.97
44	22	44	781.733	445.37	23.66	23.00	22.90
45	10	44	793.733	445.34	23.67	23.00	22.87
45	22	50	805.833	445.37	23.66	22.97	22.84
46	10	52	817.867	445.47	23.61	22.92	22.84
46	22	50	829.833	445.57	23.57	22.86	22.78
47	8	59	839.983	445.70	23.51	22.80	22.72
47	22	54	853.900	445.77	23.48	22.75	22.70
48	6	58	861.967	445.93	23.41	22.67	22.64
48	10	29	865.483	446.00	23.38	22.64	22.61
48	14	20	869.333	446.03	23.37	22.62	22.59
48	20	30	875.500	446.10	23.34	22.59	22.55
49	2	37	881.617	446.16	23.31	22.55	22.51
49	8	38	887.633	446.19	23.30	22.54	22.49
49	14	16	893.267	446.26	23.27	22.50	22.43
49	20	33	899.550	446.29	23.26	22.48	22.40
50	2	27	905.450	446.33	23.24	22.46	22.38
50	8	45	911.750	446.36	23.23	22.44	22.37
50	15	35	918.583	446.42	23.20	22.41	22.34
50	22	45	925.750	446.49	23.17	22.37	22.32
51	7	18	934.300	446.59	23.13	22.32	22.30
51	15	0	942.000	446.69	23.08	22.27	22.25
51	22	45	949.750	446.82	23.03	22.20	22.18
52	9	25	960.417	446.88	23.00	22.16	22.12
52	15	3	966.050	446.92	22.98	22.14	22.08
52	23	8	974.133	446.98	22.96	22.11	22.08
53	9	21	984.350	447.08	22.91	22.05	22.04
53	15	0	990.000	447.15	22.88	22.02	21.97
53	22	43	997.717	447.21	22.86	21.98	21.92
54	8	57	1007.950	447.24	22.84	21.96	21.88
54	14	45	1013.750	447.24	22.84	21.95	21.84
54	23	3	1022.050	447.31	22.82	21.92	21.83

(continued)

Table A-5. (continued)

Day	Hr	Min	Elapsed Time (hr)	Depth to Water (ft)	Pressure (psi)	Modified Pressure (psi)	Compensated Pressure (psi)
55	9	30	1032.500	447.38	22.78	21.88	21.80
55	14	36	1037.600	447.41	22.77	21.86	21.77
55	22	59	1045.983	447.51	22.73	21.81	21.73
56	9	55	1056.917	447.57	22.70	21.77	21.70
56	15	10	1062.167	447.57	22.70	21.76	21.67
56	22	56	1069.933	447.64	22.67	21.73	21.64
57	9	21	1080.350	447.64	22.67	21.72	21.64
57	15	15	1086.250	447.70	22.65	21.68	21.59
57	22	51	1093.850	447.74	22.63	21.66	21.58
58	8	18	1103.300	447.74	22.63	21.65	21.56
58	15	36	1110.600	447.74	22.63	21.64	21.54
58	23	0	1118.000	447.80	22.60	21.61	21.52
59	9	40	1128.667	447.87	22.57	21.57	21.51
59	15	6	1134.100	447.90	22.56	21.55	21.48
59	23	0	1142.000	447.93	22.55	21.53	21.48
60	9	15	1152.250	448.03	22.50	21.48	21.46
60	15	13	1158.217	448.06	22.49	21.46	21.41
60	22	22	1165.367	448.10	22.47	21.43	21.39
61	10	39	1177.650	448.13	22.46	21.41	21.37
61	21	15	1188.250	448.20	22.43	21.37	21.33
62	9	3	1200.050	448.29	22.39	21.32	21.33
62	15	23	1206.383	448.36	22.36	21.28	21.28
62	22	6	1213.100	448.39	22.35	21.26	21.29
63	10	23	1225.383	448.49	22.30	21.20	21.26
63	15	17	1230.283	448.52	22.29	21.18	21.22
63	22	4	1237.067	448.56	22.27	21.16	21.20
64	10	30	1249.500	448.52	22.29	21.17	21.19
64	15	23	1254.383	448.52	22.29	21.16	21.17
64	22	0	1261.000	448.52	22.29	21.15	21.14
65	13	30	1276.500	448.39	22.35	21.20	21.16
65	22	20	1285.333	448.39	22.35	21.19	21.15
66	9	3	1296.050	448.33	22.37	21.20	21.17
66	15	15	1302.250	448.29	22.39	21.21	21.15
66	22	20	1309.333	448.26	22.40	21.22	21.17
67	9	3	1320.050	448.20	22.43	21.23	21.18
67	14	30	1325.500	448.16	22.45	21.25	21.16
67	22	15	1333.250	448.13	22.46	21.25	21.18
68	10	47	1345.783	448.10	22.47	21.25	21.22
69	8	50	1367.833	448.10	22.47	21.23	21.22
70	10	42	1393.700	448.10	22.47	21.20	21.22

(continued)

Table A-5. (concluded)

Day	Hr	Min	Elapsed Time (hr)	Depth to Water (ft)	Pressure (psi)	Modified Pressure (psi)	Compensated Pressure (psi)
71	11	58	1418.967	447.97	22.53	21.23	21.24
72	12	5	1443.083	447.87	22.57	21.25	21.24
73	10	33	1465.550	447.60	22.69	21.35	21.27
74	10	40	1489.667	447.38	22.78	21.42	21.33
75	10	40	1513.667	447.15	22.88	21.50	21.37
76	10	55	1537.917	446.98	22.96	21.55	21.41
77	10	40	1561.667	446.88	23.00	21.57	21.47
78	12	48	1587.800	446.78	23.04	21.58	21.49
79	13	50	1612.833	446.65	23.10	21.61	21.51
80	12	45	1635.750	446.56	23.14	21.63	21.52
81	10	40	1657.667	446.36	23.23	21.69	21.58
82	10	25	1681.417	446.19	23.30	21.74	21.63
83	9	35	1704.583	446.13	23.33	21.75	21.66
84	11	3	1730.050	446.06	23.36	21.75	21.69
85	13	0	1756.000	446.06	23.36	21.73	21.65
86	11	24	1778.400	445.90	23.43	21.77	21.68
87	11	55	1802.917	445.80	23.47	21.79	21.74
88	10	30	1825.500	445.80	23.47	21.77	21.75
89	11	35	1850.583	445.83	23.46	21.73	21.74
91	10	25	1897.417	445.57	23.57	21.80	21.74
92	14	0	1925.000	445.54	23.58	21.78	21.75
93	9	47	1944.783	445.41	23.64	21.82	21.80
95	13	35	1996.583	445.08	23.78	21.91	21.90
96	13	15	2020.250	445.05	23.79	21.90	21.89
98	10	30	2065.500	444.88	23.87	21.93	21.93
100	11	23	2114.383	444.55	24.01	22.02	21.98
102	8	55	2159.917	444.16	24.18	22.14	22.11
103	11	15	2186.250	444.13	24.19	22.13	22.10
105	14	15	2237.250	444.03	24.23	22.12	22.07
108	10	50	2305.833	443.54	24.45	22.27	22.18
110	10	45	2353.750	443.34	24.53	22.31	22.28
113	9	40	2424.667	443.08	24.65	22.35	22.34
114	14	51	2453.850	442.98	24.69	22.36	22.35
118	11	40	2546.667	442.55	24.88	22.46	22.48
120	9	45	2592.750	442.13	25.06	22.59	22.59
126	9	55	2736.917	441.54	25.31	22.70	22.70
135	14	5	2957.083	440.55	25.74	22.91	22.91

Table A-6. Water Levels and Pressures in Observation Well WIPP-22 During the WIPP-13 Multipad Pumping Test

Day	Hr	Min	Elapsed Time (hr)	Depth to Water (ft)	Pressure* (psi)	Modified+ Pressure (psi)
336	10	48	-982.200	436.94	31.21	31.79
343	11	42	-813.300	437.07	31.15	31.63
349	11	46	-669.233	436.78	31.29	31.70
357	13	30	-475.500	436.58	31.39	31.69
363	14	28	-330.533	436.61	31.38	31.59
365	10	57	-286.050	436.42	31.47	31.66
5	13	0	-164.000	436.09	31.64	31.76
8	10	0	-95.000	436.22	31.57	31.65
9	15	25	-65.583	436.12	31.62	31.69
13	13	40	28.667	435.96	31.70	31.71
14	14	10	53.167	435.83	31.76	31.76
16	15	0	102.000	436.02	31.67	31.64
19	17	35	176.583	436.19	31.59	31.52
21	13	35	220.583	436.32	31.52	31.43
23	15	6	270.100	436.88	31.24	31.12
26	15	15	342.250	437.66	30.86	30.70
28	10	14	385.233	438.29	30.55	30.36
30	16	24	439.400	438.94	30.23	30.01
33	13	20	508.333	439.76	29.82	29.57
35	8	35	551.583	440.29	29.56	29.28
37	14	34	605.567	441.27	29.07	28.77
40	12	35	675.583	442.19	28.62	28.27
42	15	30	726.500	442.59	28.42	28.04
44	15	0	774.000	443.11	28.16	27.76
47	9	14	840.233	444.16	27.64	27.20
48	12	10	867.167	444.49	27.48	27.03
48	14	45	869.750	444.59	27.43	26.98
48	20	50	875.833	444.59	27.43	26.97
49	2	24	881.400	444.69	27.38	26.92
49	10	0	889.000	444.69	27.38	26.91
49	15	30	894.500	444.82	27.31	26.85
49	20	25	899.417	444.85	27.30	26.83
50	2	20	905.333	444.85	27.30	26.83
50	8	30	911.500	444.95	27.25	26.77
50	15	25	918.417	445.01	27.22	26.74
50	22	40	925.667	445.08	27.18	26.70
51	10	45	937.750	445.21	27.12	26.63
51	14	53	941.883	445.14	27.16	26.66
51	22	40	949.667	445.37	27.04	26.54
52	9	20	960.333	445.47	26.99	26.49
52	14	57	965.950	445.54	26.96	26.45

*Pressure = (500 ft – Depth to Water) × 0.495 psi/ft

+ Modified Pressure = (500 ft – {Depth to Water + [0.269 ft/240 hrs × (Elapsed Time – 53 hrs)]}) × 0.495 psi/ft

(continued)

Table A-6. (continued)

Day	Hr	Min	Elapsed Time (hr)	Depth to Water (ft)	Pressure (psi)	Modified Pressure (psi)
52	22	58	973.967	445.60	26.93	26.42
53	9	18	984.300	445.70	26.88	26.36
53	14	56	989.933	445.73	26.86	26.34
53	22	40	997.667	445.80	26.83	26.30
54	8	53	1007.883	445.90	26.78	26.25
54	14	42	1013.700	445.80	26.83	26.30
54	23	0	1022.000	445.87	26.79	26.26
55	9	26	1032.433	445.93	26.77	26.22
55	14	32	1037.533	445.93	26.77	26.22
55	22	55	1045.917	446.00	26.73	26.18
56	9	45	1056.750	446.13	26.67	26.11
56	15	8	1062.133	446.06	26.70	26.14
56	22	52	1069.867	446.06	26.70	26.14
57	10	55	1081.917	446.10	26.68	26.11
57	15	5	1086.083	446.03	26.71	26.14
57	22	48	1093.800	445.93	26.77	26.19
58	10	7	1105.117	446.06	26.70	26.12
58	15	30	1110.500	446.06	26.70	26.11
58	22	40	1117.667	446.26	26.60	26.01
59	9	36	1128.600	446.13	26.67	26.07
59	15	0	1134.000	446.13	26.67	26.07
59	22	40	1141.667	446.19	26.64	26.03
60	9	10	1152.167	446.29	26.59	25.98
60	15	10	1158.167	446.23	26.62	26.00
60	22	18	1165.300	446.16	26.65	26.03
61	8	30	1175.500	446.23	26.62	25.99
61	15	15	1182.250	446.06	26.70	26.07
61	21	10	1188.167	446.13	26.67	26.04
62	9	0	1200.000	446.13	26.67	26.03
62	15	20	1206.333	446.13	26.67	26.03
62	22	3	1213.050	446.19	26.64	25.99
63	10	20	1225.333	446.06	26.70	26.05
63	16	3	1231.050	446.10	26.68	26.03
63	22	0	1237.000	446.16	26.65	25.99
64	10	24	1249.400	446.00	26.73	26.07
64	16	30	1255.500	446.00	26.73	26.06
64	21	55	1260.917	446.06	26.70	26.03
65	15	50	1278.833	445.64	26.91	26.23
65	22	10	1285.167	445.87	26.79	26.11
66	9	0	1296.000	445.70	26.88	26.19
66	15	10	1302.167	445.60	26.93	26.23

(continued)

Table A-6. (concluded)

Day	Hr	Min	Elapsed Time (hr)	Depth to Water (ft)	Pressure (psi)	Modified Pressure (psi)
66	22	10	1309.167	445.70	26.88	26.18
67	9	0	1320.000	445.57	26.94	26.24
67	14	25	1325.417	445.41	27.02	26.32
67	22	10	1333.167	445.44	27.01	26.30
68	10	44	1345.733	445.37	27.04	26.32
69	8	40	1367.667	445.44	27.01	26.28
70	10	34	1393.567	445.28	27.09	26.34
71	13	40	1420.667	445.01	27.22	26.46
72	12	0	1443.000	444.95	27.25	26.48
73	10	30	1465.500	444.59	27.43	26.64
74	10	35	1489.583	444.23	27.61	26.81
75	10	35	1513.583	444.23	27.61	26.80
76	10	45	1537.750	444.13	27.66	26.83
77	10	35	1561.583	443.83	27.80	26.97
78	12	45	1587.750	443.64	27.90	27.05
79	14	0	1613.000	443.44	28.00	27.13
83	9	30	1704.500	442.85	28.29	27.37
84	11	0	1730.000	442.85	28.29	27.36
86	11	22	1778.367	442.45	28.49	27.53
89	11	30	1850.500	442.22	28.60	27.60
91	8	35	1895.583	441.90	28.76	27.74
93	9	45	1944.750	441.70	28.86	27.81
96	13	10	2020.167	441.27	29.07	27.98
98	10	25	2065.417	441.08	29.16	28.05
100	11	42	2114.700	440.49	29.46	28.31
103	11	0	2186.000	440.22	29.59	28.41
105	14	10	2237.167	439.86	29.77	28.56
108	10	45	2305.750	439.50	29.95	28.70
110	10	40	2353.667	439.37	30.01	28.73
113	9	35	2424.583	439.11	30.14	28.82
114	14	48	2453.800	438.98	30.20	28.87
118	11	30	2546.500	438.45	30.47	29.08
120	7	25	2590.417	438.19	30.60	29.19
126	9	50	2736.833	437.80	30.79	29.30
135	14	0	2957.000	436.61	31.38	29.77

Table A-7. Water Levels and Pressures in Observation Well WIPP-25 During the WIPP-13 Multipad Pumping Test

Day	Hr	Min	Elapsed Time (hr)	Depth to Water (ft)	Pressure* (psi)	Compensated+ Pressure (psi)
338	13	35	-931.417	163.85	15.82	15.82
6	10	0	-143.000	163.78	15.85	15.85
12	17	28	8.467	163.71	15.88	15.88
13	9	25	24.417	163.81	15.84	15.82
13	21	30	36.500	163.78	15.85	15.81
14	11	50	50.833	163.71	15.88	15.84
15	13	0	76.000	163.78	15.85	15.82
16	13	0	100.000	163.91	15.80	15.76
17	13	0	124.000	163.85	15.82	15.78
18	12	55	147.917	163.85	15.82	15.79
19	12	45	171.750	163.91	15.80	15.76
20	12	51	195.850	163.94	15.78	15.78
21	12	50	219.833	163.98	15.77	15.74
22	12	50	243.833	164.04	15.74	15.74
23	12	45	267.750	163.91	15.80	15.75
24	14	30	293.500	163.94	15.78	15.75
25	12	50	315.833	164.11	15.71	15.70
26	13	0	340.000	164.11	15.71	15.72
27	13	0	364.000	163.98	15.77	15.75
28	13	0	388.000	163.98	15.77	15.74
29	17	20	416.333	164.01	15.75	15.74
30	12	50	435.833	164.17	15.68	15.69
31	13	0	460.000	164.04	15.74	15.69
32	13	35	484.583	164.07	15.73	15.69
33	12	55	507.917	164.11	15.71	15.67
34	14	30	533.500	164.11	15.71	15.67
35	12	30	555.500	164.17	15.68	15.65
36	13	0	580.000	164.40	15.58	15.59
37	13	15	604.250	164.44	15.56	15.60
38	13	0	628.000	164.37	15.60	15.63
39	13	15	652.250	164.30	15.63	15.64
40	13	15	676.250	164.30	15.63	15.64
41	13	15	700.250	164.21	15.66	15.65
42	13	0	724.000	164.14	15.70	15.68
43	12	30	747.500	164.24	15.65	15.64
44	13	55	772.917	164.34	15.61	15.58
45	11	15	794.250	164.27	15.64	15.56
46	13	15	820.250	164.34	15.61	15.56
47	12	26	843.433	164.50	15.54	15.49
49	11	35	890.583	164.44	15.56	15.53
51	11	24	938.400	164.44	15.56	15.56

*Pressure = (200 ft – Depth to Water) × 0.4377 psi/ft
+Compensated Pressure = Pressure + 0.3 (Barometric Pressure – 13.1 psi)

(continued)

Table A-7. (concluded)

Day	Hr	Min	Elapsed Time (hr)	Depth to Water (ft)	Pressure (psi)	Compensated Pressure (psi)
54	10	20	1009.333	164.27	15.64	15.59
56	8	55	1055.917	164.34	15.61	15.57
58	14	0	1109.000	164.30	15.63	15.57
61	11	0	1178.000	164.34	15.61	15.59
63	14	25	1229.417	164.40	15.58	15.61
65	12	48	1275.800	164.14	15.70	15.68
68	10	4	1345.067	164.24	15.65	15.63
70	9	30	1392.500	164.34	15.61	15.62
72	10	55	1441.917	164.24	15.65	15.65
75	13	45	1516.750	164.11	15.71	15.63
77	12	45	1563.750	164.11	15.71	15.65
85	11	30	1754.500	164.27	15.64	15.59
92	10	5	1921.083	164.30	15.63	15.61

Table A-8. Water Levels and Pressures in Observation Well WIPP-30 During the WIPP-13 Multipad Pumping Test

Day	Hr	Min	Elapsed Time (hr)	Depth to Water (ft)	Pressure* (psi)	Modified+ Pressure (psi)
311	10	15	-1582.750	380.84	8.85	9.40
318	11	7	-1413.883	380.64	8.94	9.44
328	9	15	-1175.750	380.84	8.85	9.27
336	9	18	-983.700	380.81	8.87	9.21
343	9	21	-815.650	380.64	8.94	9.24
349	10	45	-670.250	380.31	9.10	9.34
363	11	16	-333.733	380.15	9.17	9.30
365	10	20	-286.667	380.12	9.19	9.30
2	10	30	-238.500	379.79	9.34	9.43
6	9	30	-143.500	379.82	9.32	9.39
7	14	38	-114.367	379.86	9.30	9.36
9	13	20	-67.667	379.82	9.32	9.36
10	12	12	-44.800	379.92	9.28	9.31
11	12	55	-20.083	379.95	9.26	9.29
12	7	8	-1.867	379.95	9.26	9.28
12	14	45	5.750	379.89	9.29	9.31
13	1	25	16.417	379.89	9.29	9.30
13	11	48	26.800	379.79	9.34	9.35
14	0	30	39.500	379.69	9.38	9.39
14	11	40	50.667	379.66	9.40	9.40
14	22	23	61.383	379.66	9.40	9.39
15	10	10	73.167	379.76	9.35	9.34
15	22	16	85.267	379.72	9.37	9.36
16	10	25	97.417	379.79	9.34	9.32
16	22	40	109.667	379.79	9.34	9.32
17	10	17	121.283	379.82	9.32	9.30
17	22	48	133.800	379.92	9.28	9.25
18	10	22	145.367	379.99	9.24	9.21
18	22	15	157.250	380.02	9.23	9.20
19	10	20	169.333	380.12	9.19	9.14
19	22	15	181.250	380.18	9.16	9.11
20	11	15	194.250	380.41	9.05	9.00
20	22	15	205.250	380.51	9.00	8.95
21	10	40	217.667	380.58	8.97	8.92
21	22	15	229.250	380.74	8.90	8.84
22	10	47	241.783	380.94	8.81	8.74
22	22	15	253.250	381.00	8.78	8.71
23	11	38	266.633	381.00	8.78	8.71
23	22	15	277.250	381.10	8.73	8.65
24	10	15	289.250	381.20	8.69	8.61
24	22	15	301.250	381.50	8.55	8.46

*Pressure = (400 ft – Depth to Water) × 0.462 psi/ft

+ Modified Pressure = (400 ft – {Depth to Water + [0.175 ft/240 hrs × (Elapsed Time – 50 hrs)]}) × 0.462 psi/ft

(continued)

Table A-8. (continued)

Day	Hr	Min	Elapsed Time (hr)	Depth to Water (ft)	Pressure (psi)	Modified Pressure (psi)
25	10	50	313.833	381.69	8.46	8.37
25	22	15	325.250	381.92	8.35	8.26
26	11	30	338.500	382.12	8.26	8.16
26	22	15	349.250	382.28	8.19	8.09
27	10	15	361.250	382.41	8.13	8.02
27	22	15	373.250	382.51	8.08	7.97
28	10	42	385.700	382.61	8.03	7.92
28	22	15	397.250	382.71	7.99	7.87
29	11	40	410.667	382.97	7.87	7.75
29	22	15	421.250	383.14	7.79	7.66
30	11	32	434.533	383.43	7.66	7.53
30	22	15	445.250	383.53	7.61	7.48
31	10	20	457.333	383.56	7.59	7.46
31	22	15	469.250	383.69	7.54	7.39
32	10	13	481.217	383.92	7.43	7.28
32	22	15	493.250	384.09	7.35	7.20
33	10	16	505.267	384.28	7.26	7.11
33	22	15	517.250	384.42	7.20	7.04
34	10	55	529.917	384.61	7.11	6.95
34	22	15	541.250	384.74	7.05	6.88
35	10	15	553.250	384.94	6.96	6.79
35	22	15	565.250	385.14	6.87	6.69
36	14	25	581.417	385.50	6.70	6.52
36	22	15	589.250	385.70	6.61	6.42
37	10	40	601.667	385.89	6.52	6.33
37	22	15	613.250	386.09	6.43	6.24
38	10	15	625.250	386.22	6.37	6.17
38	22	15	637.250	386.35	6.31	6.11
39	10	15	649.250	386.42	6.27	6.07
39	22	15	661.250	386.58	6.20	5.99
40	10	30	673.500	386.71	6.14	5.93
40	22	15	685.250	386.81	6.09	5.88
41	10	15	697.250	386.88	6.06	5.84
41	22	15	709.250	386.98	6.01	5.79
42	10	30	721.500	387.14	5.94	5.71
42	22	15	733.250	387.24	5.89	5.67
43	11	18	746.300	387.43	5.81	5.57
43	22	17	757.283	387.53	5.76	5.52
44	11	36	770.600	387.63	5.71	5.47
44	22	13	781.217	387.66	5.70	5.46
45	10	15	793.250	387.66	5.70	5.45

(continued)

Table A-8. (continued)

Day	Hr	Min	Elapsed Time (hr)	Depth to Water (ft)	Pressure (psi)	Modified Pressure (psi)
45	22	15	805.250	387.70	5.68	5.43
46	10	15	817.250	387.93	5.58	5.32
46	22	15	829.250	388.12	5.49	5.23
47	11	13	842.217	388.25	5.43	5.16
47	22	15	853.250	388.39	5.36	5.09
48	7	40	862.667	388.55	5.29	5.02
48	13	33	868.550	388.65	5.24	4.97
48	16	36	871.600	388.71	5.22	4.94
48	21	20	876.333	388.71	5.22	4.94
49	3	15	882.250	388.78	5.18	4.90
49	8	15	887.250	388.81	5.17	4.89
49	14	30	893.500	388.85	5.15	4.87
49	21	12	900.200	388.85	5.15	4.87
50	3	15	906.250	388.91	5.12	4.83
50	9	40	912.667	388.94	5.11	4.82
50	14	50	917.833	389.01	5.08	4.79
50	23	45	926.750	389.14	5.02	4.72
51	6	50	933.833	389.24	4.97	4.67
51	16	50	943.833	389.37	4.91	4.61
51	23	45	950.750	389.44	4.88	4.58
52	9	50	960.833	389.40	4.90	4.59
52	15	30	966.500	389.40	4.90	4.59
52	23	40	974.667	389.50	4.85	4.54
53	9	50	984.833	389.57	4.82	4.50
53	15	30	990.500	389.57	4.82	4.50
53	23	40	998.667	389.60	4.80	4.49
54	9	27	1008.450	389.50	4.85	4.53
54	15	15	1014.250	389.44	4.88	4.55
54	23	35	1022.583	389.50	4.85	4.52
55	10	0	1033.000	389.50	4.85	4.52
55	15	5	1038.083	389.50	4.85	4.52
55	23	35	1046.583	389.57	4.82	4.48
56	10	40	1057.667	389.53	4.84	4.50
56	15	43	1062.717	389.50	4.85	4.51
56	23	30	1070.500	389.50	4.85	4.51
57	8	36	1079.600	389.44	4.88	4.53
57	15	55	1086.917	389.40	4.90	4.55
57	23	30	1094.500	389.40	4.90	4.54
58	10	33	1105.550	389.34	4.92	4.57
58	21	45	1116.750	389.27	4.96	4.60
59	10	10	1129.167	389.30	4.94	4.58

(continued)

Table A-8. (continued)

Day	Hr	Min	Elapsed Time (hr)	Depth to Water (ft)	Pressure (psi)	Modified Pressure (psi)
59	21	45	1140.750	389.24	4.97	4.60
60	9	40	1152.667	389.27	4.96	4.59
60	22	45	1165.750	389.17	5.00	4.63
61	9	35	1176.583	389.11	5.03	4.65
61	22	0	1189.000	389.01	5.08	4.69
62	9	30	1200.500	389.01	5.08	4.69
62	22	45	1213.750	388.98	5.09	4.70
63	8	35	1223.583	388.98	5.09	4.70
63	22	45	1237.750	388.88	5.14	4.74
64	7	55	1246.917	388.71	5.22	4.81
64	22	40	1261.667	388.52	5.30	4.90
65	11	45	1274.750	388.35	5.38	4.97
65	22	55	1285.917	388.19	5.46	5.04
66	9	35	1296.583	388.06	5.52	5.10
66	22	55	1309.917	387.93	5.58	5.15
67	9	30	1320.500	387.80	5.64	5.21
67	22	45	1333.750	387.63	5.71	5.28
68	8	50	1343.833	387.57	5.74	5.31
69	8	17	1367.283	387.43	5.81	5.36
70	8	51	1391.850	387.30	5.87	5.42
71	11	6	1418.100	387.01	6.00	5.54
72	9	48	1440.800	386.81	6.09	5.62
73	9	20	1464.333	386.38	6.29	5.82
74	9	20	1488.333	386.09	6.43	5.94
75	9	20	1512.333	385.79	6.57	6.07
76	9	35	1536.583	385.56	6.67	6.17
77	9	20	1560.333	385.43	6.73	6.22
78	8	53	1583.883	385.27	6.80	6.29
79	12	35	1611.583	385.07	6.90	6.37
82	9	15	1680.250	384.48	7.17	6.62
84	9	45	1728.750	384.32	7.24	6.68
86	10	18	1777.300	383.99	7.40	6.82
89	9	15	1848.250	383.86	7.46	6.85
91	9	20	1896.333	383.40	7.67	7.05
93	8	40	1943.667	383.27	7.73	7.09
96	11	10	2018.167	382.94	7.88	7.22
98	9	15	2064.250	382.74	7.97	7.30
100	8	32	2111.533	382.41	8.13	7.43
103	9	35	2184.583	382.12	8.26	7.54
105	13	0	2236.000	382.05	8.29	7.56
108	9	25	2304.417	381.63	8.49	7.73

(continued)

Table A-8. (concluded)

Day	Hr	Min	Elapsed Time (hr)	Depth to Water (ft)	Pressure (psi)	Modified Pressure (psi)
110	9	20	2352.333	381.63	8.49	7.71
113	8	35	2423.583	381.53	8.53	7.73
114	12	30	2451.500	381.50	8.55	7.74
118	10	10	2545.167	381.33	8.63	7.79
120	6	50	2589.833	381.04	8.76	7.90
126	8	45	2735.750	380.94	8.81	7.90
135	14	20	2957.333	380.51	9.00	8.03

Table A-9. Water Levels and Pressures in Observation Well H-1 Culebra During the WIPP-13 Multipad Pumping Test

Day	Hr	Min	Elapsed Time (hr)	Depth to Water (ft)	Pressure* (psi)	Modified+ Pressure (psi)
303	11	35	-1773.417	416.55	36.74	38.62
307	11	10	-1677.833	416.46	36.78	38.59
308	7	55	-1657.083	416.42	36.80	38.59
309	10	0	-1631.000	416.37	36.82	38.59
310	14	35	-1602.417	416.33	36.84	38.58
311	10	40	-1582.333	416.30	36.85	38.58
315	8	10	-1488.833	416.28	36.86	38.51
316	13	40	-1459.333	416.27	36.87	38.49
317	10	43	-1438.283	416.28	36.86	38.47
318	8	30	-1416.500	416.30	36.85	38.44
325	9	23	-1247.617	416.42	36.80	38.25
328	11	20	-1173.667	416.45	36.79	38.18
336	11	11	-981.817	416.40	36.81	38.04
343	12	36	-812.400	416.30	36.85	37.95
349	12	24	-668.600	416.18	36.91	37.88
357	10	20	-478.667	416.00	36.98	37.81
363	13	52	-331.133	415.79	37.08	37.78
365	11	3	-285.950	415.67	37.13	37.80
2	11	35	-237.417	415.58	37.17	37.80
5	13	50	-163.167	415.49	37.21	37.78
7	10	53	-118.117	415.42	37.24	37.77
9	13	55	-67.083	415.32	37.28	37.77
10	11	32	-45.467	415.28	37.30	37.77
11	13	25	-19.583	415.25	37.31	37.76
12	6	38	-2.367	415.23	37.32	37.76
12	16	40	7.667	415.21	37.33	37.76
13	0	51	15.850	415.19	37.34	37.76
13	12	12	27.200	415.17	37.35	37.76
14	0	51	39.850	415.15	37.36	37.76
14	12	52	51.867	415.12	37.37	37.76
14	22	35	61.583	415.11	37.38	37.76
15	10	30	73.500	415.08	37.39	37.76
15	22	35	85.583	415.06	37.40	37.76
16	10	56	97.933	415.00	37.42	37.78
16	22	55	109.917	415.00	37.42	37.77
17	10	59	121.983	414.99	37.43	37.76
17	22	20	133.333	415.00	37.42	37.75
18	10	50	145.833	414.96	37.44	37.76
18	22	40	157.667	414.92	37.46	37.77
19	10	49	169.817	414.90	37.47	37.76
19	22	35	181.583	414.87	37.48	37.77

*Pressure = (500 ft – Depth to Water) × 0.4403 psi/ft

+ Modified Pressure = (500 ft – {Depth to Water + [0.445 ft/240 hrs × (Elapsed Time – 530 hrs)]}) × 0.4403 psi/ft

(continued)

Table A-9. (continued)

Day	Hr	Min	Elapsed Time (hr)	Depth to Water (ft)	Pressure (psi)	Modified Pressure (psi)
20	10	45	193.750	414.85	37.49	37.77
20	22	35	205.583	414.83	37.50	37.77
21	11	0	218.000	414.82	37.51	37.76
21	22	35	229.583	414.79	37.52	37.76
22	10	25	241.417	414.75	37.54	37.77
22	22	30	253.500	414.74	37.54	37.77
23	11	21	266.350	414.73	37.54	37.76
23	22	30	277.500	414.70	37.56	37.76
24	10	45	289.750	414.67	37.57	37.77
24	22	30	301.500	414.65	37.58	37.77
25	10	25	313.417	414.63	37.59	37.77
25	22	35	325.583	414.60	37.60	37.77
26	11	12	338.200	414.55	37.62	37.78
26	22	30	349.500	414.56	37.62	37.77
27	10	28	361.467	414.55	37.62	37.76
27	22	30	373.500	414.52	37.64	37.77
28	11	28	386.467	414.50	37.65	37.76
28	22	30	397.500	414.47	37.66	37.77
29	11	20	410.333	414.47	37.66	37.76
29	22	30	421.500	414.43	37.68	37.77
30	10	42	433.700	414.42	37.68	37.76
30	22	30	445.500	414.40	37.69	37.76
31	11	6	458.100	414.38	37.70	37.76
31	22	30	469.500	414.35	37.71	37.76
32	10	44	481.733	414.33	37.72	37.76
32	22	30	493.500	414.30	37.73	37.76
33	10	49	505.817	414.29	37.74	37.76
33	22	30	517.500	414.25	37.76	37.77
34	11	17	530.283	414.23	37.77	37.76
34	22	30	541.500	414.21	37.77	37.76
35	10	33	553.550	414.20	37.78	37.76
35	22	30	565.500	414.17	37.79	37.76
36	15	12	582.200	414.15	37.80	37.76
36	22	30	589.500	414.13	37.81	37.76
37	11	20	602.333	414.12	37.81	37.75
37	22	32	613.533	414.11	37.82	37.75
38	10	36	625.600	414.10	37.82	37.74
38	22	32	637.533	414.07	37.84	37.75
39	10	35	649.583	414.06	37.84	37.74
39	22	30	661.500	414.04	37.85	37.74
40	11	8	674.133	414.01	37.86	37.74

(continued)

Table A-9. (continued)

Day	Hr	Min	Elapsed Time (hr)	Depth to Water (ft)	Pressure (psi)	Modified Pressure (psi)
40	22	30	685.500	414.00	37.87	37.74
41	10	35	697.583	414.00	37.87	37.73
41	22	30	709.500	413.97	37.88	37.73
42	11	20	722.333	413.96	37.88	37.73
42	22	30	733.500	413.94	37.89	37.73
43	10	30	745.500	413.92	37.90	37.73
43	22	41	757.683	413.91	37.91	37.72
44	10	47	769.783	413.90	37.91	37.71
44	22	30	781.500	413.89	37.91	37.71
45	10	30	793.500	413.86	37.93	37.71
45	22	35	805.583	413.84	37.94	37.71
46	10	30	817.500	413.82	37.95	37.71
46	22	35	829.583	413.81	37.95	37.70
47	9	3	840.050	413.79	37.96	37.70
47	22	39	853.650	413.79	37.96	37.69
48	7	8	862.133	413.76	37.97	37.70
48	10	42	865.700	413.77	37.97	37.69
48	14	15	869.250	413.77	37.97	37.69
48	20	59	875.983	413.76	37.97	37.69
49	8	33	887.550	413.75	37.98	37.68
49	14	10	893.167	413.75	37.98	37.68
49	20	39	899.650	413.73	37.98	37.68
50	9	0	912.000	413.71	37.99	37.68
50	15	50	918.833	413.72	37.99	37.67
50	22	59	925.983	413.71	37.99	37.67
51	7	30	934.500	413.70	38.00	37.67
51	15	11	942.183	413.70	38.00	37.66
51	23	0	950.000	413.70	38.00	37.66
52	9	32	960.533	413.69	38.00	37.65
52	15	15	966.250	413.68	38.01	37.65
52	23	18	974.300	413.68	38.01	37.64
53	9	35	984.583	413.67	38.01	37.64
53	15	15	990.250	413.67	38.01	37.63
53	22	55	997.917	413.66	38.02	37.63
54	9	10	1008.167	413.65	38.02	37.63
54	15	0	1014.000	413.64	38.02	37.63
54	23	15	1022.250	413.64	38.02	37.62
55	9	42	1032.700	413.63	38.03	37.62
55	14	48	1037.800	413.63	38.03	37.61
55	23	10	1046.167	413.62	38.03	37.61
57	9	30	1080.500	413.60	38.04	37.59

(continued)

Table A-9. (continued)

Day	Hr	Min	Elapsed Time (hr)	Depth to Water (ft)	Pressure (psi)	Modified Pressure (psi)
56	10	8	1057.133	413.60	38.04	37.61
56	15	23	1062.383	413.61	38.04	37.60
56	23	6	1070.100	413.61	38.04	37.60
57	15	30	1086.500	413.60	38.04	37.59
57	23	3	1094.050	413.60	38.04	37.58
58	9	49	1104.817	413.59	38.05	37.58
58	15	47	1110.783	413.58	38.05	37.58
58	23	10	1118.167	413.58	38.05	37.57
59	9	53	1128.883	413.57	38.05	37.57
59	15	20	1134.333	413.57	38.05	37.56
59	23	10	1142.167	413.56	38.06	37.56
60	9	25	1152.417	413.58	38.05	37.54
60	15	30	1158.500	413.58	38.05	37.54
60	21	43	1164.717	413.58	38.05	37.53
61	10	43	1177.717	413.57	38.05	37.53
61	14	50	1181.833	413.57	38.05	37.52
61	21	30	1188.500	413.57	38.05	37.52
62	9	15	1200.250	413.58	38.05	37.50
62	15	35	1206.583	413.58	38.05	37.50
62	22	25	1213.417	413.58	38.05	37.49
63	10	42	1225.700	413.58	38.05	37.48
63	15	13	1230.217	413.58	38.05	37.48
63	22	20	1237.333	413.59	38.05	37.47
64	10	42	1249.700	413.59	38.05	37.46
64	15	20	1254.333	413.59	38.05	37.45
64	21	15	1260.250	413.60	38.04	37.45
65	15	10	1278.167	413.59	38.05	37.44
65	22	35	1285.583	413.60	38.04	37.42
66	9	20	1296.333	413.60	38.04	37.42
66	15	25	1302.417	413.60	38.04	37.41
66	22	35	1309.583	413.60	38.04	37.41
67	9	15	1320.250	413.60	38.04	37.40
67	14	35	1325.583	413.60	38.04	37.39
67	22	26	1333.433	413.59	38.05	37.39
68	10	58	1345.967	413.60	38.04	37.38
69	9	5	1368.083	413.61	38.04	37.35
70	10	54	1393.900	413.61	38.04	37.33
71	12	2	1419.033	413.60	38.04	37.32
72	11	28	1442.467	413.61	38.04	37.29
73	10	45	1465.750	413.62	38.03	37.27
74	10	50	1489.833	413.62	38.03	37.25

(continued)

Table A-9. (concluded)

Day	Hr	Min	Elapsed Time (hr)	Depth to Water (ft)	Pressure (psi)	Modified Pressure (psi)
75	10	50	1513.833	413.61	38.04	37.23
76	11	5	1538.083	413.60	38.04	37.22
77	10	50	1561.833	413.60	38.04	37.20
78	11	58	1586.967	413.59	38.05	37.18
79	13	40	1612.667	413.57	38.05	37.17
80	12	55	1635.917	413.57	38.05	37.15
81	10	45	1657.750	413.56	38.06	37.14
82	10	40	1681.667	413.55	38.06	37.12
83	9	40	1704.667	413.54	38.07	37.11
84	11	25	1730.417	413.53	38.07	37.09
85	12	30	1755.500	413.52	38.08	37.08
86	13	15	1780.250	413.51	38.08	37.06
87	12	0	1803.000	413.50	38.09	37.05
88	10	35	1825.583	413.49	38.09	37.03
89	11	50	1850.833	413.49	38.09	37.01
91	10	35	1897.583	413.46	38.10	36.99
92	13	55	1924.917	413.45	38.11	36.97
93	10	0	1945.000	413.44	38.11	36.96
95	13	40	1996.667	413.41	38.13	36.93
96	13	25	2020.417	413.40	38.13	36.91
98	10	45	2065.750	413.37	38.14	36.89
100	11	2	2114.033	413.34	38.16	36.86
102	9	0	2160.000	413.28	38.18	36.85
103	11	30	2186.500	413.26	38.19	36.84
105	14	30	2237.500	413.21	38.21	36.82
108	11	5	2306.083	413.15	38.24	36.79
110	11	0	2354.000	413.10	38.26	36.77
113	9	55	2424.917	413.02	38.30	36.75
114	14	15	2453.250	412.98	38.31	36.74
118	11	55	2546.917	412.87	38.36	36.72
120	9	55	2592.917	412.79	38.40	36.71
126	10	10	2737.167	412.54	38.51	36.71
134	6	0	2925.000	412.20	38.66	36.70
135	8	48	2951.800	412.15	38.68	36.70

Table A-10. Water Levels and Pressures in Observation Well H-2b2 During the WIPP-13 Multipad Pumping Test

Day	Hr	Min	Elapsed Time (hr)	Depth to Water (ft)	Pressure* (psi)	Compensated+ Pressure (psi)	Modified# Pressure (psi)
336	10	20	-982.667	366.70	14.52	14.52	15.02
343	11	8	-813.867	366.57	14.58	14.58	15.02
349	11	55	-669.083	366.50	14.61	14.61	15.00
357	9	30	-479.500	366.34	14.68	14.68	15.00
363	13	15	-331.750	366.21	14.73	14.73	15.00
365	8	50	-288.167	366.17	14.75	14.75	15.00
2	11	25	-237.583	365.91	14.86	14.86	15.10
5	14	25	-162.583	365.81	14.91	14.91	15.12
7	11	45	-117.250	365.94	14.85	14.85	15.04
9	14	10	-66.833	365.88	14.88	14.88	15.05
10	11	25	-45.583	365.94	14.85	14.85	15.02
11	13	30	-19.500	365.98	14.83	14.83	14.99
12	6	35	-2.417	365.94	14.85	14.85	15.00
12	16	47	7.783	365.88	14.88	14.86	15.01
13	0	48	15.800	365.91	14.86	14.84	14.99
13	12	7	27.117	365.78	14.92	14.86	15.00
14	0	46	39.767	365.72	14.95	14.85	14.99
14	12	47	51.783	365.62	14.99	14.89	15.02
14	22	39	61.650	365.58	15.01	14.93	15.06
15	10	25	73.417	365.68	14.96	14.91	15.03
15	22	30	85.500	365.65	14.98	14.91	15.03
16	11	0	98.000	365.65	14.98	14.91	15.03
16	23	5	110.083	365.65	14.98	14.91	15.02
17	12	4	123.067	365.58	15.01	14.92	15.03
17	22	27	133.450	365.65	14.98	14.93	15.03
18	10	43	145.717	365.65	14.98	14.93	15.03
18	22	35	157.583	365.62	14.99	14.94	15.03
19	10	40	169.667	365.62	14.99	14.94	15.03
19	22	30	181.500	365.58	15.01	14.97	15.06
20	10	50	193.833	365.68	14.96	14.97	15.05
20	22	30	205.500	365.68	14.96	14.96	15.03
21	10	57	217.950	365.62	14.99	14.95	15.02
21	22	30	229.500	365.68	14.96	14.97	15.03
22	10	30	241.500	365.72	14.95	14.94	15.00
22	22	25	253.417	365.62	14.99	14.95	15.00
23	11	25	266.417	365.52	15.03	14.95	15.00
23	22	35	277.583	365.45	15.06	14.96	15.00
24	10	40	289.667	365.42	15.08	14.99	15.03
24	22	35	301.583	365.55	15.02	14.99	15.02
25	10	33	313.550	365.55	15.02	15.01	15.04

*Pressure = (400 ft − Depth to Water) × 0.436 psi/ft

+Compensated Pressure = Pressure + 0.6 (Barometric Pressure − 13.1 psi)

#Modified Pressure = Compensated Pressure − [0.086 psi/240 hrs × (Elapsed Time − 420 hrs)]

(continued)

Table A-10. (continued)

Day	Hr	Min	Elapsed Time (hr)	Depth to Water (ft)	Pressure (psi)	Compensated Pressure (psi)	Modified Pressure (psi)
25	22	30	325.500	365.65	14.98	14.98	15.01
26	11	16	338.267	365.65	14.98	15.00	15.02
26	22	25	349.417	365.65	14.98	14.98	15.00
27	10	33	361.550	365.62	14.99	14.98	15.00
27	22	25	373.417	365.55	15.02	14.98	14.99
28	11	34	386.567	365.45	15.06	15.01	15.01
28	22	25	397.417	365.42	15.08	15.01	15.01
29	11	26	410.433	365.49	15.05	15.02	15.02
29	22	25	421.417	365.49	15.05	15.02	15.02
30	22	25	445.417	365.52	15.03	15.00	14.98
31	11	12	458.200	365.39	15.09	15.00	14.98
31	22	25	469.417	365.35	15.11	15.02	15.00
32	10	40	481.667	365.42	15.08	15.01	14.98
32	22	25	493.417	365.42	15.08	15.01	14.98
33	10	29	505.483	365.42	15.08	15.01	14.98
33	22	25	517.417	365.39	15.09	15.01	14.97
34	11	13	530.217	365.42	15.08	15.01	14.97
34	22	25	541.417	365.42	15.08	15.00	14.95
35	10	28	553.467	365.45	15.06	15.00	14.95
35	22	25	565.417	365.49	15.05	14.99	14.94
36	15	16	582.267	365.68	14.96	14.99	14.93
36	22	25	589.417	365.75	14.93	14.98	14.92
37	11	25	602.417	365.81	14.91	14.97	14.90
37	22	26	613.433	365.88	14.88	14.94	14.87
38	10	31	625.517	365.88	14.88	14.95	14.87
38	22	26	637.433	365.85	14.89	14.92	14.84
39	10	30	649.500	365.81	14.91	14.93	14.85
39	22	25	661.417	365.81	14.91	14.93	14.85
40	10	52	673.867	365.85	14.89	14.92	14.83
40	22	25	685.417	365.78	14.92	14.90	14.81
41	10	30	697.500	365.75	14.93	14.91	14.81
41	22	25	709.417	365.75	14.93	14.90	14.80
42	10	50	721.833	365.78	14.92	14.90	14.79
42	22	25	733.417	365.81	14.91	14.87	14.76
43	10	34	745.567	365.81	14.91	14.89	14.77
43	22	35	757.583	365.81	14.91	14.87	14.75
44	10	52	769.867	365.78	14.92	14.87	14.74
44	22	25	781.417	365.75	14.93	14.83	14.70
45	10	25	793.417	365.62	14.99	14.84	14.70
45	22	30	805.500	365.55	15.02	14.86	14.72

(continued)

Table A-10. (continued)

Day	Hr	Min	Elapsed Time (hr)	Depth to Water (ft)	Pressure (psi)	Compensated Pressure (psi)	Modified Pressure (psi)
46	10	25	817.417	365.72	14.95	14.86	14.71
46	22	30	829.500	365.75	14.93	14.84	14.69
47	9	6	840.100	365.75	14.93	14.84	14.69
47	22	32	853.533	365.85	14.89	14.82	14.67
48	7	13	862.217	365.94	14.85	14.82	14.65
48	10	46	865.767	365.98	14.83	14.80	14.64
48	14	10	869.167	366.01	14.82	14.78	14.62
48	20	55	875.917	366.01	14.82	14.78	14.62
49	2	7	881.117	366.04	14.81	14.76	14.60
49	8	26	887.433	366.04	14.81	14.76	14.59
49	14	6	893.100	366.04	14.81	14.73	14.56
49	20	44	899.733	365.98	14.83	14.74	14.57
50	2	39	905.650	366.01	14.82	14.73	14.56
50	9	5	912.083	366.04	14.81	14.74	14.56
50	16	35	919.583	366.08	14.79	14.72	14.54
50	23	5	926.083	366.11	14.78	14.73	14.55
51	7	35	934.583	366.17	14.75	14.74	14.56
51	15	14	942.233	366.24	14.72	14.70	14.52
51	23	5	950.083	366.27	14.71	14.69	14.50
52	9	37	960.617	366.21	14.73	14.69	14.49
52	15	20	966.333	366.21	14.73	14.67	14.47
52	23	24	974.400	366.27	14.71	14.68	14.48
53	9	40	984.667	366.31	14.69	14.67	14.47
53	15	20	990.333	366.31	14.69	14.64	14.43
53	23	0	998.000	366.34	14.68	14.61	14.40
54	9	15	1008.250	366.24	14.72	14.62	14.41
54	15	5	1014.083	366.17	14.75	14.61	14.40
54	23	20	1022.333	366.24	14.72	14.62	14.40
55	9	47	1032.783	366.27	14.71	14.62	14.40
55	14	53	1037.883	366.27	14.71	14.61	14.38
55	23	15	1046.250	366.34	14.68	14.59	14.36
56	10	25	1057.417	366.34	14.68	14.59	14.36
56	15	30	1062.500	366.31	14.69	14.58	14.35
56	23	11	1070.183	366.37	14.66	14.56	14.33
57	9	33	1080.550	366.37	14.66	14.57	14.33
57	15	35	1086.583	366.37	14.66	14.55	14.31
57	23	7	1094.117	366.37	14.66	14.57	14.32
58	9	53	1104.883	366.40	14.65	14.54	14.29
58	21	25	1116.417	366.44	14.63	14.53	14.28
59	9	58	1128.967	366.54	14.59	14.52	14.26

(continued)

Table A-10. (continued)

Day	Hr	Min	Elapsed Time (hr)	Depth to Water (ft)	Pressure (psi)	Compensated Pressure (psi)	Modified Pressure (psi)
59	21	25	1140.417	366.60	14.56	14.51	14.25
60	9	30	1152.500	366.73	14.51	14.49	14.22
60	15	35	1158.583	366.77	14.49	14.44	14.17
60	21	37	1164.617	366.73	14.51	14.46	14.20
61	10	48	1177.800	366.80	14.47	14.44	14.17
61	14	46	1181.767	366.80	14.47	14.42	14.15
61	21	35	1188.583	366.80	14.47	14.44	14.17
62	9	20	1200.333	366.93	14.42	14.44	14.16
62	22	30	1213.500	367.03	14.38	14.42	14.13
63	10	48	1225.800	367.03	14.38	14.44	14.15
63	22	25	1237.417	367.19	14.30	14.36	14.06
64	10	46	1249.767	367.13	14.33	14.36	14.07
64	22	20	1261.333	367.13	14.33	14.32	14.02
65	19	5	1282.083	367.06	14.36	14.32	14.01
65	22	40	1285.667	367.06	14.36	14.32	14.01
66	9	25	1296.417	367.06	14.36	14.32	14.00
66	22	40	1309.667	367.06	14.36	14.30	13.98
67	9	20	1320.333	367.03	14.38	14.30	13.98
67	22	32	1333.533	367.03	14.38	14.29	13.96
68	11	2	1346.033	367.13	14.33	14.29	13.96
69	9	10	1368.167	367.26	14.28	14.27	13.93
70	9	5	1392.083	367.36	14.23	14.25	13.90
71	12	10	1419.167	367.39	14.22	14.22	13.87
72	11	14	1442.233	367.42	14.21	14.19	13.82
73	10	50	1465.833	367.22	14.29	14.20	13.83
74	10	55	1489.917	367.22	14.29	14.19	13.80
75	10	55	1513.917	367.13	14.33	14.18	13.79
76	11	10	1538.167	367.13	14.33	14.17	13.77
77	10	55	1561.917	367.22	14.29	14.17	13.76
78	13	2	1588.033	367.26	14.28	14.16	13.74
79	13	20	1612.333	367.26	14.28	14.16	13.73
82	10	45	1681.750	367.19	14.30	14.17	13.72
84	11	30	1730.500	367.36	14.23	14.16	13.69
86	13	10	1780.167	367.26	14.28	14.16	13.68
89	12	10	1851.167	367.59	14.13	14.14	13.63
91	10	40	1897.667	367.36	14.23	14.17	13.64
93	10	15	1945.250	367.42	14.21	14.19	13.64
96	14	0	2021.000	367.32	14.25	14.24	13.66
98	12	30	2067.500	367.32	14.25	14.25	13.66
100	10	35	2113.583	367.09	14.35	14.30	13.69

(continued)

Table A-10. (concluded)

Day	Hr	Min	Elapsed Time (hr)	Depth to Water (ft)	Pressure (psi)	Compensated Pressure (psi)	Modified Pressure (psi)
103	11	50	2186.833	366.99	14.39	14.36	13.72
105	14	50	2237.833	366.99	14.39	14.32	13.67
108	11	9	2306.150	366.70	14.52	14.41	13.74
110	11	20	2354.333	366.80	14.47	14.45	13.76
113	10	30	2425.500	366.77	14.49	14.47	13.75
114	9	10	2448.167	366.73	14.51	14.50	13.77
118	12	0	2547.000	366.70	14.52	14.54	13.78
120	10	20	2593.333	366.40	14.65	14.65	13.87
126	10	35	2737.583	366.37	14.66	14.66	13.83
135	15	25	2958.417	365.91	14.86	14.86	13.95

Table A-11. Water Levels in Observation Well H-3b2 During the WIPP-13 Multipad Pumping Test

Day	Hr	Min	Elapsed Time (hr)	Depth to Water (ft)
336	11	48	-981.200	414.11
343	13	15	-811.750	413.88
349	13	8	-667.867	413.71
357	9	16	-479.733	413.52
363	13	46	-331.233	413.32
365	11	12	-285.800	413.29
5	14	15	-162.750	412.86
8	9	25	-95.583	412.93
9	13	50	-67.167	412.89
12	19	50	10.833	412.86
14	13	15	52.250	412.47
16	15	40	102.667	412.73
19	17	10	176.167	412.60
20	9	25	192.417	412.83
21	10	40	217.667	412.60
23	15	34	270.567	412.66
26	15	50	342.833	412.40
28	8	55	383.917	412.34
30	15	19	438.317	412.37
33	10	39	505.650	412.14
35	9	18	552.300	412.11
37	15	16	606.267	412.40
40	11	2	674.033	412.37
42	15	0	726.000	411.88
44	16	58	775.967	411.75
47	10	13	841.217	412.01
49	13	12	892.200	411.88
51	13	8	940.133	411.94
54	10	45	1009.750	411.68
56	10	15	1057.250	411.71
58	13	6	1108.100	411.42
61	13	5	1180.083	411.65
63	16	13	1231.217	411.84
65	15	19	1278.317	411.42
68	11	14	1346.233	411.55
70	10	4	1393.067	411.58
72	11	24	1442.400	411.61
75	14	50	1517.833	411.29
77	11	25	1562.417	411.15
79	13	30	1612.500	411.09
83	9	50	1704.833	411.29
84	11	20	1730.333	411.32

(continued)

Table A-11. (concluded)

Day	Hr	Min	Elapsed Time (hr)	Depth to Water (ft)
86	13	36	1780.600	411.32
89	12	0	1851.000	411.52
91	14	45	1901.750	410.99
93	10	10	1945.167	411.19
96	13	40	2020.667	411.25
98	10	55	2065.917	411.19
100	10	46	2113.767	411.08
103	11	35	2186.583	410.99
105	14	40	2237.667	410.70
114	14	11	2453.183	410.79
135	12	55	2955.917	410.40

Table A-12. Water Levels in Observation Well H-5b During the WIPP-13 Multipad Pumping Test

Day	Hr	Min	Elapsed Time (hr)	Depth to Water (ft)
339	10	45	-910.250	486.84
357	11	27	-477.550	486.61
363	13	4	-331.933	486.68
6	11	17	-141.717	486.48
9	14	35	-66.417	486.42
13	11	5	26.083	486.48
14	13	45	52.750	486.19
16	17	0	104.000	486.55
19	16	45	175.750	486.45
21	11	15	218.250	486.48
23	14	46	269.767	486.45
26	16	50	343.833	486.25
28	9	40	384.667	486.52
30	14	56	437.933	486.42
33	8	55	503.917	486.29
35	9	48	552.800	486.25
37	17	15	608.250	486.58
40	9	37	672.617	486.65
42	14	20	725.333	486.15
44	18	25	777.417	486.12
47	11	7	842.117	486.35
49	12	0	891.000	486.25
51	12	50	939.833	486.35
54	9	55	1008.917	486.22
56	11	5	1058.083	486.15
58	13	28	1108.467	486.02
61	12	15	1179.250	486.12
63	15	2	1230.033	486.29
65	13	15	1276.250	486.09
68	16	30	1351.500	485.96
70	8	40	1391.667	486.35
72	10	12	1441.200	486.38
75	14	30	1517.500	486.09
77	11	45	1562.750	485.93
85	11	55	1754.917	486.32
92	12	10	1923.167	486.45
100	9	55	2112.917	486.25
106	10	0	2257.000	488.85
114	13	5	2452.083	486.42
136	11	40	2978.667	486.48

Table A-13. Water Levels and Pressures in Observation Well H-6a During the WIPP-13 Multipad Pumping Test

Day	Hr	Min	Elapsed Time (hr)	Depth to Water (ft)	Pressure* (psi)
336	10	10	-982.833	303.08	43.76
343	10	22	-814.633	303.08	43.76
349	10	25	-670.583	303.08	43.76
363	11	50	-333.167	303.02	43.79
365	9	25	-287.583	302.85	43.86
2	11	0	-238.000	302.69	43.94
5	10	42	-166.300	302.72	43.92
6	14	8	-138.867	302.72	43.92
7	14	0	-115.000	302.89	43.84
9	14	55	-66.083	302.95	43.82
10	10	40	-46.333	303.25	43.68
11	14	0	-19.000	303.25	43.68
12	7	33	-1.450	303.22	43.70
12	9	2	0.033	303.15	43.73
12	10	5	1.083	303.18	43.71
12	11	0	2.000	303.18	43.71
12	12	13	3.217	303.15	43.73
12	13	0	4.000	303.12	43.74
12	14	0	5.000	303.08	43.76
12	15	0	6.000	303.08	43.76
12	16	0	7.000	303.08	43.76
12	16	57	7.950	303.12	43.74
12	19	0	10.000	303.22	43.70
12	20	30	11.500	303.28	43.67
12	21	30	12.500	303.35	43.64
12	22	0	13.000	303.38	43.62
12	23	13	14.217	303.44	43.60
13	0	15	15.250	303.44	43.60
13	1	45	16.750	303.44	43.60
13	3	11	18.183	303.48	43.58
13	4	1	19.017	303.48	43.58
13	5	4	20.067	303.51	43.56
13	6	4	21.067	303.58	43.53
13	7	0	22.000	303.61	43.52
13	8	25	23.417	303.71	43.48
13	9	37	24.617	303.77	43.45
13	10	25	25.417	303.84	43.42
13	11	31	26.517	303.87	43.40
13	12	33	27.550	303.87	43.40
13	13	30	28.500	303.90	43.39
13	14	30	29.500	303.94	43.37

*Pressure = (400 ft – Depth to Water) × 0.4515 psi/ft

(continued)

Table A-13. (continued)

Day	Hr	Min	Elapsed Time (hr)	Depth to Water (ft)	Pressure (psi)
13	15	30	30.500	303.97	43.36
13	16	30	31.500	304.00	43.34
13	17	30	32.500	304.10	43.30
13	18	30	33.500	304.17	43.27
13	19	30	34.500	304.27	43.22
13	20	35	35.583	304.36	43.18
13	21	54	36.900	304.46	43.14
13	23	44	38.733	304.59	43.08
14	1	31	40.517	304.66	43.05
14	4	55	43.917	304.76	43.00
14	7	0	46.000	304.86	42.96
14	9	40	48.667	305.12	42.84
14	11	0	50.000	305.18	42.81
14	13	15	52.250	305.25	42.78
14	15	0	54.000	305.31	42.75
14	17	35	56.583	305.45	42.69
14	21	35	60.583	305.64	42.60
15	7	35	70.583	306.40	42.26
15	11	30	74.500	306.66	42.14
15	15	30	78.500	306.79	42.08
15	19	35	82.583	306.96	42.01
15	23	30	86.500	307.32	41.84
16	7	35	94.583	307.58	41.73
16	19	30	106.500	308.14	41.48
16	23	35	110.583	308.46	41.33
17	7	35	118.583	308.66	41.24
17	19	35	130.583	309.19	41.00
18	7	30	142.500	309.71	40.77
18	19	35	154.583	310.04	40.62
19	7	30	166.500	310.50	40.41
19	19	35	178.583	310.86	40.25
20	7	30	190.500	311.35	40.02
20	19	25	202.417	311.71	39.86
21	7	35	214.583	311.88	39.79
21	19	25	226.417	312.37	39.56
22	7	35	238.583	312.73	39.40
22	19	25	250.417	312.93	39.31
23	7	30	262.500	313.06	39.25
23	19	25	274.417	313.25	39.17
24	7	30	286.500	313.48	39.06
24	19	25	298.417	313.98	38.84

(continued)

Table A-13. (continued)

Day	Hr	Min	Elapsed Time (hr)	Depth to Water (ft)	Pressure (psi)
25	7	30	310.500	314.17	38.75
25	19	25	322.417	314.53	38.59
26	7	35	334.583	314.80	38.47
26	19	25	346.417	314.96	38.40
27	7	40	358.667	315.06	38.35
27	19	25	370.417	315.22	38.28
28	9	15	384.250	315.45	38.17
29	8	30	407.500	315.78	38.02
30	10	54	433.900	316.31	37.79
31	8	30	455.500	316.34	37.77
32	7	30	478.500	316.67	37.62
33	8	15	503.250	317.03	37.46
34	10	20	529.333	317.26	37.36
35	8	28	551.467	317.55	37.23
36	15	5	582.083	318.14	36.96
37	6	35	597.583	318.34	36.87
38	8	25	623.417	318.57	36.77
39	9	10	648.167	318.67	36.72
40	9	4	672.067	318.90	36.62
41	11	30	698.500	318.93	36.60
42	8	30	719.500	319.13	36.51
43	10	52	745.867	319.36	36.41
44	11	6	770.100	319.42	36.38
45	8	43	791.717	319.29	36.44
46	8	25	815.417	319.62	36.29
47	10	26	841.433	319.85	36.19
48	9	0	864.000	320.11	36.07
48	10	0	865.000	320.14	36.06
48	10	55	865.917	320.14	36.06
48	11	55	866.917	320.18	36.04
48	13	0	868.000	320.21	36.02
48	13	55	868.917	320.21	36.02
48	15	12	870.200	320.21	36.02
48	16	0	871.000	320.18	36.04
48	17	5	872.083	320.14	36.06
48	17	55	872.917	320.11	36.07
48	19	0	874.000	320.08	36.08
48	19	55	874.917	320.05	36.10
48	21	10	876.167	320.05	36.10
48	22	0	877.000	320.01	36.12
48	22	54	877.900	320.01	36.12

(continued)

Table A-13. (continued)

Day	Hr	Min	Elapsed Time (hr)	Depth to Water (ft)	Pressure (psi)
49	0	0	879.000	320.01	36.12
49	0	55	879.917	319.98	36.13
49	2	0	881.000	319.95	36.14
49	2	55	881.917	319.91	36.16
49	4	0	883.000	319.88	36.17
49	4	55	883.917	319.78	36.22
49	6	0	885.000	319.72	36.25
49	6	55	885.917	319.65	36.28
49	8	5	887.083	319.59	36.30
49	9	1	888.017	319.55	36.32
49	11	30	890.500	319.46	36.36
49	13	0	892.000	319.36	36.41
49	15	0	894.000	319.26	36.45
49	17	0	896.000	319.13	36.51
49	19	5	898.083	319.00	36.57
49	20	55	899.917	318.86	36.63
49	23	0	902.000	318.77	36.67
50	0	55	903.917	318.67	36.72
50	3	0	906.000	318.57	36.77
50	4	55	907.917	318.44	36.82
50	7	0	910.000	318.34	36.87
50	8	9	911.150	318.34	36.87
50	12	11	915.183	318.14	36.96
50	16	15	919.250	317.98	37.03
50	20	15	923.250	317.75	37.14
50	23	24	926.400	317.59	37.21
51	8	8	935.133	317.22	37.38
51	12	12	939.200	317.09	37.43
51	15	30	942.500	316.96	37.49
51	23	25	950.417	316.50	37.70
52	8	30	959.500	316.04	37.91
52	14	10	965.167	315.78	38.02
52	22	10	973.167	315.58	38.12
53	8	35	983.583	315.19	38.29
53	14	10	989.167	314.90	38.42
53	23	21	998.350	314.57	38.57
54	8	5	1007.083	314.14	38.77
55	8	43	1031.717	313.48	39.06
56	8	25	1055.417	312.86	39.34
57	8	54	1079.900	312.24	39.62
58	10	4	1105.067	311.68	39.88

(continued)

Table A-13. (concluded)

Day	Hr	Min	Elapsed Time (hr)	Depth to Water (ft)	Pressure (psi)
59	8	45	1127.750	311.29	40.05
60	8	25	1151.417	311.02	40.17
61	10	0	1177.000	310.60	40.36
62	8	10	1199.167	310.33	40.49
63	8	56	1223.933	310.14	40.57
64	8	15	1247.250	309.88	40.69
65	12	6	1275.100	309.28	40.96
66	8	15	1295.250	308.99	41.09
67	8	15	1319.250	308.69	41.23
68	9	22	1344.367	308.53	41.30
69	8	41	1367.683	308.43	41.34
70	9	20	1392.333	308.27	41.42
71	11	26	1418.433	308.01	41.53
72	10	34	1441.567	307.81	41.62
73	9	40	1464.667	307.41	41.80
74	9	40	1488.667	307.25	41.88
75	9	40	1512.667	307.02	41.98
76	9	55	1536.917	306.86	42.05
77	9	40	1560.667	306.82	42.07
78	10	32	1585.533	306.73	42.11
79	12	55	1611.917	306.59	42.17
82	9	35	1680.583	306.23	42.34
84	10	5	1729.083	306.23	42.34
86	10	38	1777.633	305.91	42.48
89	10	40	1849.667	306.04	42.42
91	9	45	1896.750	305.58	42.63
93	9	5	1944.083	305.54	42.65
96	11	30	2018.500	305.38	42.72
98	9	35	2064.583	305.31	42.75
100	10	7	2113.117	305.09	42.85
103	10	0	2185.000	305.12	42.84
105	13	25	2236.417	305.02	42.88
106	10	22	2257.367	304.89	42.94
108	9	50	2304.833	304.66	43.05
110	9	45	2352.750	304.76	43.00
113	9	0	2424.000	304.72	43.02
114	13	16	2452.267	304.66	43.05
119	9	50	2568.833	304.43	43.15
120	9	15	2592.250	304.27	43.22
126	14	10	2741.167	304.36	43.18
135	14	55	2957.917	304.20	43.25

Table A-14. Water Levels and Pressures in Observation Well H-6b During the WIPP-13 Multipad Pumping Test

Day	Hr	Min	Elapsed Time (hr)	Depth to Water (ft)	Pressure* (psi)
338	14	5	-930.917	303.71	43.48
357	12	5	-476.917	303.35	43.64
363	11	58	-333.033	303.54	43.55
365	9	32	-287.467	303.44	43.60
12	9	13	0.217	303.64	43.51
12	10	0	1.000	303.67	43.49
12	11	5	2.083	303.67	43.49
12	12	0	3.000	303.64	43.51
12	13	5	4.083	303.61	43.52
12	13	55	4.917	303.58	43.53
12	15	5	6.083	303.58	43.53
12	15	55	6.917	303.58	43.53
12	17	2	8.033	303.61	43.52
12	18	11	9.183	303.64	43.51
12	18	55	9.917	303.71	43.48
12	20	36	11.600	303.77	43.45
12	21	37	12.617	303.84	43.42
12	22	9	13.150	303.87	43.40
12	23	5	14.083	303.94	43.37
13	0	21	15.350	303.97	43.36
13	1	53	16.883	303.97	43.36
13	3	5	18.083	304.00	43.34
13	4	9	19.150	304.00	43.34
13	4	55	19.917	304.04	43.33
13	6	11	21.183	304.10	43.30
13	6	55	21.917	304.13	43.28
13	8	28	23.467	304.27	43.22
13	9	32	24.533	304.33	43.20
13	10	29	25.483	304.36	43.18
13	11	27	26.450	304.40	43.16
13	12	37	27.617	304.40	43.16
13	13	25	28.417	304.40	43.16
13	14	35	29.583	304.46	43.14
13	15	36	30.600	304.49	43.12
13	16	35	31.583	304.56	43.09
13	17	35	32.583	304.63	43.06
13	18	34	33.567	304.69	43.03
13	19	35	34.583	304.79	42.99
13	20	30	35.500	304.89	42.94
13	21	37	36.617	305.02	42.88
13	23	40	38.667	305.15	42.83

*Pressure = (400 ft – Depth to Water) × 0.4515 psi/ft

(continued)

Table A-14. (continued)

Day	Hr	Min	Elapsed Time (hr)	Depth to Water (ft)	Pressure (psi)
14	1	35	40.583	305.22	42.79
14	4	45	43.750	305.31	42.75
14	7	10	46.167	305.41	42.71
14	9	46	48.767	305.61	42.62
14	11	4	50.067	305.71	42.57
14	13	20	52.333	305.81	42.53
14	15	4	54.067	305.87	42.50
14	17	30	56.500	306.04	42.42
14	19	30	58.500	306.23	42.34
14	21	30	60.500	306.36	42.28
14	23	28	62.467	306.43	42.25
15	7	30	70.500	306.99	41.99
15	11	35	74.583	307.22	41.89
15	15	35	78.583	307.38	41.82
15	19	30	82.500	307.51	41.76
15	23	25	86.417	307.78	41.64
16	7	30	94.500	308.20	41.45
16	19	35	106.583	308.76	41.20
16	23	40	110.667	309.09	41.05
17	7	30	118.500	309.28	40.96
17	19	30	130.500	309.84	40.71
18	7	37	142.617	310.33	40.49
18	19	30	154.500	310.70	40.32
19	7	35	166.583	311.19	40.10
19	19	30	178.500	311.55	39.94
20	7	35	190.583	312.04	39.71
20	19	30	202.500	312.40	39.55
21	7	30	214.500	312.63	39.45
21	19	30	226.500	313.09	39.24
22	7	30	238.500	313.48	39.06
22	19	30	250.500	313.62	39.00
23	7	35	262.583	313.75	38.94
23	19	30	274.500	313.98	38.84
24	7	35	286.583	314.21	38.73
24	19	30	298.500	314.73	38.50
25	7	30	310.500	314.93	38.41
25	19	30	322.500	315.29	38.25
26	7	30	334.500	315.49	38.16
26	19	30	346.500	315.72	38.05
27	7	35	358.583	315.85	37.99
27	19	30	370.500	316.01	37.92

(continued)

Table A-14. (continued)

Day	Hr	Min	Elapsed Time (hr)	Depth to Water (ft)	Pressure (psi)
28	9	11	384.183	316.14	37.86
28	18	30	393.500	316.34	37.77
29	8	35	407.583	316.57	37.67
29	20	30	419.500	316.77	37.58
30	11	0	434.000	317.09	37.43
30	20	30	443.500	317.09	37.43
31	8	36	455.600	317.03	37.46
31	20	30	467.500	317.22	37.38
32	7	38	478.633	317.42	37.28
32	20	30	491.500	317.62	37.20
33	8	23	503.383	317.75	37.14
33	20	30	515.500	317.88	37.08
34	10	24	529.400	318.08	36.99
34	20	30	539.500	318.18	36.94
35	8	35	551.583	318.34	36.87
35	20	30	563.500	318.54	36.78
36	15	9	582.150	318.93	36.60
36	20	30	587.500	319.09	36.53
37	6	40	597.667	319.13	36.51
37	20	30	611.500	319.36	36.41
38	8	31	623.517	319.39	36.40
38	20	30	635.500	319.49	36.35
39	9	16	648.267	319.49	36.35
39	20	30	659.500	319.65	36.28
40	9	8	672.133	319.72	36.25
40	20	30	683.500	319.78	36.22
41	11	35	698.583	319.78	36.22
41	20	30	707.500	319.91	36.16
42	8	35	719.583	319.95	36.14
42	20	30	731.500	320.08	36.08
43	10	46	745.767	320.21	36.02
43	20	30	755.500	320.21	36.02
44	11	10	770.167	320.28	35.99
44	20	30	779.500	320.21	36.02
45	8	50	791.833	320.14	36.06
45	20	30	803.500	320.18	36.04
46	8	30	815.500	320.47	35.91
46	20	35	827.583	320.54	35.88
47	10	22	841.367	320.70	35.80
47	20	30	851.500	320.80	35.76
48	9	5	864.083	320.96	35.69

(continued)

Table A-14. (continued)

Day	Hr	Min	Elapsed Time (hr)	Depth to Water (ft)	Pressure (psi)
48	9	55	864.917	321.00	35.67
48	11	0	866.000	321.03	35.66
48	12	0	867.000	321.06	35.64
48	12	57	867.950	321.10	35.62
48	13	58	868.967	321.10	35.62
48	15	8	870.133	321.06	35.64
48	16	4	871.067	321.03	35.66
48	17	0	872.000	321.00	35.67
48	18	0	873.000	320.96	35.69
48	18	55	873.917	320.93	35.70
48	19	58	874.967	320.90	35.71
48	21	15	876.250	320.90	35.71
48	21	55	876.917	320.87	35.73
48	23	0	878.000	320.87	35.73
48	23	55	878.917	320.83	35.74
49	1	0	880.000	320.80	35.76
49	1	55	880.917	320.77	35.77
49	3	0	882.000	320.73	35.79
49	3	55	882.917	320.70	35.80
49	5	0	884.000	320.60	35.85
49	5	55	884.917	320.57	35.86
49	7	0	886.000	320.51	35.89
49	8	0	887.000	320.41	35.94
49	9	6	888.100	320.37	35.95
49	11	25	890.417	320.28	35.99
49	13	5	892.083	320.21	36.02
49	14	55	893.917	320.08	36.08
49	17	5	896.083	319.95	36.14
49	19	0	898.000	319.78	36.22
49	21	0	900.000	319.65	36.28
49	22	55	901.917	319.59	36.30
50	1	0	904.000	319.49	36.35
50	2	55	905.917	319.42	36.38
50	5	0	908.000	319.29	36.44
50	6	55	909.917	319.19	36.49
50	8	14	911.233	319.09	36.53
50	12	15	915.250	318.90	36.62
50	16	20	919.333	318.77	36.67
50	20	20	923.333	318.54	36.78
50	23	20	926.333	318.34	36.87
51	8	15	935.250	317.98	37.03

(continued)

Table A-14. (continued)

Day	Hr	Min	Elapsed Time (hr)	Depth to Water (ft)	Pressure (psi)
51	12	18	939.300	317.81	37.11
51	15	34	942.567	317.72	37.15
51	23	30	950.500	317.26	37.36
52	8	35	959.583	316.77	37.58
52	14	15	965.250	316.54	37.68
52	22	15	973.250	316.31	37.79
53	8	40	983.667	315.88	37.98
53	14	15	989.250	315.58	38.12
53	23	17	998.283	315.35	38.22
54	8	10	1007.167	314.86	38.44
54	22	15	1021.250	314.53	38.59
55	8	50	1031.833	314.17	38.75
55	22	20	1045.333	313.91	38.87
56	8	30	1055.500	313.52	39.05
56	22	20	1069.333	313.22	39.18
57	8	57	1079.950	312.93	39.31
57	22	15	1093.250	312.70	39.42
58	10	4	1105.067	312.34	39.58
58	20	15	1115.250	312.11	39.68
59	8	50	1127.833	311.94	39.76
59	20	15	1139.250	311.78	39.83
60	8	30	1151.500	311.65	39.89
60	21	15	1164.250	311.38	40.01
61	10	5	1177.083	311.22	40.08
61	20	15	1187.250	310.96	40.20
62	8	15	1199.250	310.93	40.22
62	21	18	1212.300	310.83	40.26
63	9	0	1224.000	310.73	40.30
63	21	15	1236.250	310.53	40.40
64	8	37	1247.617	310.33	40.49
65	12	10	1275.167	309.81	40.72
65	21	15	1284.250	309.71	40.77
66	8	20	1295.333	309.55	40.84
66	21	15	1308.250	309.45	40.88
67	8	20	1319.333	309.25	40.97
67	21	15	1332.250	309.12	41.03
68	9	28	1344.467	309.09	41.05
69	8	37	1367.617	309.02	41.08
70	9	25	1392.417	308.86	41.15
71	11	30	1418.500	308.60	41.27
72	10	30	1441.500	308.37	41.37

(continued)

Table A-14. (concluded)

Day	Hr	Min	Elapsed Time (hr)	Depth to Water (ft)	Pressure (psi)
73	9	45	1464.750	307.97	41.55
74	9	45	1488.750	307.81	41.62
75	9	45	1512.750	307.58	41.73
76	10	0	1537.000	307.41	41.80
77	9	45	1560.750	307.38	41.82
78	10	28	1585.467	307.25	41.88
79	13	0	1612.000	307.15	41.92
82	9	40	1680.667	306.76	42.10
84	10	10	1729.167	306.76	42.10
86	10	44	1777.733	306.43	42.25
89	10	45	1849.750	306.53	42.20
91	9	50	1896.833	306.07	42.41
93	9	0	1944.000	306.04	42.42
96	11	35	2018.583	305.87	42.50
98	9	40	2064.667	305.81	42.53
100	10	13	2113.217	305.71	42.57
103	10	5	2185.083	305.61	42.62
105	13	20	2236.333	305.48	42.68
108	9	55	2304.917	305.28	42.77
110	9	50	2352.833	305.25	42.78
113	8	55	2423.917	305.18	42.81
114	13	21	2452.350	305.15	42.83
118	10	30	2545.500	305.09	42.85
120	9	10	2592.167	304.72	43.02
121	12	0	2619.000	304.36	43.18
126	9	15	2736.250	304.46	43.14
135	15	0	2958.000	304.69	43.03

Table A-15. Water Levels in Observation Well H-15 During the WIPP-13 Multipad Pumping Test

Day	Hr	Min	Elapsed Time (hr)	Depth to Water (ft)
357	13	50	-475.167	483.37
357	14	0	-475.000	483.33
5	13	35	-163.417	483.23
8	9	36	-95.400	483.37
9	14	20	-66.667	483.20
13	10	45	25.750	483.30
14	13	25	52.417	483.04
16	15	15	102.250	483.33
19	17	0	176.000	483.17
20	9	38	192.633	483.33
21	10	50	217.833	483.27
23	13	30	268.500	483.23
26	15	38	342.633	482.94
28	9	5	384.083	483.17
30	15	46	438.767	483.07
33	9	33	504.550	483.17
35	8	53	551.883	482.94
37	14	50	605.833	482.97
40	11	35	674.583	483.20
42	14	35	725.583	482.84
44	14	23	773.383	482.81
47	9	58	840.967	482.81
50	12	50	915.833	482.78
57	10	25	1081.417	482.68
64	15	11	1254.183	482.64
71	13	14	1420.233	482.58
78	12	9	1587.150	482.25
85	12	10	1755.167	482.38
91	15	40	1902.667	482.28
100	11	11	2114.183	482.25

Table A-16. Water Levels and Pressures in Observation Well DOE-2 During the WIPP-13 Multipad Pumping Test

Day	Hr	Min	Elapsed Time (hr)	Depth to Water (ft)	Pressure* (psi)
336	9	40	-983.333	364.63	61.05
343	9	50	-815.167	364.63	61.05
349	11	5	-669.917	364.57	61.08
357	9	25	-479.583	364.60	61.06
363	11	37	-333.383	364.53	61.10
365	9	0	-288.000	364.53	61.10
2	9	55	-239.083	364.01	61.33
5	14	45	-162.250	363.91	61.38
7	12	10	-116.833	363.88	61.39
8	12	20	-92.667	364.07	61.30
8	13	30	-91.500	364.07	61.30
9	13	30	-67.500	364.47	61.12
10	12	0	-45.000	364.60	61.06
11	13	6	-19.900	364.50	61.11
12	6	57	-2.050	364.44	61.14
12	9	0	0.000	364.53	61.10
12	9	30	0.500	364.53	61.10
12	10	0	1.000	364.57	61.08
12	10	30	1.500	364.60	61.06
12	11	0	2.000	364.67	61.03
12	11	30	2.500	364.73	61.01
12	12	0	3.000	364.83	60.96
12	12	30	3.500	364.93	60.92
12	13	0	4.000	365.03	60.87
12	13	30	4.500	365.12	60.83
12	14	0	5.000	365.26	60.77
12	15	0	6.000	365.49	60.66
12	16	0	7.000	365.72	60.56
12	17	0	8.000	366.01	60.43
12	18	0	9.000	366.21	60.34
12	19	0	10.000	366.54	60.19
12	21	0	12.000	367.06	59.96
12	22	0	13.000	367.32	59.84
12	23	0	14.000	367.55	59.73
13	0	0	15.000	367.75	59.65
13	1	0	16.000	367.95	59.55
13	2	0	17.000	368.11	59.48
13	3	0	18.000	368.27	59.41
13	4	0	19.000	368.44	59.33
13	5	0	20.000	368.64	59.24
13	6	0	21.000	368.83	59.16

*Pressure = (500 ft − Depth to Water) × 0.451 psi/ft

(continued)

Table A-16. (continued)

Day	Hr	Min	Elapsed Time (hr)	Depth to Water (ft)	Pressure (psi)
13	7	44	22.733	369.16	59.01
13	10	7	25.117	369.62	58.80
13	12	0	27.000	369.88	58.68
13	14	0	29.000	370.14	58.57
13	16	0	31.000	370.44	58.43
13	18	0	33.000	370.77	58.28
13	20	0	35.000	371.13	58.12
13	22	11	37.183	371.56	57.93
14	0	0	39.000	371.82	57.81
14	1	50	40.833	372.05	57.70
14	4	55	43.917	372.38	57.56
14	7	0	46.000	372.64	57.44
14	10	0	49.000	373.10	57.23
14	12	0	51.000	373.33	57.13
14	16	0	55.000	373.85	56.89
14	19	50	58.833	374.38	56.66
14	23	41	62.683	374.61	56.55
15	11	55	74.917	376.38	55.75
15	23	50	86.833	377.66	55.17
16	11	55	98.917	378.74	54.69
17	0	8	111.133	379.89	54.17
17	18	10	129.167	380.91	53.71
17	23	15	134.250	381.73	53.34
18	11	50	146.833	382.58	52.96
18	23	50	158.833	383.40	52.59
19	11	50	170.833	384.09	52.27
19	23	50	182.833	384.94	51.89
20	11	50	194.833	385.66	51.57
20	23	50	206.833	386.29	51.28
21	11	50	218.833	386.81	51.05
21	23	50	230.833	387.63	50.68
22	11	50	242.833	388.16	50.44
22	23	50	254.833	388.55	50.26
23	11	50	266.833	389.01	50.06
23	23	50	278.833	389.47	49.85
24	11	35	290.583	389.99	49.62
24	23	50	302.833	390.68	49.30
25	11	45	314.750	391.11	49.11
25	23	50	326.833	391.73	48.83
26	11	40	338.667	392.06	48.68
26	23	50	350.833	392.65	48.41

(continued)

Table A-16. (continued)

Day	Hr	Min	Elapsed Time (hr)	Depth to Water (ft)	Pressure (psi)
27	11	50	362.833	392.91	48.30
27	23	50	374.833	393.41	48.07
28	11	40	386.667	393.60	47.99
28	23	50	398.833	394.03	47.79
29	11	50	410.833	394.36	47.64
29	23	50	422.833	394.78	47.45
30	11	45	434.750	395.11	47.30
30	23	50	446.833	395.34	47.20
31	11	46	458.767	395.51	47.12
31	23	50	470.833	395.87	46.96
32	11	40	482.667	396.23	46.80
32	23	50	494.833	396.56	46.65
33	11	43	506.717	396.72	46.58
33	23	50	518.833	397.01	46.45
34	13	7	532.117	397.31	46.31
34	23	50	542.833	397.51	46.22
35	11	30	554.500	397.77	46.11
35	23	50	566.833	398.10	45.96
36	14	36	581.600	398.62	45.72
36	23	50	590.833	398.85	45.62
37	10	50	601.833	399.05	45.53
37	23	50	614.833	399.31	45.41
38	11	10	626.167	399.48	45.34
38	23	50	638.833	399.64	45.26
39	11	15	650.250	399.80	45.19
39	23	50	662.833	400.13	45.04
40	11	45	674.750	400.23	45.00
40	23	50	686.833	400.43	44.91
41	12	5	699.083	400.52	44.87
41	23	50	710.833	400.79	44.74
42	12	5	723.083	400.92	44.69
42	23	50	734.833	401.18	44.57
43	11	45	746.750	401.25	44.54
43	23	30	758.500	401.38	44.48
44	11	50	770.833	401.31	44.51
44	23	50	782.833	401.57	44.39
45	11	50	794.833	401.54	44.41
45	23	50	806.833	401.77	44.30
46	11	50	818.833	402.10	44.15
46	23	50	830.833	402.23	44.09
47	11	30	842.500	402.36	44.04

(continued)

Table A-16. (continued)

Day	Hr	Min	Elapsed Time (hr)	Depth to Water (ft)	Pressure (psi)
47	23	45	854.750	402.66	43.90
48	7	29	862.483	402.72	43.87
48	9	0	864.000	402.79	43.84
48	9	30	864.500	402.82	43.83
48	10	0	865.000	402.82	43.83
48	10	30	865.500	402.79	43.84
48	11	0	866.000	402.72	43.87
48	11	30	866.500	402.62	43.92
48	12	0	867.000	402.53	43.96
48	12	30	867.500	402.43	44.00
48	13	0	868.000	402.33	44.05
48	13	30	868.500	402.20	44.11
48	14	0	869.000	402.07	44.17
48	14	30	869.500	401.97	44.21
48	15	0	870.000	401.84	44.27
48	15	30	870.500	401.71	44.33
48	16	0	871.000	401.54	44.41
48	16	30	871.500	401.41	44.46
48	17	0	872.000	401.28	44.52
48	17	30	872.500	401.15	44.58
48	18	0	873.000	401.02	44.64
48	18	30	873.500	400.89	44.70
48	19	0	874.000	400.79	44.74
48	19	30	874.500	400.62	44.82
48	20	0	875.000	400.49	44.88
48	21	0	876.000	400.30	44.97
48	22	0	877.000	400.07	45.07
48	23	0	878.000	399.84	45.17
49	0	0	879.000	399.64	45.26
49	1	0	880.000	399.48	45.34
49	2	0	881.000	399.31	45.41
49	3	0	882.000	399.08	45.52
49	4	0	883.000	398.88	45.60
49	5	5	884.083	398.65	45.71
49	6	0	885.000	398.43	45.81
49	7	0	886.000	398.23	45.90
49	8	0	887.000	398.06	45.98
49	9	0	888.000	397.93	46.03
49	11	0	890.000	397.57	46.20
49	13	0	892.000	397.24	46.34
49	15	0	894.000	396.92	46.49

(continued)

Table A-16. (continued)

Day	Hr	Min	Elapsed Time (hr)	Depth to Water (ft)	Pressure (psi)
49	17	0	896.000	396.59	46.64
49	19	0	898.000	396.23	46.80
49	21	0	900.000	395.90	46.95
49	23	5	902.083	395.64	47.07
50	1	0	904.000	395.41	47.17
50	3	0	906.000	395.11	47.30
50	5	0	908.000	394.82	47.44
50	7	0	910.000	394.59	47.54
50	8	2	911.033	394.46	47.60
50	12	0	915.000	394.00	47.81
50	16	0	919.000	393.54	48.01
50	20	0	923.000	393.08	48.22
51	0	0	927.000	392.65	48.41
51	8	0	935.000	391.90	48.75
51	12	0	939.000	391.54	48.91
51	16	0	943.000	391.17	49.08
52	0	0	951.000	390.35	49.45
52	8	20	959.333	389.57	49.80
52	14	0	965.000	389.07	50.03
53	0	0	975.000	388.48	50.30
53	10	10	985.167	387.73	50.63
53	14	0	989.000	387.37	50.80
54	0	0	999.000	386.68	51.11
54	7	55	1006.917	386.02	51.41
55	0	0	1023.000	385.04	51.85
55	8	30	1031.500	384.68	52.01
56	0	0	1047.000	383.92	52.35
56	8	10	1055.167	383.40	52.59
57	0	0	1071.000	382.74	52.88
57	8	25	1079.417	382.28	53.09
58	0	0	1095.000	381.69	53.36
58	8	5	1103.083	381.14	53.61
58	20	0	1115.000	380.71	53.80
59	8	20	1127.333	380.41	53.94
59	20	0	1139.000	379.95	54.14
60	8	10	1151.167	379.63	54.29
60	21	0	1164.000	379.13	54.51
61	9	20	1176.333	378.77	54.67
61	20	0	1187.000	378.41	54.84
62	8	0	1199.000	378.22	54.92
62	21	5	1212.083	377.92	55.06

(continued)

Table A-16. (concluded)

Day	Hr	Min	Elapsed Time (hr)	Depth to Water (ft)	Pressure (psi)
63	8	23	1223.383	377.66	55.17
63	21	0	1236.000	377.30	55.34
64	7	45	1246.750	377.03	55.46
64	21	0	1260.000	376.57	55.67
65	11	35	1274.583	376.18	55.84
65	21	5	1284.083	375.92	55.96
66	8	5	1295.083	375.66	56.08
66	21	0	1308.000	375.39	56.20
67	8	5	1319.083	375.10	56.33
67	21	0	1332.000	374.80	56.47
68	8	40	1343.667	374.67	56.52
69	8	6	1367.100	374.64	56.54
70	8	39	1391.650	374.15	56.76
71	10	52	1417.867	373.52	57.04
72	9	35	1440.583	373.16	57.20
73	9	0	1464.000	372.60	57.46
74	9	0	1488.000	372.21	57.63
75	9	0	1512.000	371.78	57.83
76	9	20	1536.333	371.46	57.97
77	9	0	1560.000	371.29	58.05
78	8	43	1583.717	371.00	58.18
79	12	45	1611.750	370.80	58.27
82	9	0	1680.000	370.08	58.59
84	9	35	1728.583	369.85	58.70
86	10	8	1777.133	369.39	58.91
89	9	0	1848.000	369.23	58.98
91	9	5	1896.083	368.67	59.23
93	8	30	1943.500	368.50	59.31
96	10	50	2017.833	368.18	59.45
98	9	0	2064.000	367.98	59.54
100	8	25	2111.417	367.62	59.70
103	9	20	2184.333	367.39	59.81
105	13	10	2236.167	367.26	59.87
108	9	40	2304.667	366.77	60.09
115	8	50	2471.833	366.70	60.12
120	9	0	2592.000	366.54	60.19
126	13	50	2740.833	366.47	60.22
132	8	48	2879.800	366.14	60.37
135	14	35	2957.583	366.11	60.38

Table A-17. Water Levels and Pressures in Observation Well P-14 During the WIPP-13 Multipad Pumping Test

Day	Hr	Min	Elapsed Time (hr)	Depth to Water (ft)	Pressure* (psi)	Compensated+ Pressure (psi)
357	12	20	-476.667	324.28	33.47	33.47#
363	12	13	-332.783	324.48	33.38	33.38#
365	9	48	-287.200	324.38	33.42	33.42#
2	14	0	-235.000	324.15	33.53	33.53#
5	13	35	-163.417	324.18	33.51	33.51#
7	14	6	-114.900	324.41	33.41	33.41#
9	14	45	-66.250	324.38	33.42	33.42#
10	10	53	-46.117	324.54	33.35	33.35#
11	13	40	-19.333	324.51	33.37	33.37#
12	7	25	-1.583	324.51	33.37	33.37#
12	12	25	3.417	324.48	33.38	33.38
12	15	15	6.250	324.41	33.41	33.39
12	17	55	8.917	324.44	33.40	33.38
13	0	34	15.567	324.48	33.38	33.36
13	9	47	24.783	324.38	33.42	33.38
13	13	40	28.667	324.28	33.47	33.38
13	16	44	31.733	324.21	33.50	33.40
13	21	42	36.700	324.31	33.45	33.35
14	1	22	40.367	324.31	33.45	33.34
14	7	20	46.333	324.21	33.50	33.39
14	11	35	50.583	324.25	33.48	33.37
14	15	20	54.333	324.18	33.51	33.39
14	19	20	58.333	324.25	33.48	33.38
14	23	10	62.167	324.21	33.50	33.42
15	8	30	71.500	324.38	33.42	33.37
15	12	30	75.500	324.38	33.42	33.35
15	16	30	79.500	324.31	33.45	33.37
16	8	30	95.500	324.38	33.42	33.36
16	12	30	99.500	324.41	33.41	33.33
16	16	30	103.500	324.38	33.42	33.34
16	20	30	107.500	324.41	33.41	33.33
17	8	30	119.500	324.41	33.41	33.32
17	12	30	123.500	324.41	33.41	33.31
17	16	30	127.500	324.51	33.37	33.28
17	20	30	131.500	324.51	33.37	33.31
18	8	30	143.500	324.54	33.35	33.31
18	12	30	147.500	324.57	33.34	33.28
18	16	30	151.500	324.57	33.34	33.27
18	20	30	155.500	324.54	33.35	33.29
19	8	30	167.500	324.61	33.32	33.28
19	12	30	171.500	324.61	33.32	33.25

*Pressure = (400 ft − Depth to Water) × 0.442 psi/ft
+Compensated Pressure = Pressure + 0.7 (Barometric Pressure − 13.1 psi)
#No barometric correction

(continued)

Table A-17. (continued)

Day	Hr	Min	Elapsed Time (hr)	Depth to Water (ft)	Pressure (psi)	Compensated Pressure (psi)
19	16	30	175.500	324.61	33.32	33.24
19	20	30	179.500	324.64	33.31	33.26
20	8	30	191.500	324.80	33.24	33.25
20	11	50	194.833	324.84	33.22	33.22
20	16	30	199.500	324.87	33.21	33.20
20	20	30	203.500	324.84	33.22	33.22
21	8	30	215.500	324.77	33.25	33.21
21	12	30	219.500	324.77	33.25	33.20
21	16	30	223.500	324.90	33.19	33.17
21	20	30	227.500	324.93	33.18	33.19
22	12	30	243.500	324.93	33.18	33.17
22	16	30	247.500	324.93	33.18	33.15
22	20	30	251.500	324.93	33.18	33.14
23	8	30	263.500	324.84	33.22	33.14
23	12	30	267.500	324.77	33.25	33.15
23	16	30	271.500	324.80	33.24	33.11
23	20	30	275.500	324.84	33.22	33.09
24	8	40	287.667	324.87	33.21	33.11
24	11	55	290.917	324.87	33.21	33.11
24	16	30	295.500	324.97	33.16	33.10
24	20	30	299.500	325.13	33.09	33.05
25	8	30	311.500	325.10	33.11	33.09
25	16	30	319.500	325.13	33.09	33.08
25	20	30	323.500	325.26	33.03	33.04
26	8	30	335.500	325.26	33.03	33.07
26	12	30	339.500	325.23	33.05	33.07
26	16	30	343.500	325.23	33.05	33.06
26	20	30	347.500	325.33	33.00	33.01
27	8	30	359.500	325.26	33.03	33.04
27	12	30	363.500	325.23	33.05	33.02
27	16	30	367.500	325.16	33.08	33.04
27	20	30	371.500	325.23	33.05	33.01
28	9	26	384.433	325.16	33.08	33.02
28	20	45	395.750	325.20	33.06	32.97
29	8	45	407.750	325.30	33.02	32.99
29	20	45	419.750	325.33	33.00	32.97
30	11	11	434.183	325.49	32.93	32.95
30	20	45	443.750	325.39	32.98	32.94
31	8	45	455.750	325.43	32.96	32.85
31	20	45	467.750	325.26	33.03	32.93
32	8	50	479.833	325.36	32.99	32.91

(continued)

Table A-17. (continued)

Day	Hr	Min	Elapsed Time (hr)	Depth to Water (ft)	Pressure (psi)	Compensated Pressure (psi)
32	20	45	491.750	325.39	32.98	32.90
33	8	35	503.583	325.39	32.98	32.90
33	20	45	515.750	325.43	32.96	32.87
34	10	31	529.517	325.49	32.93	32.86
34	20	45	539.750	325.49	32.93	32.84
35	8	45	551.750	325.52	32.92	32.85
35	20	45	563.750	325.59	32.89	32.82
36	14	50	581.833	325.89	32.76	32.79
36	20	45	587.750	325.95	32.73	32.79
37	6	48	597.800	325.95	32.73	32.80
37	20	45	611.750	326.05	32.69	32.76
38	8	45	623.750	326.02	32.70	32.79
38	20	45	635.750	325.98	32.72	32.76
39	9	25	648.417	325.92	32.74	32.77
39	20	45	659.750	326.02	32.70	32.73
40	9	16	672.267	325.98	32.72	32.76
40	20	45	683.750	325.95	32.73	32.71
41	11	45	698.750	325.89	32.76	32.73
41	20	45	707.750	325.92	32.74	32.71
42	8	45	719.750	325.89	32.76	32.73
42	20	45	731.750	325.92	32.74	32.70
43	11	0	746.000	325.98	32.72	32.70
43	20	45	755.750	325.98	32.72	32.68
44	11	18	770.300	325.92	32.74	32.69
44	20	45	779.750	325.82	32.79	32.68
45	9	0	792.000	325.69	32.84	32.67
45	20	45	803.750	325.66	32.86	32.66
46	8	45	815.750	325.85	32.77	32.67
46	20	45	827.750	325.89	32.76	32.65
47	10	34	841.567	325.95	32.73	32.62
47	20	45	851.750	325.95	32.73	32.65
48	8	0	863.000	326.08	32.67	32.63
48	9	30	864.500	326.12	32.66	32.62
48	13	12	868.200	326.18	32.63	32.58
48	16	14	871.233	326.15	32.64	32.59
48	21	25	876.417	326.12	32.66	32.61
49	3	10	882.167	326.15	32.64	32.59
49	9	16	888.267	326.08	32.67	32.62
49	14	35	893.583	326.08	32.67	32.57
49	21	13	900.217	325.98	32.72	32.61
50	3	10	906.167	326.05	32.69	32.59

(continued)

Table A-17. (continued)

Day	Hr	Min	Elapsed Time (hr)	Depth to Water (ft)	Pressure (psi)	Compensated Pressure (psi)
50	8	23	911.383	326.05	32.69	32.60
50	14	30	917.500	326.12	32.66	32.56
50	22	0	925.000	326.15	32.64	32.59
51	8	25	935.417	326.21	32.62	32.61
51	15	43	942.717	326.28	32.58	32.57
51	22	0	949.000	326.25	32.60	32.58
52	8	45	959.750	326.12	32.66	32.61
52	14	25	965.417	326.12	32.66	32.59
52	22	25	973.417	326.21	32.62	32.58
53	8	49	983.817	326.18	32.63	32.61
53	14	25	989.417	326.12	32.66	32.60
54	8	20	1007.333	325.95	32.73	32.62
54	14	5	1013.083	325.82	32.79	32.63
54	22	0	1021.000	325.75	32.82	32.69
55	8	45	1031.750	325.95	32.73	32.64
55	14	0	1037.000	325.89	32.76	32.64
55	22	0	1045.000	326.02	32.70	32.60
56	8	40	1055.667	325.92	32.74	32.65
56	14	30	1061.500	325.82	32.79	32.67
56	22	0	1069.000	325.92	32.74	32.62
57	9	5	1080.083	325.85	32.77	32.66
57	14	30	1085.500	325.75	32.82	32.68
57	22	0	1093.000	325.79	32.80	32.69
58	10	17	1105.283	325.79	32.80	32.67
58	14	15	1109.250	325.75	32.82	32.68
58	22	15	1117.250	325.85	32.77	32.66
59	9	0	1128.000	325.82	32.79	32.71
59	14	30	1133.500	325.85	32.77	32.68
59	22	15	1141.250	325.92	32.74	32.68
60	8	37	1151.617	325.92	32.74	32.72
60	14	45	1157.750	325.89	32.76	32.70
60	21	25	1164.417	325.82	32.79	32.74
61	10	15	1177.250	325.85	32.77	32.74
61	14	34	1181.567	325.82	32.79	32.73
61	20	30	1187.500	325.82	32.79	32.75
62	8	25	1199.417	325.89	32.76	32.78
62	15	0	1206.000	325.95	32.73	32.74
62	21	30	1212.500	325.92	32.74	32.79
63	9	11	1224.183	325.98	32.72	32.80
63	14	36	1229.600	326.02	32.70	32.76
63	21	25	1236.417	325.92	32.74	32.81

(continued)

Table A-17. (concluded)

Day	Hr	Min	Elapsed Time (hr)	Depth to Water (ft)	Pressure (psi)	Compensated Pressure (psi)
64	8	47	1247.783	325.85	32.77	32.82
64	21	12	1260.200	325.72	32.83	32.82
65	12	22	1275.367	325.66	32.86	32.82
65	21	30	1284.500	325.62	32.88	32.83
66	8	30	1295.500	325.59	32.89	32.84
66	14	45	1301.750	325.52	32.92	32.84
66	21	30	1308.500	325.56	32.90	32.83
67	8	30	1319.500	325.49	32.93	32.85
67	14	0	1325.000	325.39	32.98	32.86
67	21	30	1332.500	325.43	32.96	32.85
68	9	45	1344.750	325.52	32.92	32.87
69	8	49	1367.817	325.56	32.90	32.90
70	9	33	1392.550	325.62	32.88	32.90
71	11	41	1418.683	325.56	32.90	32.91
72	10	42	1441.700	325.49	32.93	32.92
73	9	55	1464.917	325.26	33.03	32.93
74	9	55	1488.917	325.20	33.06	32.94
75	9	55	1512.917	325.07	33.12	32.95
76	10	15	1537.250	325.03	33.14	32.95
77	9	55	1560.917	325.10	33.11	32.97
78	10	40	1585.667	325.10	33.11	32.98
79	13	10	1612.167	325.13	33.09	32.96
82	9	50	1680.833	325.00	33.15	33.00
84	10	20	1729.333	325.16	33.08	33.00
86	10	53	1777.883	325.03	33.14	33.00
89	10	55	1849.917	325.33	33.00	33.02
91	10	0	1897.000	325.00	33.15	33.08
93	9	15	1944.250	325.07	33.12	33.11
96	11	50	2018.833	325.03	33.14	33.13
98	9	55	2064.917	325.07	33.12	33.12
100	10	25	2113.417	325.03	33.14	33.08
103	10	20	2185.333	325.13	33.09	33.05
105	13	35	2236.583	325.20	33.06	32.99
108	10	5	2305.083	325.16	33.08	32.96
110	10	0	2353.000	325.03	33.14	33.11
113	9	10	2424.167	325.00	33.15	33.14
114	13	30	2452.500	325.00	33.15	33.14
118	10	50	2545.833	325.00	33.15	33.18
120	9	20	2592.333	324.70	33.28	33.28
126	9	25	2736.417	324.93	33.18	33.18
135	15	15	2958.250	324.74	33.26	33.26

Table A-18. Water Levels and Pressures in Observation Well ERDA-9 During the WIPP-13 Multipad Pumping Test

Day	Hr	Min	Elapsed Time (hr)	Depth to Water (ft)	Pressure* (psi)	Modified+ Pressure (psi)
357	10	30	-478.500	458.14	19.21	20.22
5	13	23	-163.617	457.78	19.38	20.07
7	15	5	-113.917	457.71	19.41	20.05
9	14	5	-66.917	457.35	19.58	20.17
23	13	20	268.333	456.73	19.86	20.12
24	10	45	289.750	458.76	18.93	19.17
26	15	25	342.417	456.33	20.05	20.23
28	11	25	386.417	456.40	20.01	20.16
29	11	15	410.250	456.33	20.05	20.16
30	10	33	433.550	456.33	20.05	20.14
31	10	58	457.967	456.27	20.07	20.14
32	10	54	481.900	456.33	20.05	20.09
33	11	20	506.333	456.17	20.12	20.14
34	11	26	530.433	456.10	20.15	20.15
35	10	42	553.700	456.10	20.15	20.13
36	15	7	582.117	456.23	20.09	20.04
37	11	15	602.250	456.30	20.06	19.99
38	10	40	625.667	456.40	20.01	19.92
39	10	42	649.700	456.43	20.00	19.88
40	11	22	674.367	456.53	19.95	19.81
41	10	42	697.700	456.53	19.95	19.79
42	11	25	722.417	456.53	19.95	19.76
43	10	24	745.400	456.56	19.94	19.73
44	10	41	769.683	456.59	19.93	19.69
46	10	39	817.650	456.53	19.95	19.67
47	9	14	840.233	456.59	19.93	19.62
48	7	4	862.067	456.76	19.85	19.52
48	12	45	867.750	456.73	19.86	19.52
48	17	45	872.750	456.79	19.83	19.49
48	21	5	876.083	456.82	19.82	19.48
49	2	40	881.667	456.82	19.82	19.47
49	9	35	888.583	456.89	19.79	19.43
49	14	18	893.300	456.89	19.79	19.43
49	20	42	899.700	456.89	19.79	19.42
50	2	40	905.667	456.96	19.75	19.38
50	8	50	911.833	457.02	19.73	19.35
50	15	40	918.667	456.99	19.74	19.36
50	22	55	925.917	457.02	19.73	19.33
51	7	25	934.417	457.15	19.67	19.27
51	14	7	941.117	457.19	19.65	19.24
51	22	55	949.917	457.25	19.62	19.20

*Pressure = (500 ft – Depth to Water) × 0.459 psi/ft
+ Modified Pressure = (500 ft – {Depth to Water + [0.52 ft/240 hrs × (Elapsed Time – 530 hrs)]}) × 0.459 psi/ft

(continued)

Table A-18. (continued)

Day	Hr	Min	Elapsed Time (hr)	Depth to Water (ft)	Pressure (psi)	Modified Pressure (psi)
52	10	10	961.167	457.32	19.59	19.16
52	15	10	966.167	457.35	19.58	19.14
52	23	15	974.250	457.38	19.56	19.12
53	9	30	984.500	457.45	19.53	19.08
53	15	10	990.167	457.48	19.52	19.06
53	22	52	997.867	457.51	19.50	19.04
54	9	5	1008.083	457.58	19.47	19.00
54	14	53	1013.883	457.58	19.47	18.99
54	23	10	1022.167	457.58	19.47	18.98
55	9	38	1032.633	457.64	19.44	18.94
55	14	45	1037.750	457.64	19.44	18.94
55	23	6	1046.100	457.68	19.43	18.91
56	10	0	1057.000	457.74	19.40	18.87
56	15	20	1062.333	457.74	19.40	18.87
56	23	2	1070.033	457.78	19.38	18.84
57	9	27	1080.450	457.84	19.35	18.80
57	15	20	1086.333	457.81	19.36	18.81
57	23	0	1094.000	457.84	19.35	18.79
58	9	45	1104.750	457.87	19.34	18.77
58	15	44	1110.733	457.87	19.34	18.76
58	23	5	1118.083	457.87	19.34	18.75
59	9	48	1128.800	457.91	19.32	18.72
59	15	15	1134.250	457.91	19.32	18.72
59	23	5	1142.083	458.01	19.27	18.66
60	9	21	1152.350	458.07	19.25	18.63
60	15	22	1158.367	458.10	19.23	18.61
60	21	50	1164.833	458.17	19.20	18.57
61	8	40	1175.667	458.27	19.15	18.51
61	15	25	1182.417	458.23	19.17	18.52
61	21	25	1188.417	458.30	19.14	18.49
62	9	10	1200.167	458.43	19.08	18.41
62	15	30	1206.500	458.46	19.07	18.39
62	22	20	1213.333	458.53	19.04	18.36
63	10	35	1225.583	458.63	18.99	18.30
63	22	16	1237.267	458.73	18.94	18.24
64	10	39	1249.650	458.73	18.94	18.23
64	22	10	1261.167	458.76	18.93	18.20
65	15	5	1278.083	458.66	18.98	18.23
65	22	25	1285.417	458.66	18.98	18.22
66	9	15	1296.250	458.63	18.99	18.23
66	15	20	1302.333	458.53	19.04	18.27

(continued)

Table A-18. (concluded)

Day	Hr	Min	Elapsed Time (hr)	Depth to Water (ft)	Pressure (psi)	Modified Pressure (psi)
66	22	25	1309.417	458.56	19.02	18.25
67	9	10	1320.167	458.53	19.04	18.25
67	22	20	1333.333	458.53	19.04	18.24
68	10	55	1345.917	458.33	19.13	18.32
69	8	55	1367.917	458.27	19.15	18.32
70	10	50	1393.833	458.17	19.20	18.34
71	13	20	1420.333	458.01	19.27	18.39
72	11	37	1442.617	457.94	19.31	18.40
73	10	40	1465.667	457.74	19.40	18.47
74	10	45	1489.750	457.55	19.48	18.53
75	10	45	1513.750	457.35	19.58	18.60
76	11	0	1538.000	457.22	19.64	18.63
77	10	45	1561.750	457.05	19.71	18.69
78	12	23	1587.383	456.92	19.77	18.72
79	13	45	1612.750	456.86	19.80	18.72
82	10	30	1681.500	456.56	19.94	18.79
84	11	10	1730.167	456.46	19.98	18.79
86	13	25	1780.417	456.33	20.05	18.80
89	11	40	1850.667	456.33	20.05	18.73
91	10	30	1897.500	456.23	20.09	18.73
93	9	55	1944.917	456.23	20.09	18.68
96	13	20	2020.333	456.00	20.20	18.71
98	10	40	2065.667	455.94	20.22	18.70
100	11	19	2114.317	455.71	20.33	18.75
103	11	20	2186.333	455.38	20.48	18.83
105	14	25	2237.417	455.25	20.54	18.84
108	11	0	2306.000	455.05	20.63	18.87
110	10	55	2353.917	454.69	20.80	18.98
113	9	50	2424.833	454.40	20.93	19.05
114	14	23	2453.383	454.23	21.01	19.10
118	11	45	2546.750	453.81	21.20	19.20
120	9	50	2592.833	453.51	21.34	19.29
126	10	5	2737.083	452.82	21.66	19.46
135	13	30	2956.500	451.84	22.11	19.69

Table A-19. Pressures in Exhaust Shaft Culebra Piezometers During the WIPP-13 Multipad Pumping Test

Day	Hr	Min	Elapsed Time (hr)	#210 Pressure (psig)	#211 Pressure (psig)	#212 Pressure (psig)	#212 Modified+ Pressure (psig)
328	13	18	-1171.700	--	108.16	112.96	115.69
330	10	11	-1126.817	113.88	108.85	112.96	115.61
335	13	2	-1003.967	114.51	108.85	112.96	115.39
339	8	12	-912.800	113.88	108.16	112.96	115.23
342	8	58	-840.033	114.51	108.85	112.96	115.10
344	12	38	-788.367	114.51	108.85	113.46	115.50
346	8	6	-744.900	114.51	108.85	113.46	115.43
352	11	27	-597.550	115.13	109.55	113.96	115.66
356	13	11	-499.817	115.13	109.55	113.96	115.49
357	10	36	-478.400	115.13	109.55	113.96	115.45
358	10	12	-454.800	115.13	109.55	113.96	115.41
363	8	37	-336.383	115.13	109.55	114.46	115.69
364	8	4	-312.933	115.13	109.55	114.46	115.65
2	14	30	-234.500	--	109.55	113.96	115.01
5	15	29	-161.517	115.76	109.55	114.46	115.38
7	8	58	-120.033	115.76	109.55	114.46	115.30
9	12	10	-68.833	115.76	110.25	114.97	115.72
12	7	44	-1.267	115.76	110.25	114.97	115.60
13	8	1	23.017	116.39	110.25	114.97	115.56
14	14	58	53.967	116.39	110.25	114.97	115.50
16	11	25	98.417	116.39	110.25	114.97	115.42
19	9	43	168.717	116.39	110.25	114.97	115.30
20	13	24	196.400	116.39	110.25	114.97	115.25
21	8	0	215.000	116.39	110.25	115.46	115.70
22	7	38	238.633	116.39	110.25	115.46	115.66
23	7	52	262.867	116.39	110.25	115.46	115.62
24	8	43	287.717	116.39	110.25	115.46	115.57
26	9	15	336.250	116.39	110.25	115.46	115.48
28	19	19	394.317	116.39	110.25	115.46	115.38
29	12	7	411.117	116.39	110.25	115.46	115.35
30	20	18	443.300	116.39	110.25	115.46	115.29
32	17	0	488.000	116.39	110.25	115.46	115.21
33	11	26	506.433	116.39	110.25	115.46	115.18
34	7	38	526.633	116.39	110.25	115.46	115.14
35	12	19	555.317	116.39	110.25	115.46	115.09
36	13	51	580.850	116.39	110.25	--	--
37	8	22	599.367	116.39	110.25	115.46	115.01
38	16	35	631.583	116.39	110.25	115.46	114.95
39	16	45	655.750	116.39	110.25	115.46	114.91

+ Modified Pressure = Pressure – [(0.431 psi/240 hrs) × (Elapsed Time – 350 hrs)]

(continued)

Table A-19. (continued)

Day	Hr	Min	Elapsed Time (hr)	#210 Pressure (psig)	#211 Pressure (psig)	#212 Pressure (psig)	#212 Modified Pressure (psig)
40	7	47	670.783	116.39	110.25	115.46	114.88
41	11	41	698.683	116.39	110.25	114.97	114.34
42	11	46	722.767	116.39	110.25	114.97	114.30
43	11	12	746.200	116.39	110.25	114.97	114.26
44	11	55	770.917	116.39	110.25	114.97	114.21
47	12	15	843.250	116.39	110.25	114.97	114.08
48	8	57	863.950	116.39	110.25	114.97	114.05
49	12	25	891.417	115.76	109.55	114.97	114.00
50	11	31	914.517	115.76	109.55	114.46	113.45
51	13	36	940.600	115.76	109.55	114.46	113.40
52	8	36	959.600	115.76	109.55	114.46	113.36
53	12	35	987.583	115.76	109.55	114.46	113.31
54	13	16	1012.267	115.76	109.55	114.46	113.27
55	13	21	1036.350	115.13	109.55	113.96	112.73
56	7	45	1054.750	115.13	109.55	113.96	112.69
57	7	50	1078.833	115.13	109.55	113.96	112.65
58	8	0	1103.000	115.13	109.55	113.96	112.61
59	8	36	1127.600	115.13	109.55	113.96	112.56
61	10	28	1177.467	115.13	108.85	113.96	112.47
63	7	53	1222.883	115.13	108.85	113.96	112.39
64	10	27	1249.450	115.13	108.85	113.96	112.34
65	7	34	1270.567	115.13	108.85	113.96	112.31
66	8	11	1295.183	115.13	108.85	113.96	112.26
67	10	15	1321.250	115.13	108.85	113.96	112.22
68	8	6	1343.100	115.76	108.85	113.96	112.18
69	9	19	1368.317	115.76	109.55	114.46	112.63
70	7	35	1390.583	115.76	109.55	114.46	112.59
71	7	58	1414.967	115.76	109.55	114.46	112.55
72	8	18	1439.300	115.76	109.55	114.46	112.50
73	9	10	1464.167	115.76	109.55	114.46	112.46
75	7	31	1510.517	115.76	109.55	114.46	112.38
76	7	45	1534.750	115.76	109.55	114.46	112.33
77	7	31	1558.517	115.76	109.55	114.97	112.80
78	8	16	1583.267	115.76	109.55	114.97	112.75
79	7	37	1606.617	116.39	109.55	114.97	112.71
80	7	49	1630.817	116.39	109.55	114.97	112.67
82	10	42	1681.700	116.39	109.55	114.97	112.58
83	7	53	1702.883	116.39	110.25	114.97	112.54
84	7	37	1726.617	116.39	110.25	114.97	112.50

(continued)

Table A-19. (concluded)

Day	Hr	Min	Elapsed Time (hr)	#210 Pressure (psig)	#211 Pressure (psig)	#212 Pressure (psig)	#212 Modified Pressure (psig)
85	7	31	1750.517	116.39	110.25	115.46	112.94
86	7	41	1774.683	116.39	110.25	115.46	112.90
89	7	35	1846.583	116.39	110.25	115.46	112.77
90	7	42	1870.700	116.39	110.25	115.46	112.73
91	7	29	1894.483	116.39	110.25	115.46	112.69
92	7	28	1918.467	116.39	110.25	115.46	112.64
93	7	38	1942.633	116.39	110.25	115.46	112.60
96	6	43	2013.717	116.39	110.25	--	--
97	6	40	2037.667	116.39	110.25	--	--
98	6	48	2061.800	116.39	110.25	115.46	112.39
100	7	9	2110.150	116.39	110.25	115.46	112.30
101	8	14	2135.233	116.39	110.25	--	--
103	6	36	2181.600	117.01	110.25	115.46	112.17
104	7	7	2206.117	117.01	110.94	115.46	112.13
105	6	24	2229.400	117.01	110.94	115.46	112.08
106	12	16	2259.267	117.01	110.94	115.46	112.03
107	6	27	2277.450	117.01	110.94	115.46	112.00
110	9	44	2352.733	117.64	110.94	115.46	111.86
111	7	54	2374.900	117.64	110.94	115.96	112.32
113	6	56	2421.933	117.64	111.63	115.96	112.24
114	6	38	2445.633	117.64	111.63	115.96	112.20
115	7	48	2470.800	117.64	111.63	115.96	112.15
117	6	11	2517.183	117.64	111.63	116.46	112.57
118	9	4	2544.067	118.26	111.63	116.46	112.52
119	6	11	2565.183	118.26	111.63	116.46	112.48
120	9	4	2592.067	118.26	111.63	116.46	112.43
121	6	48	2613.800	118.26	111.63	116.46	112.39
125	8	38	2711.633	118.89	112.33	116.46	112.22
132	6	37	2877.617	118.89	112.33	116.96	112.42
140	6	25	3069.417	119.51	113.02	117.46	112.58
141	9	24	3096.400	119.51	113.02	117.46	112.53
142	8	40	3119.667	119.51	113.02	117.46	112.49
148	8	12	3263.200	120.75	113.71	117.96	112.73
149	6	57	3285.950	120.13	113.71	117.96	112.69
150	15	24	3318.400	120.13	--	117.96	112.63
151	8	41	3335.683	120.13	--	117.96	112.60
152	8	44	3359.733	120.13	113.71	117.96	112.56
153	12	22	3387.367	120.13	113.71	117.96	112.50

Table A-20. Water Levels in Observation Well H-1 Magenta During the WIPP-13 Multipad Pumping Test

Day	Hr	Min	Elapsed Time (hr)	Depth to Water (ft)
336	11	14	-981.767	257.84
343	12	40	-812.333	258.43
349	12	30	-668.500	260.40
357	9	40	-479.333	262.73
5	13	45	-163.250	263.19
14	16	32	55.533	259.97
16	15	30	102.500	259.51
19	17	15	176.250	258.69
20	9	50	192.833	258.96
21	13	50	220.833	258.92
23	13	41	268.683	258.69
26	16	0	343.000	259.12
28	9	20	384.333	259.12
30	15	35	438.583	259.28
33	11	7	506.117	258.40
35	9	5	552.083	258.20
37	15	5	606.083	259.51
40	11	14	674.233	259.88
42	14	50	725.833	257.87
44	16	37	775.617	257.22
47	9	40	840.667	256.17
61	11	40	1178.667	259.42
78	14	45	1589.750	259.78
91	15	25	1902.417	263.68
91	15	30	1902.500	263.65
106	11	10	2258.167	265.16
120	10	20	2593.333	267.55

Table A-21. Water Levels in Observation Well H-6c Magenta During the WIPP-13 Multipad Pumping Test

Day	Hr	Min	Elapsed Time (hr)	Depth to Water (ft)
338	14	0	-931.000	296.75
357	12	11	-476.817	294.95
6	14	5	-138.917	294.36
13	12	30	27.500	293.90
14	14	30	53.500	293.73
16	13	40	100.667	293.93
19	16	15	175.250	293.64
20	8	45	191.750	293.67
21	9	45	216.750	293.70
23	12	21	267.350	293.57
26	13	21	340.350	293.57
28	11	21	386.350	293.44
30	13	15	436.250	293.37
33	9	14	504.233	293.27
35	10	25	553.417	293.04
37	13	40	604.667	293.31
41	11	20	698.333	292.91
42	12	20	723.333	292.78
44	14	25	773.417	292.78
47	11	28	842.467	292.78
61	11	20	1178.333	292.42
92	10	25	1921.417	291.96
119	9	45	2568.750	291.50
135	15	5	2958.083	291.17

APPENDIX B

Techniques for Analyzing Multiwell Pumping-Test Data

Techniques for Analyzing Multiwell Pumping-Test Data

The analysis of data from multiwell pumping tests may be divided into analysis of the pumping-well data and analysis of the observation-well data. The different techniques that may be used for these analyses are presented below. The well-test interpretation code INTERPRET is also described.

B.1 Pumping-Well Data Analysis

Pumping-well data, both from the drawdown and recovery periods, may be analyzed with either single-porosity or double-porosity interpretation techniques and with log-log and semilog plotting techniques. These are described below. The drawdown and recovery analyses should provide nearly identical results. Consistency of results validates the conceptual model used in the analysis.

B.1.1 Single-Porosity Log-Log Analysis

Single-porosity log-log analysis of drawdown and buildup (recovery) data may be performed using a method presented by Gringarten et al. (1979) and modified to include the pressure-derivative technique of Bourdet et al. (1984). This method applies to both the drawdown and buildup during or after a constant-rate flow period of a well that fully penetrates a homogeneous, isotropic, horizontal, confined porous medium. When used to interpret a test performed in a heterogeneous, anisotropic aquifer, the method provides volumetrically averaged results.

Gringarten et al. (1979) constructed a family of log-log type curves of dimensionless pressure, p_D, versus a dimensionless time group defined as dimensionless time, t_D, divided by dimensionless wellbore storage, C_D,

where:

$$p_D = \frac{kh}{141.2qB\mu}\Delta p \qquad \textbf{(B-1)}$$

$$t_D = \frac{0.000264\ kt}{\phi\mu c_t r_w^2} \qquad \textbf{(B-2)}$$

$$C_D = \frac{0.8936\ C}{\phi c_t h r_w^2} \qquad \textbf{(B-3)}$$

$$\frac{t_D}{C_D} = \frac{0.000295\ kht}{\mu C} \qquad \textbf{(B-4)}$$

and:

k = permeability, millidarcies (md)
h = test interval thickness, ft
Δp = change in pressure, psi
q = flow rate, barrels/day (bpd)
B = formation volume factor (B = 1.0 in single-phase water reservoir)
μ = fluid viscosity, centipoises (cp)
t = elapsed time, hours
ϕ = porosity
c_t = total-system compressibility, 1/psi
r_w = wellbore radius, ft
C = wellbore storage coefficient, barrels/psi

Each type curve in the family of curves (Figure B-1) is characterized by a distinct value of the parameter $C_D e^{2s}$, where:

s = skin factor

A positive value of s indicates wellbore damage or a wellbore with a lower permeability than the formation as a whole as a result of drilling effects. A negative value of s indicates a wellbore with enhanced permeability, usually caused by one or more fractures intersecting the wellbore.

The type curves begin with an initial segment having a unit slope corresponding to early-time wellbore storage and skin effects. The duration of this unit slope segment is proportional to the amount of wellbore storage and skin that are present. At late time, the curves flatten as infinite-acting radial-flow effects dominate.

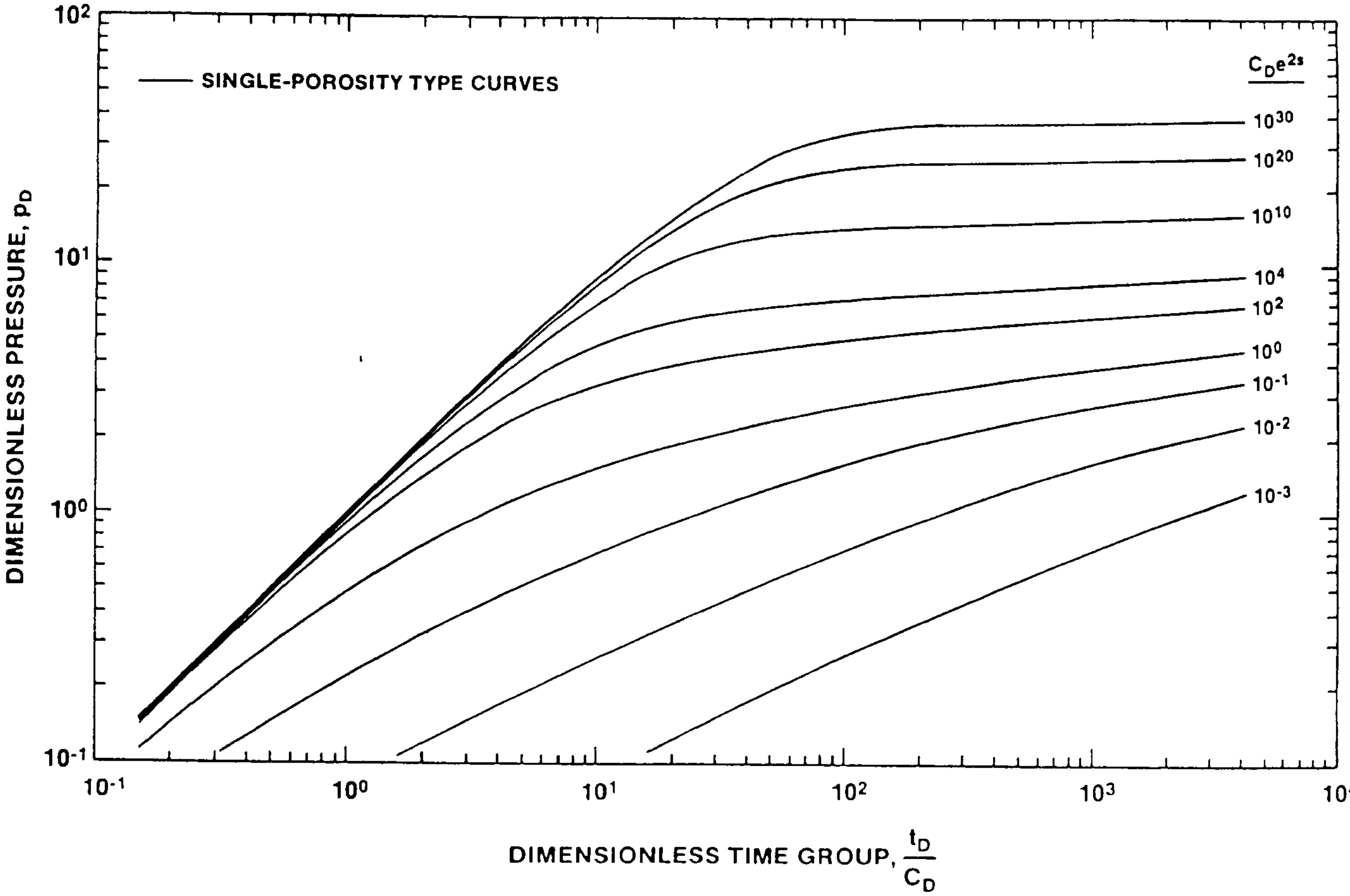

Figure B-1. Single-Porosity Type Curves for Wells With Wellbore Storage and Skin

Bourdet et al. (1984) added the pressure derivative to the analytical procedure by constructing a family of type curves of the semilog slope of the dimensionless pressure response versus the same dimensionless time group, tD/C_D. The semilog slope of the dimensionless pressure response is defined as:

$$\frac{dp_D}{d\ln(t_D/C_D)} = \frac{t_D}{C_D}\frac{dp_D}{d(t_D/C_D)} = \frac{t_D}{C_D}p'_D \qquad \textbf{(B-5)}$$

where:

p'_D = dimensionless pressure derivative

These curves are plotted on the same log-log graphs as the type curves of Gringarten et al. (1979), with the vertical axis now also labeled $(t_D/C_D)p'_D$ (Figure B-2). Again, each individual type curve is characterized by a distinct value of C_De^{2s}. Pressure-derivative type curves begin with an initial segment with unit slope corresponding to early-time wellbore storage and skin effects. This segment reaches a maximum that is proportional to the amount of wellbore storage and skin, and then the curve declines and stabilizes at a dimensionless pressure/semilog slope value of 0.5, corresponding to late-time, infinite-acting, radial-flow effects.

Pressure-derivative data in combination with pressure data are much more sensitive indicators of double-porosity effects, boundary effects, nonstatic antecedent test conditions, and other phenomena than are pressure data alone. For this reason, pressure-derivative data are useful in choosing between conflicting phenomenological models that often cannot be differentiated on the basis of pressure data alone. Pressure-derivative data are also useful in determining when infinite-acting, radial-flow conditions occur during a test because these conditions cause the pressure derivative to stabilize at a constant value.

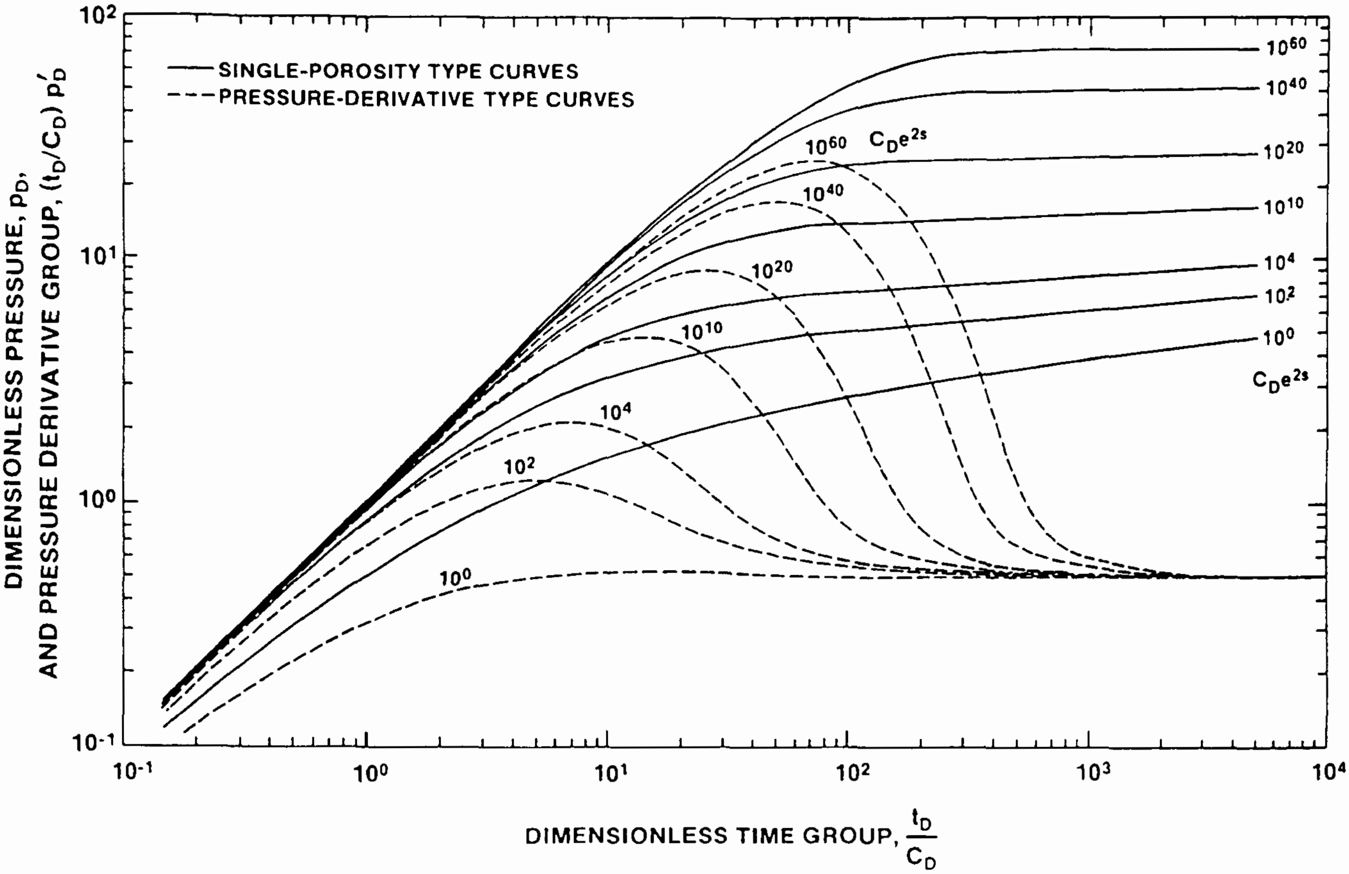

Figure B-2. Single-Porosity Type Curves and Pressure-Derivative Type Curves for Wells With Wellbore Storage and Skin

For any given point, the pressure derivative is calculated as the linear-regression slope of a semilog line fit through that point and any chosen number of neighboring points on either side. The equation for the derivative follows:

$$p' = \frac{n\sum_{i=1}^{n} x_i y_i - \sum_{i=1}^{n} x_i \sum_{i=1}^{n} y_i}{n\sum_{i=1}^{n} x_i^2 - \sum_{i=1}^{n} x_i^2} \quad \textbf{(B-6)}$$

where, for a single constant-rate flow period:

n = number of points to be fitted
$x_i = \ln \Delta t_i$
$y_i = \Delta p_i$
Δt_i = elapsed test time at point i, hr
Δp_i = pressure change at Δt_i, psi

For a multirate flow period or a buildup period, the time parameter is a superposition function calculated as:

$$x_i = \left\{ \sum_{i=1}^{n-1} (q_i - q_{i-1}) \log \left[\left(\sum_{j=1}^{n-1} \Delta t_j \right) + \Delta t \right] \right\} + (q_n - q_{n-1}) \log \Delta t \quad \textbf{(B-7)}$$

where:

q = flowrate, bpd
Δt = elapsed time during a flow period, hr

with subscripts:

i = individual flow period
j = individual flow period
n = number of flow periods considered

In general, the fewer the number of points used in calculating the derivative, the more accurate it will be. Three-point derivatives, calculated using only the nearest neighbor on either side of a point, usually provide enough resolution to distinguish most important features. However, excessive noise in the data sometimes makes it necessary to use five- or seven-point derivatives, or various "windowing" procedures, to obtain a smooth curve. Unfortunately, this may also smooth out some of the features sought.

The type curves published by both Gringarten et al. (1979) and Bourdet et al. (1984) were derived for flow-period (drawdown) analysis. In general, the curves can also be used for buildup-period analysis, so long as it is recognized that, at late time, buildup data will fall below the drawdown type curves because of superposition effects.

If the test analysis is to be done manually, the buildup data are plotted as pressure change since buildup began (Δp) versus elapsed time since buildup began (t) on log-log paper of the same scale as the type curves. The derivative of the pressure change is also plotted using the same vertical axis as the Δp data. The data plot is then laid over the type curves and moved both laterally and vertically, so long as the axes remain parallel, until a fit is achieved between the data and pressure and pressure-derivative curves with the same C_De^{2s} value. When the data fit the curves, an arbitrary match point is selected, and the coordinates of that point on both the data plot, t and Δp, and on the type-curve plot, p_D and t_D/C_D, are noted. The permeability-thickness product is then calculated from a rearrangement of Eq (B-1):

$$kh = 141.2qB\mu \frac{p_D}{\Delta p} \qquad \textbf{(B-8)}$$

The groundwater-hydrology parameter transmissivity, T, is related to the permeability-thickness product by the following relationship, modified from Freeze and Cherry (1979):

$$T = kh\rho g/\mu \qquad \textbf{(B-9)}$$

where:

ρ = fluid density, M/L^3
g = gravitational acceleration, L/T^2
μ = fluid viscosity, M/LT

When T is given in ft^2/day, kh is given in millidarcy-feet, ρ is given in g/cm^3, g is set equal to 980.665 cm/s^2, and μ is given in centipoises, Eq (B-9) becomes:

$$T = 2.7435 \times 10^{-3}\, kh\rho/\mu \qquad \textbf{(B-10)}$$

The wellbore storage coefficient is calculated from a rearrangement of Eq (B-4):

$$C = \frac{0.000295\, kht}{\mu t_D/C_D} \qquad \textbf{(B-11)}$$

Finally, if estimates of porosity and total-system compressibility are available, the skin factor can be calculated from the value of the C_De^{2s} curve selected and Eq (B-3):

$$s = 0.5 \ln\left[\frac{C_De^{2s}}{0.8936C/\phi c_t h r_w^{\,2}}\right] \qquad \textbf{(B-12)}$$

B.1.2 Double-Porosity Log-Log Analysis

Double-porosity media have two porosity sets that differ in terms of storage volume and permeability. Typically, the two porosity sets are (1) a fracture network with higher permeability and lower storage, and (2) the primary porosity of the rock matrix with lower permeability and higher storage. During a hydraulic test, these two porosity sets respond differently. With high-quality test data, the hydraulic parameters of both porosity sets can be quantified.

During a hydraulic test in a double-porosity medium, the fracture system responds first. Initially, most of the water pumped comes from the fractures, and the pressure in the fractures drops accordingly. With time, the matrix begins to supply water to the fractures, causing the fracture pressure to stabilize and the matrix pressure to drop. As the pressures in the fractures and matrix equalize, both systems produce water to the well. The total-system response is then observed for the balance of the test.

The initial fracture response and the final total-system response both follow the single-porosity type curves described earlier. By simultaneously fitting the fracture response and the total-system response to two different C_De^{2s} curves, we can derive fracture-system and total-system properties. Information on the matrix, and additional information on the fracture system, can be obtained by interpretation of the data from the transition period when the matrix begins to produce to the fractures. Two different sets of type curves can be used to try to fit the transition-period data.

Transition-period data are affected by the nature, or degree, of interconnection between the matrix and the fractures. Warren and Root (1963) published the first line-source solution for well tests in double-porosity systems. They assumed that flow from the matrix to the fractures (interporosity flow) occurred under pseudosteady-state conditions; that is, that the flow between the matrix and the fractures was directly proportional to the average head difference between those two systems. Other authors, such as Kazemi (1969) and de Swaan (1976), derived solutions using the diffusivity equation to govern interporosity flow. These are known as transient interporosity flow solutions. Mavor and Cinco-Ley (1979) added wellbore storage and skin to the double-porosity solution, but still used pseudosteady-state interporosity flow. Bourdet and Gringarten (1980) modified Mavor and Cinco-Ley's (1979) theory to include transient interporosity flow and generated type curves for double-porosity systems with both pseudosteady-state and transient interporosity flow.

Pseudosteady-state and transient interporosity flow represent two extremes; all intermediate behaviors are also possible. Gringarten (1984), however, indicates that the majority of tests he has seen exhibit pseudosteady-state interporosity flow behavior.

In recent years, Gringarten (1984, 1986) has suggested that the terms "restricted" and "unrestricted" interporosity flow replace the terms "pseudosteady-state" and "transient" interporosity flow. He believes that all interporosity flow is transient in the sense that it is governed by the diffusivity equation. But in the case where the fractures possess a positive skin similar to a wellbore skin (caused, for example, by secondary mineralization on the fracture surfaces) that restricts the flow from the matrix to the fractures, the observed behavior is similar to that described by the pseudo-steady-state formulation (Moench, 1984; Cinco-Ley et al., 1985). "Transient" interporosity flow is observed when there are no such restrictions. Hence, the terms "restricted" and "unrestricted" more accurately describe conditions than do the terms "pseudosteady-state" and "transient." The recent terminology of Gringarten is followed in this report.

Restricted Interporosity Flow

Warren and Root (1963) defined two parameters to aid in characterizing double-porosity behavior. These are the storativity ratio, ω, and the interporosity flow coefficient, λ. The storativity ratio is defined as:

$$\omega = \frac{(\phi V c_t)_f}{(\phi V c_t)_{f+m}} \qquad \textbf{(B-13)}$$

where:

ϕ = ratio of the pore volume in the system to the total-system volume
V = the ratio of the total volume of one system to the bulk volume
c_t = total compressibility of the system

with subscripts:

f = fracture system
m = matrix

The interporosity flow coefficient is defined as:

$$\lambda = \alpha r_w^2 \frac{k_m}{k_f} \qquad \textbf{(B-14)}$$

where α is a shape factor characteristic of the geometry of the system and other terms are as defined earlier.

The shape factor, α, is defined as:

$$\alpha = \frac{4n(n+2)}{\ell^2} \qquad \textbf{(B-15)}$$

where:

n = number of normal sets of planes limiting the matrix
ℓ = characteristic dimension of a matrix block (ft)

Bourdet and Gringarten (1980) constructed a family of transition type curves for restricted interporosity flow on the same axes as the C_De^{2s} curves of Gringarten et al. (1979), with each transition curve characterized by a distinct value of the parameter λe^{-2s}. Together, the single-porosity type curves and the transition type curves make up the double-porosity type curves (Figure B-3).

In manual double-porosity type-curve matching, a log-log plot of the data is prepared as in single-porosity type-curve matching. The data plot is then laid over the double-porosity type curves and moved both laterally and vertically, so long as the axes remain parallel, until (1) the early-time (fracture flow only) data fall on one C_De^{2s} curve, (2) the middle portion of the transition data falls on a λe^{-2s} curve, and (3) the late-time (total-system) data fall on a lower C_De^{2s} curve. In computer-aided analysis, pressure-derivative curves for double-porosity systems may also be prepared (Gringarten, 1986). The number of possible curve combinations, however, precludes preparation of generic pressure-derivative curves for manual double-porosity curve fitting.

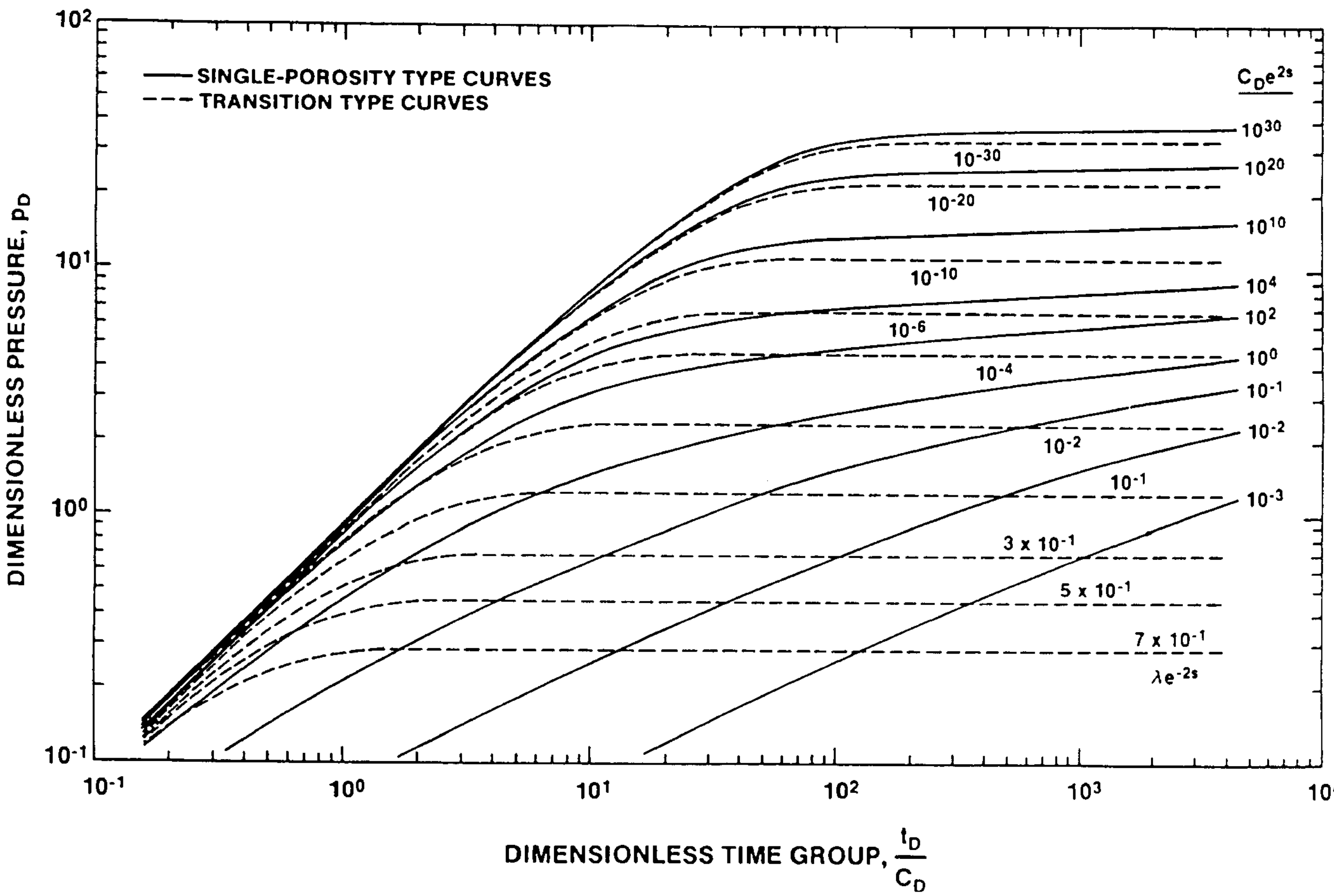

Figure B-3. Double-Porosity Type Curves for Wells With Wellbore Storage, Skin, and Restricted Interporosity Flow

When a fit of the data plot to the type curves is achieved, an arbitrary match point is selected, and the coordinates of that point on both the data plot, t and Δp, and the type-curve plot, t_D/C_D and p_D, are noted. The values of C_De^{2s} and λe^{-2s} of the matched curves are also noted. The permeability-thickness product of the fracture system (and also of the total system because fracture permeability dominates) and the wellbore storage coefficient are calculated from Eqs (B-8) and (B-11). The storativity ratio, ω, is calculated from:

$$\omega = \frac{(C_De^{2s})_{f+m}}{(C_De^{2s})_f} \quad \textbf{(B-16)}$$

The dimensionless wellbore storage coefficient for the matrix is calculated as:

$$(C_D)m = \frac{0.8936\ C}{(V\phi c_t)_m h r_w^2} \quad \textbf{(B-17)}$$

This leads to the dimensionless wellbore storage coefficient for the total system:

$$(C_D)_{f+m} = (C_D)_m \times (1-\omega) \quad \textbf{(B-18)}$$

Then the skin factor is calculated as:

$$s = 0.5 \ln\left[\frac{(C_De^{2s})_{f+m}}{(C_D)_{f+m}}\right] \quad \textbf{(B-19)}$$

The interporosity flow coefficient is calculated from:

$$\lambda = \frac{\lambda e^{-2s}}{e^{-2s}} \quad \textbf{(B-20)}$$

If matrix permeability and geometry are known independently, Eqs (B-14) and (B-15) can be used to determine the effective dimensions of the matrix blocks.

Unrestricted Interporosity Flow

Matrix geometry is more important for unrestricted interporosity flow than for restricted interporosity flow because the former is governed by the diffusivity equation. A different set of type curves is used, therefore, to match transition-period data when unrestricted interporosity flow conditions exist (Figure B-4). Bourdet and Gringarten (1980) characterize each curve with a different value of the parameter β, the exact definition of which is a function of the matrix geometry. For example, for slab-shaped matrix blocks, they give:

$$\beta = \frac{6}{\gamma^2} \frac{(C_D e^{2s})_{f+m}}{\lambda e^{-2s}} \qquad \textbf{(B-21)}$$

and for spherical blocks they give:

$$\beta = \frac{10}{3\gamma^2} \frac{(C_D e^{2s})_{f+m}}{\lambda e^{-2s}} \qquad \textbf{(B-22)}$$

where:

γ = exponential of Euler's constant (= 1.781)

Moench (1984) provides an extensive discussion on the effects of matrix geometry on unrestricted interporosity flow.

Manual double-porosity type-curve matching with unrestricted-interporosity-flow transition curves is performed in exactly the same manner as with restricted-interporosity-flow transition curves, described earlier. The same equations are used to derive the fracture and matrix parameters, except that the matrix geometry must now be known or assumed to obtain the interporosity flow coefficient, λ, from rearrangement of Eq (B-21) or (B-22).

B.1.3 Semilog Analysis

Two semilog plotting techniques are commonly used in the interpretation of hydraulic-test data. These produce a Horner plot and a dimensionless Horner plot.

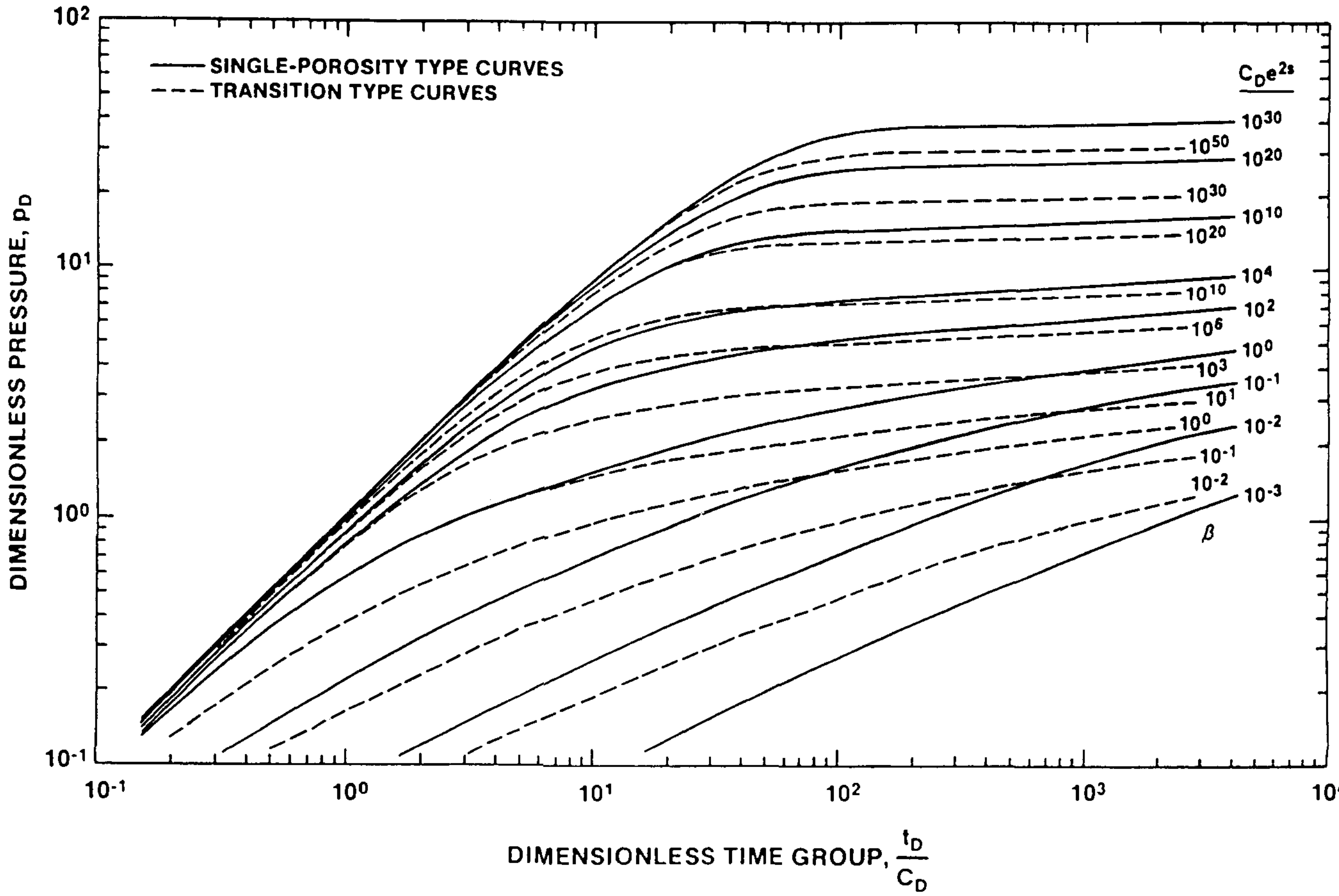

Figure B-4. Double-Porosity Type Curves for Wells With Wellbore Storage, Skin, and Unrestricted Interporosity Flow

Horner Plot

Horner (1951) provided a method of obtaining permeability and static formation pressure values independent of log-log type-curve matching, although the two methods are best used in conjunction. Horner's method applies to the buildup (recovery) of the pressure after a constant-rate flow period in a well that fully penetrates a homogeneous, isotropic, horizontal, infinite, confined reservoir. For a recovery after a single flow period, Horner's solution is:

$$p(t) = p^* - \frac{162.6qB\mu}{kh}\log\left[\frac{t_p + dt}{dt}\right] \qquad \textbf{(B-23)}$$

where:

$p(t)$ = pressure at time t, psi
p^* = static formation pressure, psi
t_p = duration of previous flow period, hr
dt = time elapsed since end of flow period, hr

and other terms are as defined earlier under Eq (B-4). For a recovery after multiple flow periods, the time group in Eq (B-23) is replaced by the superposition function given in the right-hand side of Eq (B-7).

The permeability-thickness product (kh) is obtained by (1) plotting p(t) versus log $[(t_p + dt)/dt]$ (or the superposition function), (2) drawing a straight line through the data determined from the log-log pressure-derivative plot to be representative of infinite-acting radial flow, and (3) measuring the change in p(t) on this line over one log cycle of time (m). Equation (B-23) can then be rearranged and reduced to:

$$kh = 162.6qB\mu/m \qquad \textbf{(B-24)}$$

Static formation pressure is estimated by extrapolating the radial-flow straight line to the pressure axis where log $[(t_p + dt)/dt] = 1$, representing infinite recovery time. In the absence of reservoir boundaries, the pressure intercept at that time should equal the static formation pressure.

Horner (1951) also suggested a modification of his method for the case where the flow rate was not held constant. This modification was later theoretically verified for the case of constant-pressure, variable-rate production by Ehlig-Economides (1979). The modification entails calculating a modified production time:

$$t_p^* = V/q_f \qquad \textbf{(B-25)}$$

where:

V = total flow produced, barrels
q_f = final flow rate, barrels/hr (bph)

The modified production time, t_p^*, is substituted for the actual production time, t_p, in Eq (B-23), and the analysis proceeds as before. The modified production time can also be used for calculation of buildup type curves for log-log analysis.

Dimensionless Horner Plot

The dimensionless Horner plot represents a second useful semilog approach to hydraulic-test interpretation. Once type-curve and match-point selections have been made through log-log analysis, this technique allows the single- or double-porosity C_De^{2s} type curves to be superimposed on a normalized semilog plot of the data. Logarithmic dimensionless times for the data are calculated using:

$$\frac{q_{n-1}-q_n}{|q_{n-1}-q_n|}\left[\sum_{i=1}^{n-1}\frac{q_i-q_{i-1}}{q_{n-1}-q_n}\log\left(\sum_{j=i}^{n-1}\Delta t_j+\Delta t\right)-\log\Delta t\right] \qquad \textbf{(B-26)}$$

where all parameters are as defined earlier. The dimensionless times calculated using Eq (B-26) are plotted on a linear scale. Dimensionless pressures for the data are calculated using:

$$\frac{p_D}{\Delta p}\,[p^* - p(t)] \qquad \textbf{(B-27)}$$

where p_D and Δp are the log-log match-point coordinates, and the other parameters are as defined earlier. Dimensionless pressures are also plotted on a linear scale.

The type curves are plotted on the same axes with dimensionless time defined as:

$$\frac{q_{n-1}-q_n}{|q_{n-1}-q_n|}\left[\sum_{i=1}^{n-1}\frac{q_i-q_{i-1}}{q_n-q_{n-1}}\log\left(\sum_{j=i}^{n-1}\Delta t_j+\Delta t\right)-\log\Delta t\right] \qquad \textbf{(B-28)}$$

and dimensionless pressure defined as:

$$\frac{q_{n-1}-q_n}{|q_{n-1}-q_n|}\left[\sum_{i=1}^{n-1}\frac{q_i-q_{i-1}}{q_n-q_{n-1}}p_D\left(\sum_{j=i}^{n-1}\Delta t_j+\Delta t\right)_D-p_D(\Delta t)_D\right] \qquad \textbf{(B-29)}$$

The dimensionless Horner plot is a very sensitive indicator of inaccuracies in type-curve, match-point, and static-formation-pressure selections (Gringarten, 1986). By iterating between dimensionless Horner and log-log plots, very accurate hydraulic parameters can be obtained.

B.2 Observation-Well Data Analysis

For distant observation wells monitored during pumping tests, the drawdown and recovery data can be analyzed using a method first described by Theis (1935) for single-porosity systems. Use of a single-porosity interpretation technique for an observation well in a double-porosity aquifer is justified when the observation well is far enough from the pumping well that only total-system responses are observed. Deruyck et al. (1982) provide the following criterion for being able to measure double-porosity responses at an observation well:

$$\ln \frac{2}{\gamma \sqrt{\lambda r_D^2}} > \text{gage resolution} + \text{noise} \qquad \textbf{(B-30)}$$

where:

$$r_D = r/r_w \qquad \textbf{(B-31)}$$

r = radial distance to pumping well, ft

and other terms are as defined earlier. Generally, this criterion limits observable double-porosity responses to a maximum distance of tens to perhaps hundreds of feet from the pumping well.

Theis (1935) created a log-log drawdown type curve of p_D versus t_D/r_D^2 using an exponential integral (Ei) solution for drawdown caused by a line-source well in a porous medium:

$$p_D = -0.5\ \mathrm{Ei}(-r_D^2/4t_D) \qquad \textbf{(B-32)}$$

where:

$$\frac{t_D}{r_D^2} = \frac{0.000264kht}{\phi \mu c_t h r^2} \qquad \textbf{(B-33)}$$

The terms p_D and t_D are defined by Eqs (B-1) and (B-2), respectively; other terms are as defined in Section B.1.1. This type curve applies to the analysis of drawdown at both pumping wells (assuming no wellbore storage) and observation wells.

Elapsed pumping time (t) and drawdown (Δp) are plotted on log-log paper of the same scale as the type curve. The observed data are matched to the line-source type curve, thus defining a match point. The two sets of coordinates of that point, t and Δp, and t_D/r_D^2 and p_D, are used with Eqs (B-8) and (B-33) to calculate the permeability-thickness product and the porosity-compressibility-thickness product, respectively.

The permeability-thickness product is related to transmissivity through Eqs (B-9) and (B-10). Narasimhan and Kanehiro (1980) give the relationship between the porosity-compressibility-thickness product and the groundwater-hydrology parameter storativity, S, in consistent units as:

$$S = \phi c_t h \rho g \qquad \textbf{(B-34)}$$

When total compressibility, c_t, is in units of 1/psi, thickness, h, is in units of ft, fluid density, ρ, is in units of g/cm^3, and gravitational acceleration, g, is set equal to 980.665 cm/s^2, Eq (B-34) becomes:

$$S = 0.4335 \phi c_t h \rho \qquad \textbf{(B-35)}$$

B.3 Interpret Well-Test Interpretation Code

Manual type-curve fitting is a time-consuming process limited by the published type curves available and by the degree of resolution/differentiation obtainable in manual curve fitting. The analyses presented in this report were not performed manually but by using the well-test analysis code INTERPRET developed by A. C. Gringarten and Scientific Software-Intercomp (SSI). INTERPRET is a proprietary code that uses analytical solutions. It can be leased from SSI.

INTERPRET can analyze drawdown (flow) and recovery (buildup) tests in single-porosity, double-porosity, and fractured media. For production-well data analysis, it incorporates the analytical techniques discussed earlier and additional techniques discussed in Gringarten et al. (1974), Bourdet and Gringarten (1980), and Gringarten (1984). Rather than relying on a finite number of drawdown type curves, INTERPRET calculates the precise drawdown or buildup type curve corresponding to the match point and data point selected by the user. For observation-well data analysis, the INTERPRET code uses the line-source solution of Theis (1935).

After type-curve selection, INTERPRET simulates the test with the chosen parameters so that the user can see how good the match truly is. Through an iterative parameter-adjustment process, the user fine-tunes the simulation until satisfied with the results. Log-log, semilog (Horner and dimensionless Horner), and linear-linear plotting techniques are all used to ensure consistency of the final model with the data in every respect. Once the final model is selected, INTERPRET carries out all necessary calculations and provides final parameter values. Analyses obtained using INTERPRET have been verified by manual checks.

In addition to standard type-curve analysis, INTERPRET allows the incorporation of constant-pressure and no-flow boundaries in analysis, using the theory of superposition and image wells discussed by Ferris et al. (1962) and others. A constant-pressure boundary can be simulated by adding a recharge (image) well to the model. A no-flow boundary can be simulated by adding a discharge (image) well to the model. Drawdowns/rises from multiple discharge/recharge wells are additive. In INTERPRET, an image well (either discharge or recharge) is included by specifying a dimensionless distance for the image well from the production or observation well and by using the line-source solution of Theis (1935; see Section B.2) to calculate the drawdown or recovery caused by that well at the well under consideration. In the case of a production well, the dimensionless distance to the image well is related to the "actual" distance to the image well, r_i, by the following:

$$r_i = r_w \sqrt{C_D D_D} \quad \textbf{(B-36)}$$

where:

D_D = dimensionless distance

and other terms are as defined earlier. The actual hydraulic boundary is then half of the distance to the image well from the production well.

Defining distances to hydraulic boundaries from observation-well data is more complex. The dimensionless distance to the image well is related to the "actual" distance to the image well, r_i, by the following:

$$r_i = r \sqrt{D_D} \quad \textbf{(B-37)}$$

The hydraulic boundary is then tangential to a circle having radius r_i centered midway between the production well and the observation well. Data from three or more observation wells are required to define the location and orientation of this boundary precisely.

APPENDIX C

Barometric-Pressure Data

Table C-1. WIPP-13 Multipad Pumping Test Barometric Pressure Data

Day	Hr	Min	Elapsed Time (hr)	Barometric Pressure (psia)
12	9	0	0.0000	13.133
12	12	30	3.5000	13.094
12	15	0	6.0000	13.077
12	18	0	9.0000	13.080
13	0	0	15.0000	13.069
13	10	0	25.0000	13.039
13	14	0	29.0000	12.971
13	17	0	32.0000	12.959
13	21	0	36.0000	12.955
14	1	0	40.0000	12.941
14	7	0	46.0000	12.940
14	11	0	50.0000	12.952
14	15	0	54.0000	12.922
14	19	0	58.0000	12.957
14	23	0	62.0000	12.980
15	8	30	71.5000	13.017
15	13	0	76.0000	12.985
15	17	0	80.0000	12.972
16	9	0	96.0000	13.003
16	13	0	100.0000	12.988
16	17	0	104.0000	12.979
16	21	0	108.0000	12.987
17	9	0	120.0000	12.972
17	13	0	124.0000	12.953
17	17	0	128.0000	12.972
17	21	0	132.0000	13.023
18	9	0	144.0000	13.041
18	13	0	148.0000	13.005
18	17	0	152.0000	12.997
18	21	0	156.0000	13.006
19	9	0	168.0000	13.039
19	13	0	172.0000	12.986
19	17	0	176.0000	12.978
19	21	0	180.0000	13.033
20	9	0	192.0000	13.116
20	12	8	195.1270	13.105
20	17	0	200.0000	13.090
20	21	0	204.0000	13.097
21	9	0	216.0000	13.039
21	13	0	220.0000	13.026
21	17	0	224.0000	13.071

(continued)

Table C-1. (continued)

Day	Hr	Min	Elapsed Time (hr)	Barometric Pressure (psia)
21	21	0	228.0000	13.116
22	13	0	244.0000	13.089
22	17	0	248.0000	13.051
22	21	0	252.0000	13.041
23	9	47	263.7780	12.987
23	13	0	268.0000	12.945
23	17	0	272.0000	12.919
23	21	0	276.0000	12.919
24	9	0	288.0000	12.966
24	11	0	290.0000	12.961
24	13	0	292.0000	12.955
24	17	0	296.0000	13.011
24	21	0	300.0000	13.043
25	9	0	312.0000	13.082
25	17	0	320.0000	13.077
25	21	0	324.0000	13.104
26	8	17	335.2840	13.145
26	13	0	340.0000	13.127
26	17	0	344.0000	13.112
26	21	0	348.0000	13.110
27	9	0	360.0000	13.105
27	13	0	364.0000	13.059
27	17	0	368.0000	13.035
27	21	0	372.0000	13.039
28	9	0	384.0000	13.011
28	21	0	396.0000	12.974
29	9	0	408.0000	13.059
29	21	0	420.0000	13.049
30	11	0	434.0000	13.124
30	21	0	444.0000	13.050
31	9	0	456.0000	12.943
31	21	0	468.0000	12.952
32	9	0	480.0000	12.990
32	21	0	492.0000	12.990
33	9	0	504.0000	12.993
33	21	0	516.0000	12.969
34	11	0	530.0000	12.994
34	21	0	540.0000	12.963
35	9	0	552.0000	12.996
35	21	0	564.0000	13.003
36	15	0	582.0000	13.145

(continued)

Table C-1. (continued)

Day	Hr	Min	Elapsed Time (hr)	Barometric Pressure (psia)
36	21	0	588.0000	13.180
37	7	0	598.0000	13.197
37	21	0	612.0000	13.208
38	9	51	623.8560	13.229
38	21	0	636.0000	13.154
39	9	0	648.0000	13.140
39	21	0	660.0000	13.144
40	9	0	672.0000	13.163
40	21	0	684.0000	13.076
41	11	0	698.0000	13.066
41	21	0	708.0000	13.045
42	9	0	720.0000	13.066
42	21	0	732.0000	13.043
43	11	0	746.0000	13.075
43	21	0	756.0000	13.042
44	11	0	770.0000	13.019
44	21	0	780.0000	12.943
45	9	0	792.0000	12.856
45	21	0	804.0000	12.821
46	9	0	816.0000	12.955
46	21	0	828.0000	12.946
47	11	0	842.0000	12.946
47	21	0	852.0000	12.981
48	8	30	863.5000	13.049
48	10	30	864.5000	13.052
48	13	15	868.2500	13.036
48	16	0	871.0000	13.027
48	16	30	871.5000	13.025
48	21	0	876.0000	13.042
49	3	0	882.0000	13.023
49	9	0	888.0000	13.023
49	15	0	894.0000	12.955
49	21	0	900.0000	12.944
50	3	0	906.0000	12.956
50	9	0	912.0000	12.983
50	15	0	918.0000	12.970
50	21	0	924.0000	13.021
50	23	0	926.0000	13.019
51	9	0	936.0000	13.097
51	15	0	942.0000	13.075
51	21	0	948.0000	13.081

(continued)

Table C-1. (continued)

Day	Hr	Min	Elapsed Time (hr)	Barometric Pressure (psia)
51	23	0	950.0000	13.074
52	9	0	960.0000	13.032
52	15	0	966.0000	12.997
52	23	0	974.0000	13.054
53	9	0	984.0000	13.080
53	15	0	990.0000	13.022
54	9	0	1008.0000	12.943
54	15	0	1014.0000	12.868
54	21	0	1020.0000	12.904
54	23	0	1022.0000	12.927
55	9	0	1032.0000	12.970
55	13	0	1036.0000	12.938
55	15	0	1038.0000	12.934
55	21	0	1044.0000	12.958
55	23	0	1046.0000	12.952
56	9	0	1056.0000	12.963
56	15	0	1062.0000	12.923
56	21	0	1068.0000	12.921
56	23	0	1070.0000	12.930
57	10	20	1081.3350	12.943
57	14	20	1085.3350	12.903
57	21	0	1092.0000	12.936
57	23	0	1094.0000	12.940
58	11	0	1106.0000	12.917
58	15	0	1110.0000	12.891
58	23	0	1118.0000	12.937
59	9	0	1128.0000	12.985
59	15	0	1134.0000	12.966
59	23	0	1142.0000	13.019
60	9	0	1152.0000	13.075
60	15	0	1158.0000	13.017
60	21	0	1164.0000	13.031
61	11	0	1178.0000	13.045
61	15	0	1182.0000	13.010
61	21	0	1188.0000	13.045
62	9	0	1200.0000	13.133
62	15	0	1206.0000	13.112
62	21	0	1212.0000	13.164
63	9	0	1224.0000	13.227
63	15	0	1230.0000	13.188
63	21	0	1236.0000	13.190

(continued)

Table C-1. (continued)

Day	Hr	Min	Elapsed Time (hr)	Barometric Pressure (psia)
64	9	0	1248.0000	13.167
64	21	0	1260.0000	13.090
65	13	0	1276.0000	13.045
65	21	0	1284.0000	13.028
66	9	0	1296.0000	13.035
66	15	0	1302.0000	12.979
66	21	0	1308.0000	12.999
67	9	0	1320.0000	12.985
67	13	0	1324.0000	12.945
67	15	0	1326.0000	12.922
67	21	0	1332.0000	12.942
68	9	0	1344.0000	13.029
69	9	0	1368.0000	13.093
70	9	0	1392.0000	13.135
71	11	0	1418.0000	13.113
72	11	0	1442.0000	13.080
73	9	0	1464.0000	12.951
74	9	0	1488.0000	12.930
75	9	0	1512.0000	12.855
76	11	0	1538.0000	12.828
77	9	0	1560.0000	12.904
78	10	35	1584.5830	12.915
78	12	35	1586.5830	12.912
79	12	35	1610.5830	12.924
79	14	35	1612.5830	12.903
82	9	0	1680.0000	12.883
82	11	0	1682.0000	12.879
84	9	0	1728.0000	12.979
84	11	0	1730.0000	12.982
86	9	0	1776.0000	12.924
86	11	0	1778.0000	12.909
89	9	0	1848.0000	13.151
89	13	37	1851.6120	13.108
91	9	0	1896.0000	13.008
91	11	0	1898.0000	12.988
93	9	0	1944.0000	13.082
93	11	0	1946.0000	13.067
96	11	0	2018.0000	13.097
96	13	0	2020.0000	13.080
98	9	0	2064.0000	13.113
98	11	0	2066.0000	13.101

(continued)

Table C-1. (concluded)

Day	Hr	Min	Elapsed Time (hr)	Barometric Pressure (psia)
100	9	0	2112.0000	13.029
100	11	0	2114.0000	13.018
103	9	0	2184.0000	13.038
103	11	0	2186.0000	13.039
105	13	0	2236.0000	13.005
105	15	0	2238.0000	12.979
108	9	0	2304.0000	12.934
108	11	0	2306.0000	12.922
110	9	0	2352.0000	13.053
110	11	0	2354.0000	13.060
113	9	0	2424.0000	13.084
113	11	0	2426.0000	13.071
114	13	0	2452.0000	13.089
114	15	0	2454.0000	13.075
118	9	0	2544.0000	13.145
118	11	0	2546.0000	13.147
120	7	0	2590.0000	12.997

References

Beauheim, R. L. 1987a. *Analysis of Pumping Tests of the Culebra Dolomite Conducted at the H-3 Hydropad at the Waste Isolation Pilot Plant (WIPP) Site*, SAND86-2311 (Albuquerque, NM: Sandia National Laboratories).

Beauheim, R. L. 1987b. *Interpretations of Single-Well Hydraulic Tests Conducted At and Near the Waste Isolation Pilot Plant (WIPP) Site, 1983-1987*, SAND 87-0039 (Albuquerque, NM: Sandia National Laboratories).

Bechtel National, Inc. 1986. *Interim Geotechnical Field Data Report, Fall 1986*. DOE-WIPP-86-012 (Carlsbad, NM: US DOE).

Bourdet, D., and Gringarten, A. C. 1980. *Determination of Fissure Volume and Block Size in Fractured Reservoirs by Type-Curve Analysis*, SPE 9293 (Richardson, TX: Soc Pet Eng).

Bourdet, D.; Ayoub, J. A.; and Pirard, Y. M. 1984. *Use of Pressure Derivative in Well Test Interpretation*, SPE 12777 (Richardson, TX: Soc Pet Eng).

Cinco-Ley, H.; Samaniego-V., F.; and Kucuk, F. 1985. *The Pressure Transient Behavior for Naturally Fractured Reservoirs with Multiple Block Size*, SPE 14168 (Richardson, TX: Soc Pet Eng).

Crawley, M. E. 1987. *Second Data Release Report for the Pressure-Density Survey Program*. (Carlsbad, NM: IT Corporation/Westinghouse WID).

Deruyck, B. G.; Bourdet, D. P.; DaPrat, G.; and Ramey, H. J., Jr. 1982. *Interpretation of Interference Tests in Reservoirs with Double Porosity Behavior—Theory and Field Examples*. SPE 11025 (Richardson, TX: Soc Pet Eng).

de Swaan, A. O. 1976. "Analytical Solutions for Determining Naturally Fractured Reservoir Properties by Well Testing," *Soc Pet Eng J* (June 1976):117-22.

Earlougher, R. C., Jr. 1977. *Advances in Well Test Analysis*. Monograph Volume 5 (Dallas, TX: Soc Pet Eng of AIME), 264 pp.

Ehlig-Economides, C. A. 1979. "Well Test Analysis for Wells Produced at a Constant Pressure," PhD Dissertation (Palo Alto, CA: Stanford Univ Dept of Pet Eng), 117 pp.

Ferris, J. G.; Knowles, D. B.; Brown, R. H.; and Stallman, R. W. 1962. *Theory of Aquifer Tests, Ground-Water Hydraulics*. USGS Water-Supply Paper 1536-E (Washington, DC: US GPO), 174 pp.

Freeze, R. A., and Cherry, J. A. 1979. *Groundwater* (Englewood Cliffs, NJ: Prentice-Hall, Inc), 604 pp.

Gringarten, A. C. 1984. "Interpretation of Tests in Fissured and Multilayered Reservoirs with Double-Porosity Behavior: Theory and Practice," *J Pet Tech* 36(4):549-64.

Gringarten, A. C. 1986. *Computer-Aided Well Test Analysis*, SPE 14099 (Richardson, TX: Soc Pet Eng).

Gringarten, A. C.; Ramey, H. J., Jr.; and Raghavan, R. 1974. "Unsteady-State Pressure Distributions Created by a Well with a Single Infinite-Conductivity Vertical Fracture," *Soc Pet Eng J* 14(4):347-60.

Gringarten, A. C.; Bourdet, D. P.; Landel, P. A.; and Kniazeff, V. J. 1979. A *Comparison Between Different Skin and Wellbore Storage Type-Curves for Early-Time Transient Analysis*, SPE 8205 (Richardson, TX: Soc Pet Eng).

Haug, A.; Kelley, V. A.; LaVenue, A. M.; and Pickens, J. F. 1987. *Modeling of Ground-Water Flow in the Culebra Dolomite at the Waste Isolation Pilot Plant (WIPP) Site: Interim Report*, SAND86-7167 (Albuquerque, NM: Sandia National Laboratories).

Horner, D. R. 1951. "Pressure Buildup in Wells," *Proc Third World Pet Cong* 2:503-23 (The Hague, Netherlands). Reprinted 1967. *Pressure Analysis Methods*, AIME Reprint Series 9:45-50 (Richardson, TX: Soc Pet Eng).

HydroGeoChem, Inc. 1985. *WIPP Hydrology Program, Waste Isolation Pilot Plant, SENM, Hydrologic Data Report #1*, SAND85-7206 (Albuquerque, NM: Sandia National Laboratories).

INTERA Technologies, Inc. 1986. *WIPP Hydrology Program, Waste Isolation Pilot Plant, Southeastern New Mexico, Hydrologic Data Report #3*, SAND86-7109 (Albuquerque, NM: Sandia National Laboratories).

INTERA Technologies, Inc., and HydroGeoChem, Inc. 1985. *WIPP Hydrology Program, Waste Isolation Pilot Plant, Southeastern New Mexico, Hydrologic Data Report #2*, SAND85-7263 (Albuquerque, NM: Sandia National Laboratories).

Jenkins, D. N., and Prentice, J. K. 1982. "Theory for Aquifer Test Analysis in Fractured Rocks Under Linear (Nonradial) Flow Conditions," *Ground Water* 20(1):12-21.

Kazemi, H. 1969. "Pressure Transient Analysis of Naturally Fractured Reservoirs with Uniform Fracture Distribution," *Soc Pet Eng J* (Dec 1969):451-62.

Mavor, M. J., and Cinco-Ley, H. 1979. *Transient Pressure Behavior of Naturally Fractured Reservoirs*, SPE 7977 (Richardson, TX: Soc Pet Eng).

Mercer, J. W. 1983. *Geohydrology of the Proposed Waste Isolation Pilot Plant Site, Los Medanos Area, Southeastern New Mexico*. USGS Water-Resources Investigations Rpt 83-4016 (Albuquerque, NM), 113 pp.

Mercer, J. W., and Orr, B. R. 1979. *Interim Data Report on the Geohydrology of the Proposed Waste Isolation Pilot Plant Site, Southeast New Mexico*. USGS Water-Resources Investigations Rpt 79-98 (Albuquerque, NM), 178 pp.

Moench, A. F. 1984. "Double-Porosity Models for a Fissured Groundwater Reservoir with Fracture Skin," *Water Resources Research* 20(7):831-46.

Narasimhan, T. N., and Kanehiro, B. Y. 1980. "A Note on the Meaning of Storage Coefficient," *Water Resources Research* 16(2):423-29.

Randall, W. S.; Crawley, M. E.; and Lyon, M. in preparation. *1988 Annual Water Quality Data Report for the Waste Isolation Pilot Plant.* DOE-WIPP-88-006 (Carlsbad, NM: US DOE).

Richey, S. F. 1987. *Water-Level Data from Wells in the Vicinity of the Waste Isolation Pilot Plant, Southeastern New Mexico.* USGS Open-File Rpt 87-120 (Albuquerque, NM), 107 pp.

Sandia Laboratories and US Geological Survey. 1979a. *Basic Data Report for Drillhole WIPP 13 (Waste Isolation Pilot Plant - WIPP)*, SAND79-0273 (Albuquerque, NM: Sandia National Laboratories).

Sandia Laboratories and US Geological Survey. 1979b. *Basic Data Report for Drillhole WIPP 25 (Waste Isolation Pilot Plant - WIPP)*, SAND79-0279 (Albuquerque, NM: Sandia National Laboratories).

Sandia Laboratories and US Geological Survey. 1980a. *Basic Data Report for Drillhole WIPP 19 (Waste Isolation Pilot Plant - WIPP)*, SAND79-0276 (Albuquerque, NM: Sandia National Laboratories).

Sandia Laboratories and US Geological Survey. 1980b. *Basic Data Report for Drillhole WIPP 30 (Waste Isolation Pilot Plant - WIPP)*, SAND79-0284 (Albuquerque, NM: Sandia National Laboratories).

Saulnier, G. J., Jr.; Freeze, G. A.; and Stensrud, W. A. 1987. *WIPP Hydrology Program, Waste Isolation Pilot Plant, Southeastern New Mexico, Hydrologic Data Report #4*, SAND86-7166 (Albuquerque, NM: Sandia National Laboratories).

Snyder, R. P. 1985. *Dissolution of Halite and Gypsum, and Hydration of Anhydrite to Gypsum, Rustler Formation, in the Vicinity of the Waste Isolation Pilot Plant, Southeastern New Mexico.* USGS Open-File Rpt 85-229 (Washington, DC: US GPO), 11 pp.

Stensrud, W. A.; Bame, M. A.; Lantz, K. D.; LaVenue, A. M.; Palmer, J. B.; and Saulnier, G. J., Jr. 1987. *WIPP Hydrology Program, Waste Isolation Pilot Plant, Southeastern New Mexico, Hydrologic Data Report #5*, SAND87-7125 (Albuquerque, NM: Sandia National Laboratories).

Stevens, K., and Beyeler, W. 1985. *Determination of Diffusivities in the Rustler Formation from Exploratory-Shaft Construction at the Waste Isolation Pilot Plant in Southeastern New Mexico.* USGS Water-Resources Investigations Rpt 85-4020 (Albuquerque, NM), 32 pp.

Theis, C. V. 1935. "The Relation Between the Lowering of the Piezometric Surface and the Rate and Duration of Discharge of a Well Using Ground-Water Storage," *Trans AGU* 2:519-24.

Uhland, D. W., and Randall, W. S. 1986. *1986 Annual Water Quality Data Report for the Waste Isolation Pilot Plant.* DOE-WIPP-86-006 (Carlsbad, NM: US DOE).

Uhland, D. W.; Randall, W. S.; and Carrasco, R. C. 1987. *1987 Annual Water Quality Data Report for the Waste Isolation Pilot Plant.* DOE-WIPP-87-006 (Carlsbad, NM: US DOE).

Warren, J. E., and Root, P. J. 1963. "The Behavior of Naturally Fractured Reservoirs," *Soc Pet Eng J* (Sept 1963):245-55.

DISTRIBUTION:

US Department of Energy (5)
Office of Civilian Radioactive Waste Management
Office of Geologic Repositories
Attn: Associate Director
W. J. Purcell, RW-20
Director, Repository Coordination Div.
T. H. Isaacs, RW-22
Director, Engineering & Licensing
R. Stein, RW-23
Director, Geosciences & Technology
R. Stein, Actg., RW-24
Director, Siting Division
E. Burton, RW-25
Forrestal Building
Washington, DC 20585

US Department of Energy (3)
Albuquerque Operations
Attn: R. G. Romatowski
D. L. Krenz
D. G. Jackson, Director, Public Affairs Division
PO Box 5400
Albuquerque, NM 87115

US Department of Energy (5)
Attn: J. Tillman,
WIPP Project Office (Carlsbad) (2)
T. Lukow, WPO (Carlsbad)
A. Hunt, WPO (Carlsbad)
B. Young, WPO (Carlsbad)
PO Box 3090
Carlsbad, NM 88221

US Department of Energy, SRPO (4)
Office of Nuclear Waste Isolation
Attn: J. O. Neff
R. Wunderlich
G. Appel
J. Sherwin
505 King Avenue
Columbus, OH 43201

US Department of Energy (2)
Idaho Operations Office
Nuclear Fuel Cycle Division
Attn: R. M. Nelson
J. Whitsett
550 Second Street
Idaho Falls, ID 83401

US Department of Energy (2)
Savannah River Operations Office
Waste Management Project Office
Attn: S. Cowan
W. J. Brumley
PO Box A
Aiken, SC 29801

US Department of Energy (3)
Office of Defense Waste and
Transportation Management
Attn: J. E. Dieckhoner, DP-122
L. H. Harmon, DP-121
A. Follett, DP-121
Washington, DC 20545

US Department of Energy
Research & Technical Support Division
Attn: D. E. Large
PO Box E
Oak Ridge, TN 37830

US Department of the Interior
Attn: E. Roedder
959 National Center
Geological Survey
Reston, VA 22092

US Nuclear Regulatory Commission (2)
Division of Waste Management
Attn: M. Bell
H. Miller
Mail Stop 623SS
Washington, DC 20555

US Geological Survey
Branch of Regional Geology
Attn: R. Snyder
MS913, Box 25046
Denver Federal Center
Denver, CO 80225

US Geological Survey (2)
Water Resources Division
Attn: C. Peters
P. Davies
Pine Tree Office Park
4501 Indian School Rd
Suite 200
Albuquerque, NM 87110

DISTRIBUTION (Continued):

State of New Mexico (3)
Environmental Evaluation Group
Attn: R. H. Neill, Director
320 Marcy Street
PO Box 968
Santa Fe, NM 87503

New Mexico State Engineer's Office
District II
Attn: A. Mason
PO Box 1717
Roswell, NM 88201

NM Department of Energy & Minerals
Attn: K. Laplante, Librarian
PO Box 2770
Santa Fe, NM 87501

New Mexico Bureau of Mines and Mineral Resources (2)
Attn: F. E. Kottolowski, Director
J. Hawley
Socorro, NM 87801

Battelle Pacific Northwest Laboratories
Attn: D. J. Bradley
Battelle Boulevard
Richland, WA 99352

Battelle Memorial Institute (13)
Project Management Division
Attn: W. Carbiener, General Manager (3)
J. Treadwell
T. Naymik
J. Kirchner
V. Adams
O. Swanson
A. Razem
S. Gupta
W. Newcomb
A. LaSala
ONWI Library
505 King Avenue
Columbus, OH 43201

Bechtel Inc. (2)
Attn: E. Weber
M. Bethard
PO Box 3965
45-11-B34
San Francisco, CA 94119

IT Corporation (2)
Attn: W. E. Coons
S. Niou
2340 Alamo, SE
Suite 306
Albuquerque, NM 87106

IT Corporation (4)
Attn: W. Patrick
R. McKinney
D. Deal
M. Crawley
PO Box 2078
Carlsbad, NM 88221

INTERA Technologies, Inc. (7)
Attn: G. E. Grisak
J. F. Pickens
G. J. Saulnier
V. A. Kelly
A. M. LaVenue
A. Haug
INTERA Library
6850 Austin Center Blvd., #300
Austin, TX 78731

INTERA Technologies, Inc.
Attn: W. Stensrud
PO Box 2123
Carlsbad, NM 88221

Martin Marietta Energy Systems, Inc.
Oak Ridge National Laboratory
Attn: J. A. Carter
Box Y
Oak Ridge, TN 37830

Martin Marietta Energy Systems, Inc.
Oak Ridge National Laboratory
Environmental Science
Attn: E. Bondietti
X10 Area, Bldg. 1505, Rm. 322
Oak Ridge, TN 37831

RE/SPEC Inc.
Attn: P. Gnirk
PO 725
Rapid City, SD 57701

DISTRIBUTION (Continued):

RE/SPEC Inc.
Attn: S. W. Key
PO Box 14984
Albuquerque, NM 87191

Rockwell International
Atomics International Division
Rockwell Hanford Operations
Attn: W. W. Schultz
PO Box 800
Richland, WA 99352

G. O. Bachman
Star Route Box 1028
Corrales, NM 87048

Stanford University
Department of Geology
Attn: K. B. Krauskopf
Stanford, CA 94305

Vanderbilt University
Department of Environmental and
Water Resources Engineering
Attn: F. L. Parker
Nashville, TN 37235

Oak Ridge National Laboratory
Attn: J. O. Blomeke
PO Box X
Oak Ridge, TN 37830

US Geological Survey
Water Resources Division
Attn: J. D. Bredehoeft
Western Region Hydrologist
345 Middlefield Road
Menlo Park, CA 94025

K. P. Cohen
928 N. California Avenue
Palo Alto, CA 94303

F. M. Ernsberger
1325 NW 10th Avenue
Gainesville, FL 32601

Johns Hopkins University
Department of Earth Sciences
Attn: H. P. Eugster
Baltimore, MD 21218

University of New Mexico
Department of Geology
Attn: R. C. Ewing
Albuquerque, NM 87131

University of Minnesota
Department of Geological Sciences
Attn: C. Fairhurst
Minneapolis, MN 55455

University of Texas at Austin
Department of Geological Sciences
Attn: W. R. Muehlberger
Austin, TX 78712

D. A. Shock
233 Virginia
Ponca City, OK 74601

National Academy of Sciences
Committee on Radioactive Waste Management
Attn: P. Meyers
2101 Constitution Avenue, NW
Washington, DC 20418

National Ground Water Information Center
Attn: J. Bix
6375 Riverside Dr.
Dublin, OH 43017

New Mexico Junior College
Panel Library
Attn: R. Hill
Lovington Highway
Hobbs, NM 88240

New Mexico Tech
Martin Speere Memorial Library
Campus Street
Socorro, NM 87810

New Mexico Tech (3)
Department of Geoscience
Attn: J. Wilson
D. Stephens
C. S. Chen
Socorro, NM 87801

New Mexico State Library
Attn: I. Vollenhofer
PO Box 1629
Santa Fe, NM 87503

DISTRIBUTION (Continued):

US Geological Survey (2)
Water Resources Division
Attn: P. Hsieh
A. F. Moench
345 Middlefield Rd.
Menlo Park, CA 94025

University of New Mexico
Zimmerman Library
Attn: Z. Vivian
Albuquerque, NM 87131

Atomic Museum
WIPP Public Reading Room
Attn: G. Schreiner
Kirtland East AFB
Albuquerque, NM 87185

Carlsbad Municipal Library
WIPP Public Reading Room
Attn: L. Hubbard, Head Librarian
101 S. Hallagueno St.
Carlsbad, NM 88220

Thomas Brannigan Library
Attn: D. Dresp, Head Librarian
106 W. Hadley St.
Las Cruces, NM 88001

Roswell Public Library
Attn: N. Langston
301 N. Pennsylvania Avenue
Roswell, NM 88201

University of Minnesota
Dept. of Energy and Materials Science
Attn: R. Oriani
151 Amundson Hall
421 Washington Ave SE
Minneapolis, MN 55455

Texas A & M University
Center of Tectonophysics
Attn: J. Handin
College Station, TX 77840

Texas A & M University
Department of Geology
Attn: P. A. Domenico
College Station, TX 77843

University of Arizona (2)
Department of Nuclear Engineering
Attn: J. G. McCray
J. J. K. Daemen
Tucson, AZ 85721

University of Arizona
Department of Hydrology
Attn: S. P. Neuman
Tucson, AZ 85721

University of New Mexico (2)
Geology Department
Attn: D. G. Brookins
Library
Albuquerque, NM 87131

University of Texas at El Paso
Department of Geological Sciences
Attn: D. W. Powers
El Paso, TX 79968

Princeton University
Department of Civil Engineering
Attn: G. Pinder
Princeton, NJ 08504

Scientific Software-Intercomp
Attn: A. C. Gringarten
1801 California, 3rd Floor
Denver, CO 80202

University of California (2)
Lawrence W. Berkeley Laboratory
Attn: J. Long
S. M. Benson
Berkeley, CA 94720

Kansas Geological Survey
Attn: J. Butler
University of Kansas
1930 Constant Ave., Campus West
Lawrence, KS 66046

University of Wisconsin-Madison
Department of Geology and Geophysics
Attn: M. P. Anderson
1215 W. Dayton St.
Madison, WI 53706

DISTRIBUTION (Continued):

Emcon Associates
Attn: F. W. Fenzel
1921 Ringwood Ave.
San Jose, CA 95131

University of British Columbia
Department of Geological Sciences
Attn: R. A. Freeze
Vancouver, British Columbia V6T 1W5
CANADA

Gartner-Lee Limited
Attn: K. G. Kennedy
140 Renfrew Dr.
Markham, Ontario L3R 6B3
CANADA

Atomic Energy of Canada, Ltd. (2)
Attn: C. C. Davison
D. R. Stevenson
Whiteshell Nuclear Research Establishment
Pinawa, Manitoba R0E 1L0
CANADA

Netherlands Energy Research Foundation ECN (2)
Attn: T. Deboer, Mgr.
L. H. Vons
3 Westerduinweg
PO Box 1
1755 ZG Petten
THE NETHERLANDS

Nationale Genossenschaft für die Lagerung
Radioaktiver Abfälle (3)
Attn: P. Hufschmied
C. McCombie
M. Thury
Parkstrasse 23
CH5401 Baden
SWITZERLAND

6000	D. L. Hartley
6230	W. C. Luth
6300	R. W. Lynch
6310	T. O. Hunter
6312	F. W. Bingham
6314	J. R. Tillerson
6330	W. D. Weart
6330	Sandia WIPP Central Files (700H INT) (2)
6331	A. R. Lappin
6331	R. L. Beauheim (2)
6331	D. J. Borns
6331	M. M. Gonzales
6331	A. L. Jensen
6331	S. J. Lambert
6331	K. L. Robinson
6331	M. D. Siegel
6332	L. D. Tyler
6333	T. M. Schultheis
6334	D. R. Anderson
6334	K. Brinster
6416	P. A. Davis
6416	L. R. Shipers
6416	C. D. Updegraff
7100	C. D. Broyles
7120	M. J. Navratil
7125	R. L. Rutter
7130	J. D. Kennedy
7133	J. W. Mercer
7135	P. D. Seward
8524	P. W. Dean
3141	S. A. Landenberger (5)
3151	W. L. Garner (3)
3154-1	C. H. Dalin (8) For DOE/OSTI

☆ U.S. GOVERNMENT PRINTING OFFICE: 1988—573-049/61051